TRANSITION METAL COMPLEXES CONTAINING CHELATING AMIDO LIGANDS

by

SCOTT WILLIAM SEIDEL

B.S. in Chemistry, with Honors
University of California, Berkeley
(December 1992)

Submitted to the Department of Chemistry
in Partial Fulfillment of the Requirements
for the Degree of

DOCTOR OF PHILOSOPHY
at the
MASSACHUSETTS INSTITUTE OF TECHNOLOGY
February, 1998

Signature of Author_____
Department of Chemistry
October 2, 1997

Certified by_____
Richard R. Schrock
Thesis Supervisor

Accepted by_____
Dietmar Seyferth
Chairman, Departmental Committee on Graduate Students

This doctoral thesis has been examined by a Committee of the Department of Chemistry as follows:

Professor Dietmar Seyferth_____

Chairman

Professor Richard R. Schrock_____

Thesis Supervisor

Professor Daniel G. Nocera_____

Dedicated to the memory of my father,

Dr. William C. Seidel

"I went to the woods because I wanted to live deliberately, to front only the essential facts of life. And see if I could not learn what it had to teach and not, when I came to die, discover that I had not lived."

– Henry David Thoreau, on his two-year stay at Walden Pond.

"I was born not knowing and have only had a little time to change that here and there."

– Prof. Richard P. Feynman

"Do not keep saying to yourself..., 'But how can it be like that?' because you will get...into a blind alley from which nobody has yet escaped. Nobody knows how it can be like that."

– Prof. Feynman, on scientific laws.

TRANSITION METAL COMPLEXES
CONTAINING CHELATING AMIDO LIGANDS

by

SCOTT WILLIAM SEIDEL

Submitted to the Department of Chemistry, October 1997,
in Partial Fulfillment of the Requirements
for the Degree of Doctor of Philosophy in Chemistry

ABSTRACT

The synthesis of a variety of paramagnetic molybdenum and tungsten alkyl complexes of the form $[N_3N]MR$ ($[N_3N]^{3-} = [(Me_3SiNCH_2CH_2)_3N]^{3-}$) has been attempted. When M = W only the Me and Ph complexes are stable, the rest decompose by α,α-double dehydrogenation to give $[N_3N]W{\equiv}C\text{-}R'$ complexes. Classical magnetic behavior of both the molybdenum and tungsten d^2 complexes is observed down to 5 K. $[N_3N]M$(cyclopentyl) complexes are in rapid equilibrium with the corresponding d^0 cyclopentylidene hydride complexes. The rate constant for the formation of $[N_3N]M$(cyclopentylidene)(H) from $[N_3N]M$(cyclopentyl) is approximately the same for M = Mo and W. Thermodynamic parameters do vary considerably with the metal. β-Hydride elimination in $[N_3N]$Mo(cyclopentyl) has been shown to be 6-7 orders of magnitude slower than α-hydride elimination. Analogous investigations have been made with complexes containing the $[N_3N_F]^{3-}$ ligand ($[N_3N_F]^{3-} = [(C_6F_5NCH_2CH_2)_3N]^{3-}$) and the results compared with $[N_3N]^{3-}$ complexes. X-ray studies of $[N_3N]MoR$ ($R = CD_3$, C_6H_{11}) and $[N_3N_F]W{\equiv}CSiMe_3$ have been carried out, revealing a wide variation in the degree of steric strain present. C_6F_5-substituted diamidoamine complexes of tungsten have also been prepared. $[N_3N_F]$W(3,5-dimethylphenyl) reacts with CO to give the corresponding acyl complex and with atom transfer reagents (pyridine-*n*-oxide, trimethylsilylazide) to give the oxo aryl and imido aryl complexes. X-ray studies for several $[N_3N_F]^{3-}$ complexes display unusual distortions, including close contacts between aryl and perfluoroaryl rings. $[N_3N_F]WX$ species are reduced in the presence of π-acid ligands (CO, CN-*t*-Bu, NO, and ethylene) to give $[N_3N_F]W(L)$ complexes. Strong backbonding from tungsten is apparent by IR spectroscopy and an X-ray study of $[N_3N_F]$W(CN-*t*-Bu). $[N_3N_F]$W(CO) reacts smoothly with Na/Hg followed by a TMSCl quench to give $[N_3N_F]W{\equiv}C\text{-}O\text{-}TMS$, and with $V(Mes)_3(THF)$ to give $[N_3N_F]W(CO)V(Mes)_3$, as evidenced by an X-ray study. Diamidophosphine complexes of zirconium and molybdenum have also been prepared and structurally characterized. $[N_2P]ZrR_2$ species polymerize ethylene at 0 °C when activated with $[Ph_3C][B(C_6F_5)_4]$. NMR studies of cationic tantalum and tungsten methyl compounds have been carried out in an attempt to obtain evidence for α-agostic interactions.

Thesis Supervisor: Dr. Richard R. Schrock

Title: Frederick G. Keyes Professor of Chemistry

TABLE OF CONTENTS

LIST OF FIGURES

Appendix I page

LIST OF TABLES

Chapter 1 page

Chapter 2 page

Chapter 3 page

Chapter 4 page

LIST OF SCHEMES

LIST OF X-RAY STRUCTURES

Chem 3D drawings of the structures are located on the indicated pages. Tables of selected bond lengths and angles; and crystallographic data, can be found in the text. Labeled ORTEP diagrams drawn at the 35% probability level are collected in Appendix II and tabulated by structure identification number.

ABBREVIATIONS USED IN THE TEXT

Bn	benzyl
br	broad
bp	boiling point
o-C_6F_5	ortho fluorines in C_6F_5R
m-C_6F_5	meta " "
p-C_6F_5	para fluorine "
C_α	carbon bound to metal
C_β, etc.	carbon bound to C_α, etc.
C_{ipso}	carbon in the ipso position of an aromatic ring
C_{meta}	carbon in the meta position "
C_{ortho}	carbon in the ortho position "
C_{para}	carbon in the para position "
Cp	cyclopentadienyl
Cp^*	permethylcyclopentadienyl
Cy	cyclohexyl
d	doublet
DME	1,2-dimethoxyethane
Bu	butyl
i-Bu	*iso*-butyl
n-Bu	normal butyl
t-Bu	tertiary butyl
eq	equation
equiv.	equivalent(s)
Et	ethyl
FABMS	Fast-ion bombardment mass spectroscopy
h	hours
H_α	hydrogen (proton) bound to C_α
Hz	Hertz
$^nJ_{AB}$	A-B coupling constant through n bonds
m	multiplet
m/e	mass/charge ratio
Me	methyl
Mes	mesityl
mesityl	2,4,6-trimethylphenyl

min	minutes
MO	molecular orbital
HOMO	highest occupied molecular orbital
$[N_3N]^{3-}$	$[(Me_3SiNCH_2CH_2)_3N]^{3-}$
$[N_3N_F]^{3-}$	$[(C_6F_5NCH_2CH_2)_3N]^{3-}$
$[N_2NH]^{2-}$	$[(C_6F_5NCH_2CH_2)_2NH]^{2-}$
$^*[N_3P_F]^{3-}$	$[(C_6F_5NCMe_2CH_2)_3P]^{3-}$
$[N_2P]^{2-}$	$[(Me_3SiNCH_2CH_2)_2PPh]^{2-}$
$[NP]^{2-}$	$[Me_3SiNCH_2CH_2PPh]^{2-}$
$[PhN_2P]^{2-}$	$[(PhMe_2SiNCH_2CH_2)_2PPh]^{2-}$
$[N_2P_F]^{2-}$	$[(C_6F_5NCH_2CH_2)_2PPh]^{2-}$
NMR	nuclear magnetic resonance
Np	neopentyl
OTf	O_3SCF_3
triflate	"
Ph	phenyl
ppm	parts per million
Pr	propyl
py	pyridine
q	quartet
IR	Infrared
s	singlet
SALC	symmetry-adapted linear combination
sec	seconds
t	triplet
THF	tetrahydrofuran
TMEDA	tetramethylethylenediamine
tol	toluene
TMS	trimethylsilyl
Ts	tosyl
Tosyl	$O_3SC_6H_4CH_3$
UV/Vis	ultraviolet/visible
V	volts
VT	variable-temperature
xylyl	dimethylphenyl
δ	chemical shift in parts per million

$\Delta_{1/2}$	peak width at half-height
ε	extinction coefficient
λ_{max}	wavelength of maximum optical absorption
ν	frequency
$\tau_{1/2}$	half-life
μ_B	Bohr magneton
μ_{eff}	effective magnetic moment
μ	magnetic moment

GENERAL INTRODUCTION

The tris(2-aminoethyl)amine (tren) ligand has been used as a chelating ligand in inorganic chemistry for some time. Werner-type complexes such as $[Co(tren)Cl(NH_3)](Cl)_2$ (**1**) and $[Cu_2(tren)_2Cl_2](BPh_4)_2$ (**2**) have played an important role in the development of coordination chemistry.[1,2] In general, five-coordinate tren complexes such as **2** are highly stable relative to their tetrakis(ammine) analogs as a result of the chelate effect. The tren ligand is particularly useful in the synthesis of complexes of low-valent, middle and late transition metals where ammine complexes are common, although octahedral $Ti(tren)Cl_3$ is known, as are some less well-characterized lanthanide complexes.[1]

Until relatively recently, the tren ligand was largely a tool of the coordination chemist. However, innovative work in the 1970's led to the development of trianionic derivatives of tren which proved quite useful for the synthesis of main-group compounds.[3] Ligands of the form $[(RHNCH_2CH_2)_3N]$ (R = H, Me, *i*-Pr, $SiMe_3$)[4] lead to complexes coined azatranes, e.g. $[(MeNCH_2CH_2)_3N]Al$ (**3**) and $[(MeNCH_2CH_2)_3N]P$ (**4**). Phosphine **4** is a commercially available nonionic superbase.[5] A unique facet of azatrane chemistry is that the ligand adopts two basic coordination modes, one with the dative amine coordinated to the main-group element and one with it dissociated (Figure 1). Such flexibility of the ligand in terms of binding modes is believed to confer some of the unique reactivity observed with these complexes, such as the highly nucleophilic nature of the phosphorus in $[(MeNCH_2CH_2)_3N]P$.[5] The ability of the dative nitrogen to coordinate to phosphorus has been proposed to stabilize the cationic P-silylated intermediate (**5**) during silylation reactions catalyzed by **4**.

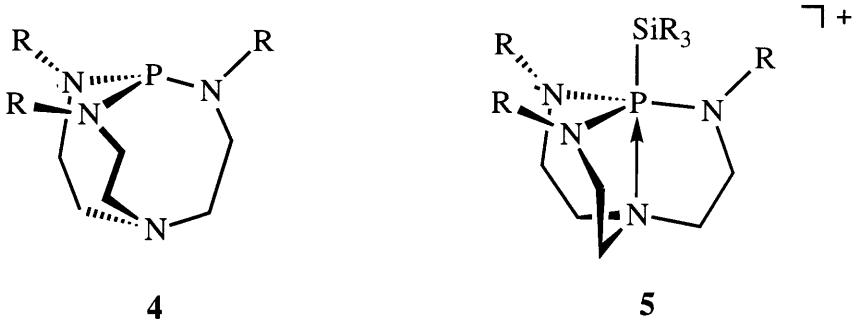

Figure 1. The two coordination modes observed for azatrane complexes.

References begin on page 22.

Transition metal chemistry with tren-derived ligands began with the idea[6] that a trianionic, TMS-substituted tren ligand might have some of the same advantages as the $(TMS)_2N^-$ ligand, namely a steric and electronic profile conducive for the synthesis of a wide variety of hydrocarbon-soluble and crystalline transition metal[7] and actinide[8] complexes. This was indeed found to be the case,[9] forwarded by the development of a facile procedure for the synthesis of $[N_3N]Li_3$ ($[N_3N]^{3-}$ = $[(TMSNCH_2CH_2)_3N]^{3-}$) in 40 gram quantities.[6] Triamidoamine complexes (we prefer this more generic nomenclature to "azatrane") of metals in Groups IV through VII are now known, and a C_6F_5-substituted version ($[N_3N_F]^{3-}$ = $[(C_6F_5NCH_2CH_2)_3N]^{3-}$) has also been prepared with similar ease,[10] resulting in the high-yield syntheses of $[N_3N_F]^{3-}$ complexes of molybdenum and tungsten. Several general chemical trends have been observed in complexes containing these ligands. In particular, a high degree of steric protection is provided for ligands in the apical site, presumably one of the reasons that a number of rarely observed species have been prepared, such as a Ta phosphinidene,[11] a Ti hydride,[6] and trigonal-monopyramidal complexes of first-row transition metals from Ti to Mn.[12] A sterically protected apical site is also probably responsible for the discovery of some unique reactions, such as the α,α-dehydrogenation of W(IV) alkyls[13] and the synthesis of a terminal phosphido complex from a W(IV) phosphide.[14] What would otherwise be unstable species are probably rendered accessible as a result of the coordination environment provided by this ligand.

The triamidoamine ligand can be at most a twelve electron donor (using the anionic convention for electron counting). Eight electrons are used in σ-bonding molecular orbitals. Only four of the six amido lone pair electrons can participate in π-bonding with the metal due to symmetry constraints. Three symmetry-adapted linear combinations of the amide p-orbitals can be constructed, one with A_2 symmetry and another doubly-degenerate set with E symmetry, however, no metal-based orbital of A_2 symmetry exists in the C_{3v} point group. Thus, the remaining two amido lone pair electrons reside in a ligand-centered nonbonding orbital. A molecular orbital diagram for amido π-bonding in a triamidoamine complex is shown in Figure 2.

References begin on page 22.

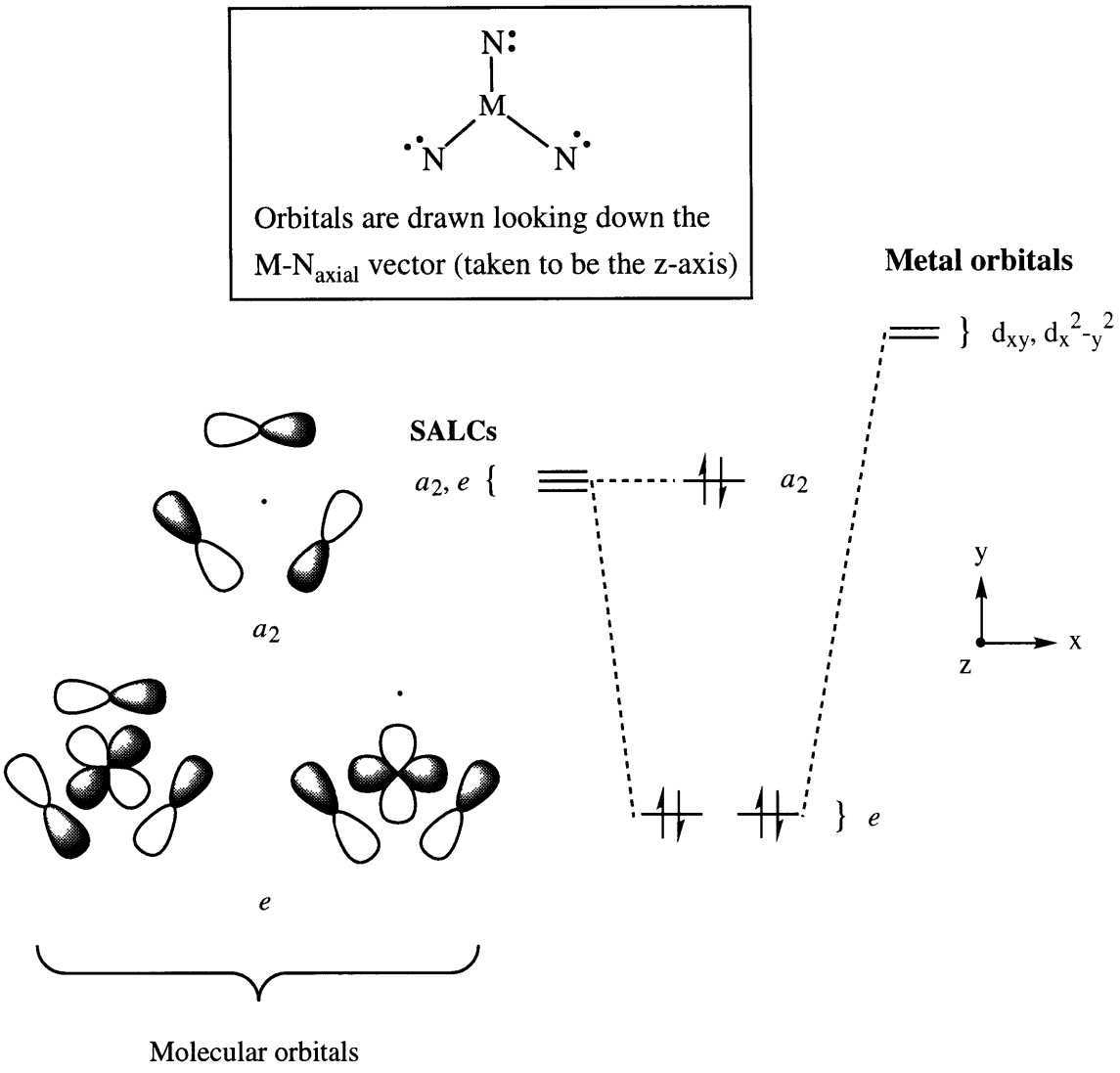

Figure 2. Molecular orbital diagram for amido π-bonding in triamidoamine complexes.

Since six molecular orbitals are used for σ- and π-bonding from the [N_3N] ligand, there are three orbitals remaining for bonding with ligands in the apical site of triamidoamine complexes, one of σ-symmetry (d_z^2) and two of π-symmetry (d_{xz} and d_{yz}) (Figure 3). The d_z^2 orbital is probably slightly higher in energy than the d_{xz}/d_{yz} set, since some dative amine-d_z^2 overlap is possible. Thus, bonding from the ligand(s) present in the "pocket" with the d_z^2 orbital will be antibonding with respect to any d_z^2-dative nitrogen interaction. The orbital arrangement present contrasts sharply with that of the ubiquitous bent metallocene core, where all three orbitals (one of

References begin on page 22.

A_1 symmetry and two of B_2 symmetry) lie in the same plane, that passing between the Cp rings.[15] The two π-symmetry frontier molecular orbitals in [N_3N] complexes are strictly degenerate, orthogonal, and probably essentially pure d-orbitals, resulting in an environment that is especially favorable for the formation of a metal-ligand triple bond. Hybridization of this set also allows for one doubly-bonded and one singly-bonded ligand in the apical site, or three singly-bonded ligands. All three of these scenarios result in an 18 electron complex for d^0 metals. This distinctive frontier molecular orbital configuration, in conjunction with the steric protection afforded by the amido substituents, has provided a fertile environment for the discovery of new complexes and the study of reaction mechanisms.

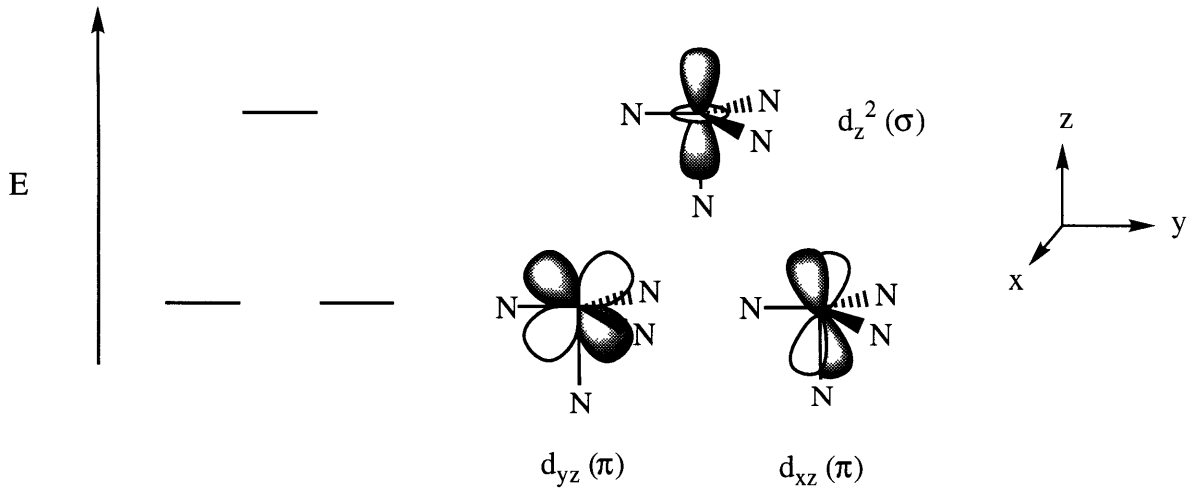

Figure 3. Frontier molecular orbitals available for bonding with apical ligands in triamidoamine complexes.

References begin on page 22.

REFERENCES

(1) *Comprehensive Coordination Chemistry;* Wilkinson, G., Ed.; Pergamon Press: New York, 1987.

(2) Laskowski, E. J.; Duggan, D. M.; Hendrickson, D. N. *Inorg. Chem.* **1975**, *14*, 2449.

(3) Verkade, J. G. *Acc. Chem. Res.* **1993**, *26*, 483.

(4) Gudat, D.; Verkade, J. G. *Organometallics* **1989**, *8*, 2772.

(5) D'Sa, B. A.; McLeod, D.; Verkade, J. G. *J. Org. Chem.* **1997**, *62*, 5057.

(6) Cummins, C. C.; Schrock, R. R.; Davis, W. M. *Organometallics* **1992**, *11*, 1452.

(7) Lappert, M. F.; Power, P. P.; Sanger, A. R.; Srivastava, R. C. *Metal and Metalloid Amides*, Halsted Press: New York, 1980.

(8) Turner, H. W.; Simpson, S. J.; Andersen, R. A. *J. Am. Chem. Soc.* **1979**, *101*, 2782.

(9) Schrock, R. R. *Acc. Chem. Res.* **1997**, *30*, 9.

(10) Kol, M.; Schrock, R. R.; Kempe, R. *J. Am. Chem. Soc.* **1994**, *116*, 4382.

(11) Cummins, C. C.; Schrock, R. R.; Davis, W. M. *Angew. Chem. Int. Ed. Eng.* **1993**, *32*, 756.

(12) Cummins, C. C.; Lee, J.; Schrock, R. R. *Angew. Chem. Int. Ed. Engl.* **1992**, *104*, 1501.

(13) Shih, K.-Y.; Totland, K.; Seidel, S. W.; Schrock, R. R. *J. Am. Chem. Soc.* **1994**, *116*, 12103.

(14) Zanetti, N. C.; Schrock, R. R.; Davis, W. M. *Angew. Chem., Int. Ed. Engl.* **1995**, *34*, 2044.

(15) Albright, T. A.; Burdett, J. K.; Whangbo, M.-H. *Orbital Interactions in Chemistry*, Wiley & Sons: New York, 1985.

CHAPTER I

Direct Detection of α-Elimination Processes That Are More Than Six Orders of Magnitude Faster Than β-Elimination Processes in Molybdenum(IV) Alkyl Complexes That Contain the $[(Me_3SiNCH_2CH_2)_3N]^{3-}$ Ligand.

Much of this material covered in this chapter has been accepted for publication:

Schrock, R. R.; Seidel, S. W.; Mösch-Zanetti, N. C.; Shih, K.-Y.; O'Donoghue, M. B.; Davis, W. M.; Reiff, W. M. *J. Am. Chem. Soc.*, in press.

INTRODUCTION

We have been interested in the chemistry of TMS-substituted triamidoamine complexes of molybdenum and tungsten from several perspectives, including dinitrogen fixation,[1-3] terminal phosphido and arsenido complexes,[4-7] and new organometallic chemistry.[3,8,9] This chapter describes the synthesis, characterization, and decomposition of a variety of alkyl complexes of molybdenum that contain the $[N_3N]^{3-}$ ligand. We have been presented with the opportunity to prove, by directly measuring rate constants, that α-elimination reactions are faster than β-elimination reactions for cyclopentyl and cyclohexyl complexes, even though the products of α-elimination (alkylidene hydrides) and β-elimination (olefin hydrides) are not observable. This was made possible by judicious use of ^2H NMR, which has a resonant frequency low enough such that these processes could be observed at temperatures where more severe decomposition reactions are still slow. These results should be compared to those obtained for related tungsten complexes,[8,9] the full details of which will be described in chapter II.

RESULTS

Characterization of Paramagnetic Molybdenum Triamidoamine Complexes

Orange, crystalline $[N_3N]MoCl$ is synthesized by reacting $[N_3N]Li_3$[10] and $MoCl_4(THF)_2$[11] in THF.[12] Yields are typically 30-35%. Despite the moderate yield, $[N_3N]MoCl$ is a practical starting material because both $[N_3N]Li_3$ and $MoCl_4(THF)_2$ can be easily prepared in large quantities. The magnetic susceptibility (χ_M) of $[N_3N]MoCl$ is plotted versus T and 1/T in Figures 1.1 and 1.2. A plot of μ_{eff} versus T is shown in Figure 1.3. The susceptibility versus T for temperatures between 50 and 300 K can be fit to curve defined by the Curie-Weiss equation ($\chi = \mu^2/8(T + \theta)$) to give values of $\mu = 2.92 \pm 0.10\ \mu_B$ and $\theta = 6.4 \pm 1.0$ K. These data suggest that $[N_3N]MoCl$ is a Curie-Weiss paramagnet between room temperature and ~50 K in the solid state with a μ value essentially equal to the spin-only value expected for two unpaired electrons (spin-only $\mu_{eff} = 2.83\ \mu_B$).[13] We assume that the two electrons are in the set of degenerate non-bonding orbitals of π symmetry (approximately d_{xz} and d_{yz} if N_{ax}-Mo-Cl is

References begin on page 63.

taken to be the z axis). The susceptibility of $[N_3N]MoCl$ in the solid state between 6 and 300 K has been reported,[14] but only Curie-Weiss behavior above 100 K (μ_{eff} = 2.35, θ = 0.148 K) was noted. It can be clearly seen from Figures 1.1 and 1.3 that below 50 K, values for χ_M and μ_{eff} are much less than expected for a Curie-Weiss paramagnet. The fairly abrupt decrease in the effective magnetic moment below ~50 K can be attributed to a combination of spin-orbit effects and low symmetry ligand field components that result in zero field splitting of the d^2 ground state triplet.[15] Table 1.1 contains the data used to generate the plots in Figures 1.1-1.3.

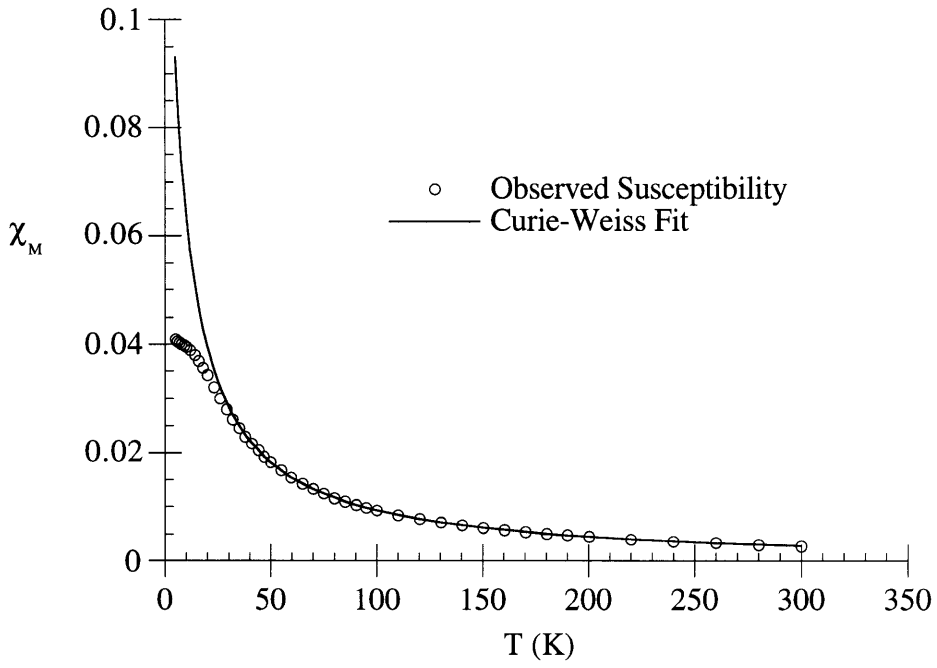

Figure 1.1. A plot of χ_M versus T for $[N_3N]MoCl$. Data between 50 and 300 K are fit to the Curie-Weiss law. The μ and θ values obtained from this fit to were used to extend the solid line in the region below 50 K. The low values in this region compared to those expected for a Curie-Weiss paramagnet are proposed to result from a combination of spin-orbit coupling and zero field splitting effects (see text).

References begin on page 63.

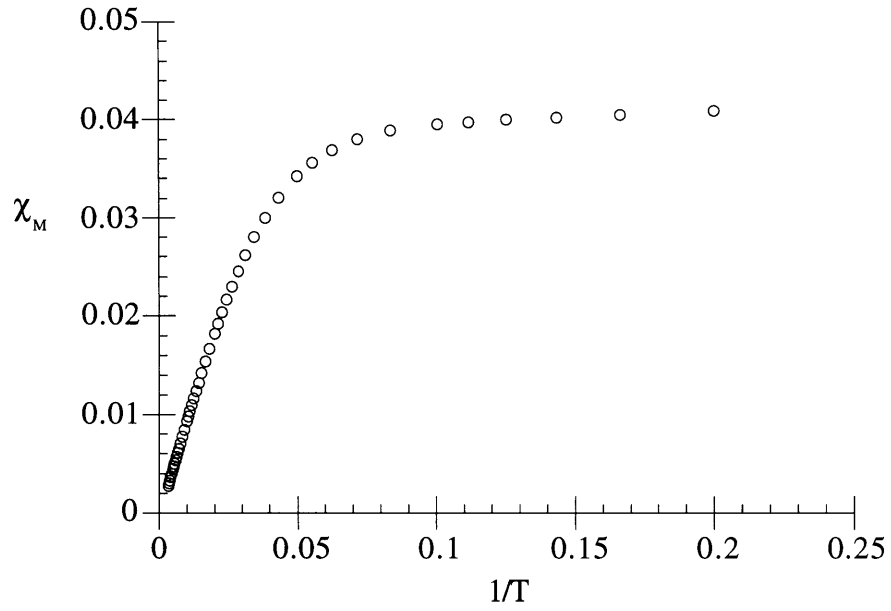

Figure 1.2. A plot of χ_M versus 1/T for $[N_3N]MoCl$.

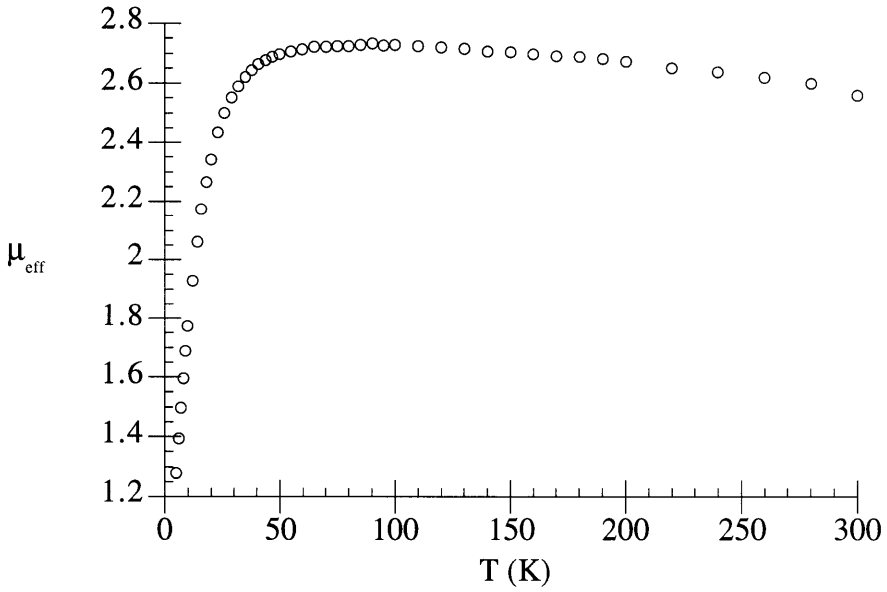

Figure 1.3. A plot of μ_{eff} versus T for $[N_3N]MoCl$.

$[N_3N]MoMe$, $[N_3N]Mo(CH_2SiMe_3)$, and $[N_3N]Mo$(cyclopentyl) are readily prepared by alkylation of $[N_3N]MoCl$ with the corresponding lithium reagent in ether.[12] The susceptibilities of these complexes in the solid state vary with temperature in ways that are entirely analogous to the behavior of $[N_3N]MoCl$. A plot of χ_M versus T for the three complexes is shown in Figure 1.4. Table 1.2 contains the values of μ and θ obtained by fitting the data at temperatures above 50 K to the Curie-Weiss law. The magnetic moment of $[N_3N]MoMe$ in C_6D_6 at 25 °C was found to be 2.9 μ_B by the Evan's method,[12] consistent with the result obtained in the solid state.

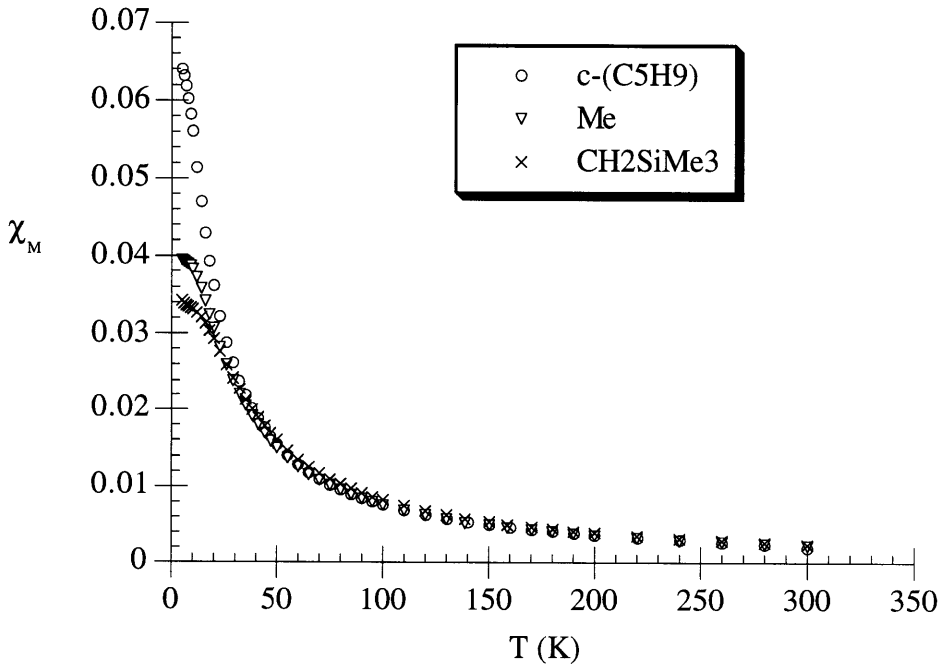

Figure 1.4. Plots of χ_M versus T for $[N_3N]MoR$ (R = Me, cyclopentyl, and CH_2SiMe_3).

References begin on page 63.

Table 1.1. Data used to generate the plots in Figures 1.1-1.3.

T (K)	Net Magnetization (EMU) [a]	χ_M [b]	μ_{eff} [c]
5.00	0.0074399	0.040853	1.2781
6.01	0.0073680	0.040461	1.3946
6.98	0.0073154	0.040174	1.4975
7.98	0.0072702	0.039927	1.5963
8.96	0.0072299	0.039707	1.6868
9.96	0.0071866	0.039471	1.7732
11.98	0.0070726	0.038849	1.9293
13.98	0.0069153	0.037990	2.0610
16.00	0.0067137	0.036890	2.1727
18.03	0.0064791	0.035610	2.2660
20.02	0.0062281	0.034241	2.3414
23.09	0.0058291	0.032063	2.4333
26.05	0.0054502	0.029996	2.4998
29.02	0.0050904	0.028032	2.5507
32.02	0.0047542	0.026197	2.5901
35.01	0.0044467	0.024519	2.6202
38.01	0.0041648	0.022981	2.6431
40.98	0.0039230	0.021662	2.6645
43.97	0.0036872	0.020375	2.6767
46.97	0.0034772	0.019229	2.6876
49.96	0.0032866	0.018189	2.6958
54.96	0.0030080	0.016668	2.7068
59.91	0.0027686	0.015362	2.7130
65.03	0.0025610	0.014229	2.7203
70.10	0.0023759	0.013219	2.7223
75.17	0.0022169	0.012351	2.7249
80.06	0.0020787	0.011597	2.7250
85.07	0.0019593	0.010945	2.7289
90.32	0.0018481	0.010339	2.7328
95.10	0.0017447	0.0097747	2.7266
100.12	0.0016565	0.0092934	2.7279
110.17	0.0014963	0.0084192	2.7236
120.20	0.0013628	0.0076906	2.7190
130.21	0.0012495	0.0070721	2.7138
140.21	0.0011508	0.0065335	2.7067
150.21	0.0010683	0.0060832	2.7033
160.21	0.00099340	0.0056746	2.6964
170.20	0.00092839	0.0053198	2.6910
180.20	0.00087297	0.0050174	2.6890
190.14	0.00081950	0.0047256	2.6807
200.20	0.00077060	0.0044588	2.6719
220.17	0.00068421	0.0039873	2.6497
240.13	0.00061661	0.0036184	2.6361
260.11	0.00055754	0.0032961	2.6185
280.08	0.00050523	0.0030106	2.5969
300.00	0.00045285	0.0027248	2.5569

[a] Corrected for the susceptibility of the empty sample holder.

[b] χ_M = [Mol. wt. (g/mol) x Net mag.] / [Field (gauss) x Sample mass (g)]. χ_M values were corrected for the diamagnetic contribution using Pascal's constants, here $\chi_{dia} = -254 \times 10^{-6}$ cgsu.

[c] $\mu_{eff} = 2.828\ (\chi_M T)^{1/2}$

References begin on page 63.

Table 1.2. Values of μ in the solid state for $[N_3N]MoX$ compounds.[a]

Compound	μ (μ_B)	θ (K)
$[N_3N]MoCl$	2.92	6.4
$[N_3N]MoMe$	2.76 (2.61)	11.1 (4.8)
$[N_3N]Mo(CH_2SiMe_3)$	2.72 (2.78)	3.8 (7.5)
$[N_3N]Mo$(cyclopentyl)	2.58 (2.60)	-2.2 (-2.4)

[a] Obtained from SQUID data between 5 and 300 K by fitting the susceptibility (corrected for core diamagnetism) between 50 and 300 K to the equation $\chi = \mu^2/8(T + \theta)$. The error in μ is estimated to be ± 0.10 μ_B and in θ to be ± 1 K. Numbers in parentheses refer to a second sample.

The proton NMR spectrum of $[N_3N]MoCl$ at 22 °C consists of three broadened, shifted resonances, one for the TMS groups and two for the backbone methylene protons of the $[N_3N]^{3-}$ ligand, consistent with a paramagnetic species that has C_{3v} symmetry on the NMR time scale. It is not known which of the two methylene resonances corresponds to which $[N_3N]^{3-}$ backbone methylene group. As the temperature of the NMR sample is lowered the spectrum changes in two ways. First, the methylene resonances shift upfield (Figure 1.5) and the TMS resonance shifts (to a lesser extent) downfield (not shown). If the chemical shift of each methylene proton set is plotted versus 1/T, nearly linear relationships are observed (Figure 1.6), as expected for a Curie-Weiss paramagnet in solution in this temperature range. (The average of the two methylene resonances below the coalescence point discussed below was employed when necessary in Figure 1.6). The second temperature-dependent process observed is a slowed interconversion between C_3-symmetric, chiral Δ and Λ conformers as shown in Figure 1.5. The backbone geminal protons in these relatively low symmetry molecules are rendered diastereotopic, thus four resonances are observed. At higher temperatures the C_3-symmetric

References begin on page 63.

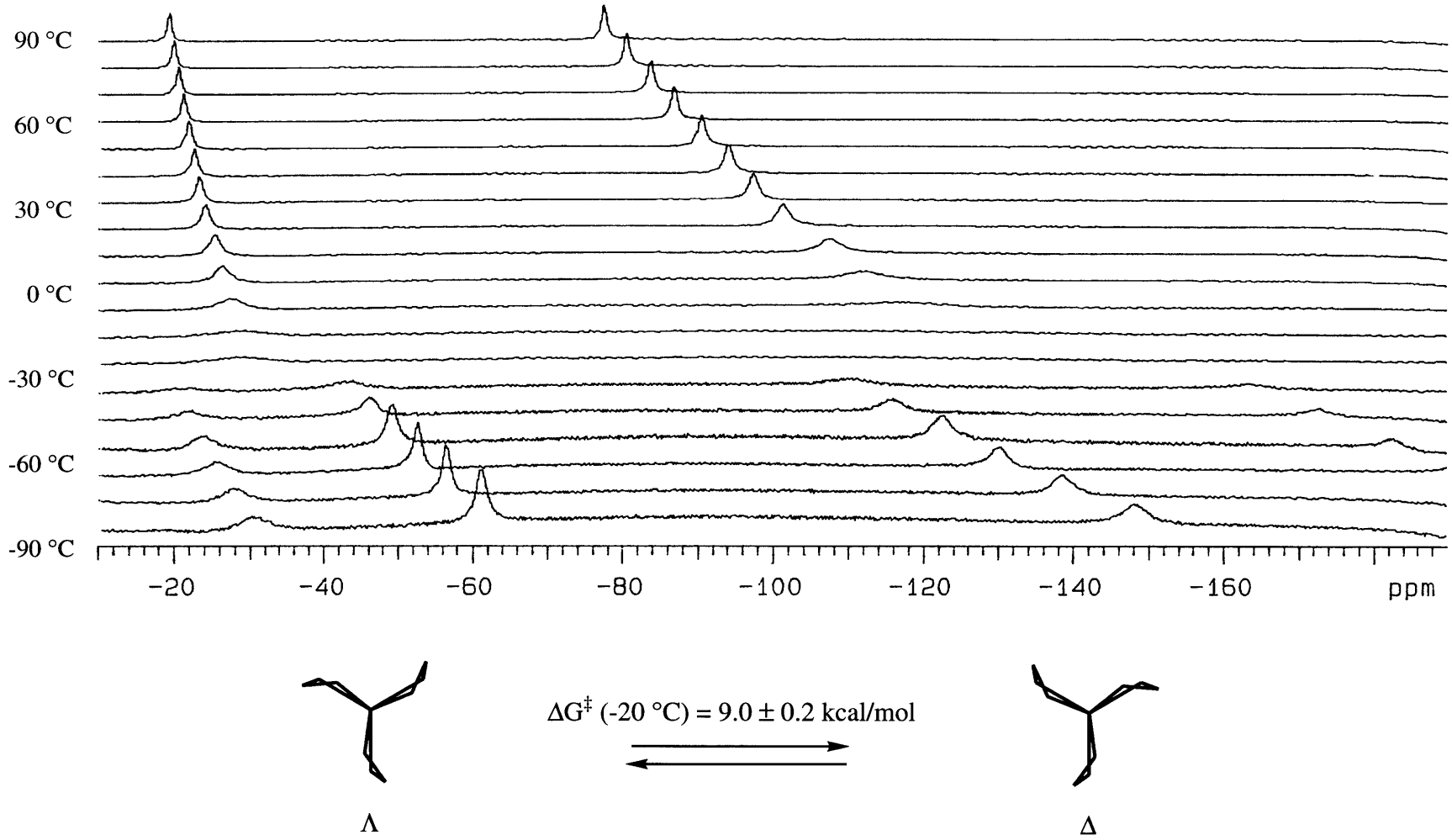

Figure 1.5. VT 500 MHz ^{1}H NMR spectra of [(TMSNCH_2CH_2)$_3$N]MoCl in toluene-d_8.

species becomes C_{3v}-symmetric on the NMR time scale as a consequence of the molecule's backbone "flipping" rapidly between the two chiral forms. Using the chemical shift difference between the two types of backbone protons at a temperature that is as close as possible to the temperature of coalescence, an approximate $\Delta G^{\ddagger}$ for the C_{3v}/C_3 fluxional process can be calculated to be 9.2 kcal/mol at ca. -30 °C and 9.0 kcal/mol at ca. -20 °C. (The errors in these values are estimated to be at least ± -0.2 kcal mol^{-1}.) A C_{3v}/C_3 fluxional process is observed for each $[N_3N]MoX$ species discussed in this chapter. This type of fluxional process can also be observed for a variety of other C_{3v}-symmetric metal complexes that contain the $[N_3N]^{3-}$ ligand, including diamagnetic species,[16] and complexes that contain the $[(C_6F_5NCH_2CH_2)_3N]^{3-}$ ligand.[17] We assume that the apical nitrogen donor does not have to dissociate from the metal in order for the C_{3v}/C_3 fluxional process to occur, mainly because $\Delta G^{\ddagger}$ values for the C_{3v}/C_3 interconversion are much the same for analogous tungsten complexes (see chapter II).

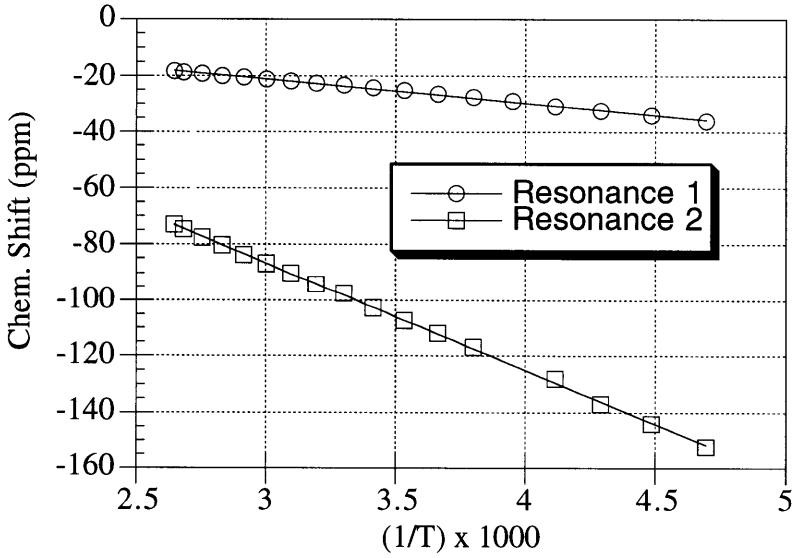

Figure 1.6. A plot of the chemical shift of the methylene backbone resonances in $[N_3N]MoCl$ versus 1/T.

References begin on page 63.

As we shall see later, $[N_3N]MoMe$ is a highly thermally stable molecule compared to some other organometallics of this type. It was thus deemed worthwhile to investigate the solid-state structure of this complex by X-ray crystallography. A view of the structure of $[N_3N]Mo(CD_3)$ is shown in Figure 1.7. Bond lengths and bond angles are compared with distances and angles in related compounds in Table 1.3. Crystallographic data are contained in Table 1.4. The choice of the CD_3 complex over the CH_3 complex was circumstantial. The structure of $[N_3N]Mo(CD_3)$ is most similar to that of $[N_3N]MoCl$[14], except that in the methyl complex the TMS groups twist out of the plane containing the metal and a given axial and equatorial nitrogen slightly, simultaneously bringing the backbone carbons, $C_{\beta,eq}$ and $C_{\beta,ax}$, out of this N(4)-Mo-N plane. We find the angle between the N(4)-M and N_{amide}-Si vectors a convenient measure of the degree of this twisting effect. Almost no "twist" is observed in the structure of $[N_3N]MoCl$, with N(4)-Mo-N-Si values of 176.6 degrees. In $[N_3N]Mo(CD_3)$, N(4)-Mo-Si-N angles range from 160 to 163 degrees. We propose that the TMS groups are twisted to a larger degree in $[N_3N]Mo(CD_3)$ than in $[N_3N]MoCl$ as a consequence of the slightly larger methyl ligand present in the apical pocket. The long Mo-N(4) distance (2.304(9) Å) could be ascribed to a less electrophilic metal center in $[N_3N]Mo(CD_3)$ compared to that in $[N_3N]MoCl$ (Mo-N(4) = 2.185(5) Å).

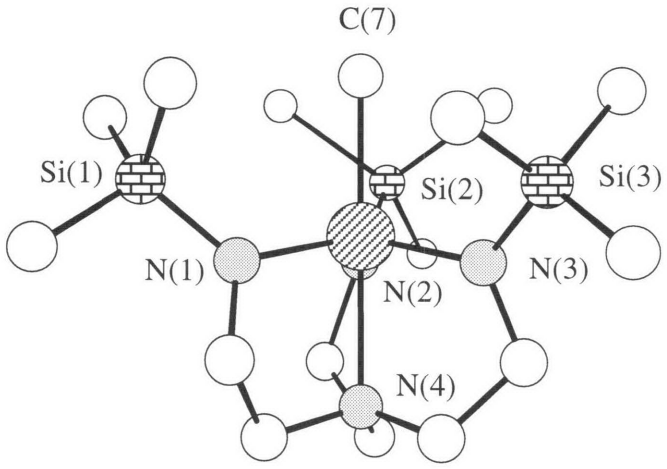

Figure 1.7. A view of the structure of $[N_3N]Mo(CD_3)$.

References begin on page 63.

A drawing of the structure of $[N_3N]$Mo(cyclohexyl) is shown in Figure 1.8. Bond lengths and bond angles are compared with distances and angles in related compounds in Table 1.3, and crystallographic data are contained in Table 1.4. The cyclohexyl ring is oriented so that it lies roughly in a plane that passes between N(1) and N(3) and between N(1) and N(2). The Mo-C(101) distance (2.167(14) Å) is the same as Mo-C(7) in $[N_3N]$Mo(CD_3). The Mo-C(101)-C(106) and Mo-C(101)-C(102) angles (117 and 120 °) are larger than tetrahedral, consistent with a significant amount of steric pressure within the trigonal pocket. The possibility of any concomitant α-agostic[18,19] interaction between the C(101)-H_α bond and the metal seems remote in view of the fact that the only available orbitals (d_{xz} and d_{yz}) each contain one electron. Interestingly, the N(4)-Mo-N_{eq}-Si dihedral angles are all dramatically smaller (129 to 136°) than those found in $[N_3N]$Mo(CD_3), and the N(4)-Mo distance is approximately 0.1 Å longer than in $[N_3N]$Mo(CD_3). We propose that both are consistent with a significantly greater degree of steric

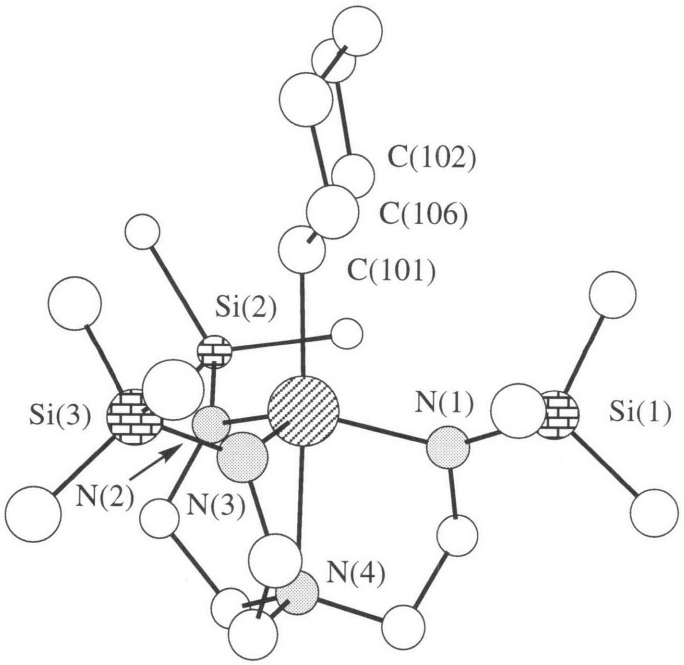

Figure 1.8. A view of the structure of $[N_3N]$Mo(cyclohexyl).

References begin on page 63.

interaction between the cyclohexyl ring and the silyl groups on the equatorial amido nitrogens. "Steric pressure" within the pocket in $[N_3N]$Mo(alkyl) complexes could sharply distinguish one complex from another in terms of the ease of some proton elimination reactions, as we shall see shortly.

Table 1.3. Selected bond distances (Å) and angles (°) for related complexes.

	$[N_3N]MoCl$[a]	$[N_3N]Mo(CD_3)$	$[N_3N]Mo(Cy)$
Mo-L_{ax}	2.398(2)	2.188(11)	2.167(14)
Mo - N(1)	1.976(3)	1.984(9)	1.991(7)
Mo - N(2)	1.976(3)	1.996(9)	2.012(7)
Mo - N(3)	1.976(3)	1.973(10)	1.987(7)
Mo - N(4)	2.185(5)	2.304(9)	2.422(10)
Mo - N(1) - Si(1)	128.2(2)	128.0(5)	128.2(4)
Mo - N(2) - Si(2)	128.2(2)	129.1(5)	126.4(4)
Mo - N(3) - Si(3)	128.2(2)	127.1(5)	131.9(4)
N(1) - Mo - N(2)	117.7(1)	117.2(4)	116.3(3)
N(2) - Mo - N(3)	117.7(1)	117.6(4)	113.9(3)
N(1) - Mo - N(3)	117.7(1)	116.4(4)	116.1(3)
N(4) - Mo - N(1) - Si(1)	176.6[b]	162.4[b]	129.1[b]
N(4) - Mo - N(2) - Si(2)	176.6[b]	163.3[b]	131.3[b]
N(4) - Mo - N(3) - Si(3)	176.6[b]	160.0[b]	135.9[b]
N(1)-Mo-L_{ax}	98.8[b]	99.9(4)	105.8(3)
N(2)-Mo-L_{ax}	98.8[b]	99.3(4)	102.0(3)
N(3)-Mo-L_{ax}	98.8[b]	100.7(4)	99.6(3)
Mo - C(101) - C(102)			120.0(7)
Mo - C(101) - C(106)			116.9(7)

[a] See reference 17.

[b] Obtained from a Chem 3D model.

References begin on page 63.

Table 1.4. Crystallographic data, collection parameters, and refinement parameters for $[N_3N]Mo(CD_3)$ and $[N_3N]Mo$(cyclohexyl).

	$[N_3N]Mo(CD_3)$	$[N_3N]Mo$(cyclohexyl)
Empirical Formula	$C_{16}H_{39}D_3MoN_4Si_3$	$C_{21}H_{50}MoN_4Si_3$
Formula Weight	473.77	538.86
Diffractometer	Siemens SMART/CCD	Siemens SMART/CCD
Crystal Dimensions (mm)	$0.17 \times 0.12 \times 0.12$	$0.20 \times 0.11 \times 0.11$
Crystal System	Monoclinic	Hexagonal
a (Å)	17.35280 (10)	20.820 (6)
b (Å)	9.6851 (2)	20.820 (6)
c (Å)	15.9445 (3)	11.680 (5)
α (deg)	90	90
β (deg)	110.6210 (10)	90
γ (deg)	90	120
V (Å^3)	2508.00 (7)	4385 (3)
Space Group	Cc	$P6_3$
Z	4	6
D_{calc} (Mg/m^3)	1.255	1.224
F_{000}	1000	1728
λ (MoK_α)	0.71073 Å	0.71073 Å
Scan Type	ω	ω
Temperature (K)	183 (2)	183 (2)
θ Range for Data Collection (deg)	2.45 to 23.28	1.13 to 20.00
Independent Reflections	2412	2728
Absorption Correction	None	None
R [I > 2σ(I)]	0.0660	0.0569
R_W [I > 2σ(I)]	0.1096	0.1488
GoF	1.085	1.113
Extinction Coefficient	0.0003 (2)	0.0003 (2)
Largest Diff. Peak and Hole (eÅ^{-3})	0.720 and -0.800	0.653 and -0.421

References begin on page 63.

NMR Studies of Paramagnetic Molybdenum(IV) Alkyl Complexes

NMR spectra of $[N_3N]MoR$ species show broadened, shifted ligand resonances and temperature dependencies that are analogous to that observed for $[N_3N]MoCl$ (Figure 1.5). For example, the high field portion of the spectrum of $[N_3N]Mo(CH_3)$ that contains the ligand backbone methylene proton resonances is shown in Figure 1.9. As the temperature is lowered, the two ligand methylene resonances shift to higher field in a linear fashion versus 1/T (Figure 1.10). Values for $\Delta G^{\ddagger}$ for the C_{3v}/C_3 fluxional process that becomes slow on the NMR time scale at ca. -60 °C in $[N_3N]Mo(CH_3)$ can be calculated as described for $[N_3N]MoCl$; the values are 8.6 ± 0.2 kcal/mol and 8.2 ± 0.2 kcal/mol. These free energies of activation are close to those found for $[N_3N]MoCl$ at -20 and -30 °C (9.0 and 9.2 kcal/mol). Therefore, it does not appear that activation energies for the C_{3v}/C_3 fluxional processes in different compounds in this general family of $[N_3N]Mo$ complexes differ dramatically.

So far we have been unable to observe an α-proton resonance in any $[N_3N]MoR$ complex. In order to be certain that we did not overlook an α-proton resonance, we searched for a ^2H resonance in $[N_3N]Mo(CD_3)$ between 400 and -400 ppm. ^2H NMR was chosen because resonances in ^2H NMR spectra of paramagnetic compounds are often significantly narrower, and therefore more readily observed, than those in ^1H NMR spectra of paramagnetic complexes.[20] Despite this theoretical advantage, we could observe no ^2H resonance that could be ascribed to the CD_3 group in $[N_3N]Mo(CD_3)$, even after hours of collection time at 76.7 MHz (500 MHz ^1H). We conclude that the CD_3 group in $[N_3N]Mo(CD_3)$ is either outside the 400 to -400 ppm region, or it is too broad to be observed, or both. In no other $[N_3N]Mo$(alkyl) species discussed here have we been able to observe any ^1H or ^2H resonance for protons or deuterons attached to a carbon directly bound to Mo.

Resonances for protons on the β-carbon of an alkyl ligand can be observed, however. For example, the ^1H NMR spectrum of $[N_3N]Mo(CH_2CH_3)$ shows a broad resonance at -51.5 ppm (at 22 °C) in addition to resonances which can be ascribed to the TMS groups and ligand

References begin on page 63.

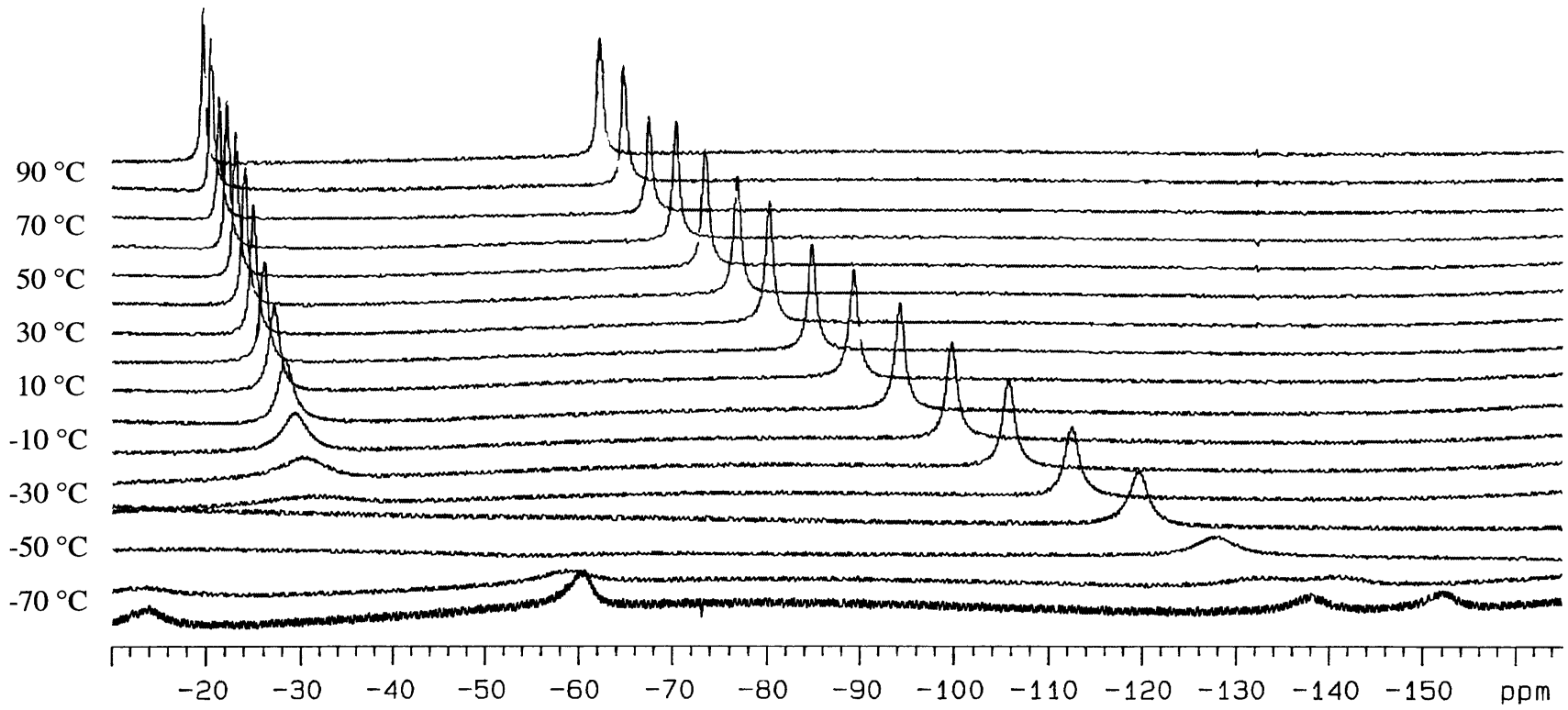

Figure 1.9. VT 500 MHz ^{1}H NMR spectra of [(TMSNCH_2CH_2)$_3$N]MoMe in toluene-d_8

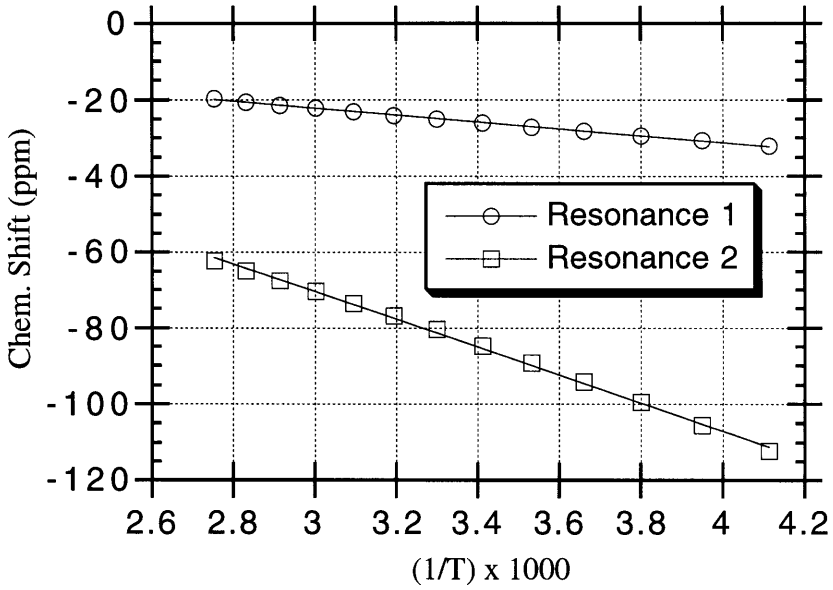

Figure 1.10. A plot of the chemical shift of the methylene backbone resonances versus 1/T for $[N_3N]MoMe$.

backbone methylene protons as described earlier for $[N_3N]MoCl$ and $[N_3N]MoMe$. Ligand backbone methylene resonances can be assigned since they split into two resonances at temperatures where the C_3/C_{3v} fluxional process becomes slow on the NMR time scale. β Proton resonances in other alkyl complexes (see below) are also typically found in the -50 to -60 ppm range. The chemical shift of the β proton resonance is temperature dependent as expected for a Curie-Weiss paramagnetic species (moving to higher field at lower temperatures).

The variable temperature ^1H NMR spectrum of $[N_3N]Mo(CH_2CH_2CH_2CH_3)$ between 60 and -60 °C shows, in addition to the TMS and ligand backbone methylene resonances, three resonances (at 22 °C) at -48, 2.9, and 5.4 ppm. The resonance at -48 ppm can be assigned to the β methylene protons, while the resonances at 2.9 and 5.4 ppm can be assigned to the γ and δ proton resonances, or vice versa. The only temperature dependent processes observed in the range 60 to -60 °C are the Curie-Weiss 1/T chemical shift dependences and slowing of the interconversion between Δ and Λ C_3-symmetric conformers at low temperatures.

References begin on page 63.

The ^{1}H NMR spectrum of [N_3N]Mo(cyclopentyl) shows four broadened and shifted resonances for the cyclopentyl ligand protons at 21.3, 15.6, -48.2, and -58.3 ppm at 22 °C (Figure 1.11). On the basis of chemical shift the resonances at 21.3 and 15.6 ppm can be ascribed to exo and endo γ protons (without specifying which is which), with endo protons being defined as those on the same side of the ring as the metal. Those resonances at -48.2 and -58.3 ppm can be assigned to exo and endo β protons (again without being able to specify which is endo and which is exo). The H_α resonance is not observable, and at low temperatures the ligand backbone becomes locked in one C_3-symmetric conformation, just as in all [N_3N]MoX complexes examined.

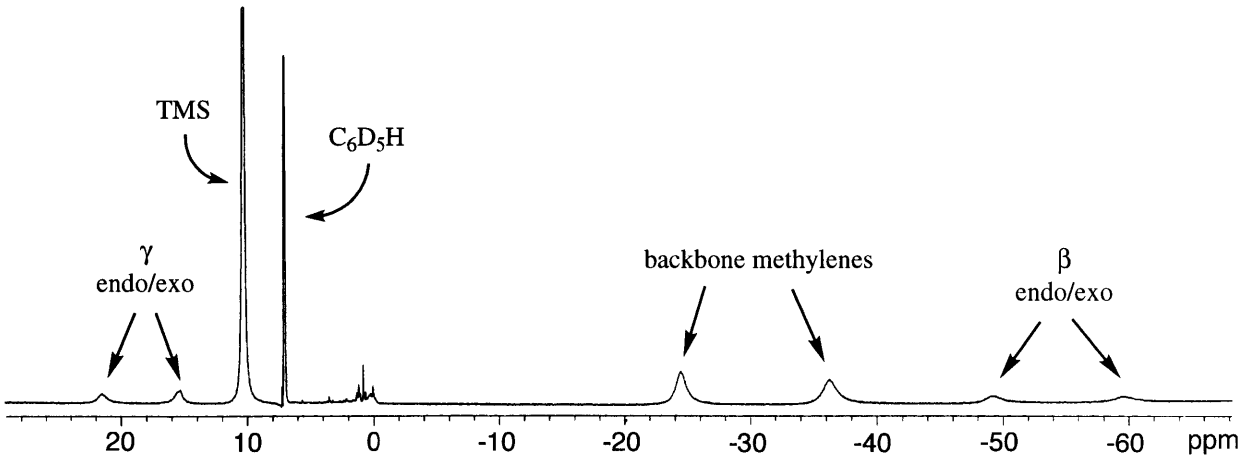

Figure 1.11. 500 MHz ^{1}H NMR spectrum of [N_3N]Mo(cyclopentyl) at 22 °C.

The ^{2}H NMR spectrum of [N_3N]Mo(C_5H_8D), prepared by reacting 1-deuterocyclopentyl-lithium with [N_3N]MoCl for 3 h at room temperature (Figure 1.12), displaced *four* broad resonances for $^2H_{\gamma,exo}$ and $^2H_{\gamma,endo}$ (or vice versa) and $^2H_{\beta,exo}$ and $^2H_{\beta,endo}$ (or vice versa) at the same chemical shifts (at a given temperature) as found in the ^{1}H NMR spectrum of [N_3N]Mo(cyclopentyl) (Figure 1.11). They are best observed when the sample is cooled to 0 °C for reasons that will be discussed below. These data confirm that the deuterium atom has washed into all exo and endo β and γ cyclopentyl positions. We cannot determine if deuterium is also

References begin on page 63.

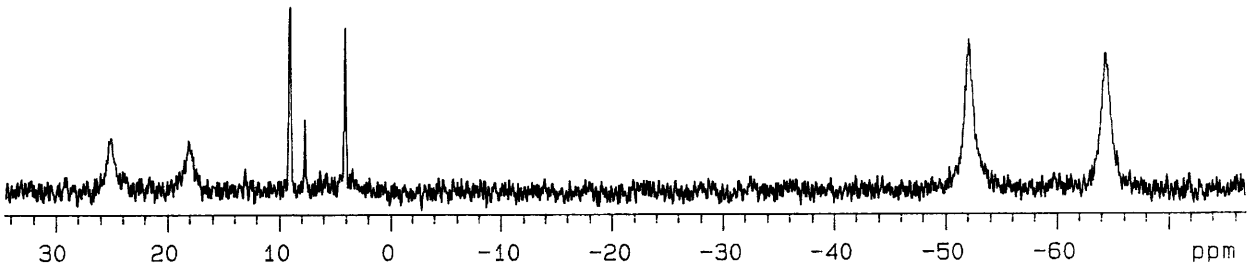

Figure 1.12. 76.7 MHz ^{2}H NMR spectrum of [N_3N]Mo(cyclopentyl-d_1) acquired at 0 °C.

present at the α-carbon, since this resonance is unobservable. When [N_3N]Mo(1-deuterocyclopentyl) was prepared by adding 1-deuterocyclopentyllithium to [N_3N]MoCl at -20 °C in a sealed NMR tube and the reaction monitored by ^{2}H NMR, the results shown in Figure 1.13 were obtained. Initially only a resonance for the deuterium in 1-deuterocyclopentyllithium was observed at 0.6 ppm. (Alkylation is relatively slow at -20 °C in toluene.) The sample was then warmed for brief periods to 22 °C and cooled to -20 °C in order to record the ^{2}H NMR spectrum. After a total of ~10 minutes at 22 °C all 1-deuterocyclopentyllithium had been consumed. However, at this stage only weak ^{2}H$_\beta$ resonances were observed (at -20 °C) at -58 and -72 ppm. No γ resonances were observed near 20 ppm. The intensity of the β resonances increased with time, reaching a maximum after the sample had stood for a total for 1-2 hours at room temperature. After 2 hours some γ deuteron intensity was observed near 20 ppm. After 24 hours the spectrum clearly revealed resonances at 18 and 27 ppm (at -20 °C) for ^{2}H in γ positions (Figure 1.13). The resonances at 18 and 27 ppm are slightly less intense than those at -58 and -72 ppm, probably as a consequence of the rapidly decreasing rate of incorporation into γ positions for statistical reasons (only one deuteron total is present). The γ resonances in the sample whose ^{2}H NMR spectrum is shown in Figure 1.12 are also less intense than the β resonances, as this sample was kept at 22 °C for only ~4 hours. Therefore we can say confidently that the α-deuteron initially present in [N_3N]Mo(1-*d*-cyclopentyl) washes into the β,exo *and* β,endo positions of the cyclopentyl ring before it washes into the γ,exo and γ,endo positions.

References begin on page 63.

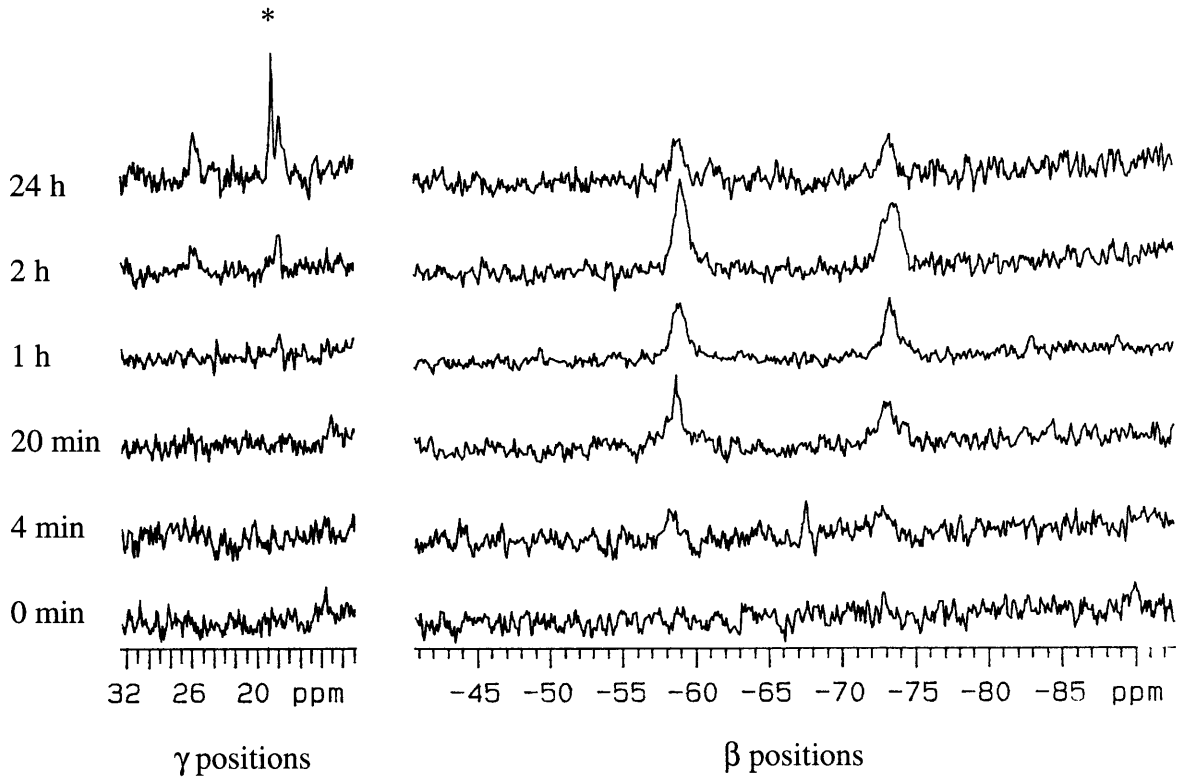

Figure 1.13. 46.0 MHz ^{2}H NMR spectra (at -20 °C) of [N_3N]Mo(cyclopentyl-d_1) as a function of time the sample was kept at 22 °C. (* a resonance due to naturally-abundant deuterium in the TMS group of [N_3N]MoH, a decomposition product, see text.)

The mechanism by which deuterium appears on a β carbon in an *exo* position is proposed to be the well-known β-hydride elimination reaction, followed by an insertion of the olefin into the Mo-H bond (equation 1). Subsequent β-hydride elimination/olefin insertion would yield the

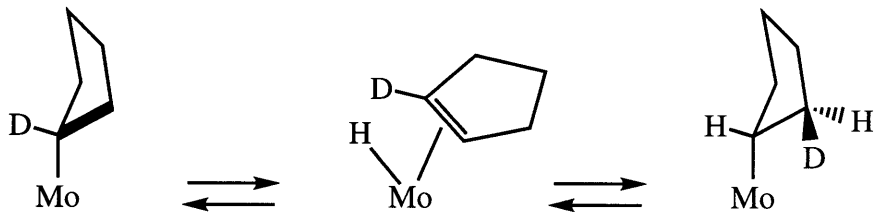

(1)

species in which deuterium appears on a γ carbon in an *exo* position (equation 2). If *only* β-hydride elimination were taking place, deuterium would appear *only* in exo positions. Therefore another faster process must interconvert exo and endo protons on β and γ carbons (see below).

References begin on page 63.

We can estimate from Figure 1.13 that scrambling of a deuteron from the α-carbon to the β-carbons (in both exo and endo positions) is complete (~5 half-lives) in 60-120 minutes. Therefore the half-life for appearance of deuterium in a β position is between 12 and 24 minutes at 22 °C or $k_\beta \approx 5 \times 10^{-4}$ sec^{-1} to 10^{-3} sec^{-1}. No significant cyclopentene is lost from the cyclopentene hydride intermediate under these conditions. It has been shown that at 66 °C $\tau_{1/2}$ = 17 min for cyclopentene elimination.[12] At equilibrium 1/9 of one deuterium should be found at each of the nine cyclopentyl positions, ignoring any equilibrium isotope effects, and assuming that deuterium is scrambled relatively rapidly between exo and endo positions by some other process.

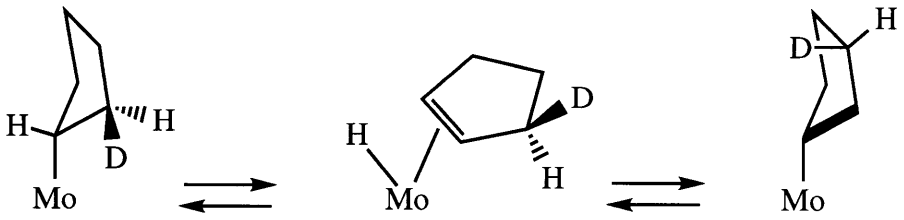

(2)

^{2}H NMR spectra of [N_3N]Mo(1-*d*-cyclopentyl) from 0 to 50 °C (Figure 1.14) reveal that deuterium present in the exo and endo sites equilibrates rapidly on the NMR time scale at the higher temperatures, where decomposition to give [N_3N]MoH (see later) is still slow. As the sample is warmed, the four broad resonances coalesce to two average resonances. Resonances also shift towards the diamagnetic region of the spectrum as a consequence of the Curie-Weiss 1/(T + θ) susceptibility dependence. Both of these temperature-dependent processes are entirely reversible. (The sharp resonances between 4 and 9 ppm in Figure 1.14 are due to naturally abundant deuterium in the toluene solvent and the small amount of cyclopentene-d_1 formed upon decomposition of [N_3N]Mo(cyclopentyl-d_1) at the higher temperatures.) This fluxional process cannot be observed unambiguously by ^{1}H NMR for several reasons, among them the factor of 6.5 difference between ^{1}H and ^{2}H frequencies at a given field strength. Note that the fluxional process that leads to interconversion of exo and endo deuterons *cannot involve any α-deuterium*

References begin on page 63.

in the averaging process. If $^2H_\alpha$ were scrambling rapidly with $^2H_\gamma$ or $^2H_\beta$, then the resulting average resonances either would be shifted significantly, or decreased in intensity dramatically, or both. Since such dramatic changes are not observed, we conclude that $^2H_{\beta,exo}$ averages with $^2H_{\beta,endo}$ and $^2H_{\gamma,exo}$ averages with $^2H_{\gamma,endo}$ as the temperature is raised. The fluxional process is not consistent with any slowed rotation of the cyclopentyl ring within the trigonal pocket, as the backbone still has pseudo-C_{3v} symmetry at 0 °C by ^1H NMR, a temperature where the cyclopentyl ^2H exo and endo resonances are resolved.

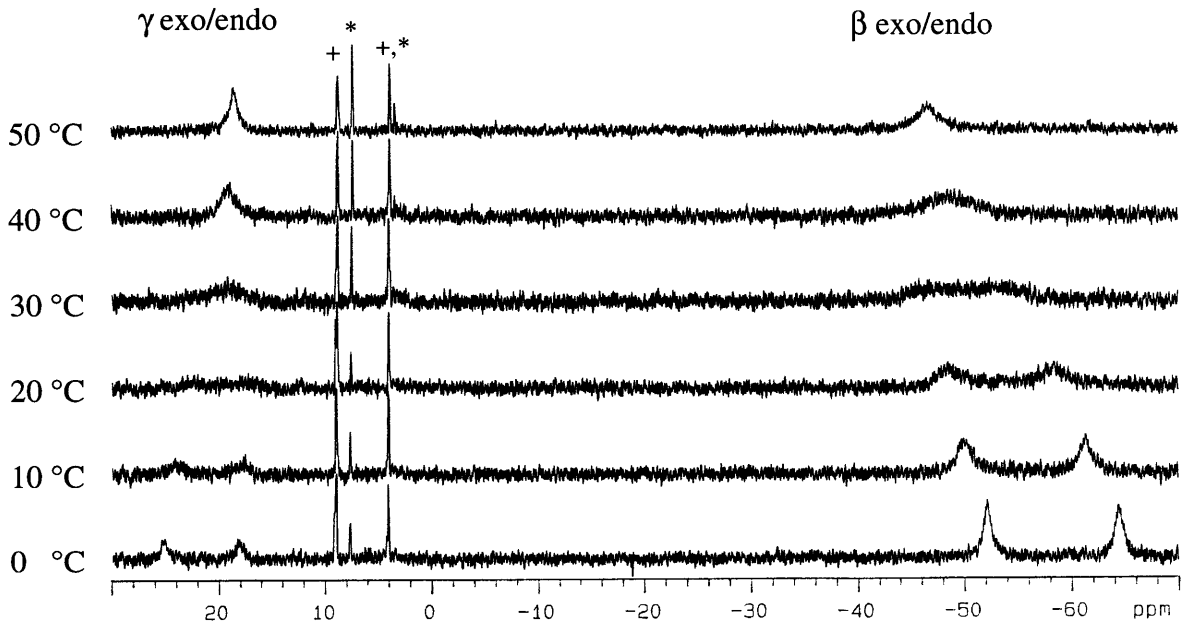

Figure 1.14. VT 76.7 MHz ^2H NMR spectra of $[N_3N]Mo(C_5H_8D)$.

+ Resonances due to residual deuterium in the toluene. * Resonances due to cyclopentene-d_1.

We propose that the fluxional process that leads to averaging of exo and endo deuterium on C_β and exo and endo deuterium on C_γ consists of *a rapid and reversible α-elimination* to give an intermediate $[N_3N]$Mo(cyclopentylidene)(H) complex (equation 3). This unusual proposal is sensible in view of the fact that an attempt to prepare $[N_3N]$W(cyclopentyl) yielded crystallographically characterized $[N_3N]$W(cyclopentylidene)(H) instead[9] (see chapter II). The

References begin on page 63.

rate constant for α-elimination (k_α) at 22 °C can be estimated to be 10^3 sec^{-1} from the NMR experiments shown in Figure 1.14. The half-life for β-elimination can be estimated to be between 12 (thus k_β would equal 5×10^{-4} sec^{-1}) and 24 (thus k_β would equal 10^{-3} sec^{-1}) minutes at 22 °C (see above). Therefore we can say that the rate constant for α-elimination *is at least six orders of magnitude larger* than the rate constant for β-elimination at room temperature, i.e., $k_\alpha > 10^6 k_\beta$ (equation 3). (An accurate comparison of the rate constants for α- and β-elimination per C-H bond would have to include a factor of two since there are two endo β protons and only one α proton present, but we need not consider that adjustment here in view of the magnitude of the rate differences in question.) We assume that [N_3N]Mo(cyclopentylidene)(H), like [N_3N]W(cyclopentylidene)(H),[9] is diamagnetic, and that [N_3N]Mo(cyclopentene)(H) also would be diamagnetic. There is no evidence that suggests that any significant amount of either is

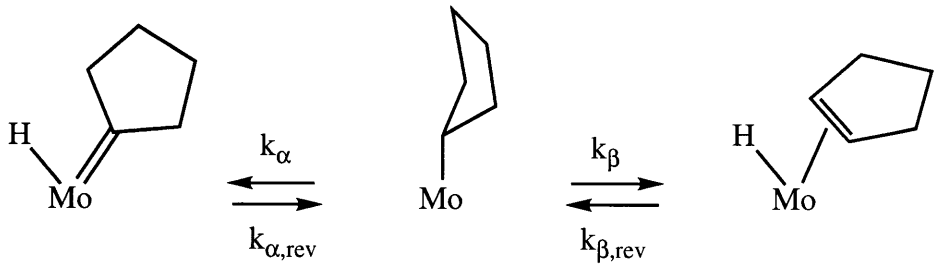

(3)

present, i.e., the equilibria for both α- and β-elimination lie well toward [N_3N]Mo(cyclopentyl). If we assume that the equilibrium constants for forming [N_3N]Mo(cyclopentyl) ($k_{\alpha,rev}/k_\alpha$ and $k_{\beta,rev}/k_\beta$) are both ~10^2 or greater, then $k_{\beta,rev} \approx 10^{-1}$ sec^{-1} (or greater) and $k_{\alpha,rev} \approx 10^5$ sec^{-1} (or greater). An alternative explanation of the phenomenon of interconversion of exo and endo cyclopentyl protons involves C-C bond cleavage and formation of a 1-molybdacyclohexene complex that has C_s symmetry, but rapid and reversible C-C bond cleavage would seem to be much less likely than rapid and reversible C-H bond cleavage. (See results and discussion below.) It should be noted that a significant primary H/D kinetic isotope effect might be expected for an α-elimination process,[21] but since only one ^2H is present among eight ^1H nuclei

References begin on page 63.

in the sample whose ^2H NMR spectrum is shown in Figure 1.14, we are most likely observing a virtually pure α-hydrogen elimination in this case.

The ^1H NMR spectrum of $[N_3N]$Mo(cyclohexyl) shows six resonances for the cyclohexyl ring exo and endo protons that average upon heating the sample. $[N_3N]$Mo(cyclohexyl) is more stable than $[N_3N]$Mo(cyclopentyl), so it is possible to heat it to higher temperatures before decomposition to $[N_3N]$MoH and cyclohexene occurs (see below). Nevertheless, resonances for $[N_3N]$MoH complicate this study, as does the TMS resonance of $[N_3N]$Mo(cyclohexyl). We assign the resonances at 15.8 and 6.1 ppm to exo and endo γ protons, those at 1.9 and -2.0 ppm to exo and endo δ protons, and those at -40.9 and -49.9 ppm to exo and endo β protons. Interference by other resonances and the breadth of the cyclohexyl β, γ, and δ resonances in the proton NMR spectrum of $[N_3N]$Mo(cyclohexyl) make these results less convincing than those for $[N_3N]$Mo(cyclopentyl-d_1). Nevertheless, we can observe coalescence of the δ proton resonances at 64 ± 2 °C and the β resonances at ~100 °C (less accurately and not shown). Unfortunately, the γ resonances coalesce under the broad resonance for the TMS group in $[N_3N]$Mo(cyclohexyl) at ~10 ppm. From coalescence of exo and endo δ protons we can obtain an approximate value for $k_{\alpha,C6}$ (2×10^3 s^{-1}) at 64 °C. This value should be compared with the value for k_α in the cyclopentyl complex, $k_{\alpha,C5} \approx 10^3$ s^{-1} at 22 °C. At 64 °C, $k_{\alpha,C5}$ perhaps would be ~16×10^3, or approximately eight times larger than $k_{\alpha,C6}$. (A second estimate at a different temperature is made below using another approach.) Note that in the cyclohexyl case it is possible to distinguish a rapid α-elimination from a rapid β-elimination on the basis of the number of averaged ring resonances alone (three ideally), regardless of assignment.

The ^2H NMR spectrum of $[N_3N]$Mo(C_6D_{11}) at 46.0 MHz is shown in Figure 1.15. The expected six C_6D_{11} resonances in the ratio of 2(γ):2(γ):1(δ):1(δ):2(β):2(β) are observed at 10 °C. Upon heating the sample these resonances broaden and coalesce pair-wise. The coalescence temperature varies for each set of resonances as a consequence of the different chemical shift difference between the respective exo and endo ^2H resonances [$\Delta\nu(\gamma) > \Delta\nu(\beta) > \Delta\nu(\delta)$] . Since a

References begin on page 63.

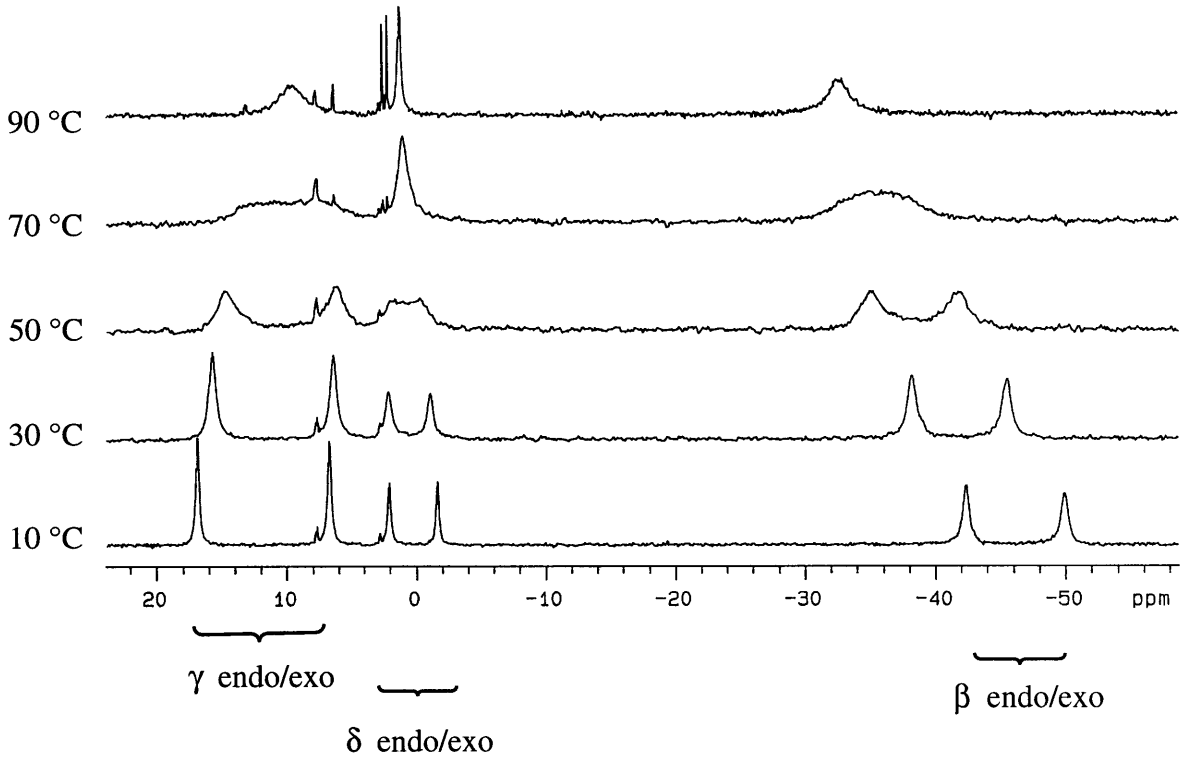

Figure 1.15. 46.0 MHz VT ^{2}H NMR spectra of [N_3N]Mo(cyclohexyl-d_{11}).

single physical process (α-elimination) is responsible for all three coalescence phenomena, we can obtain a rate for that process at three different temperatures from the spectra shown in Figure 1.15. The results for a ~0.1 M sample in toluene are k_α = 378 sec^{-1} at 324 K, 755 sec^{-1} at 339 K, and 955 sec^{-1} at 343 K. By performing a similar experiment at 76.7 MHz with a ~0.1 M sample three additional points were obtained: k_α = 606 sec^{-1} at 331 K, 1273 sec^{-1} at 346 K, and 1555 sec^{-1} at 352 K. Virtually identical values were obtained for a sample that was half the concentration (~0.05 M). A plot of ln(k/T) versus 1/T for these six points gave $\Delta H^\ddagger$ = 11 ± 1 kcal mol^{-1} and $\Delta S^\ddagger$ = -14 ± 3 e.u. (exact values may be found in the Experimental Section). The rate constant for α-elimination in [N_3N]Mo(C_6H_{11}) at 337 K was found to be 2155 sec^{-1} (see

References begin on page 63.

above). Since the rate of α-elimination in $[N_3N]Mo(C_6D_{11})$ at 337 K can be calculated to be 696 sec^{-1} from the Eyring plot, k_H/k_D for α elimination at 337 K is 3.1 ± 0.3. Observation of a substantial isotope effect confirms that a C-H bond cleavage is involved in the process that gives rise to interconversion of exo and endo protons, and therefore rules out a possible, if implausible, alternative equilibration by C-C bond cleavage and formation of a metallacycloheptene ring. We also can compare the rate constant for α-elimination at 22 °C for $[N_3N]Mo(C_6D_{11})$ (calculated to be ~64 sec^{-1}) and $[N_3N]Mo(C_5H_9)$ (estimated to be ~1000 sec^{-1}). The k_α at 22 °C for $[N_3N]Mo(C_6H_{11})$ should be ~200 sec^{-1} on the basis of $k_H/k_D \approx 3$. Thus, the rate of α-elimination in $[N_3N]Mo(C_5H_9)$ is approximately five times faster than the rate of α-elimination in $[N_3N]Mo(C_6H_{11})$ at 22 °C (cf. the estimate of eight times faster at 64 °C above).

Both $[N_3N]$Mo(cyclobutyl) and $[N_3N]$Mo(cyclopropyl) have also been studied by VT ^1H NMR in order to determine if a similar rapid α-elimination process is occurring. The endo and exo β protons in the cyclopropyl complex are separated by > 110 ppm. If a reversible α-elimination process was taking place, the large peak separation would require too high of a temperature in order to observe coalescence, since the cyclopropyl complex decomposes to $[N_3N]Mo{\equiv}CH$ with a half-life of ~1 h at 50 °C.[12] In $[N_3N]$Mo(cyclobutyl), endo and exo β protons are separated by > 70 ppm, a margin which is again too large to observe any coalescence before the molecule decomposes to $[N_3N]Mo{\equiv}CH_2CH_2CH_2CH_3$ ($\tau_{1/2}$ for this process = 23 min at 60 °C).[12] Endo and exo γ protons in the cyclobutyl complex are too broad and too close together to evaluate whether they coalesce. As the sample is warmed, the γ resonances simply shift to give one broad resonance, presumably as a result of Curie-Weiss $1/(\theta + T)$ dependence. Therefore we cannot confirm or exclude a reversible α-elimination process in $[N_3N]$Mo(cyclopropyl) or $[N_3N]$Mo(cyclobutyl).

Thermolysis of $[N_3N]$MoX Complexes

Thermolysis of several $[N_3N]Mo(CH_2R)$ complexes leads to formation of $[N_3N]Mo{\equiv}CR$ complexes with loss of molecular hydrogen (equation 4).[12] The reaction is fastest when R =

References begin on page 63.

CMe_3, but can also be observed when R = $SiMe_3$, Ph, or *n*-propyl. This decomposition is analogous to the faster and better documented decompositions of tungsten complexes of this type.[8] It is proposed that $[N_3N]Mo(CH_2R)$ is converted into $[N_3N]Mo(H)(CHR)$, and that dihydrogen is lost from $[N_3N]Mo(H)(CHR)$ by a type of "α-hydrogen abstraction" reaction

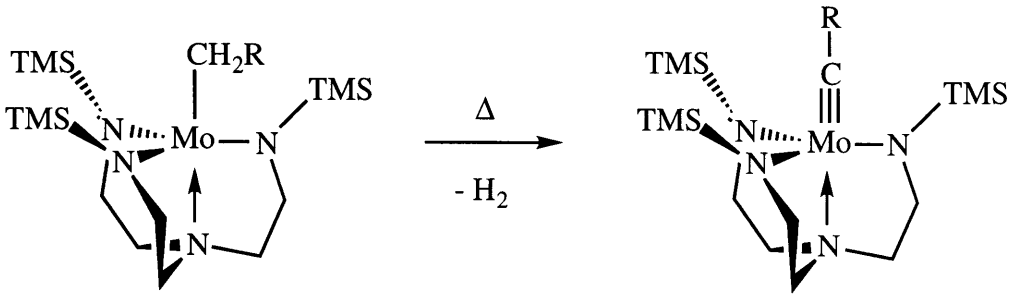

(4)

(equation 5).[21] We have shown that the rates of forming a cyclopentylidene hydride from $[N_3N]Mo$(cyclopentyl) and a cyclohexylidene hydride from $[N_3N]Mo$(cyclohexyl) can be relatively fast. Since the difference between the rates of α-elimination in $[N_3N]Mo$(cyclopentyl) and $[N_3N]Mo$(cyclohexyl) is already significant (ca. one order of magnitude), we suspect that the rates of forming $[N_3N]Mo(H)(CHR)$ complexes from various $[N_3N]Mo(CH_2R)$ complexes will also differ dramatically (see discussion section).

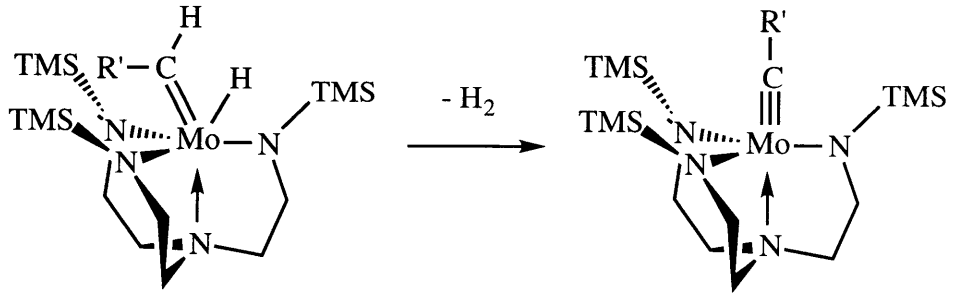

(5)

The thermolysis of $[N_3N]Mo(CH_2CH_2CH_2CH_3)$ warranted further study, since $[N_3N]MoH$ (the ultimate product of a β-hydride elimination/olefin loss reaction sequence) is formed in significant amounts as well as $[N_3N]Mo{\equiv}CCH_2CH_2CH_3$. It seems that the rates of

References begin on page 63.

α,α-dehydrogenation (equation 5) and β-hydride elimination followed by loss of olefin (equation 6) are competitive in this case. When $[N_3N]Mo(^{13}CH_2CH_2CH_2CH_3)$ is heated to 80 °C for 6 days, 90% of the labeled product is 1-butene, with a 6 : 1 ratio of $H_2{}^{13}C{=}CHCH_2CH_3$ and $H_2C{=}CHCH_2{}^{13}CH_3$. The remaining 10% is a 10 : 1 mixture of $[N_3N]Mo(^{13}CH_2CH_2CH_2CH_3)$

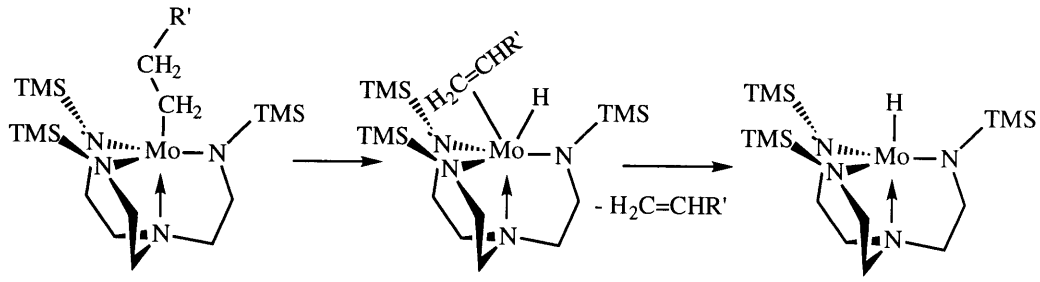

(6)

and $[N_3N]Mo(CH_2CH_2CH_2{}^{13}CH_3)$. This is the result expected if the metal cannot easily "walk" to the other end of the butyl chain (by forming $[N_3N]Mo$(sec-butyl) and $[N_3N]Mo$(2-butene)(H) intermediates) before 1-butene is lost. If an isomerization of this type *were* rapid relative to the rate of loss of 1-butene, then a 1:1 mixture of $^{13}CH_2{=}CHCH_2CH_3$ and $CH_2{=}CHCH_2{}^{13}CH_3$ would be obtained. Formation of mainly $[N_3N]Mo{\equiv}{}^{13}CCH_2CH_2CH_3$ is also consistent with no $[N_3N]Mo(CH_2CH_2CH_2{}^{13}CH_3)$ being formed before the α,α-dehydrogenation.

Upon heating a solution of the cyclopentyl complex, cyclopentene is lost and yellow, paramagnetic $[N_3N]MoH$ (equation 7) is formed quantitatively, according to NMR spectra. It

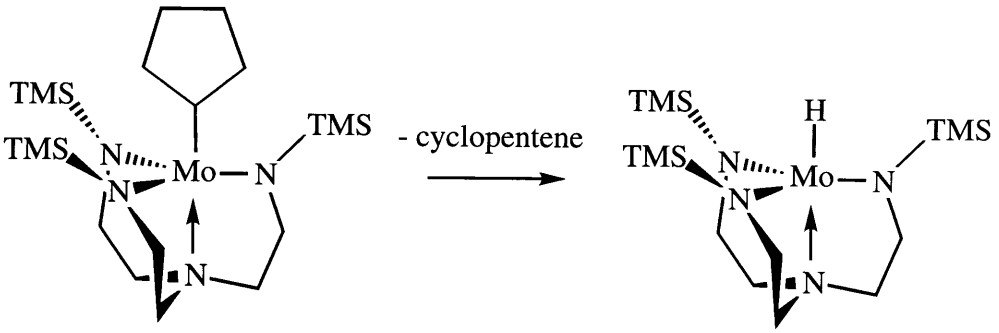

(7)

can be isolated in 65% yield on a scale of 1 mmol. Evidence for irreversible cyclopentene loss is provided by the following experiment. When $[N_3N]MoD^{12}$ is dissolved in neat cyclopentene

References begin on page 63.

and the solution is heated to 50 °C for 18 h, no deuterium is incorporated into the cyclopentene solvent, as can be sensitively ascertained by ^2H NMR.

$[N_3N]Mo(cyclohexyl)$ also decomposes cleanly to give $[N_3N]MoH$, as determined by ^1H NMR and by monitoring the reaction in toluene by UV/Vis at 562 nm. The first order conversion of $[N_3N]Mo(cyclohexyl)$ into $[N_3N]MoH$ was followed at five temperatures between 323 and 363 K, and the values of $\Delta H^{\ddagger}$ and $\Delta S^{\ddagger}$ from an Eyring plot (Figure 1.16) are 24.5 (2) kcal mol^{-1} and -5 (1) e.u. Plots of ln $[(A - A_\infty)/(A_0 - A_\infty)]$ versus T at the five different temperatures are shown in Figure 1.17. The decomposition of $[N_3N]Mo(cyclohexyl)$ is ~10 times slower than that of $[N_3N]Mo(cyclopentyl)$.[12] (At 298 K the rate constants are calculated to be 4.7 x 10^{-7} sec^{-1} for $[N_3N]Mo(cyclohexyl)$ and 6.2 x 10^{-6} sec^{-1} for $[N_3N]Mo(cyclopentyl)$.) At 343 K $[N_3N]Mo(C_6D_{11})$ was found to decompose with k = 3.0 x 10^{-5} and 3.3 x 10^{-5} sec^{-1}. Rate constants were independent of concentration over a fivefold range. Since the rate constant for decomposition of $[N_3N]Mo(C_6H_{11})$ at 343 K is calculated to be 12.3 x 10^{-5} s^{-1}, the isotope effect at that temperature is 3.9 (2). A deuterium isotope effect of this magnitude is consistent C-H bond cleavage in the transition state.

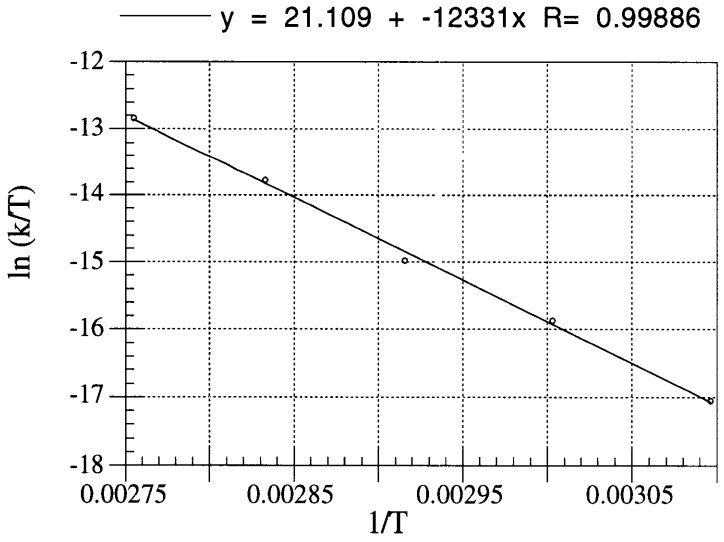

Figure 1.16. An Eyring plot for the decomposition of $[N_3N]Mo(cyclohexyl)$ from 323 to 363 K.

References begin on page 63.

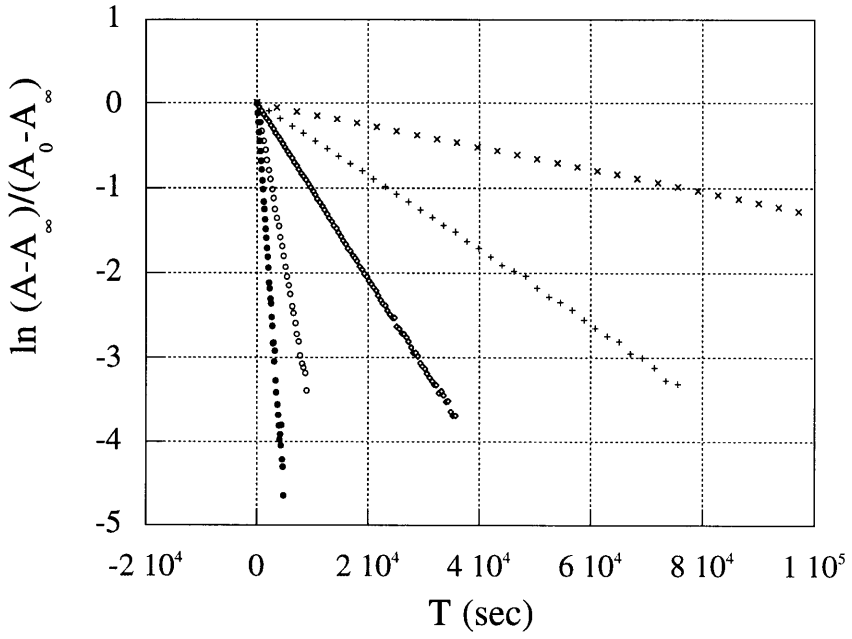

Figure 1.17. First-order kinetic plots for the decomposition of [N_3N]Mo(cyclohexyl).

At 100 °C [N_3N]MoH begins to evolve dihydrogen to give the paramagnetic "[bitN_3N]Mo" complex[12] shown in equation 8. When [N_3N]MoH is heated to 105 °C in toluene-d_8 in an evacuated, sealed NMR tube, a 50/50 mixture of [N_3N]MoH and [bitN_3N] is observed

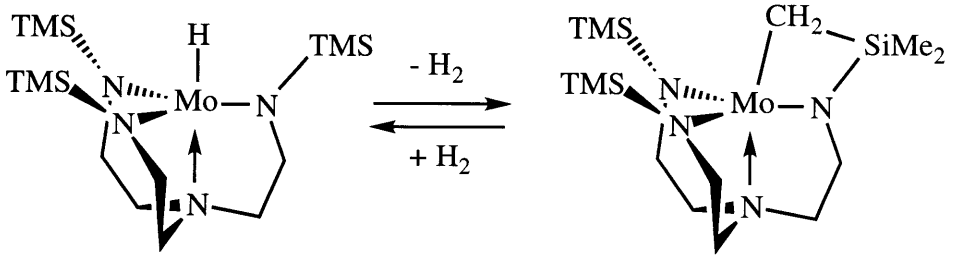

(8)

after 22 h. Removal of the H_2 from this solution and further heating for another 22 h yields a 70/30 mixture of [bitN_3N] and [N_3N]MoH. Heating for another 24 h gave a 80/20 mixture. [bitN_3N]Mo reacts with D_2 slowly to give largely [N_3N]MoD in which a second deuterium is

References begin on page 63.

located in a TMS group,[12] thereby confirming that loss of hydrogen (equation 8) is reversible. However, both loss of hydrogen from $[N_3N]MoH$ and reaction of $[bitN_3N]Mo$ with hydrogen are relatively slow. $[bitN_3N]Mo$ is not formed upon heating $[N_3N]MoR$ complexes that are relatively stable toward decomposition by other pathways. For example, $[N_3N]MoPh$ is quite stable thermally (decomposition is slow at 120 °C), and there is no evidence that $[bitN_3N]Mo$ forms over a period of 24 h at 120 °C. Likewise, no $[bitN_3N]Mo$ is formed when $[N_3N]MoMe$ decomposes.

DISCUSSION

The β-hydride elimination reaction has been a predominant mode of decomposition for transition metal alkyls, especially compared to an α-elimination to give an alkylidene hydride.[22] Evidence for an equilibrium between an alkyl complex and alkylidene hydride has usually involved high oxidation state tungsten[23-25] or tantalum[26-30] alkyl complexes. In the Cp^*_2Ta system observable $Cp^*_2Ta(CH_2)(H)$ was found to be in equilibrium with unobservable $Cp^*_2Ta(CH_3)$.[29] It was also shown that $Cp^*_2(H)Ta{=}C{=}CH_2$ decomposed via intermediate $Cp^*(\eta^5\text{-}C_5Me_4CH_2CH_2CH_2)Ta$ to the kinetic product, $Cp^*(\eta^5\text{-}C_5Me_4CH_2CH_2CH)Ta(H)$, by α-elimination, and to the thermodynamic product, $Cp^*(\eta^5\text{-}C_5Me_4CH_2\text{-}\eta^2\text{-}CH{=}CH_2)Ta(H)$, by β-elimination.[30] It was noted that "the rate of α-H elimination is 10^8 times greater than the rate of β-H elimination" in this circumstance. However, it was also noted that "...the generality of faster α-H elimination versus β-H elimination is questionable, since the transition state for β-H elimination in this system is highly strained, whereas that for α-H elimination is much less so." Finally, it was argued that "for a general alkyl ligand in the permethyltantalocene system, α-H elimination cannot be kinetically favored over β-H elimination by more than...a factor of ~30 in rate at 25 °C." Similar statements could be made about many of the alkyl complexes reported here, although the validity and generality of such statements are limited by the experimental data available. It is generally assumed that an agostic interaction[19] between the metal and the α- or β-

References begin on page 63.

hydrogen is on the pathway for α- or β-elimination, respectively, even though definitive evidence for α-agostic interactions is still sparse.[18]

α-Abstraction in a dialkyl complex (to give alkane and an alkylidene complex)[21] is closely related to α-elimination, and an α-agostic activation of an α-proton in one of the alkyls is thought to precede α-abstraction. It has long been known that neopentyl complexes are most prone to α-abstraction, with trimethylsilylmethyl, benzyl, and especially methyl being progressively less so.[21] It was also noted in early studies that α-abstraction is faster in sterically crowded environments, e.g., when additional ligands coordinate to the metal.[21] Recently it has been shown that α-abstraction and β-abstraction can compete in $[(Me_3SiNCH_2CH_2N)_3N]Ta$ dialkyl species,[31] that the rate of α-abstraction can be enhanced by increasing the size of the alkyls in the apical "pocket,"[32] and that α-abstraction to give an alkylidene can be forced to be virtually the only sterically tenable process by increasing the size of the silyl substituent in $[(R_3SiNCH_2CH_2N)_3N]Ta(alkyl)_2$ species from R = Me to R = Et. In a more crowded "pocket," the β-agostic interaction that precedes β-abstraction in the alkyl becomes sterically disfavored, while the α-agostic interaction that precedes α-abstraction at the same time is encouraged.

The preceding discussion would suggest that α-processes (abstraction or elimination) can be dramatically accelerated *at the expense of* β-processes (abstraction or elimination), and that steric (or "conformational") factors play a key role in determining the relative rates of α- versus β-processes in a given complex. Therefore, it is becoming increasingly clear that broad statements concerning the relative rates of α- versus β-processes simply cannot be justified, even for a given metal with the same ligand coordination sphere. Nevertheless, it seems relatively safe to say that competition between α-and β-processes will continue to be found among the earlier, heavier metals (Ta, Mo, W, Re) where multiple metal-carbon bonds (alkylidenes and alkylidynes) are relatively common.[21] Whether α-elimination is faster than β-elimination for later metals (e.g., iridium[33]) has yet to be investigated thoroughly.

We have observed that α-elimination is fast relative to β-elimination in two $[N_3N]Mo$(cycloalkyl) systems, even though no alkylidene hydride complex is observed in either

References begin on page 63.

case. To our knowledge any consequence of rapid and reversible α-elimination has never been observed *directly* before, perhaps largely because no net change in the alkyl itself occurs. Rapid α-elimination could be documented here in part because of the paramagnetic nature of the [N_3N]Mo(cycloalkyl) complexes and the resulting dispersion of all cycloalkyl resonances (including exo and endo resonances) in NMR spectra, a phenomenon that has proved useful in the coordination chemistry of paramagnetic coordination complexes for some time.[20] We suspect that α-elimination in some [N_3N]Mo(n-alkyl) complexes can also be "rapid" (e.g., 10^{-1} sec^{-1} or greater), but perhaps only when the Mo-C_α-C_β angle is opened up as a consequence of steric interactions (e.g., in [N_3N]Mo(neopentyl)). Unfortunately, we have not been able to devise a way to measure the rate of conversion of (e.g.) [N_3N]Mo(CH_2CMe_3) to [N_3N]Mo($CHCMe_3$)(H) in order to compare the rate of α-elimination with that found in [N_3N]Mo(cyclopentyl) and [N_3N]Mo(cyclohexyl). For alkyls in general the situation is complicated by competitive α-abstraction reaction (α,α-dehydrogenation) and β-hydride elimination processes. A plausible scenario is that the rate of α-elimination in [N_3N]Mo(CH_2CMe_3) could be of the same order of magnitude as it is in [N_3N]Mo(cyclopentyl) or [N_3N]Mo(cyclohexyl) (i.e., 10^2 to 10^3 sec^{-1} at 22 °C), but [N_3N]Mo≡$CCMe_3$ does not form readily because [N_3N]Mo($CHCMe_3$)(H) does not lose hydrogen rapidly enough to compete with the back reaction to reform [N_3N]Mo(CH_2CMe_3). Therefore a plausible explanation as to why other [N_3N]Mo(CH_2R) complexes decompose to [N_3N]Mo≡CR complexes progressively less readily as the size of R decreases is that the equilibrium between [N_3N]Mo(H)(CHR) and [N_3N]Mo(CH_2R) complexes becomes prohibitively large, i.e., virtually no [N_3N]Mo(H)(CHR) is present. The equilibrium between [N_3N]Mo(H)(CHR) and [N_3N]Mo(CH_2R) could become large either as a consequence of a precipitous drop in the rate of α-elimination, or as a consequence of a dramatic increase of the rate of forming an alkyl complex from an alkylidene hydride complex. If it is the former, then α-elimination could even become rate limiting in the reaction in which an alkylidyne complex is formed from an alkyl complex, e.g., hypothetical α,α-dehydrogenation in [N_3N]MoMe to form [N_3N]Mo≡CH. It is interesting to note that the

References begin on page 63.

overall relative ease of forming an alkylidyne complex via loss of H_2 from the alkyl (CH_2CMe_3 > CH_2SiMe_3 > CH_2Ph >> Me) is analogous to what has been observed qualitatively for α-hydrogen abstraction in tantalum dialkyl complexes to give alkylidene complexes.[21] Less data for formation of alkylidyne complexes from alkylidene complexes[34] by α-hydrogen abstraction is available, but it is in accord with a general trend toward more facile α-abstraction from bulkier alkylidenes.

The X-ray structures of the methyl and cyclohexyl $[N_3N]MoR$ species illustrate semi-quantitatively the differences in the degree of steric congestion within the trigonal pocket. These differences suggest that a greater rate of α-elimination *in part* could be traced to a relief of steric strain within the pocket. However, so many other factors must be taken into account that we can only in a very general sense feel secure in concluding that steric congestion increases the rate of α-elimination. In fact, the rate of α-elimination in the cyclohexyl complex is significantly *slower* than the rate of α-elimination in the cyclopentyl complex at 22 °C, even though one would expect steric congestion in the *ground* state of the cyclohexyl species to be *greater*. However, a greater degree of steric congestion in $[N_3N]$Mo(cyclohexylidene)(H) (versus $[N_3N]$Mo(cyclopentylidene)(H)) should oppose that trend and lead to a slower rate of α-elimination. Correlating the rates of β-elimination with steric congestion in either the ground state or in the olefin hydride intermediate species in these systems is also virtually impossible for similar reasons at this stage.

In contrast to the equilibria observed here, the equilibrium between $[N_3N]$W(cycloalkyl) and $[N_3N]$W(cycloalkylidene)(H) complexes has been observed to lie toward the latter for cyclopentyl[9] and cyclohexyl.[35] However, $[N_3N]WMe$ is observable.[8] These results are consistent with a substantially slower rate of α-elimination in the methyl complex and/or a relatively small equilibrium constant for forming $[N_3N]W(CH_2)(H)$. The observation of tungsten(VI) alkylidene hydride complexes, but molybdenum(IV) alkyl complexes, could be explained using oxidation state and/or bond strength arguments. The fact that α,α-dehydrogenation reactions in $[N_3N]W(CH_2R)$ complexes are orders of magnitude faster than in

References begin on page 63.

the analogous $[N_3N]Mo(CH_2R)$ complexes also could be explained in terms of a higher concentration of alkylidene hydride in a W system versus an analogous Mo system. A more detailed discussion and relevant results may be found in chapter II.

It may be worth pointing out that we have assumed throughout this work that the $[N_3N]$ ligand is not directly involved in proton migration reactions, i.e., a proton does not migrate from carbon to nitrogen to produce a $[(Me_3SiNCH_2CH_2)_2N(CH_2CH_2NHSiMe_3)]^{2-}$ ligand. However, such a ligand has been observed in the analogous C_6F_5-substituted ligand system.[36] Therefore the possibility of forming an intermediate via proton migration to an amido nitrogen (e.g., equation 9) must be considered. Unlike the α-elimination reaction, there is no change in oxidation state of the metal in such a reaction if we assume that the alkylidene is a dianion. A rapid process of this nature *could* explain interconversion of exo and endo protons in $[N_3N]$Mo(cyclopentyl), *if* the alkylidene could rotate readily by 180 degrees before the amido proton migrates back to the alkylidene carbon atom.

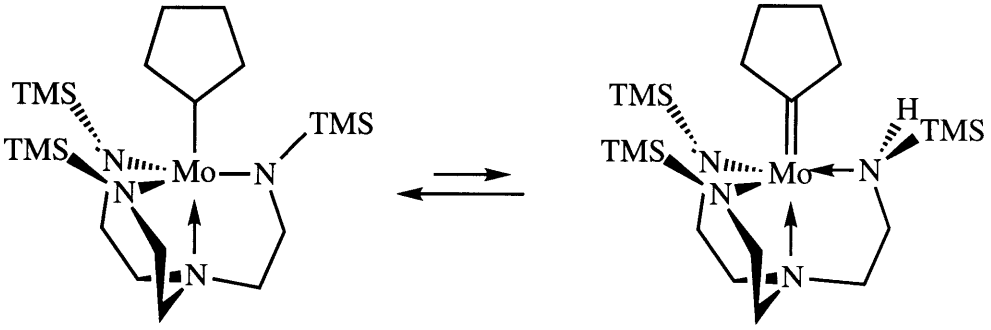

(9)

As alluded to previously, an alternative explanation for the changes in the ^2H NMR spectrum of $[N_3N]$Mo(cyclopentyl-d_1) upon warming is that a rapid and reversible carbon-carbon bond cleavage reaction is taking place (equation 10). Fast access of this C_s-symmetric metallacyclohexene complex on the NMR time scale would lead to the same interconversion of endo and exo ring positions. A C-C bond cleavage process occurring at 10^3 sec^{-1} would seem unlikely compared to a C-H_α bond cleavage, although for $[N_3N]$Mo(cyclopentyl) we cannot entirely rule out this possibility. However, in $[N_3N]$Mo(cyclohexyl), the substantial kinetic

References begin on page 63.

isotope effect (k_H/k_D = 3.1 at 64 °C) does demonstrate that a C-H bond is cleaved during the reaction. Considering that the rate constants for the endo/exo interconversion process in the cyclopentyl and cyclohexyl complexes are within one order of magnitude (see results section), it seems likely that a rapid and reversible α-elimination is also in effect with the cyclopentyl complex.

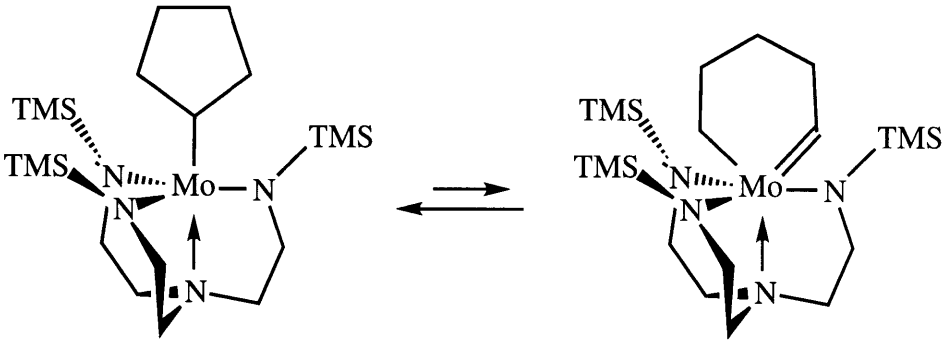

(10)

It is perhaps largely a consequence of the relative stability of the $[N_3N]^{3-}$ ligand system to various other decomposition reactions, especially *inter*molecular decomposition reactions and reactions involving ligand dissociation, that such a variety of intramolecular reactions can be observed. However, it is also somewhat surprising that the trimethylsilyl substituents do not undergo C-H activation more readily than they do (e.g., to form [bitN_3N]Mo), as carbon-hydrogen bond activation in (usually hydride) complexes that contain one or more trimethylsilyl-substituted ligands has been observed in several systems,[37-39] including [N_3N]TiH.[10] Other possible decomposition reactions, e.g., loss of Me_3SiH[31] or degradation of the tren backbone by cleavage of an N_{ax}-C bond,[31,32] so far have not been observed with in [N_3N]Mo alkyl complexes.

A potentially important feature of the alkyl systems studied here is the fact that they are all 16 electron, high spin d^2 species. Many of the reactions discussed here, α-hydride elimination in particular, would seem to require an empty orbital in order to activate a C-H bond through an agostic interaction. However, so far there is no evidence that the rate of any of the

References begin on page 63.

reactions discussed here is limited as a consequence of the high spin ground state alone, a possibility that was proposed in a preliminary communication.[9] Arguments concerning the degree to which spin state alone can alter the rate of an organometallic reaction have been in the literature for some time,[40-42] and the conclusion in every case so far has been that it cannot have such effects. However, since the vast majority of examples in the literature concern metals in lower oxidation states (usually carbonyl complexes), we will keep an open mind concerning the possibility that accessibility of some ^1A spin state (with an accompanying structural change) is an important feature of some of the chemistry of d^2 complexes of the type described here.

EXPERIMENTAL

General Details. All experiments were conducted under nitrogen in a Vacuum Atmospheres drybox, using standard Schlenk techniques, or on a high vacuum line (< 10^{-4} torr). Pentane was washed with HNO_3/H_2SO_4 (5/95 v/v), sodium bicarbonate, H_2O, stored over $CaCl_2$ and then distilled from sodium benzophenone under nitrogen. Regent grade benzene was distilled from sodium benzophenone under nitrogen. Toluene was distilled from molten sodium. Methylene chloride was distilled from CaH_2. Reagent grade ether and THF were sparged with nitrogen and passed through alumina columns.[43] All solvents were stored in the drybox over activated 4 Å molecular sieves. Deuterated solvents were freeze-pump-thaw degassed and vacuum transferred from an appropriate drying agent, or sparged with argon and stored over sieves. NMR spectra are recorded in C_6D_6 unless noted otherwise. ^1H and ^{13}C data are listed in parts per million downfield from tetramethylsilane and were referenced using the residual protonated solvent peak. ^2H NMR spectra usually were obtained at 46.0 MHz and are referenced externally to C_6D_6 (7.15 ppm) in C_6H_6. Probe temperatures during variable temperature studies were calibrated with methanol (low T) or ethylene glycol (high T). Coupling constants are given in Hertz, and routine couplings are not listed. Elemental analyses (C, H, N) were performed on a Perkin-Elmer 2400 CHN analyzer in our own laboratory.

References begin on page 63.

Preparation of Starting Materials. $[N_3N]MoCl$, $[N_3N]MoMe$, $[N_3N]Mo(cyclopentyl)$, $[N_3N]Mo(CH_2SiMe_3)$, $[N_3N]Mo$-(cyclohexyl), $[N_3N]Mo(ethyl)$, $[N_3N]MoH$, and $[N_3N]Mo(butyl)$ were prepared as described in the literature.[12] Preparations of isotopically-labeled molybdenum complexes are given below. Perdeuterocyclohexyl chloride was prepared from commercially available $C_6D_{11}OH$ and DCl by a modification (described below) of a literature method.[44] 1-Deuterocyclopentyllithium was prepared by reduction of cyclopentanone with lithium aluminum deuteride followed by treatment with Ph_3PBr_2 in DMF.[45] The bromide was converted to the lithium reagent by reaction with lithium powder in refluxing hexane. The lithium reagent was recrystallized from pentane before use. Cyclohexyllithium was prepared by the literature method.[46] $Li^{13}CH_2CH_2CH_2CH_3$ was prepared by treating $^{13}CO_2$ with n-PrMgCl, reducing the acid with $LiAlH_4$ to the alcohol, chlorinating the alcohol with $SOCl_2$/pyridine in hexane (procedure described below), and finally treating the chloride with lithium wire in the usual manner; overall yield ~20% .

In UV/Vis studies the following equation was employed to follow the disappearance of an alkyl species: $\ln[(A_0 - A_\infty)/(A - A_\infty)] = kt$, where A_0 = absorbance at wavelength λ at time 0, A_∞ = absorbance at wavelength λ at infinite time, and A = absorbance at wavelength λ at time t.

Rate constants of dynamic NMR processes were obtained by using the equation $k = (\pi/\sqrt{2}) \cdot (\Delta\nu)$; where $\Delta\nu$ = the frequency difference between the two resonances which are exchanging and k is the rate constant at the coalescence temperature.

$C_6D_{11}Cl$. The compound was synthesized by a modification of the literature procedure. An oven-dried 100 mL flask was charged with $C_6D_{11}OD$ (9.3 g, 82.8 mmol), followed by DCl (12 M in D_2O, 35 mL). The flask was fitted with a condenser and purged with argon. It was placed in a 95 °C oil bath for 30 min. It is important for the temperature not to exceed 95 °C at this point so that the cyclohexene-d_{10} intermediate does not boil out of the flask. The temperature was then increased to 115 °C for ~3 h. The reaction was cooled to room temperature and the product separated from the acid layer. ^2H NMR showed complete consumption of the

References begin on page 63.

starting material, and that a trace of cyclohexene-d_{10} was present. The product was washed with water, $NaHCO_3$, and dried over $CaCl_2$. Purification was effected by flash chromatography on silica (5 cm x 13 cm) with hexanes as the eluant. 25 mL fractions were collected and the first 12 fractions were combined and rotovaped. Gas chromatography and ^2H NMR showed no olefin was present. After freeze-pump-thawing and passing through activated Al_2O_3 in the drybox, the product was of sufficient purity to be converted to the lithium reagent, 3.77 g chloride obtained (35%). ^2H NMR ($CHCl_3$) δ 3.96 (C*D*Cl), 2.00, 1.73, 1.60, 1.45, 1.28 (CD_2).

[N_3N]Mo(cyclopentyl-d_1). A solution of 1-deuterocyclopentyllithium (94 mg, 1.22 mmol, 2 equiv.) dissolved in 6 mL of pentane was added to a solution of [N_3N]MoCl (300 mg, 0.610 mmol) in 15 mL of ether in a 100 mL flask. The solution changed color immediately to purple. After one hour at room temperature the volatile materials were removed *in vacuo* and the residue was extracted with minimum (~4 mL) pentane. This extract was concentrated to ~1.5 mL and cooled to -40 °C to give purple crystals (209 mg, 65%): ^1H NMR δ 21.2 (cyclopentyl), 15.3 (cyclopentyl), 10.2 ($SiMe_3$), -24.0 (NCH_2), -35.6 (NCH_2), -48.8 (cyclopentyl), -58.8 (cyclopentyl). Variable-temperature deuterium NMR spectra are shown in Figure 1.14.

[N_3N]Mo(C_6D_{11}). Undecadeuterocyclohexyllithium (21 mg, 0.21 mmol) was added as a solid to a solution of [N_3N]MoCl (92 mg, 0.19 mmol) in 10 mL of ether. The solution turned deep purple immediately. After 45 min the solvent was removed in vacuo and the residue was extracted with pentane. Cooling the extract to -40 °C afforded 82 mg (80 %) of purple crystals. The variable-temperature ^2H NMR spectra are shown in Figure 1.15.

NMR monitoring of the thermolysis of [N_3N]MoH to give [bitN_3N]Mo. A more direct synthesis of [bitN_3N]Mo is available in the literature.[12] [N_3N]MoH (20 mg, 44 μmol) was dissolved in 0.7 mL toluene-d_8 an NMR tube with a J. Young valve was charged with the solution. The reaction was degassed by freeze-pump-thaw cycles. The reaction was heated to 105 °C for 22 h. ^1H NMR showed a 50/50 mixture of [N_3N]MoH and [bitN_3N]Mo. The hydrogen was removed by freeze-pump-thaw cycles and heating was continued at 110 °C for 24 hours, ^1H NMR now showed a 70:30 mixture of [bitN_3N]Mo and [N_3N]MoH. ^1H NMR of

References begin on page 63.

[bitN_3N] δ 18.58 (CH_2), 14.81 ($SiMe_3$), 1.10 ($SiMe_2$), -18.95 (CH_2), -20.26 (CH_2), -98.65 (CH_2), -103.55 (CH_2), -125.06 (CH_2).

Procedure for determining the rate of β-hydride elimination in [N_3N]Mo (cyclopentyl). In the drybox, a 9" NMR tube with a female 14/20 joint attached was charged with solid 1-d-cyclopentyllithium (18 mg, 0.23 mmol, 2.3 equiv.). A slurry of [N_3N]MoCl (50 mg, 0.102 mmol) in 0.6 mL toluene-d_8 was prepared and cooled to -40 °C. The cold solution was added to the NMR tube containing the lithium reagent. The tube was quickly fitted with a vacuum adapter and removed from the drybox. It was frozen, evacuated, and flame sealed. The tube was kept in liquid nitrogen during transport to the NMR spectrometer. It was then thawed and monitored by ^2H NMR. The NMR spectra were acquired at -20 °C, a temperature at which α-elimination is slow on the NMR time scale. The reaction times listed in Figure 1.13 represent total reaction time at room temperature.

Kinetic study of the conversion of [N_3N]Mo(cyclohexyl) to [N_3N]MoH. The reaction was followed by UV/Vis in toluene at 562 nm. Runs were performed with a 3 mM stock solution of the cyclohexyl complex. Runs were repeated at each temperature, average values (in units of 10^{-4} sec^{-1}) at temperature T (deg. K) are 0.127 (323), 0.428 (333), 1.07 (343), 3.68 (353), and 9.64 (363). A plot of ln(k/T) versus 1/T gave $\Delta H^{\ddagger}$ = 24,501 cal/mol and $\Delta S^{\ddagger}$ = -5.27 e.u. with R = 0.99886. At 343 K the rate constant for decomposition of [N_3N]Mo(C_6H_{11}) was calculated to be 1.23 x 10^{-4} sec^{-1}, while [N_3N]Mo(C_6D_{11}) was found in two experiments to be 3.0 x 10^{-5} and 3.3 x 10^{-5} sec^{-1} for a $k_H/k_D = 3.9 \pm 0.2$.

Kinetic study of the α-elimination process in [N_3N]Mo(C_6D_{11}). The rate of α-elimination was determined by VT ^2H NMR as shown in 1.15 and described in the text. Values for k obtained at 46.0 MHz at a concentration of ca. 0.1 M are: 378 sec^{-1} at 324 K, 755 sec^{-1} at 339 K, and 955 sec^{-1} at 343 K. By performing a similar experiment at 76.7 MHz with a ~0.1 M sample three additional points were obtained: k_α = 606 sec^{-1} at 331 K, 1273 sec^{-1} at 346 K, and 1555 sec^{-1} at 352 K. A plot of ln(k/T) versus 1/T for these six points gave $\Delta H^{\ddagger}$ = 10,588 cal/mol

References begin on page 63.

and $\Delta S^{\ddagger}$ = -14.189 e.u. with R = 0.988. Using these values k at 337 K was calculated to be 696 sec^{-1}. The rate of α-elimination in $[N_3N]Mo(C_6H_{11})$ was determined by ^1H NMR to be 2155 sec^{-1} at 337 K. Thus k_H/k_D at this temperature is 3.1 ± 0.3.

X-ray Structures of $[N_3N]Mo(CD_3)$ and $[N_3N]Mo$(cyclohexyl). Crystallographic data, collection parameters, and refinement parameters for these studies can be found in Table 1.4. Both crystals were grown from pentane at -40 °C. General details for the experimental procedures[36] and tables of atomic coordinates and all bond lengths and angles can be found elsewhere.[12]

Solid-State Magnetic Susceptibility Measurements. SQUID experiments were performed on a Quantum Design 5.5 T instrument running MSRP2 software. Samples were prepared in an N_2-filled drybox. A gelatin capsule and 2.2 × 1.9 cm piece of parafilm were weighed. The capsule was then loaded with the sample and the parafilm was folded and packed on top using plastic tongs. The capsule was closed and weighed again to determine the sample mass. It was then suspended in a straw. The straw was placed in a plastic bottle with a screw cap and the bottle was tightly sealed. At the instrument the straw was quickly attached to the sample rod and transferred to the helium atmosphere. Measurements were taken in 1 degree intervals from 5-10 K, 2 degree intervals from 12-20 K, 3 degree intervals from 23-50 K, 5 degree intervals from 55-100 K, 10 degree intervals from 110-200 K, and 20 degree intervals from 220-300 K, see Table 1.1. A background measurement of an empty gel capsule, parafilm square, and straw was taken over the entire temperature range. These values were subtracted from the observed susceptibility at each temperature.

References begin on page 63.

REFERENCES

(1) Albright, T. A.; Burdett, J. K.; Whangbo, M.-H. *Orbital Interactions in Chemistry*, Wiley & Sons: New York, 1985.

(2) O'Donoghue, M. B.; Zanetti, N. C.; Davis, W. M.; Schrock, R. R. *J. Am. Chem. Soc.* **1997**, *119*, 2753.

(3) Shih, K.-Y.; Schrock, R. R.; Kempe, R. *J. Am. Chem. Soc.* **1994**, *116*, 8804.

(4) Zanetti-Mösch, N. C.; Davis, W. M.; Schrock, R. R.; Wanniger, K.; Seidel, S. W.; O'Donoghue, M. B. , in press.

(5) Zanetti, N. C.; Schrock, R. R.; Davis, W. M. *Angew. Chem., Int. Ed. Engl.* **1995**, *34*, 2044.

(6) Wu, G.; Rovnyak, K.; Johnson, M. J. A.; Zanetti, N. C.; Musaev, D. G.; Morokuma, K.; Schrock, R. R.; Griffin, R. G.; Cummins, C. C. *J. Am. Chem. Soc.* **1996**, *118*, 10654.

(7) Johnson-Carr, J. A.; Zanetti, N. C.; Schrock, R. R.; Hopkins, M. D. *J. Am. Chem. Soc.* **1996**, *118*, 11305.

(8) Shih, K.-Y.; Totland, K.; Seidel, S. W.; Schrock, R. R. *J. Am. Chem. Soc.* **1994**, *116*, 12103.

(9) Schrock, R. R.; Shih, K.-Y.; Dobbs, D.; Davis, W. M. *J. Am. Chem. Soc.* **1995**, *117*, 6609.

(10) Cummins, C. C.; Schrock, R. R.; Davis, W. M. *Organometallics* **1992**, *11*, 1452.

(11) Nugent, W. A.; Mayer, J. A. *Metal-Ligand Multiple Bonds*, Wiley: New York, 1988.

(12) Schrock, R. R.; Seidel, S. W.; Mösch-Zanetti, N. C.; Shih, K.-Y.; O'Donoghue, M. B.; Davis, W. M.; Reiff, W. M. *J. Am. Chem. Soc.* , in press.

(13) Figgis, B. N. *Introduction to Ligand Fields*, Wiley: New York, 1966.

(14) Duan, Z.; Verkade, J. G. *Inorg. Chem.* **1995**, *34*, 1576.

(15) Figgis, B. N.; Lewis, J. *Prog. Inorg. Chem.* **1964**, *6*, 37.

(16) Schrock, R. R. *Acc. Chem. Res.* **1997**, *30*, 9.

(17) Reid, S. M., unpublished results.

(18) Maus, D. C.; Copié, V.; Sun, B.; Griffiths, J. M.; Griffin, R. G.; Luo, S.; Schrock, R. R.; Liu, A. H.; Seidel, S. W.; Davis, W. M.; Grohmann, A. *J. Am. Chem. Soc.* **1996**, *118*, 5665.

(19) Brookhart, M.; Green, M. L. H. *Prog. Inorg. Chem.* **1988**, *36*, 1.

(20) LaMar, G. N.; Horrocks, W. D., Jr.; Holm, R. H. *NMR of Paramagnetic Molecules*, Academic: New York, 1973.

(21) Schrock, R. R. In *Reactions of Coordinated Ligands*; Braterman, P. R., Ed.; Plenum: New York, 1986.

(22) Collman, J. P.; Hegedus, L. S.; Norton, J. R.; Finke, R. G. *Principles and Applications of Organotransition Metal Chemistry*, University Science Books: Mill Valley, 1987.

(23) Cooper, N. J.; Green, M. L. H. *J. Chem. Soc., Dalton Trans.* **1979**, 1121.

(24) Cooper, N. J.; Green, M. L. H. *J. Chem. Soc., Chem. Commun.* **1974**, 761.

(25) Cooper, N. J.; Green, M. L. H. *J. Chem. Soc., Chem. Commun.* **1974**, 209.

(26) Turner, H. W.; Schrock, R. R. *J. Am. Chem. Soc.* **1982**, *104*, 2331.

(27) Turner, H. W.; Schrock, R. R.; Fellmann, J. D.; Holmes, S. J. *J. Am. Chem. Soc.* **1983**, *105*, 4942.

(28) Fellmann, J. D.; Schrock, R. R.; Traficante, D. D. *Organometallics* **1982**, *1*, 481.

(29) van Asselt, A.; Burger, B. J.; Gibson, V. C.; Bercaw, J. E. *J. Am. Chem. Soc.* **1986**, *108*, 5347.

(30) Parkin, G.; Bunel, E.; Burger, B. J.; Trimmer, M. S.; Asselt, A. v.; Bercaw, J. E. *J. Molec. Catal.* **1987**, *41*, 21.

(31) Freundlich, J. S.; Schrock, R. R.; Davis, W. M. *J. Am. Chem. Soc.* **1996**, *118*, 3643.

(32) Freundlich, J. S.; Schrock, R. R.; Davis, W. M. *Organometallics* **1996**, *15*, 2777.

(33) Burk, M. J.; McGrath, M. P.; Crabtree, R. H. *J. Am. Chem. Soc.* **1988**, *110*, 620.

(34) Murdzek, J. S.; Schrock, R. R. In *Carbyne Complexes*; VCH: New York, 1988.

(35) Schrock, R. R.; Seidel, S. W.; Zanetti-Mösch, N. C.; Dobbs, D. A.; Shih, K.-Y.; Davis, W. M. *Organometallics* , in press.

(36) Rosenberger, C.; Schrock, R. R.; Davis, W. M. *Inorg. Chem.* **1997**, *36*, 123.

(37) Simpson, S. J.; Andersen, R. A. *Inorg. Chem.* **1981**, *20*, 3627.

(38) Simpson, S. J.; Andersen, R. A. *Inorg. Chem.* **1981**, *20*, 2991.

(39) Turner, H. W.; Simpson, S. J.; Andersen, R. A. *J. Am. Chem. Soc.* **1979**, *101*, 2782.

(40) Detrich, J. L.; Reinaud, O. M.; Rheingold, A. L.; Theopold, K. H. *J. Am. Chem. Soc.* **1995**, *117*, 11745.

(41) Gadd, G. E.; Upmacis, R. K.; Poliakoff, M.; Turner, J. J. *J. Am. Chem. Soc.* **1986**, *108*, 2547-2552.

(42) Janowicz, A. H.; Bryndza, H. E.; Bergman, R. G. *J. Am. Chem. Soc.* **1981**, *103*, 1516.

(43) Pangborn, A. B.; Giardello, M. A.; Grubbs, R. H.; Rosen, R. K.; Timmers, F. J. *Organometallics* **1996**, *15*, 1518.

(44) Perlman, D.; Davidson, D.; Bogert, M. T. *J. Org. Chem.* **1936**, *1*, 288.

(45) Wiley, G. A.; Hershkowitz, R. L.; Rein, B. M.; Chung, B. C. *J. Am. Chem. Soc.* **1964**, *86*, 964.

(46) Liang, L.-C., unpublished results.

CHAPTER II

Kinetic Studies on α- and β-Elimination Reactions of Paramagnetic Tungsten(IV) Alkyl Complexes That Contain the $[(Me_3SiNCH_2CH_2)_3N]^{3-}$ Ligand.

Much of the material covered in this chapter has been accepted for publication:

Schrock, R. R.; Seidel, S. W.; Mösch-Zanetti, N. C.; Dobbs, D. A.; Shih, K.-Y.; Davis, W. M. *Organometallics*, in press.

INTRODUCTION

The preceding chapter describes studies on the rates of α- and β-elimination reactions of molybdenum cyclopentyl and cyclohexyl complexes that contain the $[N_3N]^{3-}$ ($[N_3N]^{3-}$ = $[(TMSNCH_2CH_2)_3N]^{3-}$) ligand. The remarkable result that α-elimination is six to seven orders of magnitude faster than β-elimination with these complexes led us to wonder if similar studies could be made with tungsten analogs of the $[N_3N]$Mo(cycloalkyl) complexes. A qualitative determination that α-elimination is faster than β-elimination at -13 °C with the $[N_3N]$W-(cyclopentyl) complex has been made by observing that only $[N_3N]$W(cyclopentylidene)(D) is formed when $[N_3N]$WCl is reacted with 1-deuterocyclopentyllithium.[1] This chapter will describe further studies towards measuring exact rate constants of these processes.

$[N_3N]W(CH_2R)$ species with R ≠ H all lose dihydrogen rapidly at room temperature to yield $[N_3N]W{\equiv}CR$ complexes.[2] The analogous molybdenum complexes undergo this α,α-double dehydrogenation reaction much more slowly.[3] Only $[N_3N]Mo(CH_2CMe_3)$ loses dihydrogen cleanly to form $[N_3N]Mo{\equiv}CCMe_3$, and the reaction occurs at reasonable rates only at temperatures above 60 °C. Additionally, differences are observed in the rates of some C-C bond cleavage reactions. $[N_3N]$Mo(cyclobutyl) is an isolable species which decomposes upon thermolysis to yield $[N_3N]Mo{\equiv}CCH_2CH_2CH_3$ whereas $[N_3N]$W(cyclobutyl) is only a presumed intermediate in the synthesis of $[N_3N]W(\text{cyclo-}CHCH_2CH_2CH_2)$ (**1**) from $[N_3N]$WCl and cyclobutyllithium, **1** is converted to $[N_3N]W{\equiv}CCH_2CH_2CH_3$ upon thermolysis. Results in this chapter describe the much greater facility with which tungsten complexes undergo this type of C-C bond cleavage reaction. The differences in the relative rates of alkylidyne formation between these congeneric complexes can be qualitatively rationalized by considering the relative "electrophilicity" of each metal, but such arguments are speculative at best. The goal of the work in this chapter is to understand the differences between the chemistry of these W and Mo complexes in a more conclusive way. We will compare kinetic, thermodynamic, and magnetic data obtained for $[N_3N]$M(cyclopentyl) (M = Mo, W) complexes with regard to understanding

References begin on page 92.

the differences between these two metals in terms of rates of alkylidyne formation and other reactions.

RESULTS

Characterization of Paramagnetic Tungsten Triamidoamine Complexes

$[N_3N]WCl$ is synthesized by reacting $[N_3N]Li_3$ [4] with $WCl_4(dme)$[5] in THF.[6] The reaction proceeds in only 15-20% yield, presumably because reduction of the metal and loss of TMSCl occur readily. $[N_3N]WCl$ is an available starting material only because both $[N_3N]Li_3$ and $WCl_4(dme)$ can be easily prepared in large quantities. A plot of the magnetic susceptibility of $[N_3N]WCl$ versus T from 5 to 300 K is shown in Figure 2.1. The susceptibility of $[N_3N]WCl$ is as much as one order of magnitude smaller than that of $[N_3N]MoCl$ at a given temperature (see chapter I). μ_{eff} is thus lower than the spin-only value for an S = 1 configuration (2.83 μ_B) at room temperature, and decreases smoothly with decreasing temperature (Figure 2.2). The

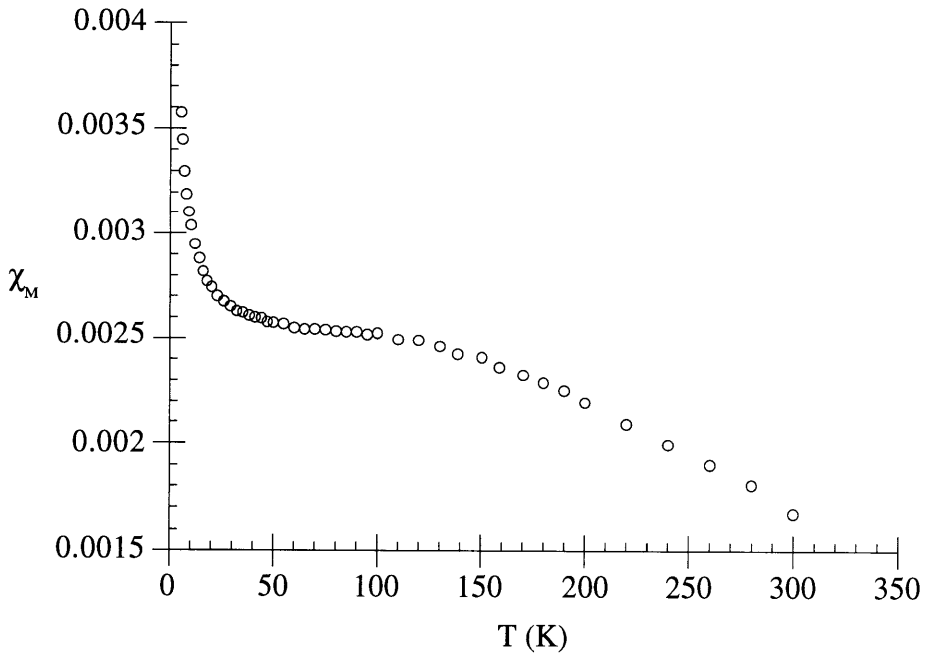

Figure 2.1. A plot of χ_M versus T for $[N_3N]WCl$.

References begin on page 92.

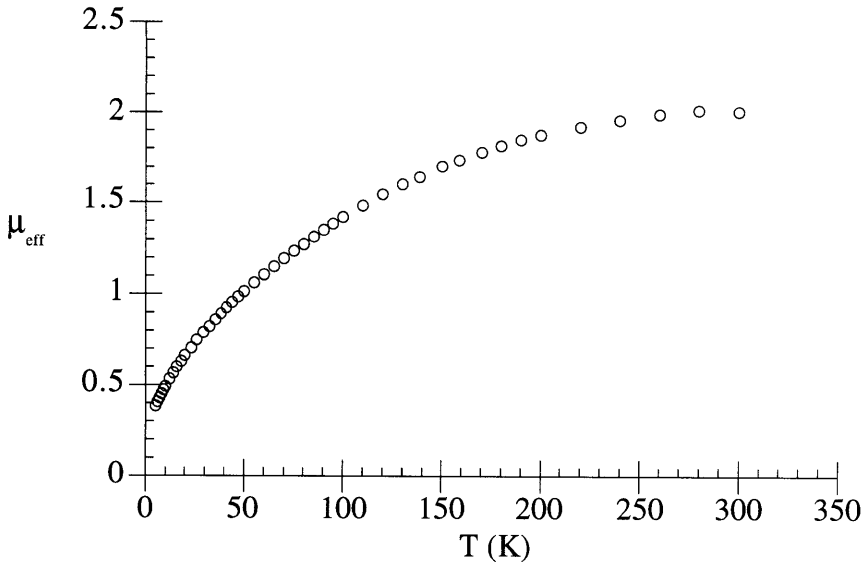

Figure 2.2. A plot of μ_{eff} versus T for $[N_3N]WCl$.

susceptibility of the tungsten compound also changes much more slowly with temperature than that of $[N_3N]MoCl$. These differences are best illustrated by plotting χ_M versus T for both $[N_3N]MoCl$ and $[N_3N]WCl$ on the same graph (Figure 2.3). The susceptibility behavior of $[N_3N]WCl$ is explained by a combination of spin-orbit coupling and low symmetry ligand field components which result in zero field splitting of the d^2 ground state triplet.[3,7] These effects were also used to explain the drop in μ_{eff} with $[N_3N]MoCl$ at temperatures below 50 K (see chapter I). The effect manifests itself at much higher temperatures in the tungsten complex because the spin-orbit coupling constant for tungsten(IV) is more than twice that of molybdenum(IV) ($\lambda(W^{4+}) \approx 1050$ cm^{-1} while $\lambda(Mo^{4+}) \approx 475$ cm^{-1}).[7] The degenerate d_{xz} and d_{yz} orbitals each contain one electron in this case, resulting in the triplet ground state. Two measurements of μ_{eff} for $[N_3N]WCl$ in solution by the Evans method[8] at 22 °C in C_6D_6 gave values of 2.4 and 2.5 μ_B,[9] consistent with the solid-state results.

References begin on page 92.

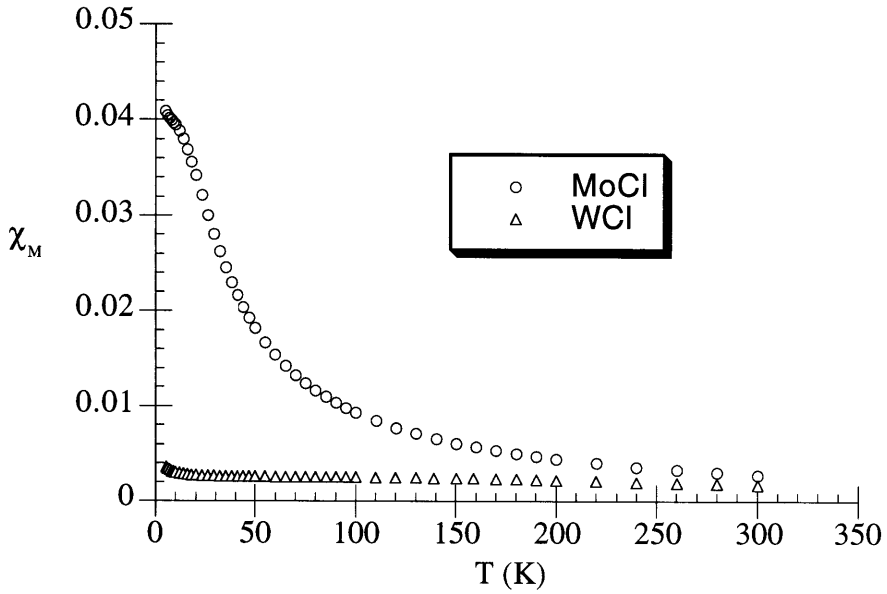

Figure 2.3. A plot of χ_M versus T for $[N_3N]MoCl$ and $[N_3N]WCl$.

$[N_3N]W(CH_3)$ and $[N_3N]W(C_6H_5)$ are readily prepared by alkylation of $[N_3N]WCl$ with the corresponding lithium reagent. $[N_3N]WH$ is prepared by heating $[N_3N]W$(cyclopentylidene)(H) (see below) to 45 °C for one day. The susceptibilities of these three compounds in the solid state vary with temperature in ways that are entirely analogous to the behavior of $[N_3N]WCl$. Apparently conjugation of the d_{xz}/d_{yz} set with the phenyl ring in $[N_3N]W(C_6H_5)$ is not significant enough to change any magnetic properties. A plot of χ_M versus T for all three compounds is shown in Figure 2.4. μ_{eff} for $[N_3N]W(CH_3)$ was found to be 2.5 μ_B in C_6D_6 at 22 °C[6] by the Evan's method.

References begin on page 92.

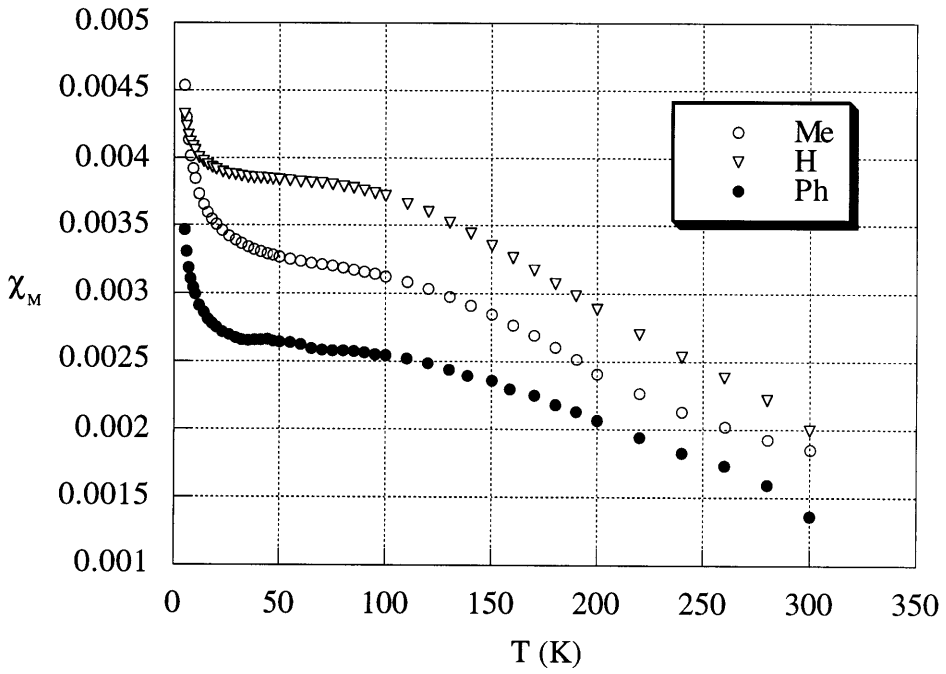

Figure 2.4. χ_M versus T plots for $[N_3N]WMe$, $[N_3N]WH$, and $[N_3N]WPh$.

The proton NMR spectrum of $[N_3N]WH$ at room temperature displays three shifted resonances, one for the TMS groups at 17.9 ppm and one for each set of geminal methylene protons at -30.1 and -94.4 ppm. As is the case with all triamidoamine complexes, we are unable to assign which methylene resonance corresponds to protons α to the amides or α to the amine. No resonance is observed for the hydride ligand, as expected for a hydrogen bonded directly to the paramagnetic center. The paramagnetic shift becomes more pronounced as the temperature decreases (Figure 2.5, TMS resonance not shown) as a consequence of the slight increase of the molar susceptibility of $[N_3N]WH$ with decreasing temperature. Peaks are noticeably sharper and more shifted than in $[N_3N]MoCl$ and $[N_3N]MoMe$ (see chapter I). At temperatures below -20 °C, geminal methylene protons become inequivalent as a consequence of a locking of the molecule into a C_3-symmetric chiral conformation. This type of fluxional process has been observed in a variety of other triamidoamine complexes, including diamagnetic species.[10]

References begin on page 92.

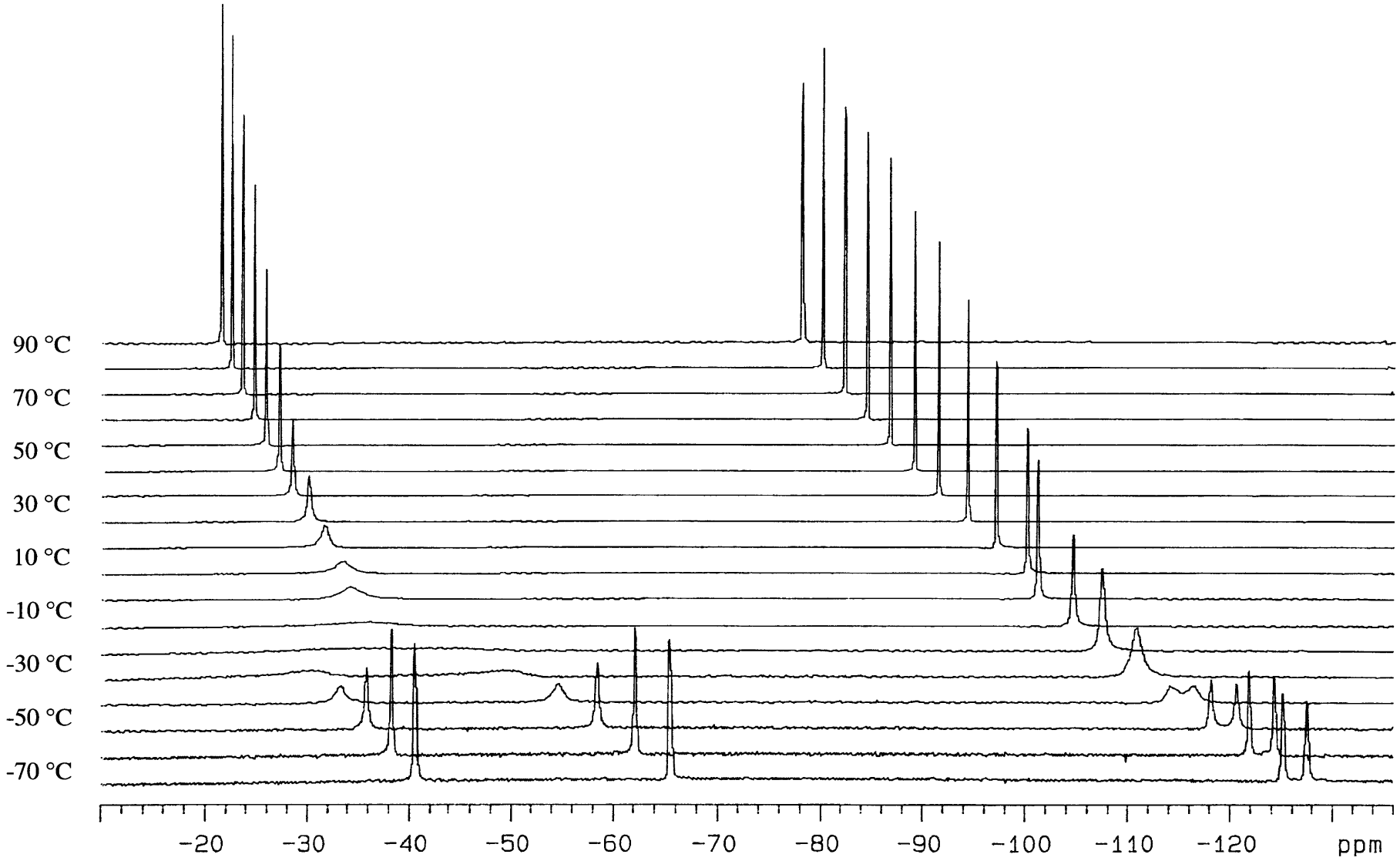

Figure 2.5. VT 500 MHz ^{1}H NMR spectra of [(TMSNCH_2CH_2)$_3$N]WH in toluene-d_8.

For $[N_3N]WH$, $\Delta G^{\ddagger}$ is 9.7 ± 0.3 kcal/mol at -20 °C and 8.5 ± 0.3 kcal/mol at -50 °C. These values are within the same range as those obtained for $[N_3N]MoCl$ and $[N_3N]MoMe$. Thus, we feel that the fluxional process is best explained by the simple C_{3v} to C_3 conformational change described above. More complicated processes involving dissociation of the amine donor would be anticipated to be considerable more energetically costly for tungsten than molybdenum since tungsten would be expected to have a stronger $M\text{-}N_{ax}$ bond.

Synthesis of Tungsten Triamidoamine Alkylidenes and Alkylidynes.

$[N_3N]WCl$ reacts with $LiCH_2R$ reagents (R = H, Me, *n*-Pr, $SiMe_3$, *t*-Bu) or KCH_2Ph in ether or THF to yield alkylidyne complexes, $[N_3N]W{\equiv}CR$ and molecular hydrogen (equation 1).[2,6] Reaction is rapid in all cases except when R = H. $[N_3N]W(CH_3)$ is an isolable species and decomposes to $[N_3N]W{\equiv}CH$ in a first-order reaction. The rate constant for this process at 330 K is 4.35 x 10^{-4} sec^{-1}.[2] $[N_3N]WCl$ reacts with $LiCD_2CH_2CH_2CH_3$ to give $[N_3N]W{\equiv}C\text{-}CH_2CH_2CH_3$ and D_2 gas exclusively. The tungsten chloride also reacts with $Li^{13}CH_2CH_2CH_2CH_3$ to yield $[N_3N]W{\equiv}^{13}CCH_2CH_2CH_3$. The J_{CW} value (242 Hz) could easily be obtained with this labeled complex and is in the range normally observed for tungsten alkylidyne complexes.[11] These experiments show that loss of dihydrogen from the α-carbon occurs faster than any processes which would result in "walking" of the metal along the butyl chain. Scrambling also does not occur to a significant degree with the molybdenum analog, $[N_3N]Mo(^{13}CH_2CH_2CH_2CH_3)$, although in this case the alkyl is isolable at room temperature

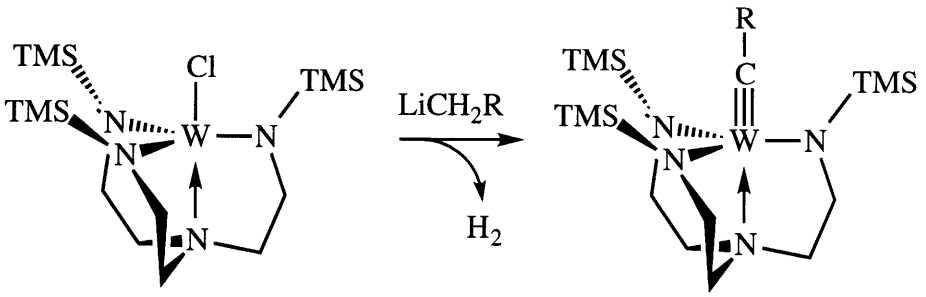

(1)

R = H, Me, *n*-Pr, Ph,
$SiMe_3$, CMe_3

References begin on page 92.

and must be heated in order to observe decomposition. Also, the major decomposition product of [N_3N]Mo(*n*-Bu) is [N_3N]MoH (see chapter II). These results should also be compared with those found in C_6F_5-substituted complexes. With the [N_3N_F] complexes, complete scrambling *is* observed with both the deuterated and ^{13}C-labeled butyllithium reagents (see chapter III for a discussion).

Addition of cyclobutyllithium to [N_3N]WCl results in the formation of a tungsten metallacyclopentene complex, **1**, as shown in equation 2. ^1H and ^{13}C NMR spectra are consistent with the metallacycle structure. The alkylidene carbon is observed at 265 ppm with $^1J_{CH}$ = 130 Hz. The ^1H NMR spectrum shows three sets of methylene protons for the complex, ruling out a fast equilibrium on the NMR time scale between **1** and [N_3N]W(cyclobutyl).

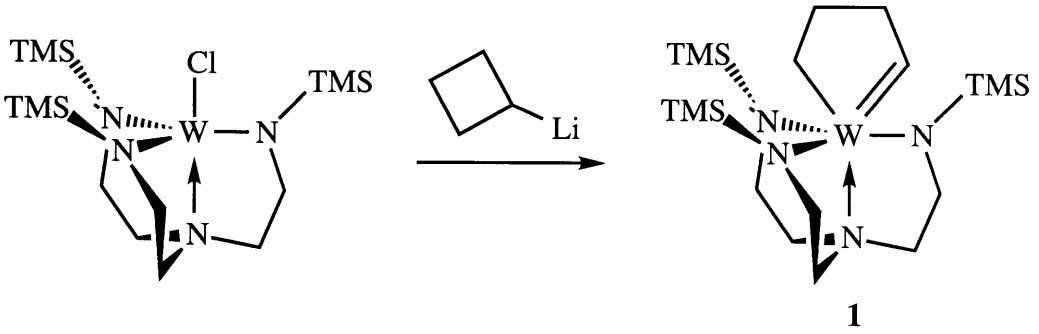

1 (2)

An X-ray structure of **1** was carried out and the metallacyclopentene structure was confirmed. A view of the structure is given in Figure 2.6, and Table 2.1 contains selected bond lengths and angles. Crystallographic data can be found in Table 2.2. As is common in TMS-substituted triamidoamine complexes with apical ligands, twisting of the TMS groups out of the W-N_{eq}-N(4) plane is observed (N(4)-W-Si-N_{eq} dihedral angles are 142, 149, and 170 deg.) This twisting effect has been documented in structurally-characterized [N_3N]Mo complexes (see chapter I) and has been used as a measure of the degree of strain present (cf. [N_3N]Mo(CD_3) and [N_3N]Mo(cyclohexyl)). The W-N(4) distance is relatively long (2.395(5) Å), also indicating a relatively high degree of steric strain in the molecule. The 1-tungstacyclopentene ring is oriented

References begin on page 92.

so that it lies roughly in the N(1)-W-N(4) plane, resulting in an opening of the N(2)-W-N(3) angle to 135.5(2) deg. The W-C(10) and W-C(7) distances are typical of W(VI) alkylidene and alkyl bonds, respectively. The W-C(10)-C(9) angle is larger than the W-C(7)-C(8) angle, and the N(4)-W-C(10) angle is much larger than the N(4)-W-C(7) angle, as expected for the alkyl-alkylidene structure.

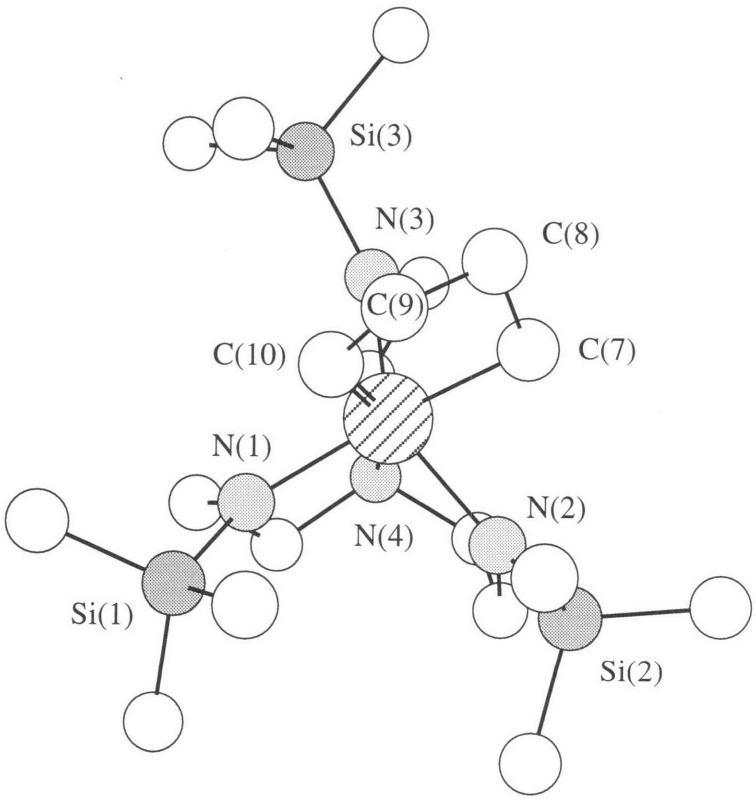

Figure 2.6. A view of the structure of $[N_3N]W(cyclo\text{-}CHCH_2CH_2CH_2)$ (**1**).

References begin on page 92.

Table 2.1. Selected bond distances (Å) and angles (deg.) for $[N_3N]W(cyclo\text{-}CHCH_2CH_2CH_2)$ (**1**).

Distances (Å)

W - N(1)	2.015(5)	W - C(10)	1.972(6)
W - N(2)	2.033(5)	C(7) - C(8)	1.527(8)
W - N(3)	2.004(5)	C(8) - C(9)	1.508(8)
W - N(4)	2.395(5)	C(9) - C(10)	1.509(8)
W - C(7)	2.216(6)		

Angles (deg.)

W - N(1) - Si(1)	134.0(3)	N(1) - W - C(7)	151.0(2)
W - N(2) - Si(2)	133.1(3)	N(2) - W - C(7)	77.9(2)
W - N(3) - Si(3)	136.3(3)	N(3) - W - C(7)	91.1(2)
N(4) - W - N(1) - Si(1)	142[a]	N(1) - W - N(2)	100.9(2)
N(4) - W - N(2) - Si(2)	170[a]	N(2) - W - N(3)	133.5(2)
N(4) - W - N(3) - Si(3)	149[a]	N(1) - W - N(3)	109.0(2)
W - C(7) - C(8)	113.0(5)	C(10) - W - C(7)	72.7(3)
C(7) - C(8) - C(9)	104.8(5)	C(10) - W - N(1)	83.8(2)
C(8) - C(9) - C(10)	105.2(5)	C(10) - W - N(3)	97.4(2)
W - C(10) - C(9)	127.1(5)	C(10) - W - N(2)	120.9(2)
C(7) - W - N(4)	130.3(2)	C(10) - W - N(4)	155.3(2)

[a] Obtained from a Chem 3D model.

References begin on page 92.

Table 2.2. Crystallographic data, collection parameters, and refinement parameters for $[N_3N]W(cyclo\text{-}CHCH_2CH_2CH_2)$ (**1**).

Empirical Formula	$C_{19}H_{43}N_4Si_3W$
Formula Weight	595.69
Diffractometer	Siemens SMART/CCD
Crystal Dimensions (mm)	$0.22 \times 0.16 \times 0.13$
Crystal System	Orthorhombic
a (Å)	17.494 (3)
b (Å)	15.860 (4)
c (Å)	19.350 (4)
V (Å^3)	5369 (2)
Space Group	Pbca
Z	8
D_{calc} (Mg/m^3)	1.474
F_{000}	2408
λ, radiation	0.71073 Å, MoK_α
Scan Type	ω
Temperature (K)	183 (2)
θ Range for Data Collection (deg)	2.03 to 23.27
Independent Reflections	3703
Absorption Correction	None
Refinement Method	Full-matrix least-squares on F^2
Data/Restraints/Parameters	3701/0/245
Final R indices [$I>2\sigma(I)$]	R1 = 0.0309, wR2 = 0.0603
R indices (all data)	R1 = 0.0590, wR2 = 0.0706
GoF	1.043
Extinction Coefficient	0.00024 (3)
Largest Diff. Peak and Hole (eÅ^{-3})	0.661 and -0.475

References begin on page 92.

Alkylation of $[N_3N]WCl$ with cyclopentyllithium in ether at room temperature results in the formation of a crystallographically-characterized cyclopentylidene hydride complex (**2**) (equation 3).[1] The X-ray structure revealed that the cyclopentylidene ring lies in the N(1)-W-N(4) plane, directly between two of the TMS groups. Electron density ascribable to the hydride ligand was found in the plane containing the alkylidene carbon, W, and N(1), but it did not

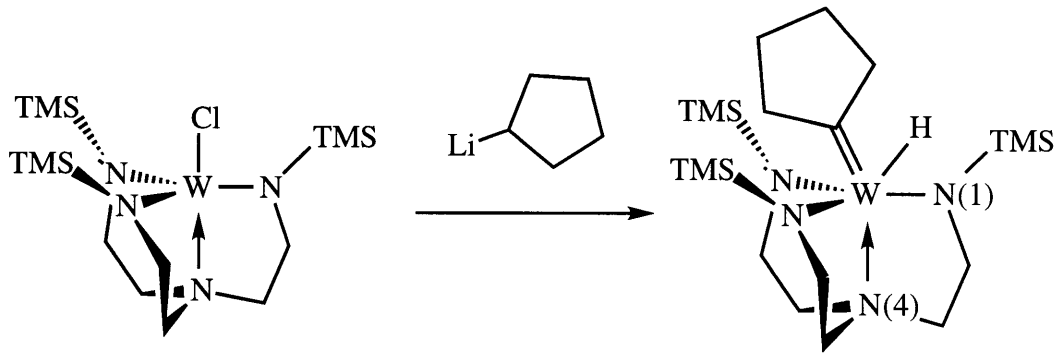

2 (3)

survive refinement. The orientation of the cyclopentylidene and hydride ligands is as expected considering the set of orbitals (d_{xz}, d_{yz}, and d_z^2) available for bonding with apical ligands. Hybridization of a d_{xz} (or d_{yz}) orbital with the d_z^2 results in two orbitals of the proper symmetry for σ-bonding with the alkylidene and the hydride. The remaining d_{yz} (or d_{xz}) orbital is then available for the formation of the alkylidene π-bond. Reaction of $[N_3N]MoCl$ with cyclopentyllithium results in the formation of paramagnetic $[N_3N]Mo$(cyclopentyl). Although in the molybdenum system only this d^2 cyclopentyl tautomer was directly observed, a rapid equilibrium between it and the molybdenum analog of **2** was the simplest way to explain changes in the NMR spectrum of $[N_3N]Mo$(cyclopentyl) upon warming. Further studies have corroborated this explanation (see chapter I).

The ^1H NMR spectrum of $[N_3N]W(C_5H_8)(H)$ at room temperature shows a broad singlet at 0.22 ppm for the TMS groups, two sets of triplets at 2.11 and 3.34 ppm for the backbone methylene protons, a multiplet for the four cyclopentylidene protons γ to the metal (ring positions 2 and 3 in equation 4), and two broad singlets at 3.97 and 5.11 ppm for the inequivalent

References begin on page 92.

cyclopentylidene protons β to the metal (ring positions 1 and 4 in equation 4). The single TMS resonance and backbone triplets indicate that the [N_3N] core spins about the N_{ax}-W vector on the NMR time scale at 22 °C. Upon cooling to -40 °C, the TMS resonance splits out

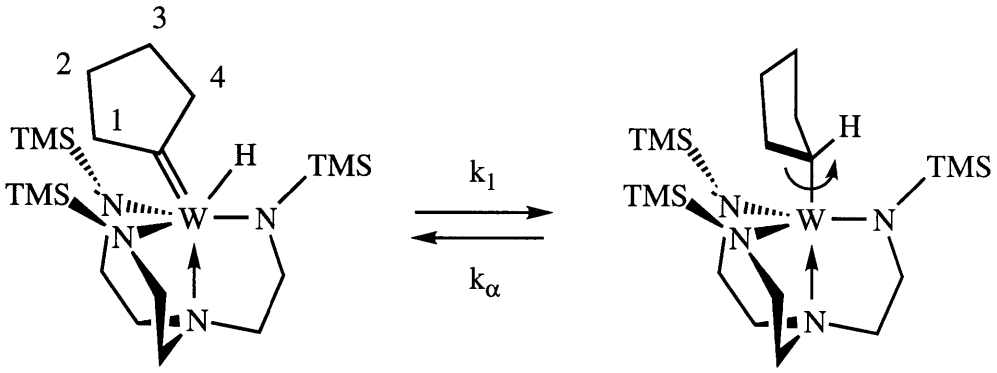

2 **3** (4)

into two resonances in a 2:1 ratio and the ligand backbone methylene protons resonances become multiplets, consistent with a "freezing out" of the C_s-symmetric structure of **2** shown in equation 3. The hydride resonance also sharpens and coupling to tungsten can be observed below 0 °C (J_{HW} = 89 Hz).

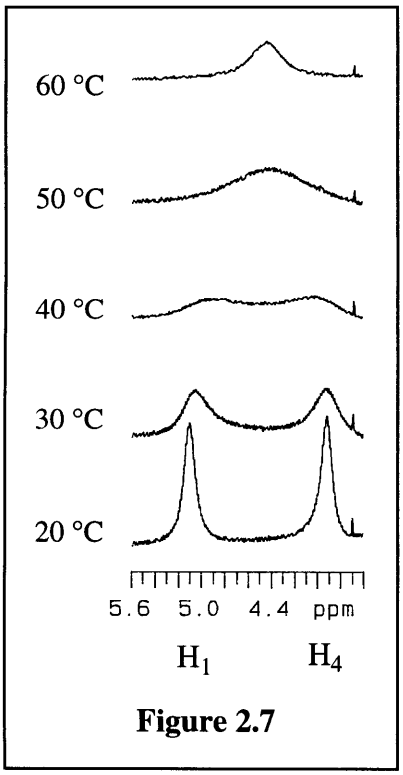

Figure 2.7

^{1}H NMR spectra of **2** above room temperature show that the cyclopentylidene ring methylene β-protons (positions 1 and 4) broaden and coalesce to a single resonance at 46 °C (Figure 2.7). We attribute this behavior to the equilibrium shown in equation 4. We propose that access of [N_3N]W(cyclopentyl) (**3**) would allow for facile rotation about the W-C single bond, resulting in interconversion of protons in positions 1 and 4. k_1 was determined to be 1.3 x 10^3 sec^{-1} at 46 °C from the peak separation of methylene protons 1 and 4 in the low-temperature spectrum. k_α is

References begin on page 92.

apparently greater than k_1, since what we believe would be paramagnetic **3** (cf. $[N_3N]WMe$ and $[N_3N]Mo(cyclopentyl)$) is not observed. A similar process was proposed to explain interconversion of endo and exo ring protons in $[N_3N]Mo(cyclopentyl)$, although in this case the equilibrium favors the paramagnetic cyclopentyl complex and no $[N_3N]Mo(C_5H_8)(H)$ was directly observed (see chapter I). The slower rate constant (the equivalent of k_α in equation 4) in the molybdenum system was found to be ~10^3 sec^{-1} at 22 °C.

As alluded to above, the hydride resonance in **2** is extremely sensitive to temperature. Upon warming, the resonance broadens dramatically and shifts to lower field (Figure 2.8). We attribute these effects to the equilibrium in equation 4. At higher temperatures, it appears that more of paramagnetic **3** is present. We have not been able to observe any protons or deuterons attached to α-carbons by ^1H or ^2H NMR in complexes such as $[N_3N]WCH_2R$ or $[N_3N]MoCH_2R$. Thus, we believe α-protons in these types of paramagnetic complexes are extremely broadened and shifted as a result of their proximity to the paramagnetic center. We presume the α-proton in **3** would therefore also be severely broadened and shifted. Since the equilibrium between **2** and **3** is fast, the observed "hydride" resonance during the NMR experiment is a summation of its diamagnetic component from **2** and paramagnetic component from **3**. The degree of shifting and broadening of the hydride resonance then depends on [**3**]/[**2**] or K_{eq}. If we assume that the chemical shift of the α-proton in **3** follows a 1/T dependence (which is probably reasonable in the 270 to 360 K range based on χ_M versus T plots for related tungsten paramagnets, see above), and that these resonances do not shift for any other reason, then we can determine $\Delta G°$ (i.e. k_1/k_α or K_{eq}) for the equilibrium in equation 4 by using equation 5,[12-14] where δ is the observed "hydride"

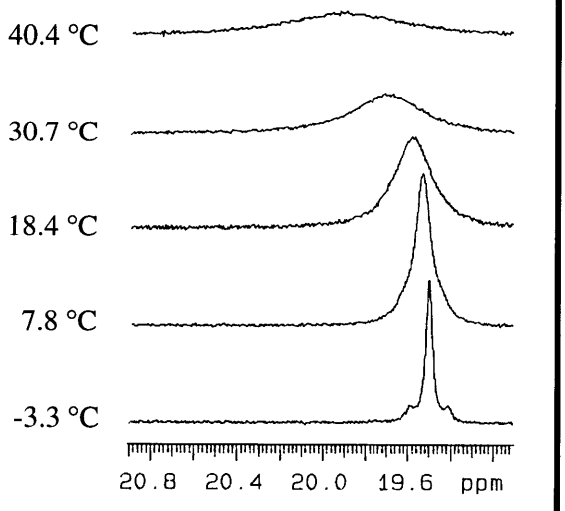

Figure 2.8

References begin on page 92.

chemical shift at a given temperature, δ_{dia} is the hydride chemical shift of **2** in the absence of any **3**, and C is a constant. The chemical shift of the hydride ligand was measured every five degrees from 270 to 360 K, and a plot of δ versus T was fit to equation 5 (Figure 2.9), which gave

$$\delta = \delta_{dia} + \frac{C}{T\left[1+\exp\left(\frac{\Delta H^\circ}{RT} - \frac{\Delta S^\circ}{R}\right)\right]} \quad (5)$$

ΔH° = 11.8(6) kcal/mol, ΔS° = 33(2) e.u., and δ_{dia} = 19.46 ppm (identical to the low-temperature chemical shift of the hydride in **2**). From these data, K_{eq} at 46 °C is calculated to be 0.13. Therefore 0.13 = $k_1/k_{\alpha W}$, and since k_1 was determined above to be 1.3 x 10^3 sec^{-1}, $k_{\alpha W}$ = 1.0 x 10^4 sec^{-1} at 46 °C. This value should be compared to $k_{\alpha Mo}$, the rate constant for the formation

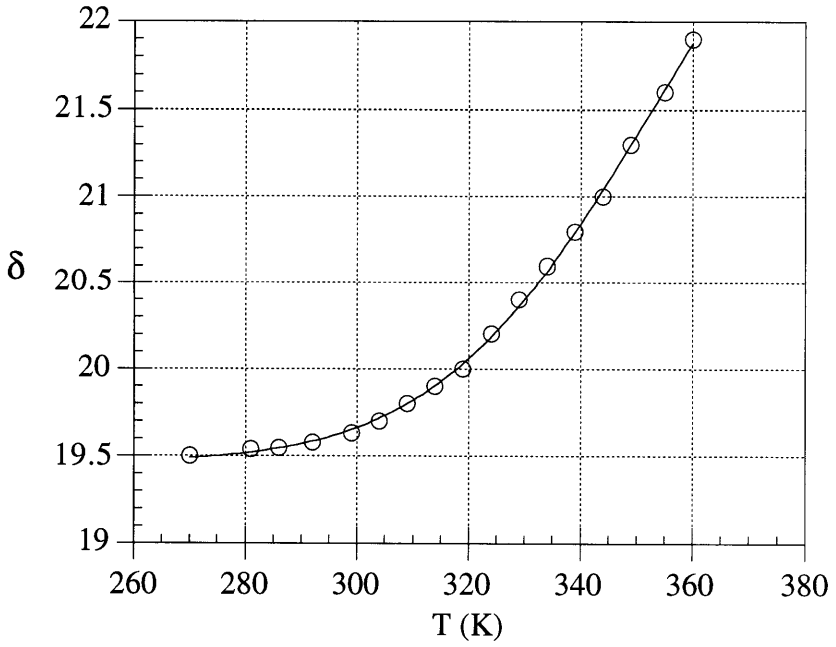

Figure 2.9. A plot of the chemical shift of [N_3N]W(*H*)(cyclopentylidene) versus T fit to equation 5.

References begin on page 92.

of $[N_3N]Mo(C_5H_8)(H)$ from [N_3N]Mo(cyclopentyl) (see chapter I). $k_{\alpha Mo}$ (10^3 sec^{-1} at 22 °C) could be as much as one order of magnitude greater than this at 46 °C. From these data, we conclude that the rate constants for α-elimination in [N_3N]Mo(cyclopentyl) and [N_3N]W(cyclopentyl) *are approximately the same* at this temperature. Therefore, the fact that the alkylidene hydride is the preferred species for tungsten, whereas for molybdenum it is the alkyl that is favored must be attributed to a much larger k_{1Mo} than k_{1W}. Unfortunately, no way has been found to accurately measure k_{1Mo} and compare it to k_{1W}. However, since no $[N_3N]Mo(H)(C_5H_8)$ is observed during the NMR experiment (which would not be difficult since the alkylidene hydride should be diamagnetic) we have estimated that k_1/k_α for Mo is 10^2 or greater. From this assessment, k_{1Mo} can be estimated at 10^6 sec^{-1} (or greater) at 46 °C. This should be compared to k_{1W}, measured to be 1.3×10^3 sec^{-1} at this temperature. The fact that the rates of α-elimination are so similar but the rates of retro-α-elimination (k_1) are so dissimilar for analogous Mo and W complexes seems peculiar and will be discussed further (see below).

Reaction of 1-deuterocyclopentyllithium with [N_3N]WCl in toluene at -13 °C led to the formation of only $[N_3N]W(D)(C_5H_8)$.[1] When the sample was warmed to room temperature for brief periods and then re-cooled to -20 °C to monitor the progress of the reaction by ^2H NMR, the spectra shown in Figure 2.10 were obtained (-20 °C is a convenient temperature to record the spectrum since at this temperature retro-α-elimination is slow on the ^2H NMR time scale and virtually no paramagnetic [N_3N]W(cyclopentyl) is present). Deuterium incorporation into the β positions (at 3.8 and 5 ppm) was observed first, followed by incorporation into the γ positions at ca. 2 ppm. We propose this process occurs by a reversible β-hydride elimination of the cyclopentyl complex (**3**) to yield an olefin hydride complex (**4**) (equation 6). Recall that we have shown that **2** and **3** are in rapid equilibrium at room temperature, although [**3**]/[**2**] at 25 °C is ~0.03. We show below that little cyclopentene is lost from the molecule under these conditions ($\tau_{1/2}$ at 22 °C = 3.1 days). We can obtain a fairly accurate value for the rate constant of

References begin on page 92.

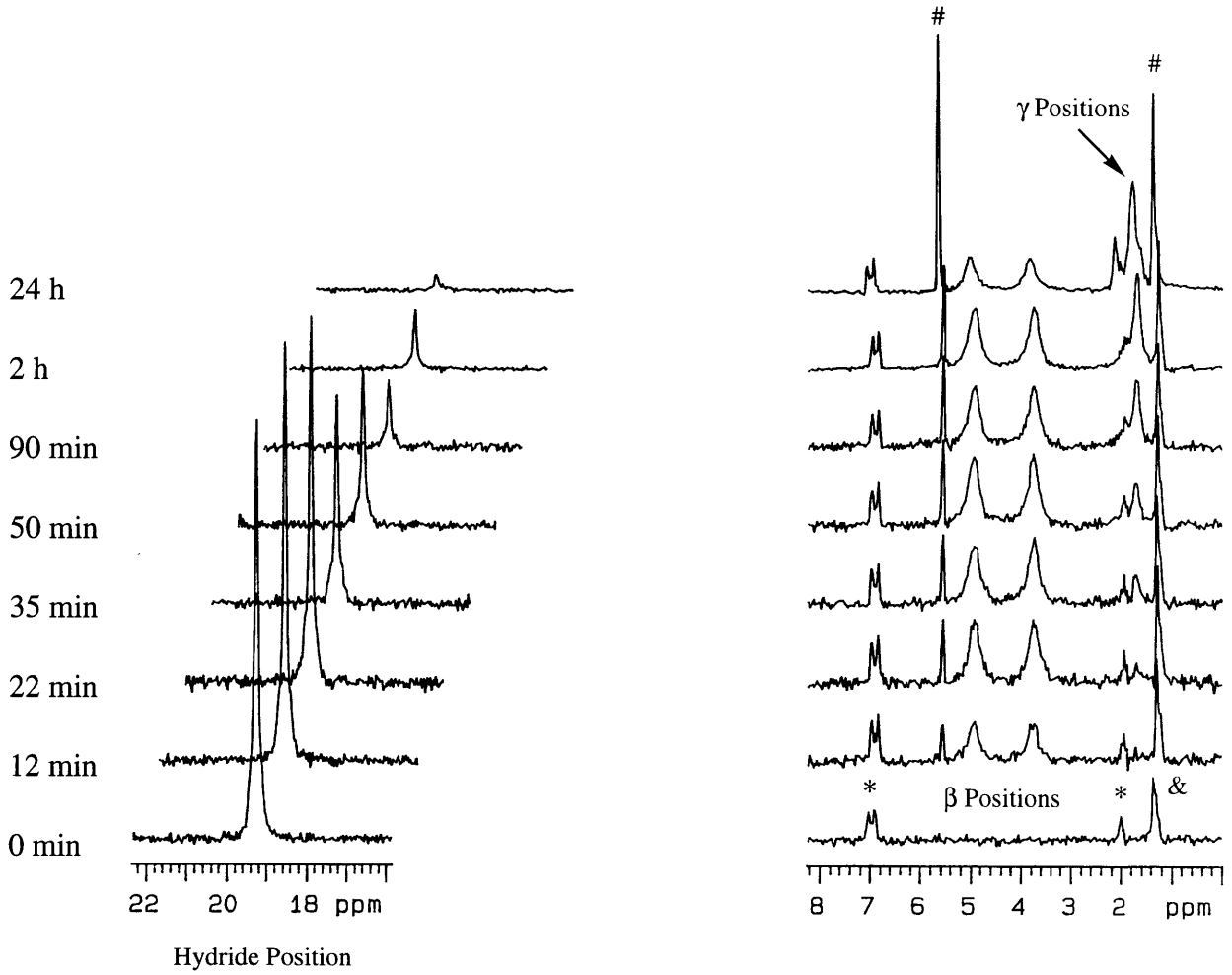

Figure 2.10. 46.0 MHz ^{2}H NMR spectra (at -20 °C) of [N_3N]W(cyclopentylidene)(H)-d_1 as a function of time the sample was kept at 22 °C.

& - cyclopentane-d_1
* - naturally abundant deuterium in the toluene
# - cyclopentene-d_1, a decomposition product (see text)

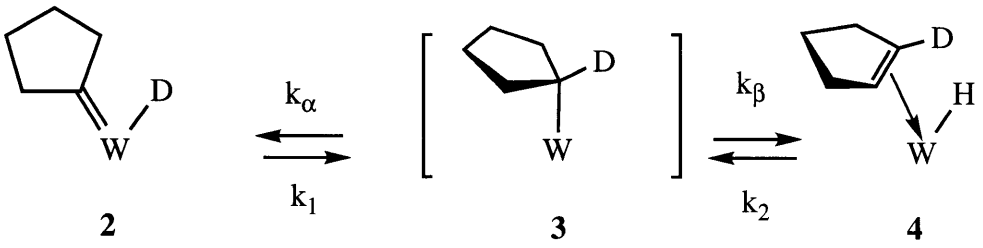

(6)

scrambling of deuterium from the hydride position into the cyclopentylidene ring by plotting the logarithm of its intensity (normalized against the toluene resonance) versus T (Figure 2.11). If we assume the reaction is first-order (the data are not of high enough quality to verify this), the rate constant at 22 °C is 3.7 x 10^{-4} sec^{-1} ($\tau_{1/2}$ = 31 min). Since neither **3** or **4** is directly observed, we have no information about which of these two complexes is the preferred species

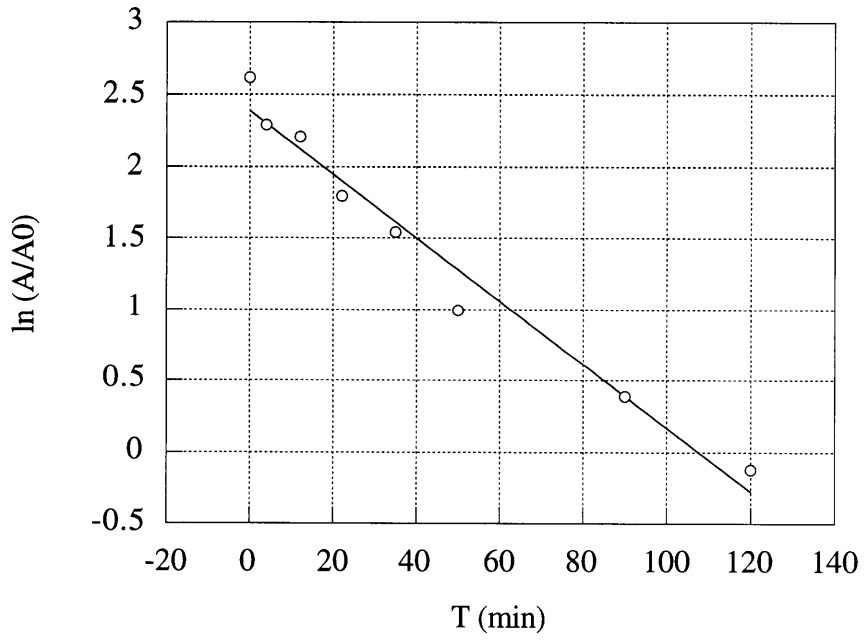

Figure 2.11. Kinetic plot for the decrease of deuterium in the hydride site of **2** over time.

References begin on page 92.

and thus no information about the relative magnitudes of k_β and k_1. Therefore we cannot determine whether we are measuring k_β or k_1 in this case and thus are unable to precisely compare k_α and k_β. The fact that only $[N_3N]W(D)(C_5H_8)$ is observed initially requires that k_α be greater than k_β, and the large difference between k_α (estimated at 10^3 sec^{-1} at 298 K) and k_{obs} for deuterium scrambling (3.7×10^{-4} sec^{-1}) would seem to assure that this is the case. We note that k_β in the molybdenum system was estimated at 5×10^{-4} sec^{-1} (see chapter I). It should also be noted that after 24 h, less deuterium than would be expected on statistical grounds (1/9 of the initial) is present in the hydride site of **2** (Figure 2.10). We attribute this observation to an equilibrium isotope effect.[15] A $\Delta G°$ for the equilibrium between $[N_3N]W(D)(C_5H_8)$ to $[N_3N]W(H)(C_5H_7D)$ can be estimated at -0.8 kcal/mol by considering the changes in the IR stretching frequencies of the bonds involved. Since the increase in bond enthalpy of a C-D bond compared to a C-H bond is greater than the increase in bond enthalpy of a W-D compared to a W-H bond, the situation most thermodynamically stable is that in which the hydrogen is bound to the metal and the deuterium is bound to a carbon on the cyclopentylidene ring. A $\Delta G°$ of -0.8 kcal/mol gives an equilibrium constant of ~4 in favor of $[N_3N]W(H)$(cyclopentylidene-d_1). Thus 25% of 1/9 (~3%) of the original deuterium signal would be expected in the deuteride site at equilibrium, and this is approximately what is observed by integration after 24 hours (Figure 2.10).

$[N_3N]W(H)$(cyclopentylidene) (**2**) decomposes above ~45 °C to give cyclopentene and $[N_3N]WH$ (**5**). Compound **5** has NMR spectra (Figure 2.5) and magnetic susceptibility behavior (Figure 2.4) similar to other d^2 tungsten $[N_3N]$ complexes. Heating **2**-d_1 to 45 °C resulted in the production of **5** and cyclopentene-d_1 in which deuterium was scrambled throughout the ring according to ^1H and ^2H NMR, as expected. The decomposition of **2** is proposed to proceed via formation of the cyclopentyl complex followed by decomposition by β-hydride elimination and olefin loss (equation 7). Kinetics of the transformation from **2** to **5** were followed at 45, 60, and 80 °C by ^1H NMR and the reaction was found to be first-order in **2** through three or more half-

References begin on page 92.

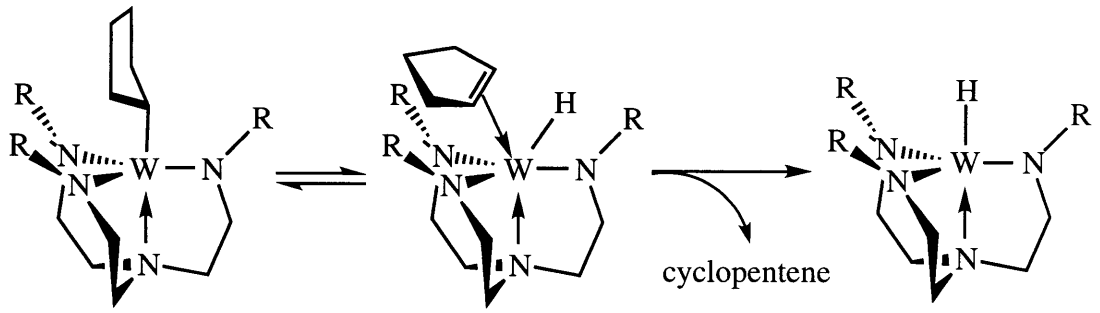

5 (7)

lives. At 80 °C, the rate constant was found to be 1.9(1) x 10^{-3} sec^{-1}. An Eyring plot yielded $\Delta H^{\ddagger}$ = 22.9(3) kcal/mol and $\Delta S^{\ddagger}$ = -6(1) e.u. (see Experimental section for exact values). Thus, the rate constant for cyclopentene loss at 22 °C is calculated to be 2.6 x 10^{-6} sec^{-1}. This is ca. 2 orders of magnitude slower than the rate of deuterium scrambling (k_{obs} = 3.7 x 10^{-4} sec^{-1}).

DISCUSSION

The β-hydride elimination reaction has dominated the decomposition of transition metal alkyls since the first syntheses of these types of complexes were attempted. In fact, it was long believed that the transition metal-carbon bond was inherently unstable because so many early synthetic attempts involved alkyls with β-protons and thus led only to decomposition.[16,17] Once the β-hydride decomposition pathway was elucidated, a wide variety of transition metal alkyls with no β-hydrogens, namely MR species with R =, e. g. Me, CH_2Ph, or CH_2CMe_3, were prepared. An α-elimination reaction to yield an alkylidene hydride complex is a much less well-documented transformation compared to β-hydride elimination to yield an often unstable olefin hydride complex, and α-elimination has always been assumed to be slower than β-elimination. This may in part be due to the fact that alkylidenes are only common for early and middle heavy transition metals such as Mo, W, Ta, and Re.

Previous observations of an equilibrium between an alkyl complex and an alkylidene hydride have usually involved high oxidation state tantalum[18-21] or tungsten[22-24] complexes. $Cp^*_2Ta(CH{=}CH_2)$ was found to decompose via intermediate $Cp^*(\eta^5\text{-}C_5Me_4CH_2CH_2CH_2)Ta$ to

References begin on page 92.

the kinetic product, $Cp^*(\eta^5\text{-}C_5Me_4CH_2CH_2CH)Ta(H)$, by α-elimination, and to the thermodynamic product, $Cp^*(\eta^5\text{-}C_5Me_4CH_2\text{-}\eta^2\text{-}CH{=}CH_2)Ta(H)$, by β-elimination.[18] The rate of α-elimination was determined to be 10^8 times that of β-elimination in this system. However, the authors stated that this result could be a consequence of a transition state for β-elimination which is much more strained than that for α-elimination. A kinetic preference for α-elimination has been demonstrated for $[N_3N]$Mo(cycloalkyl) complexes (see chapter I). We will now compare several $[N_3N]$W(alkyl) complexes with their molybdenum analogs in terms of the alkyl/alkylidene hydride equilibrium.

The equilibrium shown in equation 8 is in effect for M = Mo and W. With the tungsten complex, k_α is greater than $k_{\alpha,rev}$ and the alkylidene hydride is the observed species. At 298 K, [alkyl]/[alkylidene hydride] = ~0.04 for tungsten, and ca. 10^2 or greater for molybdenum. This difference between the two metals can be explained by bond strength and oxidation state arguments. One M-C bond is traded for a M=C bond and a M-H bond with concomitant oxidation of the metal center. A greater difference between the metal-alkylidene and metal-hydride bond strengths compared to the metal-alkyl bond strength would be expected for M = W, since in general tungsten forms stronger bonds than molybdenum. Additionally, tungsten is

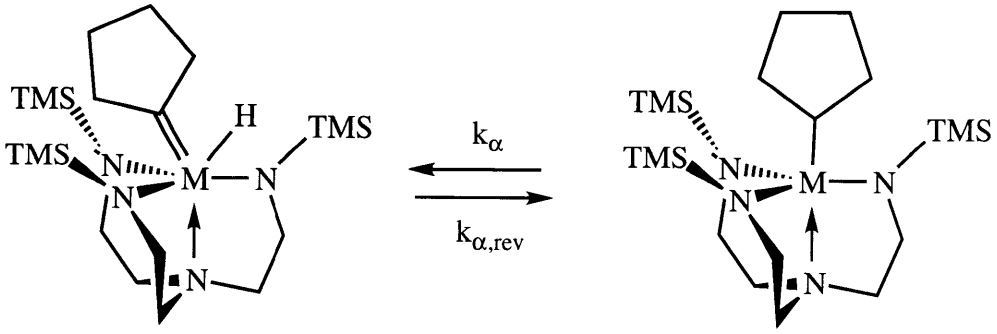

(8)

more easily oxidized than molybdenum, thus providing further thermodynamic drive towards the tungsten alkylidene hydride complex. A ΔΔG° between the tungsten and molybdenum complexes of as little as 5 kcal/mol is all that is required for the observed shifts in K_{eq}. It is perhaps surprising that the α-elimination process occurs at nearly the same rate for molybdenum

References begin on page 92.

and tungsten ($k_{\alpha W}$ and $k_{\alpha Mo}$ are probably within one order of magnitude of each other). This result may be circumstantial, or it may be that the transition state for α-elimination is early on the reaction pathway and hence relatively independent of the nature of the product.

The α,α-dehydrogenation reaction (equation 9) of tungsten alkyls of the type $[N_3N]W(CH_2R)$ has been determined to be many orders of magnitude faster than with $[N_3N]Mo(CH_2R)$ complexes,[2,3] despite the fact that the rates of α-elimination (equation 9; k_α) are nearly the same. The studies performed with $[N_3N]M$(cyclopentyl) complexes provide some explanation for this difference. A thermodynamic preference for the alkylidene hydride species shown in equation 9 with tungsten complexes would mean it is present at an appreciable concentration. Although we have no data on the relative rate of α-abstraction of the alkylidene proton by the hydride for tungsten and molybdenum complexes, the fact that concentration of the molybdenum alkylidene hydride is so low compared to the concentration of the tungsten alkylidene hydride intermediate (as a result of thermodynamic constraints) certainly impedes the final step, loss of H_2, for the molybdenum complexes. These arguments are all consistent with a high thermodynamic stability of the tungsten(VI) species with a triply bonded ligand present in the apical site.

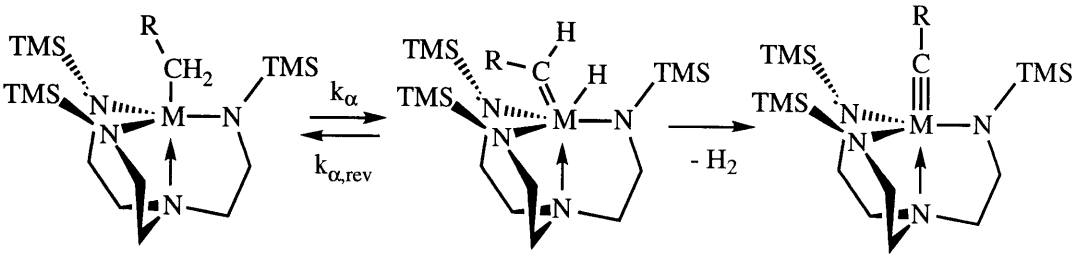

(9)

The transformation of $[N_3N]W$(cyclopentyl) into $[N_3N]W(H)$(cyclopentylidene) must involve conversion to a low-spin species at some point along the reaction path. Presumably, the α-elimination reaction begins with an agostic interaction of the α-proton with the tungsten center. Since $[N_3N]W$(cyclopentyl) has a ^3E ground state, both orbitals available for forming this agostic interaction (the d_{xz} and d_{yz}) contain one electron. Thus, an α-agostic interaction is

References begin on page 92.

not possible unless these electrons pair into one orbital, leading to a ^1A electronic configuration. In earlier work,[1] we raised the possibility that a reaction could be slowed by crossover to a singlet ground state. We thus entertained the notion that the α,α-dehydrogenation reaction could be much faster for tungsten than molybdenum because of a more facile ^3E to ^1A conversion with tungsten. However, all magnetic behavior observed so far has been of the classical type, with the lower moments observed for tungsten complexes readily ascribed to the larger spin-orbit coupling constant for tungsten compared to molybdenum. We conclude that thermodynamic considerations (as discussed above) are better explanations for the faster alkylidyne formation with tungsten as opposed to a more facile spin crossover. We also have no data on whether the triamidoamine ligand remains a true ancillary ligand during the reaction, or if α-proton abstraction is assisted by the amides. Whether or not dissociation of the dative amine donor is required for the reaction to occur is also still unresolved. We hope to be able to test this issue in the future by employing new multiamido/donor ligands with donors other than nitrogen (see chapter V).

EXPERIMENTAL

General Details. All experiments were conducted under nitrogen in a Vacuum Atmospheres drybox, using standard Schlenk techniques, or on a high vacuum line (< 10^{-4} torr). Pentane was washed with HNO_3/H_2SO_4 (5/95 v/v), sodium bicarbonate, H_2O, stored over $CaCl_2$ and then distilled from sodium benzophenone under nitrogen. Regent grade benzene was distilled from sodium benzophenone under nitrogen. Toluene was distilled from molten sodium. Methylene chloride was distilled from CaH_2. Reagent grade ether and THF were sparged with nitrogen and passed through alumina columns.[25] All solvents were stored in the drybox over activated 4 Å molecular sieves. Deuterated solvents were freeze-pump-thaw degassed and vacuum transferred from an appropriate drying agent, or sparged with argon and stored over 4 Å sieves. NMR spectra are recorded in C_6D_6 unless noted otherwise. ^1H and ^{13}C data are listed in parts per million downfield from tetramethylsilane and were referenced using the residual

References begin on page 92.

protonated solvent peak. ^2H NMR spectra usually were obtained at 46.0 MHz and are referenced externally to C_6D_6 (7.15 ppm) in C_6H_6. Probe temperatures during variable temperature studies were calibrated with methanol (low T) or ethylene glycol (high T). Coupling constants are given in hertz, and routine couplings are not listed. Elemental analyses (C, H, N) were performed on a Perkin-Elmer 2400 CHN analyzer in our own laboratory.

$[N_3N]WCl$, $[N_3N]WMe$, $[N_3N]WPh$, $[N_3N]WH$, $[N_3N]W{\equiv}CR$ complexes, $[N_3N]W$-(cyclo-$CHCH_2CH_2CH_2$), and $[N_3N]W$(cyclopentylidene)(H) were synthesized as described in the literature.[6] 1-Deuterocyclopentyllithium was prepared by reduction of cyclopentanone with lithium aluminum deuteride followed by treatment with Ph_3PBr_2 in DMF.[26] The bromide was converted to the lithium reagent by reaction with lithium powder in refluxing hexane. The lithium reagent was recrystallized from pentane before use. $Li^{13}CH_2CH_2CH_2CH_3$ was prepared by treating $^{13}CO_2$ with n-PrMgCl, reducing the acid with $LiAlH_4$ to the alcohol, chlorinating the alcohol with $SOCl_2$/pyridine in hexane, and finally treating the chloride with lithium wire in the usual manner; overall yield ~20%. $LiCD_2CH_2CH_2CH_3$ was prepared by treating butyryl chloride with $LiAlD_4$ in ether and then following subsequent steps as described for the ^{13}C-labeled reagent.

Rate constants of dynamic NMR processes were obtained by using the equation $k = (\pi/\sqrt{2}) \cdot (\Delta\nu)$; where $\Delta\nu$ = the frequency difference between the two resonances which are exchanging and k is the rate constant at the coalescence temperature.

Procedure for determining the rate of deuterium scrambling in $[N_3N]W(D)$-(cyclopentylidene). A solution of 1-deuterocyclopentyllithium (10 mg, 0.13 mmol) in ~300 μL toluene was prepared and cooled to -40 °C in the drybox. This was added to a -40 °C slurry of $[N_3N]WCl$ (50 mg, 0.086 mmol) in ~200 μL toluene. After the solution was quickly mixed, it was added to a 9" NMR tube with a female 14/20 joint. A needle valve was placed on top and the tube was removed from the drybox, frozen, and flame-sealed. The tube was kept in liquid nitrogen during transport to the NMR spectrometer. It was then thawed and monitored by ^2H

References begin on page 92.

NMR. NMR spectra were acquired at -20 °C, a temperature where interconversion with [N_3N]W(cyclopentyl) is slow on the NMR time scale. The reaction times in Figure 2.10 represent total reaction time at room temperature.

Kinetic study of the decomposition of [N_3N]W(H)(cyclopentylidene). The reaction was followed by ^1H NMR in toluene-d_8 at 0.02 M. Protio toluene was used as an internal standard. Probe temperatures were calibrated with either methanol or ethylene glycol both before and after runs were performed, temperature drift was less than 0.5 K. Values for the rate constants (10^{-4} sec^{-1}) at temperature T (deg K) are: 0.48 (318), 2.3 (333), 18 (353), 20 (353). A plot of ln(k/T) versus 1/T gave $\Delta H^{\ddagger}$ = 22,916 cal/mol and $\Delta S^{\ddagger}$ = -6.44 e.u.

X-ray Structure of [N_3N]W(cyclo-$CHCH_2CH_2CH_2$). Suitable crystals were grown from pentane at -40 °C. Crystallographic data, collection parameters, and refinement parameters for this study can be found in Table 2.2, and selected bond lengths and angles are located in Table 2.1. General details for the experimental procedures[27] can be found elsewhere.

Solid-State Magnetic Susceptibility Measurements. SQUID experiments were performed on a Quantum Design 5.5 T instrument running MSRP2 software. Samples were prepared in an N_2-filled drybox. A gelatin capsule and 2.2 × 1.9 cm piece of parafilm were weighed. The capsule was then loaded with the sample and the parafilm was folded and packed on top using plastic tongs. The capsule was closed and weighed again to determine the sample mass. It was then suspended in a straw. The straw was placed in a plastic bottle with a screw cap and the bottle was tightly sealed. At the instrument the straw was quickly attached to the sample rod and transferred to the helium atmosphere. Measurements were taken in 1 degree intervals from 5-10 K, 2 degree intervals from 12-20 K, 3 degree intervals from 23-50 K, 5 degree intervals from 55-100 K, 10 degree intervals from 110-200 K, and 20 degree intervals from 220-300 K, see Table 1.1. A background measurement of an empty gel capsule, parafilm square, and straw was taken over the entire temperature range. These values were subtracted from the observed susceptibility at each temperature.

References begin on page 92.

REFERENCES

(1) Schrock, R. R.; Shih, K.-Y.; Dobbs, D.; Davis, W. M. *J. Am. Chem. Soc.* **1995**, *117*, 6609.

(2) Shih, K.-Y.; Totland, K.; Seidel, S. W.; Schrock, R. R. *J. Am. Chem. Soc.* **1994**, *116*, 12103.

(3) Schrock, R. R.; Seidel, S. W.; Mösch-Zanetti, N. C.; Shih, K.-Y.; O'Donoghue, M. B.; Davis, W. M.; Reiff, W. M. *J. Am. Chem. Soc.* , in press.

(4) Cummins, C. C.; Schrock, R. R.; Davis, W. M. *Organometallics* **1992**, *11*, 1452.

(5) Persson, C.; Andersson, C. *Inorg. Chim. Acta* **1993**, *203*, 235.

(6) Schrock, R. R.; Seidel, S. W.; Zanetti-Mösch, N. C.; Dobbs, D. A.; Shih, K.-Y.; Davis, W. M. *Organometallics* , in press.

(7) Figgis, B. N.; Lewis, J. *Prog. Inorg. Chem.* **1964**, *6*, 37.

(8) Evans, D. F. *J. Chem. Soc.* **1959**, 2003.

(9) Liang, L.-C., unpublished results.

(10) Schrock, R. R. *Acc. Chem. Res.* **1997**, *30*, 9.

(11) Murdzek, J. S.; Schrock, R. R. In *Carbyne Complexes*; VCH: New York, 1988.

(12) Gütlich, P.; McGarvey, B. R.; Kläui, W. *Inorg. Chem.* **1980**, *19*, 3704.

(13) Kläui, W.; Eberspach, W.; Gütlich, P. *Inorg. Chem.* **1987**, *26*, 3977.

(14) Smith, M. E.; Andersen, R. A. *J. Am. Chem. Soc.* **1996**, *118*, 1119.

(15) Carpenter, B. K. *Determination of Organic Reaction Mechanisms*, Wiley: New York, 1984.

(16) Collman, J. P.; Hegedus, L. S.; Norton, J. R.; Finke, R. G. *Principles and Applications of Organotransition Metal Chemistry*, University Science Books: Mill Valley, 1987.

(17) Schrock, R. R.; Parshall, G. W. *Chem. Rev.* **1976**, *76*, 243.

(18) Parkin, G.; Bunel, E.; Burger, B. J.; Trimmer, M. S.; Asselt, A. v.; Bercaw, J. E. *J. Molec. Catal.* **1987**, *41*, 21.

(19) Turner, H. W.; Schrock, R. R. *J. Am. Chem. Soc.* **1982**, *104*, 2331.

(20) Turner, H. W.; Schrock, R. R.; Fellmann, J. D.; Holmes, S. J. *J. Am. Chem. Soc.* **1983**, *105*, 4942.

(21) van Asselt, A.; Burger, B. J.; Gibson, V. C.; Bercaw, J. E. *J. Am. Chem. Soc.* **1986**, *108*, 5347.

(22) Cooper, N. J.; Green, M. L. H. *J. Chem. Soc., Chem. Commun.* **1974**, 209.

(23) Cooper, N. J.; Green, M. L. H. *J. Chem. Soc., Chem. Commun.* **1974**, 761.

(24) Cooper, N. J.; Green, M. L. H. *J. Chem. Soc., Dalton Trans.* **1979**, 1121.

(25) Pangborn, A. B.; Giardello, M. A.; Grubbs, R. H.; Rosen, R. K.; Timmers, F. J. *Organometallics* **1996**, *15*, 1518.

(26) Wiley, G. A.; Hershkowitz, R. L.; Rein, B. M.; Chung, B. C. *J. Am. Chem. Soc.* **1964**, *86*, 964.

(27) Rosenberger, C.; Schrock, R. R.; Davis, W. M. *Inorg. Chem.* **1997**, *36*, 123.

CHAPTER III

Tungsten(VI) and Molybdenum(VI) Alkyl and Alkylidyne Complexes

That Contain the $[(C_6F_5NCH_2CH_2)_3N]^{3-}$ Ligand.

A portion of the material covered in this chapter has appeared in print:

Shih, K.-Y.; Totland, K.; Seidel, S. W.; Schrock, R. R. *J. Am. Chem. Soc.*, **1994**, *116*, 12103.

INTRODUCTION

The chemistry of triamidoamine ligands with molybdenum and tungsten in mid- to high oxidation states has interested us for some time. The triamidoamine ligand allows for the preparation of group six metal complexes in the relatively rare +4 oxidation state. Organometallic compounds of the type $[(Me_3SiNCH_2CH_2)_3N]MR$ (M = Mo, W) have displayed a wide variety of unique reactivity patterns. A molybdenum cyclopentyl complex with this ligand undergoes rapid and reversible α-hydride elimination at a rate many orders of magnitude faster than it undergoes β-hydride elimination.[1] Additional studies have shown that alkyls of the type $[N_3N]MCH_2R$ (M = Mo, W, $[N_3N] = [(Me_3SiNCH_2CH_2)_3N]^{3-}$) can decompose thermally to give alkylidynes and molecular hydrogen, in some cases rapidly at room temperature.[2,3] Alkylidynes are formed by many other unusual routes, including coupling of terminal acetylides[4] and cleavage of C-C bonds in strained cycloalkane rings.[1,3] $[N_3N]$ ligands provide a sterically protected environment for the apical ligand, which is shrouded by the trialkylsilyl groups on the amido nitrogens. This steric shielding is likely the reason such unconventional reactivity has been discovered; reactive intermediates are kinetically stabilized by the bulky amido nitrogen substituents.

One limitation with the use of silylated triamidoamine ligands for molybdenum and tungsten complexes is that the $[N_3N]MCl$ starting materials can be prepared only in low yield (15-35%). We suspect that loss of TMSCl and reduction of the metal are side reactions which limit the efficiencies of these metatheses. A related triamidoamine ligand, $[(C_6F_5NHCH_2CH_2)_3N]$, abbreviated as $[N_3N_F]H_3$, reacts with metal tetrachlorides in the presence of triethylamine to give $[N_3N_F]MCl$ (M = Mo, W) complexes in good yields (70-80%).[5] Presumably, such reactions proceed in better yield because of the decreased lability of the $N\text{-}C_6F_5$ linkage relative to the $N\text{-}SiR_3$ bond, and less reducing nature of these perfluorophenyl ligands. The $[N_3N_F]^{3-}$ ligand provides a different steric and electronic environment around the metal, and we wondered how this difference would affect the chemistry of $[N_3N_F]$ complexes as compared to their silylated tren analogs. This chapter will describe the

References begin on page 122.

synthesis of alkyl and alkylidyne complexes that contain the $[N_3N_F]^{3-}$ ligand. The alkylidyne syntheses utilize reactions which were first discovered with the silylated tren ligand system, such as the loss of molecular hydrogen from complexes of the type $[N_3N]M(CH_2R)$ and the loss of ethylene from tungsten cyclopropyl complexes.

$[N_3N_F]$-based alkylidynes can be synthesized by more conventional methods as well. We have recently become interested in complexes containing dianionic, tridentate diamidoamine ligands for titanium, zirconium, and tantalum complexes.[6,7] Changing from a triamido to a diamido ligand opens up another coordination site at the metal, potentially allowing for a wider variety of reactivity. C_6F_5-substituted diamidoamine ligands, such as $[(C_6F_5NCH_2CH_2)_2NH]^{2-}$, have been prepared and used for the synthesis of tantalum complexes.[6] This chapter will describe more a customary synthesis of alkylidyne complexes that contain the C_6F_5-substituted diamidoamine ligand.

RESULTS

Synthesis of Tungsten and Molybdenum Organometallic Complexes

Alkylation of paramagnetic $[N_3N_F]WCl$[5] with $LiCH_2R$ (R = CMe_3, $SiMe_3$, Me, *n*-Pr) reagents in toluene at room temperature leads to evolution of molecular hydrogen and formation of the corresponding tungsten(VI) alkylidynes as shown in equation 1. $[N_3N_F]W{\equiv}CPh$ (**1c**) can be prepared similarly from $[N_3N_F]WI$ (**1f**). Hydrogen was observed by ^1H NMR analysis of a

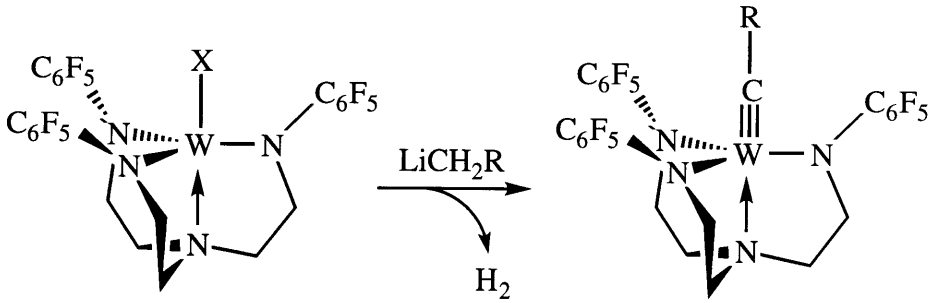

(1)

R = Me (**1a**), *n*-Pr (**1b**), Ph (**1c**), $SiMe_3$ (**1d**), or CMe_3 (**1e**)
X = Cl, I

References begin on page 122.

reaction between $[N_3N_F]WCl$ and $LiCH_2SiMe_3$ run in a flame-sealed NMR tube (the chemical shift of dihydrogen in toluene-d_8 is 4.5 ppm). We presume that the first step in this process is formation of $[N_3N_F]W(CH_2R)$, which then undergoes loss of molecular hydrogen to give the alkylidyne. The light tan or brown solids are isolated in 50-70% yield. These alkylidynes are not very soluble in hydrocarbons, and the alkylation reactions proceed essentially heterogeneously in toluene ($[N_3N_F]WCl$ is only sparingly soluble in that solvent). Interestingly, attempts to alkylate $[N_3N_F]WCl$ homogeneously in THF led only to decomposition. We also note that $[N_3N_F]WCl$ does not react with Grignard reagents at room temperature. Alkylidyne ^{13}C chemical shifts range from 281 to 296 ppm. J_{CW} for $[N_3N_F]W{\equiv}^{13}CCH_2CH_2CH_3$ was determined to be 254 Hz by alkylating with $Li^{13}CH_2CH_2CH_2CH_3$. These NMR parameters are in line with those of other d^0 alkylidyne complexes.[8]

Qualitative differences are noticed in the rates of alkylidyne formation depending on the nature of the alkylating agent. In particular, when $LiCH_2SiMe_3$ reacts with $[N_3N_F]WCl$, the solution turns red initially, but over the course of a day the color lightens. After two days, $[N_3N_F]W{\equiv}CSiMe_3$ can be isolated in 72% yield. This relatively slow reaction led us to wonder if an intermediate alkyl complex could be isolated before decomposition to the trimethylsilylmethylidyne occurs. Reaction of the tungsten chloride with $LiCH_2SiMe_3$ at -10 °C for one hour gave a red solid precipitate which displayed ^1H and ^{19}F NMR spectra indicative of a paramagnetic complex, as expected for d^2 $[N_3N_F]W(CH_2SiMe_3)$ (**1g**). This complex decomposes in a first-order manner to yield $[N_3N_F]W{\equiv}CSiMe_3$. The transformation was followed by ^{19}F NMR with 0.01 M THF solutions of **1g** at five temperatures from 16 to 53 °C (see experimental section for details). A plot of ln(k/T) versus 1/T (Figure 3.1) yielded a $\Delta H^{\ddagger}$ of 20.3 ± 0.2 kcal/mol and a $\Delta S^{\ddagger}$ of -7 ± 1 e.u. (R = 0.999). The rate constant at 298 K is calculated to be 2.3×10^{-4} sec^{-1}. These values may be compared only qualitatively to those found with trimethylsilyl-substituted complexes. During the alkylation of $[(TMSNCH_2CH_2)_3N]WCl$ with $LiCH_2SiMe_3$, alkylidyne formation is complete within 2 h and no evidence of intermediate $[N_3N]W(CH_2SiMe_3)$ is observed.[3] If we assume that 2 h (or less) represents five half-lives for

References begin on page 122.

this decomposition, then the rate constant is ~5 x 10^{-4} (or greater). Thus, the trimethylsilyl-substituted analog decomposes at least twice as fast as $[N_3N_F]W(CH_2SiMe_3)$ does at room temperature.

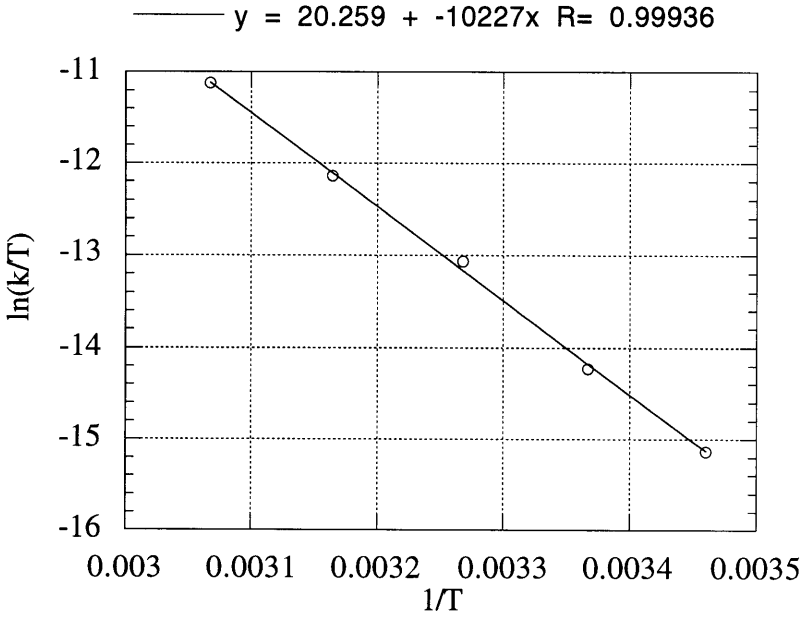

Figure 3.1. Eyring plot for the decomposition of $[N_3N_F]W(CH_2SiMe_3)$ between 16 and 53 °C.

An X-ray study of $[N_3N_F]W{\equiv}CSiMe_3$ (**1d**) was carried out. A view of its structure is shown in Figure 3.2. Bond distances and angles can be found in Table 3.1. Crystallographic data can be found in Table 3.2. As is typically observed in structures of complexes containing the $[(C_6F_5NCH_2CH_2)_3N]^{3-}$ ligand, the aryl rings form a "bowl" around the ligand trans to the dative amine donor. Qualitatively, the size of the cavity in which the apical ligand resides is much greater than in complexes containing the $[(TMSNCH_2CH_2)_3N]^{3-}$ ligand (see Chapter I).[1] Whether or not this cavity is maintained in solution cannot be ascertained for this particular complex, however, in a related diamidoamine complex, restricted rotation of the aryl rings is observed on the NMR timescale up to 110 °C (see below). The W-C triple bond distance (1.768(6) Å) is in the range normally observed for tungsten alkylidynes.[8] The W-N(4) distance

References begin on page 122.

(2.323(4) Å) and the W-N(1), N(2), and N(3) distances (1.963(5) to 1.973(4) Å) are similar to those observed in other W(VI) triamidoamine complexes. The dihedral angle between N(4)-W and the N(1)-C(1) is 173.6° and values for the other amides are similar. These angles are close to what is observed in the structure of $[N_3N_F]MoCl$,[5] and are indicative of little steric strain in the molecule (cf. $[N_3N]Mo$(cyclohexyl), Table 1.3).

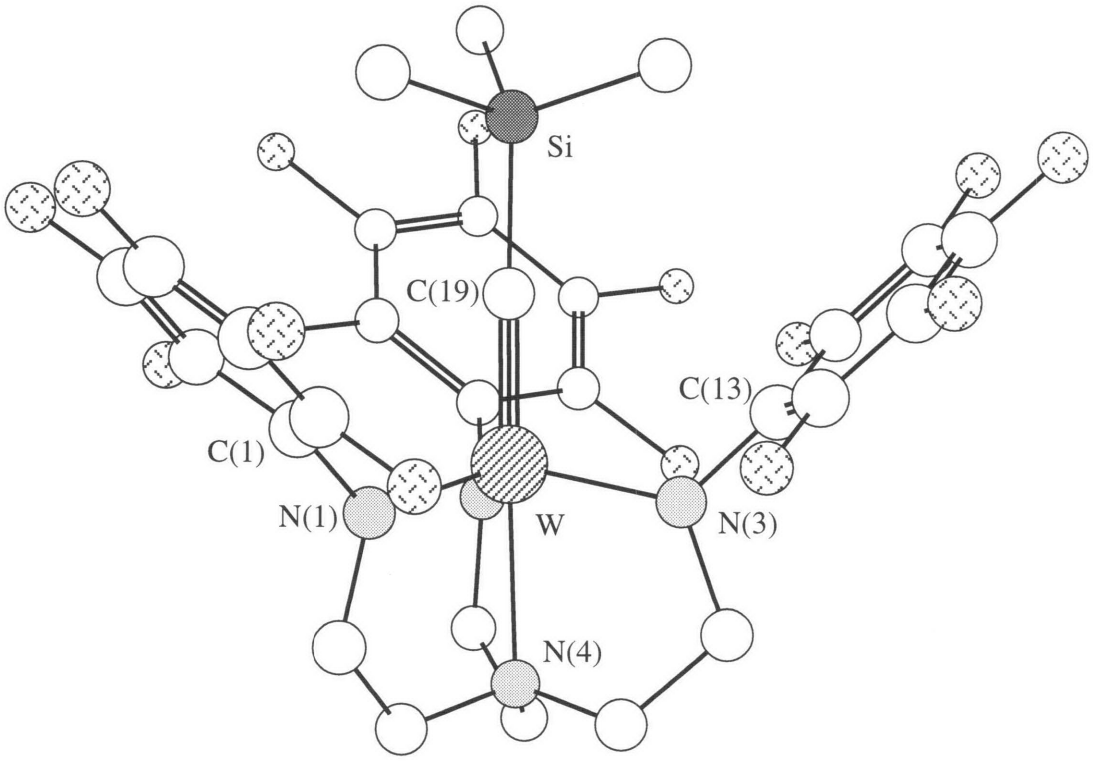

Figure 3.2. A view of the structure of $[N_3N_F]W{\equiv}CSiMe_3$ (**1d**).

Table 3.1. Selected bond distances (Å) and angles (deg.) for $[N_3N_F]W{\equiv}CSiMe_3$ (**1d**).

Distances (Å)

W - C(19)	1.768(6)	W - N(1)	1.973(4)
W - N(2)	1.963(5)	W - N(3)	1.968(4)
W - N(4)	2.323(4)	Si - C(19)	1.876(6)
C(1) - N(1)	1.411(7)	C(13) - N(3)	1.422(7)

Angles (deg.)

W - C(19) - Si	176.9(4)	N(1) - W - N(2)	116.4(2)
N(2) - W - N(3)	114.8(2)	C(13) - N(3) - W	126.5(3)
W - N(1) - C(1)	126.8(3)	N(4) - W - C(19)	177.3(2)
N(1) - W - C(19)	102.0(2)	N(3) - W - N(4)	78.0(2)

Dihedral Angles (deg.)[a]

N(4) - W - N(1) - C(1)	173.6
N(4) - W - N(3) - C(13)	175.4

[a] From a Chem 3D drawing

References begin on page 122.

Table 3.2. Crystallographic data, collection parameters, and refinement parameters for $[N_3N_F]W{\equiv}CSiMe_3$ (**1d**).

Empirical Formula	$C_{28}H_{23}N_4F_{15}SiW$
Formula Weight	912.43
Diffractometer	Enraf-Nonius CAD-4
Crystal Dimensions (mm)	$0.280 \times 0.280 \times 0.240$
Crystal Color, Habit	Yellow, Prismatic
Crystal System	Monoclinic
a (Å)	9.285(2)
b (Å)	28.268(5)
c (Å)	12.054(2)
β (deg)	100.25(2)
V (Å^3)	3133(2)
Space Group	$P2_1/c$
Z	4
D_{calc} (Mg/m^3)	1.946
F_{000}	1768
μ (MoK_α)	39.41 cm^{-1}
Scan Type	ω
Temperature (K)	187
λ (MoK_α)	0.71069 Å
Absorption Correction	Lorentz-polarization (Trans. factors: 0.92 - 1.10)
Structure Solution	Patterson Method
Refinement	Full-matrix least-squares
Number of Observations [I>3σ(I)]	5512
R	0.032
R_W	0.035
GoF	1.37
Largest Diff. Peak and Hole (eÅ^{-3})	0.99 and -0.96

References begin on page 122.

Attempts to prepare $[N_3N_F]W(CH_3)$ were not successful, and therefore we were unable to determine if this methyl compound undergoes the α,α-double dehydrogenation reaction to yield $[N_3N_F]W{\equiv}CH$ (**1h**). $[N_3N_F]WX$ (X = Cl, I, OTf, 3,5-dimethylphenoxide) slowly decomposes when treated with MeLi or MeLi·TMEDA in toluene (not every permutation was attempted). Ethereal solvents led to more rapid decomposition. Treating $[N_3N_F]WI$ with MeMgCl in CH_2Cl_2 results in almost no reaction. In some cases during reactions with MeMgCl or MeLi, a trace of diamagnetic product was observed which might be $[N_3N_F]W{\equiv}CH$, but none could ever be isolated. $[N_3N_F]WCl$ does not react with Me_3Al in toluene at 60 °C for 2 h. $[N_3N_F]W{\equiv}CH$ could be prepared, however, by reacting $[N_3N_F]WCl$ with cyclopropyllithium in toluene. We presume that this reaction proceeds as in the analogous silylated tren complex, where an initially formed tungsten cyclopropyl complex loses ethylene to yield the methylidyne (equation 2).[3] The light orange microcrystalline solid displays a characteristic low-field ^{13}C resonance[8] for the methylidyne carbon at 284.3 ppm, and a resonance at 5.24 ppm ($^2J_{HW}$ = 76 Hz) in the ^1H NMR spectrum for the methylidyne proton. When a C_6H_6 solution of **1h** is treated with ~4 atm D_2 in a sealed NMR tube at 70 °C for 18 h, no $[N_3N_F]W{\equiv}C\text{-}D$ was detected by ^2H NMR. It appears that, just as with the TMS-substituted alkylidynes,[2] the α,α-double dehydrogenation reaction is irreversible.

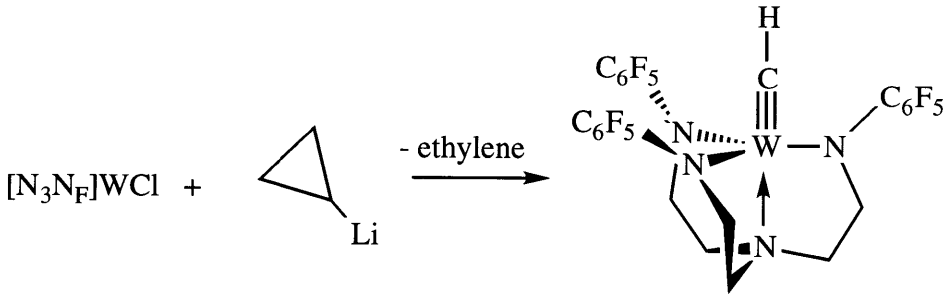

(2)

1h

$[N_3N_F]MoCl$[5] reacts with $LiCH_2SiMe_3$ and $LiCH_2CMe_3$ in toluene to yield the corresponding alkyl complexes, $[N_3N_F]Mo(CH_2CMe_3)$ (**2a**) and $[N_3N_F]Mo(CH_2SiMe_3)$ (**2b**). In stark contrast to the tungsten analogs discussed above, these complexes are stable towards

References begin on page 122.

dihydrogen loss at room temperature. Increased stability of molybdenum alkyls is also observed with $[N_3N]^{3-}$ complexes.[1] Upon thermolysis at 121 °C, **2a** is converted cleanly to $[N_3N_F]Mo{\equiv}CCMe_3$ (**2c**) in a first-order reaction. The rate constant at 121 °C in toluene is 7.9(5) x 10^{-5} sec^{-1} and is independent of concentration over a threefold range. as determined via UV-Vis spectroscopy. This value should be compared to the rate constant for the decomposition of the silylated analog, $[N_3N]Mo(CH_2CMe_3)$, which was found to be 9.41 x 10^{-4} sec^{-1} at 121 °C.[1] $[N_3N_F]Mo(CH_2SiMe_3)$ could not be converted to the corresponding alkylidyne by thermolysis at 85 °C for 5 days.

Mechanistic Studies of Alkylidyne Formation

We propose that the loss of molecular hydrogen from $[N_3N]^{3-}$ and $[N_3N_F]^{3-}$ tungsten(IV) alkyl complexes involves an α-elimination to yield an unobserved alkylidene hydride complex, which then undergoes intramolecular α-abstraction of the alkylidene proton by the hydride, yielding dihydrogen and the alkylidyne (equation 3). Corroboration of this mechanism came with the observation that paramagnetic $[N_3N]W$(cyclopentyl) is in equilibrium with its α-elimination product, $[N_3N]W(H)(C_5H_8)$, and that the equilibrium constant is ~28 in favor of the alkylidene hydride complex at room temperature.[3,9]

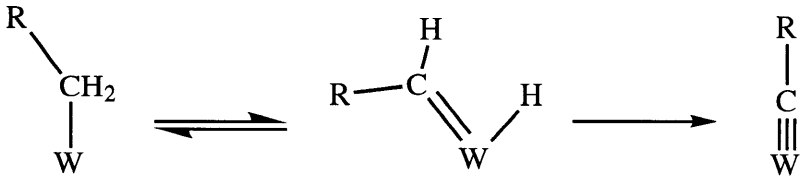

(3)

The observation that alkylidynes are still formed smoothly even when β-protons are present on the alkyl, as in the reaction between $[N_3N_F]WCl$ and BuLi to give **1b**, led us to wonder if the α-processes involved in the loss of molecular hydrogen from unobserved $[N_3N_F]W(CH_2CH_2CH_2CH_3)$ were actually occurring faster than β-hydride elimination. A kinetic preference for α-elimination over β-elimination has been demonstrated for both tungsten

References begin on page 122.

and molybdenum complexes that contain the TMS-substituted triamidoamine ligand.[1,3] Reaction of $[N_3N_F]WCl$ and $LiCD_2CH_2CH_2CH_3$ leads to the formation of **1b** which contains a statistical amount of deuterium scrambled throughout the propyl chain.

We propose that the mechanism for scrambling involves a β-hydride elimination of $[N_3N_F]W(CD_2CH_2CH_2CH_3)$ to give an olefin hydride complex, which can then undergo migratory insertion of the olefin into the hydride to yield the *sec*-butyl complex. A series of β-hydride elimination-migratory insertion reaction sequences could eventually afford to an *n*-butyl complex with scrambled deuterons which then finally undergoes the loss of dihydrogen (Scheme 3.1). Further support of this mechanism was obtained by reacting $[N_3N_F]WCl$ with $Li^{13}CH_2CH_2CH_2CH_3$, yielding **1b** with ~50% ^{13}C label at the alkylidyne carbon, and ~50% ^{13}C label at the terminal carbon on the propyl chain. These results with the C_6F_5-triamidoamine ligand system should be compared to those observed with the TMS-triamidoamine ligand complexes. When $[N_3N]WCl$ is reacted with $LiCD_2CH_2CH_2CH_3$, D_2 gas is lost and the butylidyne product contains only hydrogen, as evidenced by ^2H NMR.[2] Similarly, when $[N_3N]WCl$ is reacted with $Li^{13}CH_2CH_2CH_2CH_3$, the product formed is labeled exclusively at the alkylidyne carbon.[3] Thus, with the TMS-substituted complexes, the α-processes involved in loss of molecular hydrogen from $[N_3N]W$(*n*-butyl) are apparently faster than the β-processes required to scramble the labels in these alkyls, in line with the previous demonstration of a kinetic preference for α-elimination with TMS-substituted complexes.[3,9] It seems reasonable to attribute this difference between the $[N_3N]^{3-}$ complexes and their $[N_3N_F]^{3-}$ analogs in terms of relative rates of α and β processes to a greater degree of steric shielding from the TMS groups which may prevent the β-hydrogen from interacting with the metal center. Steric effects have been used in the past to rationalize preferential α versus β abstraction[10,11] and elimination[12-14] processes. Additionally, the α-process resulting in alkylidyne formation may be slower with complexes containing the fluorinated ligand system as a result of a metal center which is more electron-poor than that in $[N_3N]^{3-}$ complexes. Since α-elimination, the proposed first step in

References begin on page 122.

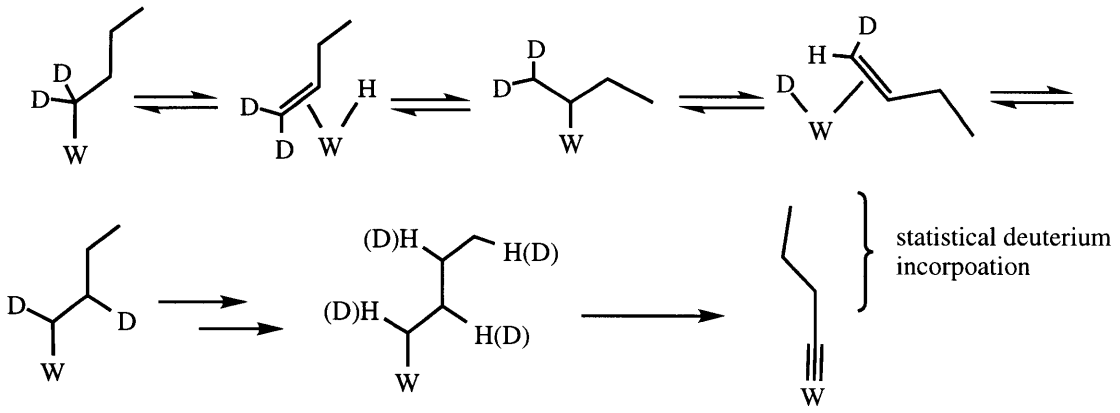

Scheme 3.1. Scrambling of deuterium during the formation of $[N_3N_F]W{\equiv}C\text{-}n\text{-}Pr\text{-}d_{1.5}$.

loss of H_2 from the alkyls (equation 3), requires oxidation of the metal from W(IV) to W(VI), it seems likely that an electron-poor metal center would be less able to undergo this first step. Cyclic voltammetry studies have shown that complexes containing the $[N_3N_F]^{3-}$ ligand are generally more difficult to oxidize than those containing the $[N_3N]^{3-}$ ligand. The inductive effect of the 15 fluorine atoms present in C_6F_5-substituted complexes is likely the reason for this difference.

Several additional experiments were carried out in order to substantiate the mechanism shown in Scheme 3.1. $[N_3N_F]WCl$ reacts with *sec*-butyllithium to yield the linear butylidyne, $[N_3N_F]W{\equiv}CCH_2CH_2CH_3$. This result lends credence to the notion that a *sec*-butyl intermediate can "walk" along the metal to yield a straight-chain butylidyne. We also investigated the formation of $[N_3N_F]W{\equiv}CMe$ (**1a**) by a similar labeling study to determine if β-hydride elimination competes with the loss of molecular hydrogen in this reaction as well. $[N_3N_F]WCl$ reacts with $LiCH_2CD_3$ to yield $[N_3N_F]W{\equiv}CMe$ which contains hydrogen scrambled with deuterium in the methyl group. Apparently β-processes again compete with α-processes during the formation of **1a**.

References begin on page 122.

Diamidoamine Alkylidyne Complexes

Addition of tungsten neopentylidyne trichloride DME adduct to an ethereal solution of $[(C_6F_5NHCH_2CH_2)_2NH]$[6] in the presence of triethylamine leads to the formation of yellow $[(C_6F_5NHCH_2CH_2)_2NH]W{\equiv}CCMe_3(Cl)$ (**3a**) in 79% yield (equation 4). ^1H NMR spectra of this complex show diastereotopic geminal methylene ligand backbone protons as well as a broad triplet for the proton bound to the dative amine. A band is observed in the infrared spectrum of the complex at 3306 cm^{-1} (Nujol mull) which we assign to the secondary amine N-H stretch. We feel that the most reasonable structure for the molecule is that shown in equation 4, a "two-armed" complex directly analogous to the $[N_3N_F]^{3-}$ tungsten alkylidyne complexes described above. The high stability of triamidoamine complexes with triply-bonded ligands in the site trans to the amine donor and the remarkably diverse routes which can be followed to form them are now well-established.[1,15,16] The decrease in symmetry upon going from a triamidoamine alkylidyne complex to **3a**, C_{3v} to C_s, should not result in large changes of the d-orbital energies. Thus, we believe that **3a** is highly stable for the same reasons the triamidoamine complexes discussed above are (see discussion section).

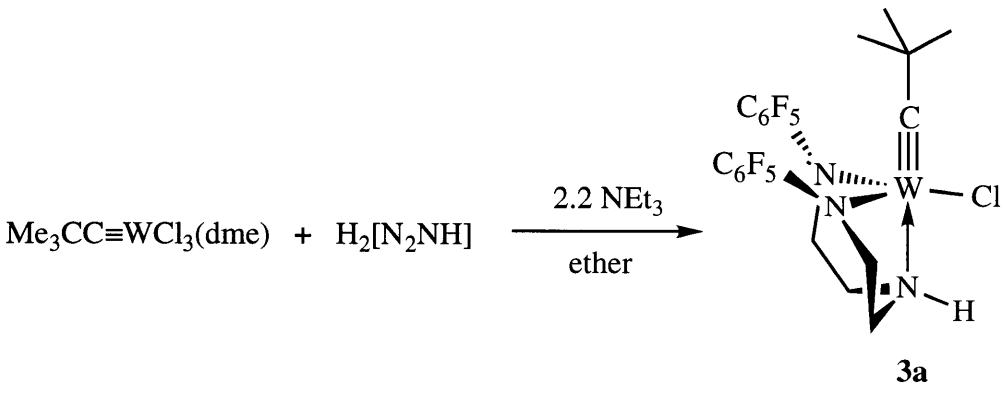

3a (4)

$[N_2NH]W{\equiv}CCMe_3(Cl)$ ($[N_2NH]^{2-}$ = $[(C_6F_5NCH_2CH_2)_2NH]^{2-}$) is smoothly alkylated with methyllithium and ethyllithium in toluene to give $[N_2NH]W{\equiv}CCMe_3(R)$ (R = Me (**3b**) or Et (**3c**)). No tendency for deprotonation of the secondary amine in **3a** is observed. In fact, $[N_2NH]W{\equiv}CCMe_3(Me)$ does not lose methane even when heated to 75 °C. **3a** also reacts with

References begin on page 122.

sodium acetylide in THF to yield a parent acetylide complex, $[N_2NH]W{\equiv}CCMe_3(C{\equiv}CH)$ (**3d**). ^{19}F NMR spectra of **3a**, **3b**, and **3c** and show that all five ring fluorines are inequivalent in these complexes on the NMR timescale at room temperature. These fluorines remain equivalent up to 110 °C for **3a**. Typically, a three-set pattern is observed in ^{19}F NMR spectra of diamagnetic complexes containing the $[N_3N_F]^{3-}$ ligand (see experimental section for $[N_3N_F]M{\equiv}CR$ complexes). We attribute the NMR parameters these $[N_2NH]^{2-}$ complexes display to hindered rotation about the F_5C_6-N bond. One would not expect rotation about this bond to be more difficult in complexes **3a** through **3c** than in their $[N_3N_F]M{\equiv}CR$ counterparts. However, the lower symmetry present in the $[N_2NH]^{2-}$ alkylidynes makes it possible to observe this hindered rotation, since the ortho and meta fluorines will have an "inside" and "outside" orientation in the slowed rotation limit. It seems likely that hindered rotation is also in effect with $[N_3N_F]^{3-}$ alkylidyne complexes, but simply cannot be observed by ^{19}F NMR because of the higher symmetry present.

$[N_2NH]W{\equiv}CCMe_3(Cl)$ reacts with silver triflate in THF to yield a complex formulated as $\{[N_2NH]W{\equiv}CCMe_3(THF)_2\}\{CF_3SO_3\}$, **3e**. ^1H NMR and elemental analysis are consistent with two equivalents of THF per metal center, and IR shows a band at 1205 cm^{-1}, consistent with ionic triflate.[17] This type of six coordinate complex has also been observed for a related diamidophosphine zirconium complex.[18]

DISCUSSION

We sought to prepare the alkylidyne complexes described above to determine, at least qualitatively, how the chemistry of silylated $[N_3N]^{3-}$ complexes and their $[N_3N_F]^{3-}$ analogs differ. In both cases, a variety of alkylidynes can be prepared by loss of molecular hydrogen from alkyls. We cannot directly compare the rates of alkylidyne formation with the two ligands since kinetics were done on $[N_3N]W(CH_3)^2$ and $[N_3N_F]W(CH_2SiMe_3)$, complexes with very different alkyl groups in terms of both sterics and electronics. It is well known that, at least for α-abstraction reactions, the alkyl substituent has a dramatic effect on the rate of reaction.[19] For

References begin on page 122.

$[N_3N]W(CH_2SiMe_3)$ and $[N_3N_F]W(CH_2SiMe_3)$, a qualitative estimate places the rate of decomposition of $[N_3N]$ complex at least twice that of $[N_3N_F]$ complex. The two systems can be directly compared, however, in the reaction between $[N_3N]WCl$ and $[N_3N_F]WCl$ with $LiCD_2CH_2CH_2CH_3$. The fact that scrambling is observed when the fluorinated complex is alkylated suggests that β-hydride elimination/migratory insertion pathways can compete kinetically with the loss of molecular hydrogen in the fluorinated system. When $[(TMSNCH_2CH_2)_3N]WCl$ is reacted with $LiCD_2CH_2CH_2CH_3$, D_2 gas is lost and the organometallic product contains no deuterium. A similar difference is observed when these two chlorides are reacted with $Li^{13}CH_2CH_2CH_2CH_3$. With the C_6F_5-substituted triamidoamine complex, scrambling of the ^{13}C label is observed during the reaction, but with the Me_3Si-substituted triamidoamine complex, only $[N_3N]W{\equiv}^{13}CCH_2CH_2CH_3$ is formed. Thus, the α-processes required to form an alkylidyne in the silylated triamidoamine complex are faster than any β-processes. It would seem that in the fluorinated system, a more conventional kinetic preference for β-elimination over α-elimination is occurring.[20] We speculate that the primary reason for these differences lies in the steric environments of the apical sites of $[N_3N]^{3-}$ and $[N_3N_F]^{3-}$ complexes. Nearly all of the C_6F_5-substituted triamidoamine complexes which have been crystallographically characterized show that the aryl rings twist in order to form a "bowl" which affords the apical ligand a relatively open coordination environment. Conversely, X-ray structures of TMS-substituted triamidoamine complexes often reveal a greater degree of steric strain for the ligand in the apical site.[1,21] It seems reasonable that transition state for β-elimination in $[N_3N]W(CH_2CH_2CH_2CH_3)$ could be considerably more strained than the transition state for β-elimination in $[N_3N_F]W(CH_2CH_2CH_2CH_3)$ as a result of this difference in steric environments. Such effects have been used to explain changes in the relative rates of α- and β-abstraction reactions in $[N_3N]TaR_2$ complexes when the amido substituent is changed from TMS to triethylsilyl.[11] Electronic effects may also be important, as it has generally been found by cyclic voltammetry that C_6F_5-substituted complexes are less easily oxidized than their

References begin on page 122.

silylated analogs. An electron-rich metal center may facilitate the formation of the proposed W(VI) alkylidene hydride intermediate in the dehydrogenation reaction (equation 3).

It is possible to make a direct comparison of the rates of alkylidyne formation from $[N_3N]Mo(CH_2CMe_3)$ and $[N_3N_F]Mo(CH_2CMe_3)$. Previous studies have shown that molybdenum alkyls also undergo reversible α-elimination reactions, although alkylidene hydride complexes analogous to [N3N]W(H)(cyclopentylidene) have not been directly observed.[1] Both decomposition reactions are first-order at 121 °C, but the fluorinated complex loses dihydrogen 12 times more slowly than the silylated complex does. We propose that this difference is due to the same factors which were discussed above regarding the differences in the reactions with labeled butyllithium reagents. A more open steric environment in $[N_3N_F]MoCl$ leads to less steric pressure between the neopentyl group and the amido substituents. Steric strain has been proposed to assist in α-abstraction reactions by forcing the α-hydrogen closer to the metal center, rendering it more easily removed.[19] It should be noted that, if our mechanistic proposals are correct, steric strain assists both the α-elimination and the α-abstraction steps leading to product (equation 3). We feel that electronic effects are also important in these reactions. The electron-withdrawing C_6F_5 rings may deactivate the complexes towards loss of dihydrogen. It is generally accepted that C-H activation processes such as the one proposed to occur in the first step of the formation of $[N_3N_F]Mo{\equiv}CCMe_3$ are facilitated by electron-rich metal centers.[20]

Another way in which complexes containing the $[N_3N_F]^{3-}$ ligand differ from their TMS-substituted analogs is in certain alkylation reactions. [N3N]WCl is smoothly alkylated with MeLi to give $[N_3N]W(CH_3)$[2] and with cyclopentyllithium to give [N3N]W(cyclopentylidene)(H).[9] Neither of the corresponding $[N_3N_F]$ complexes could be prepared, either no reaction or decomposition was observed (see Results section). Similarly, $[N_3N]Mo(CH_3)$ is readily synthesized in high yield whereas $[N_3N_F]Mo(CH_3)$ was never isolated.[22] We propose that the $[N_3N_F]$ complexes are more problematic in these reactions for two reasons. First of all, the C_6F_5 ring in $[N_3N_F]WX$ starting materials may be susceptible to nucleophilic attack or electron transfer from the alkylating agent (in these cases highly reducing alkyllithium reagents).

References begin on page 122.

Secondly, it has been generally observed that $[N_3N_F]$ complexes are more susceptible to decomposition reactions where the ligand becomes stripped off the metal, such as protonolysis. It seems that the C_5F_6 amides are less tightly bound to the metal than their TMS counterparts, perhaps for both steric (the amide lone pair is less well-protected) and electronic reasons. It could be that, rather than alkylate at the metal, MeLi causes removal and subsequent decomposition of the $[N_3N_F]$ ligand. Interestingly, reagents such as $LiCH_2SiMe_3$ and $LiCH_2CMe_3$ *do* alkylate $[N_3N_F]MCl$ (M = Mo, W) cleanly, perhaps because these larger alkyls are less able to react with the C_6F_5 rings on steric grounds and therefore alkylate the metal relatively rapidly.

Although we were initially surprised to find that $[N_2NH]W{\equiv}CCMe_3(Cl)$ (**3a**) reacts with methyllithium to yield $[N_2NH]W{\equiv}CCMe_3(Me)$ with no deprotonation of the secondary amine, consideration of the molecular orbital picture of this complex provides an explanation for its stability. Dehydrohalogenation of **3a** would yield a C_{2v}-symmetric species as shown in equation 5. If all three amide donors in this species participate in π-bonding with the metal, the alkylidyne group cannot be triply-bonded to the metal. The frontier molecular orbitals for the C_{2v}-symmetric triamide ligand are shown in Figure 3.3. Only one σ-type and one π-type MO is

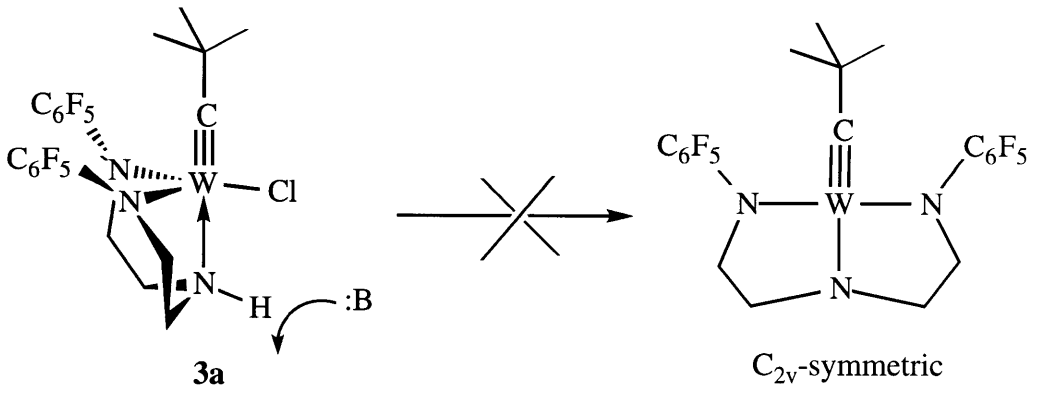

(5)

available for bonding of the ligand in between the C_6F_5 rings (in this case the alkylidyne). Therefore, a triply bonded alkylidyne ligand is not possible with the planar triamide ligand. Additionally, π-bonding from both the C_6F_5-substituted amides can only occur with one metal d

References begin on page 122.

orbital, whereas in C_s-symmetric **3a**, π-bonding from these amides can occur with both the d_{xy} and $d_{x^2-y^2}$ orbitals. It seems that the net result of these effects is that the C_s structure with a tetrahedral dative secondary amine donor is favored when the apical ligand is triply bonded. A similar preference has been observed in tantalum chemistry with an apical nitride donor.[23]

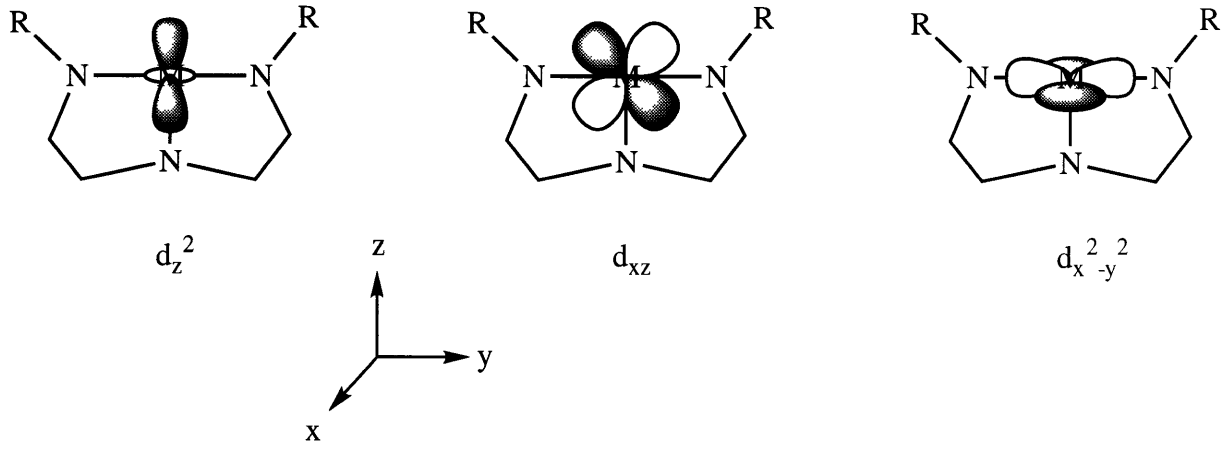

Figure 3.3. Frontier molecular orbitals for C_{2v}-symmetric triamido ligands.

CONCLUSION

Triamidoamine complexes of molybdenum and tungsten have shown a remarkable tendency to form triply-bonded ligands in the apical site. This proclivity stems from the fact that the two π-type frontier molecular orbitals in these C_{3v}-symmetric complexes, d_{xz} and d_{yz}, are strictly degenerate and probably almost pure d-orbitals. Thus, 18-electron $[N_3N_F]$ tungsten alkylidynes are sufficiently thermodynamically stable that 16-electron $[N_3N_F]W(CH_2R)$ complexes will eject dihydrogen rapidly at room temperature to form $[N_3N_F]W{\equiv}CR$ complexes. In this chapter, a comparison between C_6F_5- and TMS-substituted complexes in terms of this dehydrogenation reaction has been made. Both $[N_3N_F]W(CH_2SiMe_3)$ and $[N_3N_F]Mo(CH_2CMe_3)$ decompose more slowly than do their silylated analogs. We attribute this difference to less steric strain and increased metal center electron-deficiency in these molecules as compared to the TMS-substituted complexes. Perhaps more interestingly, it seems that when

References begin on page 122.

β-protons are present on the alkyl, as in $[N_3N_F]W(n\text{-Bu})$ and $[N_3N_F]W(Et)$, β-elimination can compete with the dehydrogenation reaction as evidenced by several types of labeling studies. This is in stark contrast to what is observed with silylated triamidoamine complexes, where labeling studies have shown that solely the α-dehydrogenation reaction occurs in $[N_3N]W(CD_2CH_2CH_2CH_3)$ (see Chapter II). It should be emphasized that the experiments performed have only shown that β-elimination competes with the *overall* dehydrogenation reaction with the $[N_3N_F]$ complexes. A reversible α-elimination process which is faster than β-elimination could be in effect with these complexes just as in their silylated analogs (see Chapters I and II). However, we are unable to make this determination with the C_6F_5 complexes, largely because the $[N_3N_F]M$(cyclopentyl) complexes could not be synthesized.

EXPERIMENTAL

General Details. All experiments were conducted under nitrogen in a Vacuum Atmospheres drybox, using standard Schlenk techniques, or on a high vacuum line ($<10^{-4}$ torr). Glassware was dried in a 135 °C oven overnight. Pentane was washed with HNO_3/H_2SO_4 (5/95 v/v), sodium bicarbonate, H_2O, stored over $CaCl_2$ and then distilled from sodium benzophenone with tetraglyme under nitrogen. Ether and THF were purified by sparging with nitrogen and passing through alumina columns.[24] Reagent grade benzene was distilled from sodium benzophenone under nitrogen. Toluene was distilled from molten sodium. Acetonitrile was distilled from P_2O_5. Methylene chloride was distilled from CaH_2. All solvents were stored in the drybox over activated 4Å molecular sieves. Deuterated solvents were freeze-pump-thaw degassed and vacuum transferred from an appropriate drying agent, or sparged with argon and stored over molecular sieves. ^1H NMR spectra were recorded at either 250 or 300 MHz at 25 °C. ^{13}C, ^{19}F, and ^{31}P NMR spectra were recorded at 75.4, 282, and 121 MHz respectively. ^1H and ^{13}C data are listed in parts per million downfield from tetramethylsilane and were referenced using the solvent peak. ^{19}F NMR are listed in parts per million downfield of $CFCl_3$ as an external standard. ^2H NMR spectra were obtained at 46.0 MHz and referenced to external C_6D_6

References begin on page 122.

(7.15 ppm). ^{31}P NMR spectra are listed in parts per million downfield from H_3PO_4. Coupling constants are given in Hertz, and routine couplings are not listed. Magnetic susceptibility measurements were done by NMR using the Evans method.[25] Elemental analyses (C, H, N) were performed on a Perkin-Elmer 2400 CHN analyzer in our own laboratory.

Preparation of starting materials. $[N_3N_F]WCl$ and $[N_3N_F]MoCl$ were synthesized as described in the literature,[5] except that $WCl_4(dme)$[26] was used instead of $WCl_4(Et_2S)_2$ for the synthesis of the tungsten chloride. $CH_3CH_2CH_2CD_2Li$ was prepared by reduction of butyryl chloride with $LiAlD_4$ in ether followed by reaction with thionyl chloride in hexane in the presence of pyridine. The hexane/butyl chloride mixture was dried and distilled together from P_2O_5. Treatment of this solution with lithium wire gave $CH_3CH_2CH_2CD_2Li$ in ~15% overall yield. D_3CCH_2Li was prepared by treatment of D_3CCH_2Br (Cambridge Isotope Labs) with lithium wire. $CH_3CH_2CH_2{}^{13}CH_2Li$ was prepared from $^{13}CO_2$ by formation of the acid with *n*-PrMgCl, followed by $LiAlH_4$ reduction to the alcohol. Treatment with $SOCl_2$ in hexane in the presence of pyridine as for $LiCD_2CH_2CH_2CH_3$ and subsequent reaction with lithium metal gave the labeled reagent in 20% overall yield. Phenyllithium and 3,5-xylyllithium were prepared by treatment of the aryl bromide with BuLi in ether/hexane at -35 °C. Ethyllithium was prepared by the literature procedure.[27] Trimethylsilylmethyllithium was purchased commercially as a solution in pentane and the pentane was removed *in vacuo*. Cyclopropyllithium was synthesized from the bromide and lithium powder in ether. Neopentyllithium was prepared by the literature procedure.[28] Benzyllithium was prepared by the transmetalation method.[29] Tungsten neopentylidyne trichloride DME was prepared by the literature procedure.[26] This material can also be prepared from $Me_3CC{\equiv}W(O\text{-}t\text{-}Bu)_3$ by treatment with BCl_3.[30]

In the UV/Vis study, the following equation was employed to follow the disappearance of an alkyl species: $\ln[(A_0 - A_\infty)/(A - A_\infty)] = kt$, where A_0 = absorbance at wavelength λ at time 0, A_∞ = absorbance at wavelength λ at infinite time, and A = absorbance at wavelength λ at time t.

References begin on page 122.

[N_3N_F]W≡CMe (1a). A room temperature suspension of [N_3N_F]WCl (0.50 g, 0.58 mmol) in 10 mL toluene had ethyllithium (31 mg, .842 mmol) added as a solid. Gas was evolved instantaneously and the reaction changed from orange to brown over 30 min. After 45 minutes the toluene was removed in vacuo and the residue extracted with 10 mL CH_2Cl_2. Filtration through a short column of Celite and removal of the solvent left the crude product. It was recrystallized by dissolving in a mixture of CH_2Cl_2 and ether and cooling to -40 °C. Two crops of tan-yellow solid were obtained. Total yield: 249 mg (50%): ^{1}H NMR ($CDCl_3$) δ 2.2 (t, W≡C-*Me*, 3, J_{WH} = 8.7 Hz), 3.1 (t, NCH_2, 6), 3.9 (t, NCH_2, 6); $^{13}C\{^1H\}$ NMR ($CDCl_3$) δ 30.1 (W≡C-*Me*), 51.8 (NCH_2), 56.8 (NCH_2), 135.6, 138.9, 140.7, 144.0 (C_6F_5), 286.3 (W≡*C*-Me); ^{19}F NMR ($CDCl_3$) δ -165.2 (t, *m*-C_6F_5, 6), -164.8 (t, *p*-C_6F_5, 3), -151.0 (d, *o*-C_6F_5, 6). Anal. Calcd. for $C_{26}H_{15}N_4F_{15}W$: C, 36.64; H, 1.77; N, 6.57. Found: C, 36.71; H, 1.90; N, 6.42.

[N_3N_F]W≡C$CH_2CH_2CH_3$ (1b). *n*-Butyllithium (0.581 mL, 1.45 mmol, 2.5 M in hexane) was added via syringe at room temperature to a suspension of [N_3N_F]WCl (1.00 g, 1.16 mmol) in 30 mL of toluene. Within minutes the color began to change from orange to brown and gas evolved. The reaction was stirred for three hours and then filtered through Celite. The filtrate was reduced in volume in vacuo until crystals began to form and then cooled to -40 °C overnight. The off-white microcrystalline product was filtered off and dried *in vacuo* . A second crop was obtained by reducing the volume of the mother liquor and cooling to -40 °C; total yield 0.673 g (66%): ^{1}H NMR C_6D_6 δ 0.25 (t, -$CH_2CH_2CH_3$, 3), 0.41 (sextet, -$CH_2CH_2CH_3$, 2), 2.05 (t, NCH_2CH_2N, 6), 2.50 (t, -$CH_2CH_2CH_3$, 2), 3.33 (t, NCH_2, 6); $^{13}C\{^1H\}$ NMR C_6D_6 δ 12.94 ($CH_2CH_2CH_3$), 22.29 ($CH_2CH_2CH_3$), 46.71 ($CH_2CH_2CH_3$), 51.22 (NCH_2), 56.92 (NCH_2), 136.2, 139.5, 141.4, 144.7 (br s, C_6F_5), 292.64 (W≡C, J_{CW} = 254 Hz) Anal. Calcd for $C_{28}H_{19}N_4F_{15}W$: C, 38.20; H, 2.18; N, 6.36. Found: C, 38.33; H, 2.27; N, 6.32.

[N_3N_F]W≡CPh (1c). $PhCH_2Li$ (325 mg, 1.70 mmol) was added as a solid to a stirred suspension of [$(C_6F_5NCH_2CH_2)_3N$]WI (750 mg, 0.788 mmol) in 25 mL of toluene. The reaction darkened immediately and gas was evolved. The reaction was stirred for 2 days, at which point the toluene was removed in vacuo. The residue was dissolved in CH_2Cl_2, filtered through Celite

References begin on page 122.

and evaporated. Dissolution in a minimum amount of CH_2Cl_2 and cooling this solution to -40 °C overnight gave the product as an off white solid, 337 mg (47%): ^{1}H NMR (C_6D_6) δ 2.09 (t, NCH_2, 6), 3.37 (t, NCH_2, 6), 6.09 (d, H_{ortho}, 2), 6.41 (t, H_{para}, 1), 6.70 (t, H_{meta}, 2); $^{13}C\{^1H\}$ NMR (CD_2Cl_2) δ 52.7 (NCH_2), 58.0 (NCH_2), 127.2 (C_6H_5), 130.5 (C_6H_5), 136.2, 137.2, 139.5, 141.8, 145.0, 146.7 (C_6F_5), 281.6 (W≡C-Ph); ^{19}F NMR (C_6D_6) -164.8 (t, *m*-C_6F_5, 6), -164.0 (t, *p*-C_6F_5, 3), -150.7 (d, *o*-C_6F_5, 6).

[N_3N_F]W≡CSiMe$_3$ (1d). $LiCH_2SiMe_3$ (66 mg, 0.70 mmol) was added as a solid to a stirred suspension of [N_3N_F]WCl (500 mg, 0.581 mmol) in 10 mL of toluene at room temperature. The reaction turned wine-red and bubbling was observed. After stirring for 2 days, the reaction mixture was evaporated to dryness and the residue was extracted with CH_2Cl_2. The extract was filtered through Celite and the solvent removed from the filtrate in vacuo to give the crude product as a pink residue. This residue was recrystallized by dissolving it in ~ 3 mL THF, layering TMS_2O on top, and standing the solution in the refrigerator at -40 °C. After two days red crystals were filtered off; yield 0.381 g (72%): ^{1}H NMR ($CDCl_3$) δ -0.80 (s, -SiC*H*$_3$, 9), 3.03 (t, NCH_2, 6), 3.97 (t, NCH_2, 6); $^{13}C\{^1H\}$ NMR ($CDCl_3$) δ -0.87 (Si*C*H$_3$), 51.13 (NCH_2), 57.35 (NCH_2), 136, 139, 142, 145 (br s, C_6F_5), 288.37 (W≡*C*); ^{19}F NMR (C_6D_6) δ -165.24 (br s, *o*-C_6F_5), -164.61 (t, *p*-C_6F_5), -150.22 (br s, *o*-C_6F_5). Anal. Calcd for $C_{28}H_{21}N_4F_{15}SiW$: C, 36.94; H, 2.32; N, 6.15. Found: C, 36.90; H, 2.42; N, 6.12.

[N_3N_F]W≡CCMe$_3$ (1e). $LiCH_2CMe_3$ (79 mg, 1.02 mmol) was added as a solid to a stirred suspension of [N_3N_F]WCl (500 mg, 0.581 mmol) in 20 mL toluene. Within seconds gas was evolved and the color began to change from orange to light yellow. After 3.5 h, the toluene was removed in vacuo and the off white residue dissolved in ~ 60 mL 1,2-dimethoxyethane. The solution was then filtered through Celite and the volume reduced *in vacuo* until microcrystals began to form. Cooling this solution to -40 °C overnight gave the product as a light yellow powder. A second crop was obtained by concentrating the mother liquor and cooling to -40 °C. Total yield 0.317 g (61%): ^{1}H NMR (THF-d_8) δ .064 (s, W≡C-C(C*H*$_3$)$_3$, 9), 3.12 (t, NCH_2, 6), 3.94 (t, NCH_2, 6); $^{13}C\{^1H\}$ NMR (THF-d_8) δ 29.90 (W≡C-C(*C*H$_3$)$_3$), 48.73 (W≡C-*C*Me$_3$),

References begin on page 122.

52.54 (NCH_2), 58.35 (NCH_2), 137, 139, 143, 146 (C_6F_5), 296.07 (W≡*C*-CMe_3); ^{19}F NMR (C_6H_6): -165.3 (d, *m*-C_6F_5), -164.6 (t, *p*-C_6F_5), -150.7 (s, *o*-C_6F_5). Anal. Calcd. for $C_{29}H_{21}N_4F_{15}W$: C, 38.95; H, 2.37; N, 6.26. Found: C, 38.82; H, 2.18; N, 6.12.

[N_3N_F]WI (1f). A solution of [N_3N_F]WCl (870 mg, 1.01 mmol) in 30 mL CH_2Cl_2 had TMSI (216 µl, 1.52 mmol, 1.5 equiv.) added via syringe. The reaction was stirred overnight and the solution evaporated. The yellow-brown residue was recrystallized from CH_2Cl_2/Et_2O mixtures, 755 mg orange crystals isolated (97% yield). ^1H NMR (C_6D_6) δ -25.5 (br s, $\Delta\nu_{1/2}$ = 156 Hz, CH_2), -50.0 (br s, $\Delta\nu_{1/2}$ = 115 Hz, CH_2); ^{19}F NMR (C_6D_6) δ -86.5 (ortho F), -124.0 (meta F), -144.5 (para F) Anal. Calcd for $C_{24}H_{12}N_4F_{15}WI$: C, 30.28; H, 1.27; N, 5.88. Found: C, 30.45; H, 1.32; N, 5.80.

[N_3N_F]W(CH_2SiMe_3) (1g). A -40 °C solution of $LiCH_2SiMe_3$ (131 mg, 1.39 mmol, 1.2 equiv.) in 40 mL of toluene was added via cannula to solid [N_3N_F]WCl (1.00 g, 1.16 mmol) in a 100 mL Schlenk flask immersed in a -10 °C bath. The heterogeneous reaction mixture was stirred at this temperature for 1 hour, the color changing gradually from orange to red. The red solid was filtered off and dried *in vacuo*; yield 908 mg (86%). Extraction with methylene chloride and recrystallization from CH_2Cl_2 layered with pentane gave the product as red crystals: ^1H NMR (C_6D_6) δ -0.82 (br s, 9, TMS), -18.3 (br s, 6, NCH_2), -52.1 (br s, 6, NCH_2); ^{19}F NMR (C_6D_6) δ -29 (br s, *o*-C_6F_5), -112 (s, *m*-C_6F_5), -140 (s, *p*-C_6F_5).

The dehydrogenation of [N_3N_F]W(CH_2SiMe_3) was followed by ^{19}F NMR at 470 MHz by monitoring the decrease in intensity of the meta fluorine resonance verses fluorobenzene as an internal standard. Runs were done in THF with an initial alkyl concentration of ~0.01 M and followed through two to five half-lives. The values for k ($x10^{-4}$ s^{-1}) at temperature T (K) are as follows: 48.1 (326), 16.9 (316), 6.47 (306), 1.97 (297), 0.774 (289). A plot of ln(k/T) versus 1/T yielded $\Delta H^{\ddagger}$ = 20,321 cal/mol and $\Delta S^{\ddagger}$ = -6.956 e.u.

[N_3N_F]W≡C-H (1h). [N_3N_F]WCl (500 mg, 0.581 mmol) was dissolved in 40 mL of toluene by stirring the solution for 1 h. A solution of cyclopropyllithium (84 mg, 0.56 mmol, 1 equiv.) was prepared by adding 3 drops of THF to the solid lithium reagent followed by 2 mL of

References begin on page 122.

toluene. This solution was added dropwise to the chloride. The reaction was stirred for twenty minutes, at which point 0.3 more equivalents of cyclopropyllithium (28 mg, 0.19 mmol) in 1 mL toluene was added. After an additional thirty minutes of stirring, ^{19}F NMR showed the reaction was complete. The solution was filtered through Celite and the solvents removed *in vacuo*. Recrystallization from CH_2Cl_2 layered with pentane yielded several crops of orange microcrystals which were isolated by decantation of the mother liquor and drying *in vacuo*; yield 394 mg (81%): ^1H NMR (C_6D_6) δ 1.99 (t, NC*H*$_2$, 6), 3.29 (t, NC*H*$_2$, 6), 5.24 (s, J_{HW} = 76 Hz, W≡C-*H*, 1); ^{13}C NMR (CD_2Cl_2) δ 52.2 (t, N*C*H$_2$), 57.9 (t, N*C*H$_2$), 136.1, 137.0, 139.4, 140.2, 141.8, 145.1, (*C*$_6$F$_5$), 284.3 (W≡*C*-H); ^{19}F NMR (C_6D_6) δ -150.9 (br s, *o*-C_6F_5), -163.4 (t, *p*-C_6F_5), -164.9 (br s, *m*-C_6F_5).

[N_3N_F]Mo(CH_2CMe_3) (2a). [N_3N_F]MoCl (750 mg, 0.971 mmol) was slurried in 50 mL toluene and stirred for ~45 minutes to dissolve. Neopentyllithium (151 mg, 1.16 mmol, 1.2 equiv.) was added as a solid to the toluene solution. The color changed instantly from orange to wine-red. After 30 minutes ^{19}F NMR showed the reaction was complete. The toluene was removed under reduced pressure and the residue extracted with methylene chloride and filtered through Celite. The methylene chloride solution was reduced in volume, layered with pentane, and cooled to -40 °C. 544 mg product crystallized in two crops (70%). ^1H NMR (C_6D_6): δ 4.5 (br s, 9, C(C*H*$_3$)$_3$), -9.5 (br s, NC*H*$_2$N), -66 (br s, NC*H*$_2$N). ^{19}F NMR (C_6D_6): δ -47.3 (br s, 6, *o*-C_6F_5), -120.7 (s, 6, *m*-C_6F_5), -139. 2 (s, 3, *p*-C_6F_5). Anal. Calcd. for $C_{29}H_{23}N_4F_{15}Mo$: C, 43.09; H, 2.87; N, 6.93. Found: C, 43.03; H, 3.16; N, 6.87. λ_{max} = 492 nm (ε = 1.6 x 10^3 $M^{-1}cm^{-1}$).

Kinetic study for the conversion of 2a into [N_3N_F]Mo≡CCMe$_3$. The reaction was followed by UV/Vis in toluene at 492 nm. Runs were performed with a 1.6 mM stock solution. A cuvette with a teflon stopcock was charged with 2.0 mL of the solution and a stir bar. It was placed in a stirred 121.0 ± 0.2 °C oil bath for 4 min. It was then removed from the bath, rinsed with hexane, and placed in the UV/Vis Peltier block kept at 70 °C during the entire run so that the absorbance measurements could all be obtained at the same temperature. After equilibration

References begin on page 122.

at 70 °C, a spectrum was recorded and used as the T_0 value. The cuvette was placed back in the 121 °C bath and, after allowing 30 seconds for temperature equilibration, timing was begun. Data points were collected approximately every 1.5 h and a rate constant of 7.9(5) x 10^{-5} sec^{-1} was obtained. Another measurement at a concentration of 0.53 mM gave a rate constant of 7.8 x 10^{-5} sec^{-1}.

[N_3N_F]Mo(CH_2SiMe_3) (2b). [N_3N_F]MoCl (153 mg, 0.198 mmol) was slurried in 10 mL toluene and stirred to dissolve for ~30 min. Trimethylsilylmethyllithium (22 mg, 0.24 mmol) was added as a solid and the color of the reaction changed instantly from orange to deep purple. The solvent was removed under reduced pressure and the residue extracted with methylene chloride. This solution was filtered through Celite and the volume reduced *in vacuo*. The solution was layered with pentane and stored at -40 °C for 15 h. Red microcrystals formed which were isolated by decantation of the mother liquor and dried under reduced pressure, yield 67 mg (41%). ^1H NMR (C_6D_6): δ 3.54 (s, $Si(CH_3)_3$), -11 (br s, NCH_2N), -67 (br s, NCH_2N). ^{19}F NMR (C_6D_6): δ -47.8 (br s, 6, *o*-C_6F_5), -121.9 (s, 6, *m*-C_6F_5), -140.1 (s, 3, *p*-C_6F_5). Anal. Calcd. for $C_{28}H_{23}N_4F_{15}SiMo$: C, 40.79; H, 2.81; N, 6.80. Found: C, 40.39; H, 2.99; N, 6.46.

[N_3N_F]Mo≡$CCMe_3$ (2c). [N_3N_F]Mo(CH_2CMe_3) (300 mg, 0.373 mmol) was heated in 10 mL toluene at 110 °C for 24 h, at which point ^{19}F NMR indicated the reaction was complete. The reaction mixture was cooled to -40 °C for 15 h. 204 mg of product crystallized (68%). ^1H NMR (C_6D_6) δ 3.26 (t, 6, NCH_2N), 2.05 (t, 6, NCH_2N), 0.074 (s, 9, CMe_3). ^{19}F NMR (toluene) δ -150.0 (d, 6, *o*-C_6F_5), -164.9 (t, 3, *p*-C_6F_5), -165.2 (t, 6, *m*-C_6F_5). ^{13}C NMR (CD_2Cl_2) δ 27.3 (CMe_3), 52.3 (NCH_2N), 58.0 (NCH_2N), 137, 139, 142, 144 (C_6F_5), 312.9 (Mo≡C).

[$HN(CH_2CH_2NC_6F_5)_2$]W≡$CCMe_3$(Cl) (3a). A solution of $HN(CH_2CH_2NC_6F_5)_2$ (1.50 g, 3.45 mmol) and triethylamine (1.06 mL, 7.58 mmol, 2.2 equiv.) in 60 mL diethyl ether was cooled to -40 °C. W≡$CCMe_3(Cl)_3$(dme) (1.55 g, 3.45 mmol) was added as a solid over 5 min to the stirred ethereal solution. The reaction was stirred overnight at room temperature and then the volatiles were removed *in vacuo*. The residue was extracted with THF, filtered and the THF removed. The yellow solid remaining was recrystallized by layering a concentrated

References begin on page 122.

dichloromethane solution with pentane and cooling to -40 °C for 15 h. The product was obtained as yellow microcrystals, 1.97 g (79%). ^{1}H NMR ($CDCl_3$) δ 3.88 (m, 4, NCH_2N), 3.38 (m, 2, NCH_2N), 3.08 (m, 2, NCH_2N), 2.86 (br t, 1, NH), 0.372 (s, 9, CMe_3). ^{19}F NMR ($CDCl_3$) δ -150.2 (d, 2, *o*-C_6F_5), -150.6 (d, 2, *o*-C_6F_5), -162.5 (t, 2, *p*-C_6F_5), -164.4 (dt, 4, *m*-C_6F_5). ^{13}C NMR ($CDCl_3$) δ 305.3 (W≡C), 145, 140, 139, 135 (br m, C_6F_5), 59.5 (NCH_2N), 48.6 (NCH_2N), 45.8 (NCH_2N), 30.2 (CMe_3) IR (Nujol mull) cm^{-1} 3306 (NH), 1500 (C_6F_5-N), 986 (C-F). Anal. Calcd for $C_{21}H_{18}N_3ClF_{10}W$: C, 34.95; H, 2.51; N, 5.82. Found: C, 35.16; H, 2.12; N, 5.60.

[HN(CH$_2$CH$_2$NC$_6$F$_5$)$_2$]W≡CCMe$_3$(Me) (3b). [HN($CH_2CH_2NC_6F_5$)$_2$]W≡CCMe$_3$(Cl) (770 mg, 1.07 mmol) was dissolved in 25 mL toluene. MeLi (1.4 M in Et_2O, 838 μL, 1.17 mmol, 1.1 equiv.) was added to the stirred solution via syringe. Stirring was continued for 3 h, and then the reaction was filtered and the volatiles were removed *in vacuo*. The residue was dissolved in 8 mL benzene and filtered again to removed the last traces of LiCl. The benzene was removed under reduced pressure and the tan residue recrystallized at -40 °C from minimum toluene layered with pentane. The product was obtained as light orange crystals, 478 mg (64%). ^{1}H NMR (C_6D_6) δ 3.17 (m, 2, NCH_2N), 2.97 (m, 2, NCH_2N), 2.12 (m, 2, NCH_2N), 2.03 (m, 2, NCH_2N), 1.60 (br t, 1, NH), 0.930 (s, $^2J_{WH}$ = 8 Hz, 3, Me), 0.514 (s, 9, CMe_3). ^{13}C NMR (C_6D_6) δ 298.2 (W≡C), 144, 142, 139, 138, 136 (m, C_6F_5), 58.3 (NCH_2N), 48.4 ($^2J_{WC}$ = 41 Hz, W≡C*C*Me$_3$), 46.2 (NCH_2N), 30.1 (CMe_3), 29.0 ($^1J_{WC}$ = 112 Hz, WMe). ^{19}F NMR ($CDCl_3$) δ -150.2 (d, 2, *o*-C_6F_5), -152.2 (d, 2, *o*-C_6F_5), -164.8 (t, 2, *p*-C_6F_5), -165.4 (br t, 2, *m*-C_6F_5), -165.8 (t, 2, *m*-C_6F_5). Anal. Calcd for $C_{22}H_{21}N_3F_{10}W$: C, 37.68; H, 3.02; N, 5.99. Found: C, 37.96; H, 3.03; N, 5.73.

[HN(CH$_2$CH$_2$NC$_6$F$_5$)$_2$]W≡CCMe$_3$(Et) (3c). [HN($CH_2CH_2NC_6F_5$)$_2$]W≡CCMe$_3$(Cl) (100 mg, 0.139 mmol) was dissolved in 5 mL toluene. Ethyllithium (6 mg, 0.166 mmol, 1.2 equiv.) was added as a solid to the stirred toluene solution. After stirring for 5 h, the solution was filtered, the volatiles were removed *in vacuo*, and the yellow-tan solid recrystallized from toluene/pentane mixtures, 43 mg (44%). ^{1}H NMR (C_6D_6) δ 3.15 (m, 2, NCH_2N), 2.95 (m, 2, NCH_2N), 2.37 (t, 3, WCH_2CH_3), 2.10 (m, 2, NCH_2N), 2.01 (m, 2, NCH_2N), 1.25 (q, 2,

References begin on page 122.

WCH_2CH_3), 0.513 (s, 9, CMe_3). ^{19}F NMR (C_6D_6) δ -150.8 (d, 2, *o*-C_6F_5), -151.9 (d, 2, *o*-C_6F_5), -164.7 (t, 2, *p*-C_6F_5), -165.1 (br t, 2, *m*-C_6F_5), -165.3 (t, 2, *m*-C_6F_5).

[HN($CH_2CH_2NC_6F_5$)$_2$]W≡CCMe$_3$(CCH) (3d). Sodium acetylide (7 mg, 0.15 mmol, 1.1 equiv.) was added as a solid to a stirred solution of [HN($CH_2CH_2NC_6F_5$)$_2$]W≡CCMe$_3$(Cl) (100 mg, 0.139 mmol) in THF. Stirring was continued for 15 h, at which point the solvent was removed under reduced pressure. The residue was extracted with toluene and NaCl filtered off. Recrystallization at -40 °C from minimum toluene layered with pentane gave the product as a tan solid, 40 mg (40%). ^1H NMR (C_6D_6) δ 11.36 (s, $^3J_{WH}$ = 23 Hz, 1, *H*C≡CW), 4.02 (br t, 1, NH), 3.10 (m, 2, NCH_2N), 2.65 (m, 2, NCH_2N), 2.46 (m, 4, NCH_2N), 0.966 (s, 9, CMe_3). ^{13}C {^1H} NMR (C_6D_6) δ 231.6 (W≡C), 187.7 (d, $^1J_{CH}$ = 212 Hz, $^2J_{CW}$ = 119 Hz, WC≡*C*H), 177.9 (d, $^2J_{CH}$ = 23 Hz, W*C*≡CH), 146, 142, 139, 136, 133 (m, C_6F_5), 59.1 (t, NCH_2N), 49.9 (t, NCH_2N), 44.1 (s, W≡C*C*Me$_3$), 30.2 (q, C*Me$_3$*). IR (Nujol mull) cm^{-1} 3213 (NH), 1501 (N-C_6F_5), 1059, 1011, 987 (C-F), 850, 700.

[HN($CH_2CH_2NC_6F_5$)$_2$]W≡CCMe$_3$(THF)$_2$(OTf) (3e). Silver triflate (107 mg, 0.416 mmol) was added to a stirred solution of [HN($CH_2CH_2NC_6F_5$)$_2$]W≡CCMe$_3$(Cl) (300 mg, 0.416 mmol) in 10 mL THF. A precipitate began forming immediately. After 2 h, the solution was filtered and the volatiles removed *in vacuo*. The yellow solid was dissolved in 10 mL warm THF, layered with pentane, and stored at -40 °C for 40 h. Yellow microcrystals were obtained, 332 mg (82%). ^1H NMR ($CDCl_3$) δ 3.97 (br m, 12, THF, NCH_2N), 3.62 (br s, 1, NH), 3.40 (m, 2, NCH_2N), 2.96 (m, 2, NCH_2N), 1.95 (q, 8, THF), 0.359 (s, 9, CMe_3). ^{19}F NMR (THF) -78.3 (s, 3, OTf), -148.1 (s, 4, *o*-C_6F_5), -166.6 (t, 2, *p*-C_6F_5), -167.1 (t, 4, *m*-C_6F_5). IR (Nujol mull) cm^{-1} 3249 (NH), 1501 (N-C_6F_5), 1205 (OTf), 1013 (C-F), 856, 633. Anal. Calc. for $C_{30}H_{34}N_3F_{13}SO_5W$: C, 36.79; H, 3.50; N, 4.29. Found: C, 36.87; H, 3.55; N, 4.29.

X-ray structure of [N_3N_F]W≡CSiMe$_3$ (1d). Crystallographic data are located in Table 3.2, and selected bond lengths and angles are given in Table 3.1. Full tables of atomic coordinates and bond lengths and angles will be published. Suitable crystals were grown from THF layered with hexamethyldisiloxane at -40 °C. A crystal was attached to a glass fiber and

References begin on page 122.

transferred to a Enraf-Nonius CAD-4 diffractometer with graphite monochromated MoK_α radiation. Cell constants and an orientation matrix for data collection, obtained from a least-squares refinement using the setting angles of 25 carefully centered reflections in the range 13.50 < 2j < 21.00° corresponded to a monoclinic cell with the dimensions given in Table 3.2. Based on the systematic absences of h0l: 1 ≠ 2n and 0k0: k ≠ 2n and the successful solution and refinement of the structure, the space group was determined to be $P2_1/c$ (#14).

References begin on page 122.

REFERENCES

(1) Schrock, R. R.; Seidel, S. W.; Mösch-Zanetti, N. C.; Shih, K.-Y.; O'Donoghue, M. B.; Davis, W. M.; Reiff, W. M. *J. Am. Chem. Soc.* , in press.

(2) Shih, K.-Y.; Totland, K.; Seidel, S. W.; Schrock, R. R. *J. Am. Chem. Soc.* **1994**, *116*, 12103.

(3) Schrock, R. R.; Seidel, S. W.; Zanetti-Mösch, N. C.; Dobbs, D. A.; Shih, K.-Y.; Davis, W. M. *Organometallics* , in press.

(4) Shih, K.-Y.; Schrock, R. R.; Kempe, R. *J. Am. Chem. Soc.* **1994**, *116*, 8804.

(5) Kol, M.; Schrock, R. R.; Kempe, R. *J. Am. Chem. Soc.* **1994**, *116*, 4382.

(6) Schrock, R. R.; Lee, J.; Liang, L.-C.; Davis, W. M. *Inorg. Chim. Acta.* , in press.

(7) Baumann, R.; Schrock, R. R.; Davis, W. M. *J. Am. Chem. Soc.* **1997**, *119*, 3830.

(8) Murdzek, J. S.; Schrock, R. R. In *Carbyne Complexes*; VCH: New York, 1988.

(9) Schrock, R. R.; Shih, K.-Y.; Dobbs, D.; Davis, W. M. *J. Am. Chem. Soc.* **1995**, *117*, 6609.

(10) Freundlich, J. S.; Schrock, R. R.; Davis, W. M. *J. Am. Chem. Soc.* **1996**, *118*, 3643.

(11) Freundlich, J. S.; Schrock, R. R.; Davis, W. M. *Organometallics* **1996**, *15*, 2777.

(12) Turner, H. W.; Schrock, R. R. *J. Am. Chem. Soc.* **1982**, *104*, 2331.

(13) Turner, H. W.; Schrock, R. R.; Fellmann, J. D.; Holmes, S. J. *J. Am. Chem. Soc.* **1983**, *105*, 4942.

(14) Parkin, G.; Bunel, E.; Burger, B. J.; Trimmer, M. S.; Asselt, A. v.; Bercaw, J. E. *J. Molec. Catal.* **1987**, *41*, 21.

(15) Zanetti-Mösch, N. C.; Davis, W. M.; Schrock, R. R.; Wanniger, K.; Seidel, S. W.; O'Donoghue, M. B. , in press.

(16) Freundlich, J. S.; Ph.D. Thesis, **1996**, Massachusetts Institute of Technology, Cambridge, MA 02139.

(17) Lawrance, G. A. *Chem. Rev.* **1986**, *86*, 17-33.

(18) Seidel, S. W., unpublished results.

(19) Schrock, R. R. In *Reactions of Coordinated Ligands*; Braterman, P. R., Ed.; Plenum: New York, 1986.

(20) Collman, J. P.; Hegedus, L. S.; Norton, J. R.; Finke, R. G. *Principles and Applications of Organotransition Metal Chemistry*, University Science Books: Mill Valley, 1987.

(21) Schrock, R. R. *Acc. Chem. Res.* **1997**, *30*, 9.

(22) Dobbs, D. A., unpublished results.

(23) Lee, J., unpublished results.

(24) Pangborn, A. B.; Giardello, M. A.; Grubbs, R. H.; Rosen, R. K.; Timmers, F. J. *Organometallics* **1996**, *15*, 1518.

(25) Evans, D. F. *J. Chem. Soc.* **1959**, 2003.

(26) Persson, C.; Andersson, C. *Inorg. Chim. Acta* **1993**, *203*, 235.

(27) Bryce-Smith, D.; Turner, E. E. *J. Chem. Soc.* **1953**, 861.

(28) Schrock, R. R.; Fellmann, J. D. *J. Am. Chem. Soc.* **1978**, *100*, 3359.

(29) Seyferth, D.; Suzuki, R.; Murphy, C. J.; Sabet, C. R. *J. Organomet. Chem.* **1964**, *2*, 431.

(30) Stevenson, M. A.; Hopkins, M. D. *Organometallics* **1997**, *16*, 3572.

CHAPTER IV

Synthesis of Tungsten and Molybdenum Complexes

That Contain the $[(C_6F_5NCH_2CH_2)_3N]^{3-}$ Ligand.

INTRODUCTION

Our interest in developing the chemistry of the $[N_3N_F]^{3-}$ ($[N_3N_F]^{3-}$ = $[(C_6F_5NCH_2CH_2)_3]^{3-}$) triamidoamine ligand arose after it was determined that syntheses of $[N_3N]^{3-}$ ($[N_3N]^{3-}$ = $[(TMSNCH_2CH_2)_3N]^{3-}$) complexes of molybdenum and tungsten were plagued by side-reactions, presumably involving cleavage of the silicon-nitrogen bond. It was postulated that a more robust triamidoamine ligand such as C_6F_5-substituted $[N_3N_F]^{3-}$ might be more amenable to forming $[N_3N_F]MCl$ complexes for molybdenum and tungsten, and that was indeed found to be the case.[1] Whereas $[N_3N]MCl$ starting materials can only be obtained in low yield (M= W, ~20%; M = Mo, ~35%),[2,3] $[N_3N_F]MCl$ complexes for both Mo and W can be prepared in nearly 80% yield from the $[N_3N_F]H_3$ ligand and $MCl_4(L)_2$ in the presence of triethylamine. Since $[N_3N_F]H_3$ and WCl_4(dme) are readily accessible, we are able to routinely prepare orange, crystalline $[N_3N_F]WCl$ in 15 gram quantities, greatly facilitating the development of the chemistry presented in this chapter.

We begin by exploring some of the chemistry of $[N_3N_F]W(IV)$ organometallic complexes. As described in chapter III, alkylation of $[N_3N_F]WCl$ with certain RCH_2Li reagents results in rapid loss of dihydrogen and formation of tungsten(VI) alkylidynes of the form $[N_3N_F]W{\equiv}CR$. We thus became interested in exploring the chemistry of some $[N_3N_F]^{3-}$-containing tungsten(IV) organometallic complexes which could not lose dihydrogen, such as phenyl compounds. Here, we describe the preparation and reactivity of these $[N_3N_F]W(Ar)$ (Ar = Ph, 3,5-Me_2Ph) complexes, rare examples of tungsten(IV) organometallics (especially considering that they do not utilize the bent metallocene core). We also report the synthesis of a variety of tungsten(III) complexes of the general form $[N_3N_F]W(L)$, where L is a high-field π-acceptor ligand. No complex where L = N_2 has been synthesized; it appears that more aggressive ligands are required for clean products to be isolated. Interesting reactivity of some of the $[N_3N_F]W(L)$ complexes is reported, with the general trend once again being toward a high stability of W(VI) complexes with triply-bonded ligands in the apical site.

References begin on page 176.

RESULTS

[N_3N_F] Tungsten Aryl Complexes

[N_3N_F]WI reacts with ArLi reagents (Ar = Ph, 3,5-Me_2Ph) to yield the corresponding aryl complexes, [N_3N_F]W(Ph) (**1a**) and [N_3N_F]W(3,5-Me_2Ph) (**1b**), as red-orange, paramagnetic solids. [N_3N_F]WCl cannot be used as a starting material because it does not react readily enough with ArLi reagents. Just as with [N_3N]W(Ph) (see chapter II), overlap of the metal d-electrons with the π system of the aryl rings in these systems is apparently not substantial enough to break the degeneracy of the d_{xz}/d_{yz} HOMO of the molecule and result in a diamagnetic complex. The observed magnetic moment of **1b** in C_6D_6 solution at 22 °C is 3.0 ± 0.1 μ_B, close to the spin-only value for two unpaired electrons (2.83 μ_B). ^{1}H NMR spectra of the complexes reveal ligand backbone resonances between -15 and -60 ppm, similar to TMS-substituted triamidoamine tungsten(IV) complexes (chapter II). Resonances for the aryl protons are not observed, but in **1b** a sharp resonance which we assign to the aryl methyls is observed at -53.9 ppm. **1a** is only sparingly soluble in hydrocarbon solvents, whereas **1b** is soluble enough in toluene to render extraction into this solvent a viable method for separating **1b** from most of the LiI side-product.

These aryl complexes react with hydrogen (3 atm) in toluene at 40 °C to yield a diamagnetic trihydride complex, [N_3N_F]W($H)_3$ (**1c**). This trihydride is a direct analog to one synthesized previously which contains the silylated triamidoamine ligand, [$N_3N]^{3-}$.[4] The

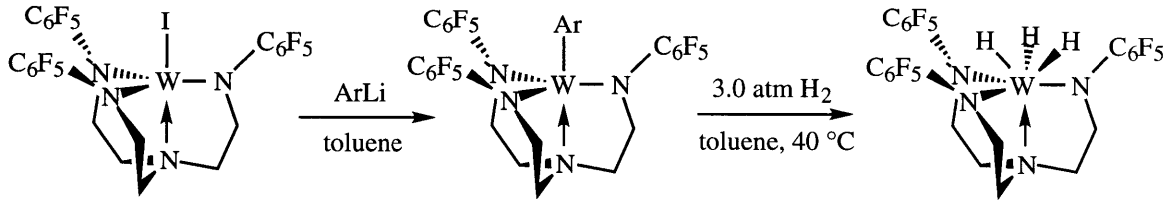

(1)

Ar = Ph (**1a**), 3,5-Me_2-Ph (**1b**) **1c**

hydride resonance of [N_3N_F]W($H)_3$ is observed at 11.1 ppm in the ^{1}H NMR spectrum with J_{HW} = 25 Hz. The relaxation time of the hydride was determined to be 344 ± 5 msec at 22 °C, indicative of a classical hydride complex.[5] A band observed at 1898 cm^{-1} in the IR spectrum is

References begin on page 176.

assignable to the W-H stretch. The trideuteride could be prepared similarly by employing D_2 gas in the synthesis. The proton NMR of $[N_3N_F]W(D)_3$ has no resonance at 11.1 ppm, whereas the ^2H NMR spectrum does display a resonance at 10.9 ppm. In addition, the IR spectrum of $[N_3N]W(D)_3$ lacks a band at 1898 cm^{-1}, but a new band at 1372 cm^{-1} is present which we assign to the deuteride stretch.

Atom-Transfer Reactions with W(IV) Aryl Complexes

Both **1a** and **1b** are cleanly oxidized in DME by pyridine *n*-oxide to yield tungsten(VI) oxo complexes, $[N_3N_F]W(O)(Ph)$ (**2a**) and $[N_3N_F]W(O)(3,5\text{-}Me_2Ph)$ (**2b**). No IR stretch for the oxo ligand is observed in either complex, presumably because the region around 1000 cm^{-1} where a tungsten oxo stretch is normally observed[6] is obscured by strong absorptions from the C_6F_5 ligand. Room temperature ^1H and ^{19}F NMR spectra for diamagnetic **2b** show a normal C_{3v}-symmetric ligand backbone. The oxo ligand in **2b** proved highly unreactive. The complex survives unchanged after treatment with TMSI at room temperature or with trimethylphosphine in C_6D_6 at 60 °C for 14 h. **2b** decomposes upon treatment with TMSCl/aniline/NEt_3 in DME at 70 °C or upon reaction with TMSOTf at room temperature in the same solvent, none of the products could be identified.

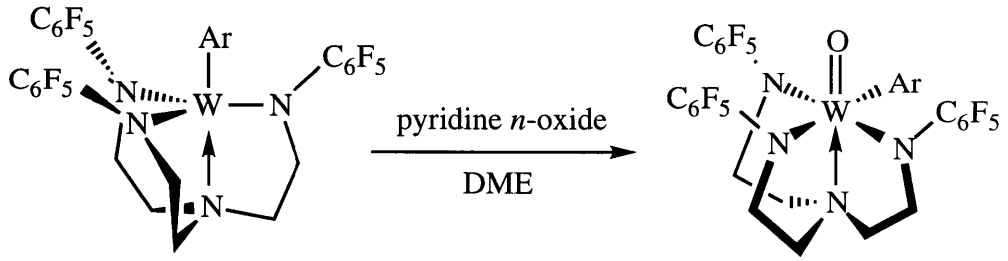

(2)

Ar = Ph (**2a**), 3,5-Me_2-Ph (**2b**)

The NMR data for **2b**, along with its high stability, rendered the structure and the tungsten-oxygen bond order in the molecule unclear (see discussion section). The X-ray structure of the complex was therefore determined. A side view is shown in Figure 4.1, and a

References begin on page 176.

view down the W-N(4) axis is shown in Figure 4.2. Table 4.1 contains selected bond lengths and angles for the complex, and Table 4.3 contains crystallographic data. The structure is of low quality, only the tungsten, fluorine, nitrogen, and oxygen atoms could be refined anisotropically (see ORTEP diagram, appendix I).

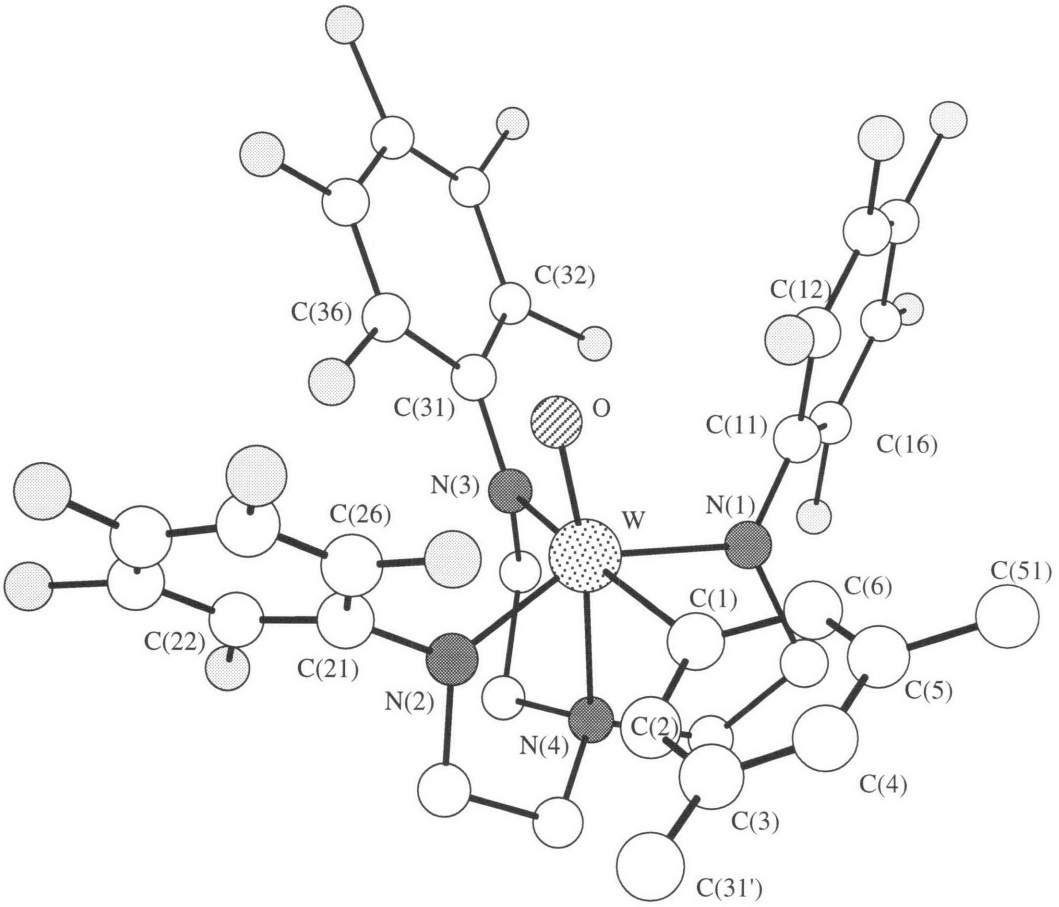

Figure 4.1. A view of the structure of [N_3N_F]W(O)(3,5-Me_2Ph) (**2b**).

However, it does display an unusually distorted conformation of the triamidoamine ligand. Rather than reside in the pocket formed by the three C_6F_5 rings, the xylyl ring is found in between N(1) and N(2), and the oxo ligand is nearly trans to N(4). The distortion can best be visualized by considering the complex to be a deformed octahedron with the O, N(1), N(2), N(3), N(4), and C(1) atoms residing at the vertices. The N(1)-W-N(2) angle is opened up from the

References begin on page 176.

~120° value expected for a C_{3v}-symmetric [N_3N_F] complex to 146.0(7)°. This is the smallest angle for ligands "trans" to one another in the distorted octahedron, with the other two such angles, O-W-N(4) and N(3)-W-C(1), equal to 165.2(7) and 167.2(7)° respectively. We use the dihedral angle between the N(4)-W bond and a N_{amide}-C_6F_5 bond as a measure of how much steric strain is present between the fluorinated aryl rings and the principal ligands. For the C_6F_5 rings closest to the xylyl ring, significant twist is observed. Dihedral angles are 154 and 140°, indicating that these C_6F_5 rings swing away from the xylyl ligand by a rotation about the W-N(1) or N(2) bonds. The C_6F_5 attached to N(3) across from the xylyl ring is almost pointed straight up from N(4), with N(4)-W-N(3)-C(31) = 178°. The tungsten-oxygen bond length of 1.685(14) Å lies in the range normally observed for pseudo-triply bonded tungsten oxo ligands.[6] The solution-state structure is apparently dynamic, since NMR data support a C_{3v}-symmetric structure at room temperature.

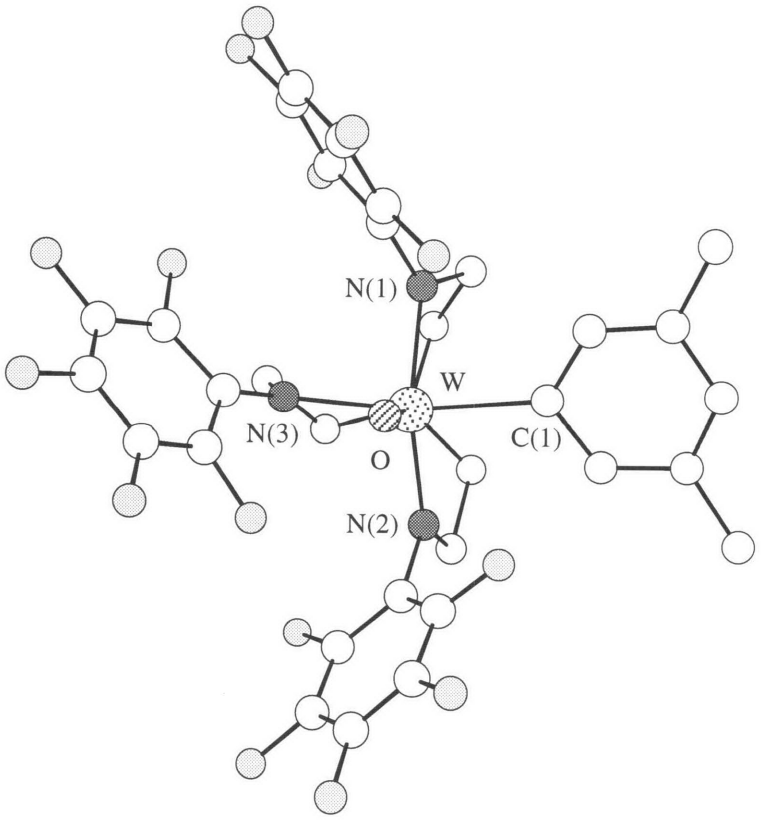

Figure 4.2. The structure of **2b** viewed down the W-N(4) axis.

References begin on page 176.

Table 4.1. Selected bond lengths (Å) and angles (deg.) for [N_3N_F]W(O)(3,5-Me_2Ph) (**2b**).

Distances (Å)

W - O	1.685(14)	W - C(1)	2.23(2)
W - N(1)	2.06(2)	N(1) - C(11)	1.37(3)
W - N(2)	1.96(2)	N(2) - C(21)	1.45(3)
W - N(3)	2.13(2)	N(3) - C(31)	1.32(3)
W - N(4)	2.33(2)		

Angles (deg.)

W - O - N(4)	165.2(7)	N(3) - W - N(1)	86.7(7)
N(1) - W - N(2)	146.0(7)	N(4) - W - N(3)	75.3(7)
C(1) - W - N(3)	167.2(7)	W- N(1) - C(11)	123.3(13)
O - W - C(1)	99.5(7)	W - N(2) - C(21)	124.7(14)

Dihedral Angles (deg.)[a]

N(4) - W - N(2) - C(21)	154.4
N(4) - W - N(1) - C(11)	139.9
N(4) - W - N(3) - C(31)	178.5

[a] Obtained from a Chem 3D drawing

References begin on page 176.

Nitrogen-atom transfer to [N_3N_F]W(3,5-Me_2Ph) can be accomplished with trimethylsilyl-azide, leading to an imido complex, [N_3N_F]W(=N-TMS)(3,5-Me_2-Ph), **3** (equation 3). This nitrogen analog of **2b** has C_s symmetry on the NMR timescale. Apparently the fluxional process which renders **2b** C_{3v}-symmetric by NMR is slower in **3**, if it is occurring at all. A related molecule containing the $[(TMSNCH_2CH_2)_3N]^{3-}$ ligand has recently been synthesized in our laboratories by a alternate method ([N_3N]Mo(=N-TMS)(Me)),[7] and is also C_s-symmetric by NMR.

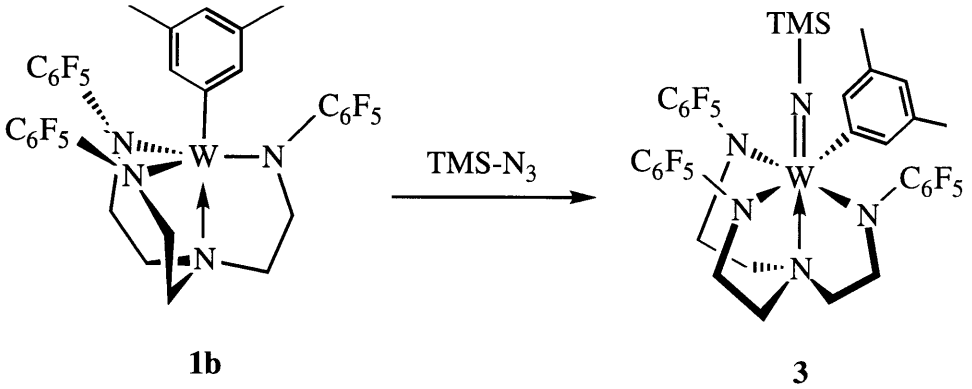

1b **3** (3)

Synthesis of [N_3N_F]W(IV) Phenoxides

[N_3N_F]WCl reacts quickly with potassium pentafluorophenoxide or potassium 3,5-dimethylphenoxide in THF to provide the corresponding tungsten(IV) phenoxides, [N_3N_F]W(O-C_6F_5), **4a**, and [N_3N_F]W(O-3,5-Me_2-Ph), **4b**, and in good yield. Both phenoxides are paramagnetic, with contact-shifted ^1H and ^{19}F NMR spectra. All six magnetically inequivalent fluorines in **4a** can be unambiguously assigned, demonstrating the utility of ^{19}F NMR in the synthesis and characterization of the paramagnetic complexes presented in this chapter. An X-ray study of **4b** was carried out, and a view of the structure is shown in Figure 4.3. Table 4.2 contains selected bond lengths and angles for the complex, and Table 4.3 contains crystallographic data. The usual C_3-symmetric structure seen for the $[N_3N_F]^{3-}$ ligand is observed, with the C_6F_5 rings forming a bowl around the phenoxide. The three F_5C_6-N_{eq}-M-N(4) dihedral angles are 161.7, 174.4, and 178.2°, suggesting that the molecule is relatively

References begin on page 176.

strain-free (cf. Table 1.3). With silylated complexes, the Si-N_{eq}-M-N(4) dihedral angle can vary from nearly 180° (as observed for [N_3N]MoCl[8]) with a small ligand in the pocket down to ~130° as seen with [N_3N]Mo(cyclohexyl) (chapter I). The W-N(4) distance (2.195(7) Å) and the W-N_{eq} distances (1.990(6)-1.975(7) Å) are in the range normally observed for triamidoamine complexes, also indicating little steric strain in the molecule. The W-O distance for the phenoxide ligand is 1.991(7) Å, and the W-O-C(41) angle is 145.0(6)°. M-O bond distances and M-O-C bond angles have been used as a measure of the degree of π-bonding between oxygen and the metal for early transition metal alkoxides and aryloxides, but careful analysis of the data has shown that there is little or no significance of the M-O-C angle in this regard.[9,10] The M-O bond distance in a series of tungsten complexes has been shown to increase with increasing formal electron count of the complex,[11] but we are reluctant to draw any conclusions at this stage regarding the degree of oxygen to tungsten π-bonding in effect in **4b** from the observed metrical data, considering that steric and electronic effects may also perturb these parameters. The 3,5-xylyl ring is oriented directly over one of the C_6F_5 rings, with short aryl carbon-fluorinated aryl carbon distances (C(41)-C(26) = 3.153 Å, C(42)-C(21) = 3.487 Å, see Table 4.2 for others). Typical phenyl-perfluorophenyl π-π stacking distances range from 3.4 to 3.6 Å.[12-14] It may be that a van der Waals interaction between the $Me_2C_6H_3$ ring and the C_6F_5 ring is responsible for the observed metrical parameters for the phenoxide ligand.

References begin on page 176.

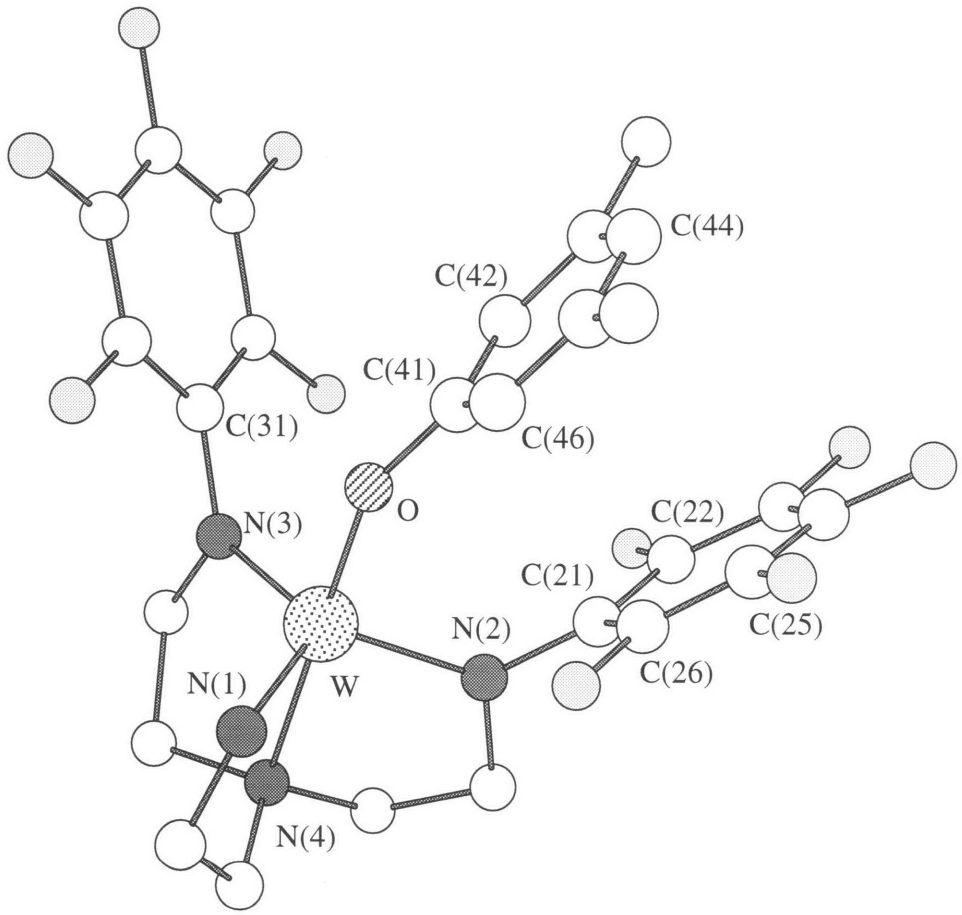

Figure 4.3. A view of the structure of [N_3N_F]W(O-3,5-Me_2Ph) (**4b**). The C_6F_5 ring attached to N(1) was removed for clarity.

Table 4.2. Selected interatomic distances (Å) and angles (deg.) for [N_3N_F]W(O-3,5-Me_2Ph) (**4b**).

Distances (Å)

W - O	1.991(7)	C(41) - C(26)	3.153[a]
W - N(1)	1.990(6)	C(41) - C(21)	3.318[a]
W - N(2)	1.968(7)	C(42) - C(21)	3.487[a]
W - N(3)	1.975(7)	C(46) - C(26)	3.398[a]
W - N(4)	2.195(7)	C(44) - C(25)	3.915[a]
N(3) - C(31)	1.392(11)	C(42) - C(22)	3.609[a]
N(2) - C(21)	1.423(10)		

Angles (deg.)

W - O - C(41)	145.0(6)	N(3) - W - N(1)	119.8(3)
W - N(3) - C(31)	127.8(6)	N(4) - O - W	176.3(3)
W - N(2) - C(21)	125.1(5)	N(3) - W - N(4)	80.3(3)
N(3) - W - N(2)	115.8(3)		

Dihedral Angles (deg.) [a]

N(4) - W - N(1) - C(11)	161.7
N(4) - W - N(2) - C(21)	178.2
N(4) - W - N(3) - C(31)	174.4

[a] Obtained from a Chem 3D drawing

References begin on page 176.

Table 4.3. Crystallographic data, collection parameters, and refinement parameters for [N_3N_F]W(O)(3,5-Me_2Ph) (**2b**) and [N_3N_F]W(O-3,5-Me_2Ph) (**4b**).

	[N_3N_F]W(O)(3,5-Me_2Ph)	[N_3N_F]W(O-3,5-Me_2Ph)
Empirical Formula	$C_{32}H_{21}F_{15}N_4OW$	$C_{32}H_{21}F_{15}N_4OW$
Formula Weight	946.38	946.38
Diffractometer	Siemens SMART/CCD	Siemens SMART/CCD
Crystal Dimensions (mm)	n/a	0.50 × 0.15 × 0.15
Crystal System	Monoclinic	Monoclinic
a (Å)	21.73 (2)	15.2959 (9)
b (Å)	14.92 (2)	13.8809 (8)
c (Å)	24.17 (3)	15.5727 (9)
β (deg)	94.94 (2)	98.9050 (10)
V (Å^3)	7804 (15)	3266.6 (3)
Space Group	I2/a	$P2_1/c$
Z	8	4
D_{calc} (Mg/m^3)	1.611	1.924
μ (absorption coefficient) (mm^{-1})	3.061	3.657
F_{000}	3664	1832
λ (MoK_α)	0.71073 Å	0.71073 Å
Temperature (K)	188 (2)	188 (2)
θ Range for Data Collection (deg)	1.61 to 18.75	1.35 to 23.28
Reflections Collected	8082	12524
Independent Reflections	3030	4657
R [I > 2σ(I)]	0.0855	0.0522
R_W [I > 2σ(I)]	0.1761	0.1247
GoF	1.160	1.128
Extinction Coefficient	0.00008 (4)	0.0023 (4)
Largest Diff. Peak and Hole (eÅ^{-3})	0.819 and -0.767	2.056 and -2.920

References begin on page 176.

[N_3N_F]W(O-3,5-Me_2Ph) (**4b**) reacts with pyridine *n*-oxide to yield a complex which analyzes correctly for [N_3N_F]W(O)(O-3,5-Me_2Ph) (**5**) (equation 4). We have no direct proof that the oxo ligand is present, since the IR spectrum is masked by the C-F absorbances in the region around 1000 cm^{-1} . However, given that **5** is diamagnetic and that pyridine is produced

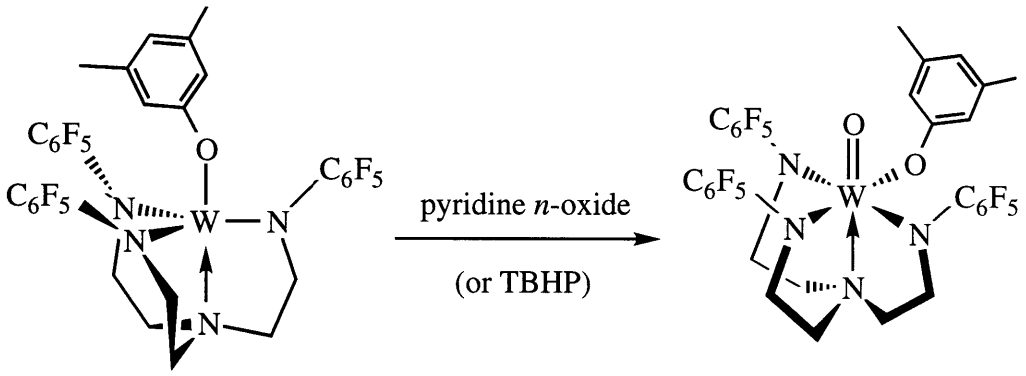

3b **5** (4)

during its formation (as evidenced by ^1H NMR) we propose that oxygen atom transfer has occurred in a manner analogous to the formation of [N_3N_F]W(O)(3,5-Me_2Ph), **2b**. Just as with [N_3N_F]W(3,5-Me_2Ph)(=N-TMS) (**3**), it seems that a fluxional process similar to the one which renders **2b** C_{3v}-symmetric on the NMR timescale at room temperature (despite its distorted solid-state structure) is slower in **5**, if it is occurring at all. Anhydrous t-butylhydroperoxide (TBHP) as a 5.5 M solution in decane also reacts with **4b** to yield **5**, although the reaction is not as clean with pyridine *n*-oxide, perhaps because **5** is susceptible to protonolysis by TBHP or the *t*-butanol side-product. Reaction of [N_3N_F]W(3,5-Me_2Ph) (**1b**) with *t*-butylhydroperoxide led only to decomposition, possibly because **1b** or **2b** is again too susceptible to protonolysis. **4b** also reacts with butyllithium to yield [N_3N_F]W≡$CCH_2CH_2CH_3$ with liberation of dihydrogen (equation 5). The reaction probably proceeds by metathesis of the phenoxide with the butyl

[N_3N_F]W(O-3,5-Me_2Ph) —BuLi→ [N_3N_F]W≡$CCH_2CH_2CH_3$ (5)

4b

References begin on page 176.

anion to lead to an intermediate [N_3N_F]W(butyl) complex, which then loses molecular hydrogen as would be expected (see chapter III).

Attempted Synthesis of Terminal Phosphido and Arsenido Complexes

[N_3N_F]WCl and [N_3N_F]MoCl[1] react smoothly with lithium phenylphosphide to give the corresponding phosphido complexes, [N_3N_F]M(PHPh), M = Mo (**6a**) or W (**6b**), in high yield as brown solids (equation 6). The phosphido proton resonance of the tungsten compound was located at 17.50 ppm in the proton NMR spectrum (J_{HP} = 295 Hz, J_{HW} = 22 Hz) and the

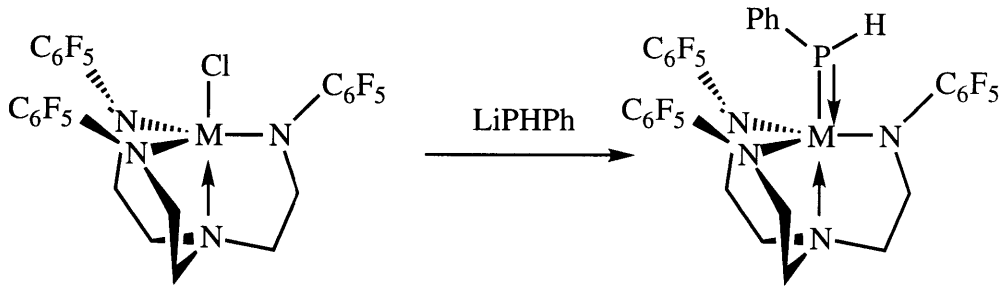

(6)

M = Mo (**6a**), W (**6b**)

phosphorus resonance at 118.1 ppm (J_{PW} = 742 Hz) in the ^{31}P spectrum. For **6a**, δ_{PPhH} = 11.20 ppm, J_{HP} = 281 Hz, and δ_P = 189.6 ppm. These data are analogous to the NMR parameters found for the TMS-substituted analogs, [N_3N]W(PPhH) and [N_3N]Mo(PPhH).[7] The diamagnetism of these d^2 phosphides can be ascribed to π donation of the lone pair on phosphorus to the metal, resulting in pairing of the two d electrons in the remaining orbital. Since the mechanism of conversion of [N_3N]W(PHPh) into the rare terminal phosphido complex, [N_3N]W≡P, is believed to involve removal of the phosphido proton, attempts were made to convert [N_3N_F]W(PPhH) into [N_3N_F]W≡P employing various lithium reagents (LiPPhH, BuLi, MeLi, PhLi) under a variety of conditions, but in all cases either no reaction occurred or no products could be identified. The cyclic voltammagram of **6b** showed a reversible oxidation wave at 0.40 V, however, chemical oxidation with [Cp_2Fe]OTf followed by addition of triethylamine did not yield a clean product. An attempt to cleave the phosphorus-phenyl linkage

References begin on page 176.

photochemically was unsuccessful, **6b** is stable towards photolysis at 30 °C. Lithium metal P-Ph cleavage was also attempted, but only decomposition was observed. The reaction between [N_3N_F]WCl and Li_2PPh also failed. We conclude that [N_3N_F]W≡P simply is not formed as readily as [N_3N]W≡P, or much less probably, [N_3N_F]W≡P is unstable under the reaction conditions. Of course, none of these results constitutes evidence that [N_3N_F]M≡P species are not stable, only that they cannot be made by the methods employed so far.

[N_3N_F]M≡N (M = Mo, W) complexes *are* readily prepared[1] from the [N_3N_F]MCl complexes and sodium azide. They are quite stable, but a nitrido complex is a far less exotic species than the [N_3N_F]W≡P target. Although both [N_3N]Mo≡As and [N_3N]W≡As are known compounds,[7] we were again unable to prepare [N_3N_F]-containing analogs of these terminal arsenido complexes. The reaction between LiAsPhH and [N_3N_F]WX (X = Cl, I, OTf, or 3,5-dimethylphenoxide) resulted either in no reaction or slight decomposition of the tungsten starting material, depending on the conditions. Similarly, despite the fact that [N_3N]WPh reacts smoothly with $PhAsH_2$ itself to yield [N_3N]W≡As, [N_3N_F]W(3,5-Me_2Ph) completely decomposes when treated with phenylarsine in CH_2Cl_2 or THF over a few days in the dark. We presume that the reasons for the inability to synthesize [N_3N_F]W≡As are related to the inability to convert [N_3N_F]M(PPhH) complexes to terminal phosphides; the more open steric environment and less electron-rich metal center present in the C_6F_5-substituted complexes compared to the TMS-substituted complexes render the reaction unfavorable, at least under the conditions attempted thus far.

Carbon Monoxide Insertion Reactions

Both [N_3N_F]W(Ph) and [N_3N_F]W(3,5-Me_2Ph) react with one equivalent of CO to yield the corresponding acyl complexes, [N_3N_F]W(OC)Ph (**7a**), and [N_3N_F]W(OC)-3,5-Me_2Ph (**7b**), as diamagnetic black microcrystalline solids (equation 7). Exactly one equivalent of carbon monoxide must be used during the synthesis, since both products decompose upon treatment

References begin on page 176.

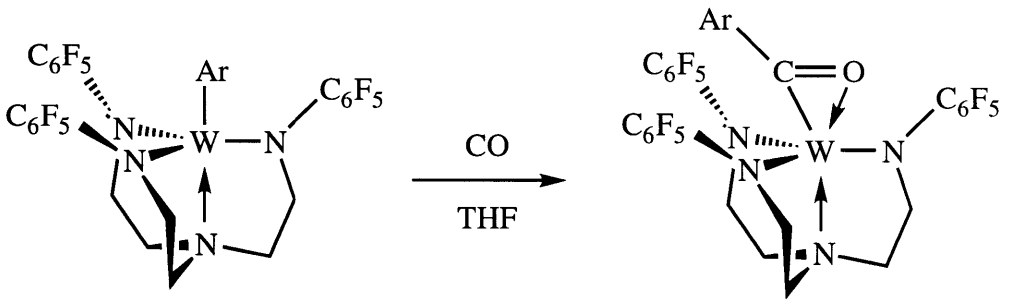

(7)

Ar = Ph (**7a**), 3,5-Me_2Ph (**7b**)

with additional CO. An X-ray study of **7b** showed an η^2 acyl structure. Dative bonding of oxygen with tungsten apparently breaks the degeneracy of the d_{xz}/d_{yz} set in the complexes, resulting in pairing of the electrons into one of these orbitals and a ^1A electronic configuration. ^1H, ^{19}F, and ^{13}C NMR show a C_{3v}-symmetric structure at 22 °C. It appears that the acyl ligand is able to rotate about the W-N_{axial} vector on the NMR timescale. This type of fluxional process is not uncommon for triamidoamine complexes with local C_s-symmetric apical ligand(s) (cf. [N_3N]W(cyclopentylidene)(H), chapter II). The IR spectra display no stretch which can be assigned to the acyl, but all compounds containing the $[N_3N_F]^{3-}$ ligand (including $[N_3N_F]H_3$) display a strong band at ~1510 cm^{-1} which we assign to the to the N-C_6F_5 stretch. Considering that the C-O stretch in many early and middle transition metal acyl complexes[15] is observed between 1500 and 1600 cm^{-1}, it is possible that the C-O stretch in **7a** and **7a** is concealed by the intense N-C_6F_5 absorbance. Both complexes have a low-field ^{13}C resonance (256.9 ppm for **7a** and 252.3 ppm for **7b**) in the range normally observed for η^2 acyl complexes,[15] although the concentration of the samples was too low to observe tungsten-carbon coupling.

Crystals of **7b** suitable for X-ray diffraction were grown by vapor diffusion of pentane into a dichloromethane solution at -40 °C, and one CH_2Cl_2 molecule per molecule of **7b** was observed in the crystal. A drawing of the structure is shown in Figure 4.4, and Table 4.4 contains selected bond lengths and angles. Table 4.8 contains the crystallographic data. The structure confirmed that the acyl ligand is bound η^2 to tungsten, with W-O, W-C(40), and C(40)-O distances of 2.177(4), 1.931(7), and 1.296(8) Å, respectively. The W-C(40) distance is

References begin on page 176.

particularly short for compounds of this type.[15] This could be a result of a significant amount of backbonding between tungsten and C(40), resulting in multiple bond character. Such backbonding would also be expected to decrease the C(40)-O bond order, elongating that bond distance. The observed distance is indeed at the long end of the spectrum for η^2 acyl C-O bonds.[15] The xylyl ring in **7b** lies in between two of the three C_6F_5 rings, resulting in a stack of the three rings with inter-ring distances short enough for a van der Waals interaction to be present. The shortest distances between ring carbons range from 3.182 Å (C(42)-C(22) to 3.497 Å (C(41)-C(11)). Consistent with an interaction between these three rings, the N(1)-W-N(2) angle is the smallest of the three N_{eq}-W-N_{eq} angles, at 113.1(3)°. One might expect this angle to be greater than 120° on steric grounds. N(4)-W-N_{eq}-C_6F_5 dihedral angles are 178.0, 170.5, and 164.0°, indicative of only a slight degree of steric strain in the molecule (cf. the dihedral angles for TMS-substituted complexes in Table 1.3). Similarly, the W-N_{eq} and W-N(4) distances are in the range normally observed for relatively sterically unobstructed triamidoamine complexes.

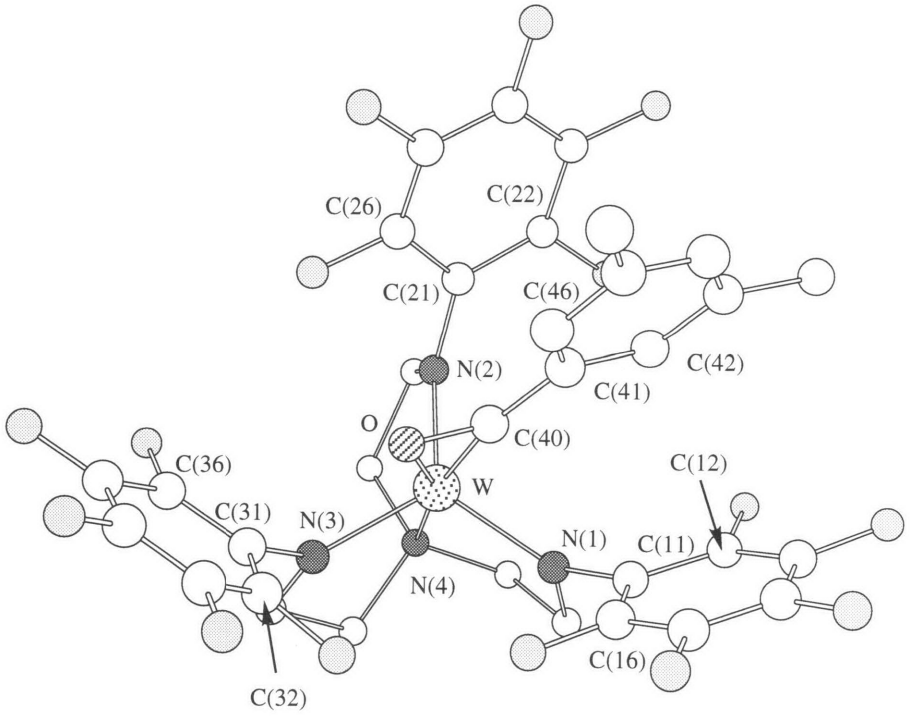

Figure 4.4. A view of the structure of [N_3N_F]W(CO)(3,5-Me_2Ph) (**7b**) (CH_2Cl_2 removed).

References begin on page 176.

Table 4.4. Selected interatomic distances (Å) and angles (deg.) for [N_3N_F]W(CO)(3,5-Me_2Ph).

Distances (Å)

W - O	2.177(4)	W - C(40)	1.931(7)
W - N(1)	1.988(6)	O - C(40)	1.296(8)
W - N(2)	1.969(6)	C(40) - C(41)	1.464(10)
W - N(3)	1.988(7)	N(1) - C(11)	1.413(9)
W - N(4)	2.227(6)	N(2) - C(21)	1.429(11)

Angles (deg.)

W - C(40) - O	82.3(4)	N(3) - W - N(1)	117.6(3)
C(40) - W - O	36.2(2)	N(2) - W - N(3)	116.7(3)
C(40) - O - W	61.5(3)	N(2) - W - N(1)	113.1(3)
W - C(40) - C(41)	151.3(5)	N(4) - W - N(3)	79.9(2)
W - N(3) - C(31)	126.6(5)	N(4) - W - N(1)	76.8(2)
W - N(1) - C(11)	125.6(4)	N(3) - W - O	82.0(2)

Dihedral Angles (deg.)[a]

N(4) - W - N(2) - C(21)	170.5	W - N(1) - C(11) - C(16)	60.0
N(4) - W - N(1) - C(11)	178.0	W - N(2) - C(21) - C(26)	71.4
N(4) - W - N(3) - C(31)	164.0	W - N(3) - C(31) - C(32)	80.0

[a] Obtained from a Chem 3D drawing

As stated above, both **7a** and **7b** decompose when treated with additional carbon monoxide, although the nature of the decomposition is not known. Decomposition with excess CO is also observed with TMS-substituted triamidoamine complexes. When $[(TMSNCH_2CH_2)_3N]Mo(CH_3)$[16] is reacted with an excess of ^{13}CO in ether at 0 °C for 15 min, a rust-colored crystalline product is isolated. ^1H and ^{13}C NMR data are consistent with an η^2 acyl complex, with δ (^{13}CO) = 245.7 ppm, a one-bond acyl carbon-methyl carbon coupling constant of 32 Hz, and a two-bond $\underline{H_3}C\text{-}^{13}\underline{C}O$ J_{CH} value of 6 Hz. The ability to measure these coupling constants allowed us to determine that the carbon monoxide had inserted into the Mo-Me bond, since these data are consistent with a single bond between H_3C and ^{13}CO.[17] When $[N_3N]Mo(CH_3)$ is treated with an excess of CO over the course of hours at room temperature in ether, a Mo(II) decomposition product (**8**) is formed (equation 8).

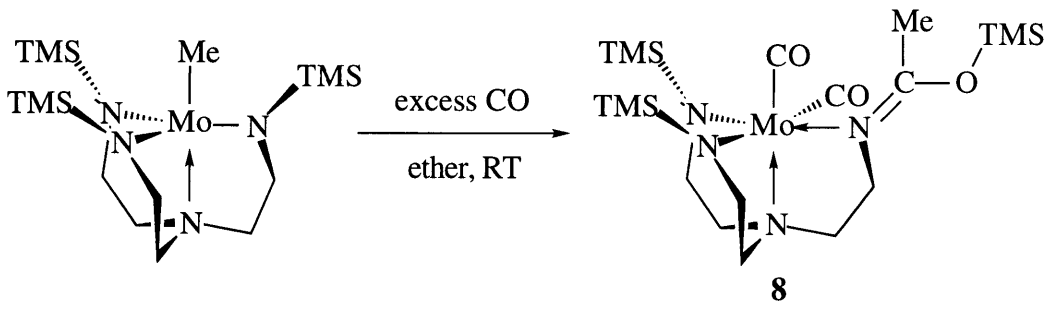

(8)

8

8 is the result of formal insertion of an acetyl fragment into an amido nitrogen-silicon bond, and two terminal carbonyl ligands are bound to the metal, as determined by an X-ray study.[18] Since I did not discover this reaction, I will not discuss mechanistic proposals for the transformation or the structure of **8**, this information will be available in the literature.[18] The high thermodynamic stability of this decomposition product is evidenced by the following experiment. When a toluene-d_8 solution of $[N_3N]Mo(CO)Me$ is heated to 65 °C in a sealed tube for 4 h, $[N_3N]Mo(CH_3)$ and **8** are formed in a 2:1 ratio (equation 9). Apparently migratory de-insertion of carbon monoxide in $[N_3N]Mo(CO)Me$ is facile enough at 65 °C that the liberated CO can react to form **8**.

References begin on page 176.

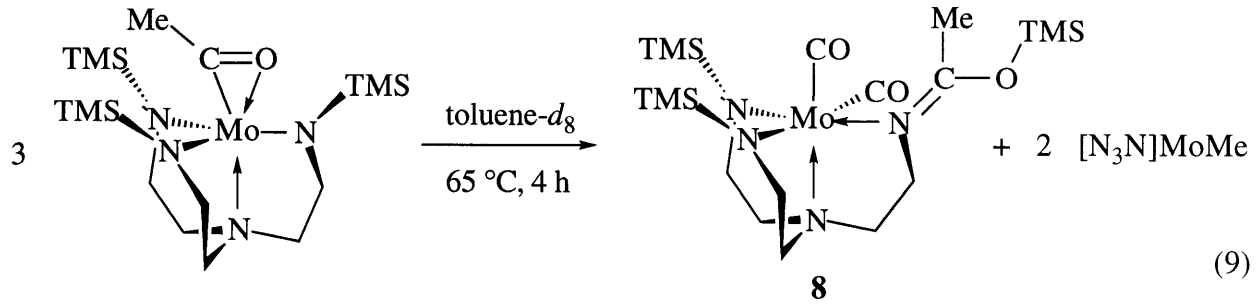

8 (9)

Adducts of [N_3N_F]W

The impetus for our work in this area came with the discovery that [N_3N_F]Mo(OTf) could be reduced with sodium amalgam under nitrogen to yield [N_3N_F]Mo(N_2)Mo[N_3N_F].[1] We sought to determine if a similar reaction would occur with the tungsten analog. When [N_3N_F]W(OTf) is reacted with sodium amalgam, a paramagnetic product of unknown structure is obtained in only moderate purity. Attempts to purify this material further were unsuccessful. The same impure product is obtained when the reaction is run under argon or *in vacuo*, ruling out the possibility of formation of a dinitrogen complex. Addition of *t*-butyl isocyanide to the mixture does not result in the formation of known [N_3N_F]W(CN-*t*-Bu) (see below), suggesting that the product is not trigonal-monopyramidal [N_3N_F]W, the complex resulting from reductive loss of sodium triflate. It appears that binding of dinitrogen in the tungsten system is not competitive with whatever processes give rise to the decomposition product observed.

In the presence of stronger π-acid ligands than dinitrogen, [N_3N_F]WX species can be reduced to give [N_3N_F]W(L) complexes. [N_3N_F]W(OTf)[1] reacts with one equivalent of 0.5% sodium amalgam under carbon monoxide to yield [N_3N_F]W(CO) (**9**) as a paramagnetic, red crystalline solid in high yield. Interestingly, [N_3N_F]WCl does not react under the same conditions. The ^{1}H NMR spectrum of **9** contains two broad signals for the ligand methylene protons at 29.3 and -19.2 ppm. One high-field and one low-field ligand backbone proton resonance is characteristic of W(III) complexes of this type (see below). In **9**, only the meta and para fluorine atoms are observed as broad resonances at -132.1 and -170.5 ppm. A magnetic moment of 2.8 ± 0.1 μ_B at 22 °C is observed in CD_2Cl_2 solution by the Evan's method, and the

References begin on page 176.

IR spectrum shows a band at 1846 cm^{-1} which we assign to the CO stretch. This value is abnormally low for a terminal carbonyl ligand, indicative of a high degree of backbonding from the metal.[19] A carbonyl hydride complex, $[(TMSNCH_2CH_2)_3N]W(H)(CO)$, has recently been prepared and crystallographically characterized in our laboratories,[4] and has an even lower CO stretching frequency (1766 cm^{-1}). We note that attempts to synthesize $[N_3N_F]W(CO)$ from $[N_3N_F]WCl$ under the same conditions lead to no reaction.

A facile, reversible reduction wave is observed in the cyclic voltammagram of $[N_3N_F]W(CO)$ (**9**) at 0.16 V, which led us to attempt to reduce it chemically. When a THF solution of **9** is stirred over one equivalent of sodium amalgam for one hour, ^{19}F NMR shows clean conversion to a diamagnetic species. Quenching with TMSCl leads to the formation of $[N_3N_F]W{\equiv}C\text{-}O\text{-}TMS$ (**10**) as a light brown solid (equation 10). The reduction of carbon

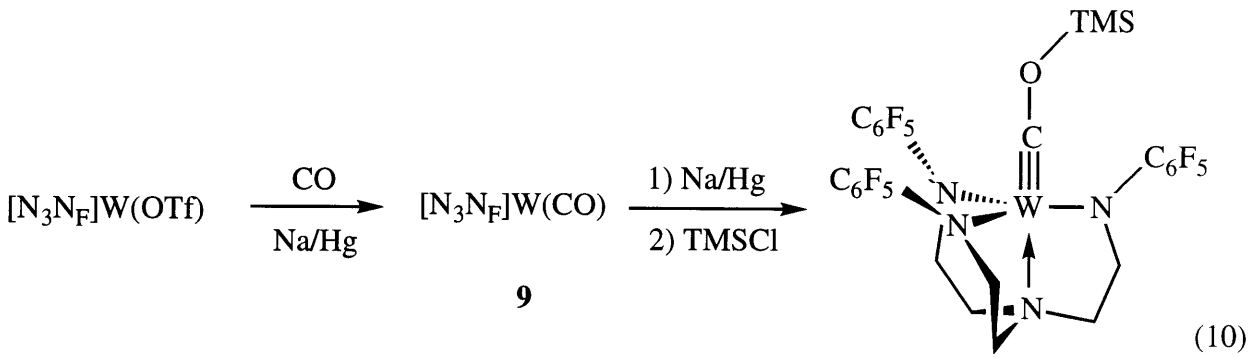

(10)

10

monoxide to yield a siloxycarbyne is rare, the only other examples to our knowledge are those of some tantalum carbonyl complexes,[20] and a related example from our laboratories.[4] Electron transfer to **9** might be facilitated by the inductive effect of the C_6F_5 rings. The formation of **10** is probably thermodynamically driven as well, considering the exceptional propensity for the formation of triple[7,21] or pseudo-triple[22] bonds in the apical site of triamidoamine complexes.

When $[N_3N_F]WCl$ is treated with one equivalent of sodium amalgam in the presence of *t*-butyl isocyanide, orange $[N_3N_F]W(C{\equiv}N\text{-}t\text{-}Bu)$ (**11**) is formed in high yield as a paramagnetic

References begin on page 176.

crystalline solid. Using [N_3N_F]W(OTf) as a starting material gives identical results. NMR parameters are similar to those for [N_3N_F]W(CO), with ligand backbone protons observed at 8.0 and -25.8 ppm, and a resonance observed at 13.8 ppm for the *t*-butyl group (Figure 4.5). The CN stretch for the isocyanide complex is observed at 1684 cm^{-1}, an abnormally low value for a coordinated isocyanide ligand.[23] It appears that extensive π-backbonding occurs into the isocyanide ligand, just as with [N_3N_F]W(CO). Cyclic voltammetry showed that the complex could be oxidized reversibly at a potential of 0.33 V. Treating a THF solution of **11** with [Cp_2Fe][OTf] leads to the formation of ferrocene and an diamagnetic product which appears to be [[N_3N_F]W(CN-*t*-Bu)][OTf] (**11b**) by NMR. C_6F_5 resonances are observed in the ^{19}F spectrum (THF) at -148.3, -162.0, and -164.6 ppm, and a broad triflate resonance is seen at -79.3 ppm. The IR shows a strong stretch at 2107 cm^{-1}, and a peak at 157.3 ppm (J_{CW} = 93 Hz) is observed in the ^{13}C spectrum which we assign to [N_3N_F]W(CN-*t*-Bu)$^+$. Satisfactory elemental analyses have not yet been obtained. The data in hand suggest that the C-N bond order in the cation is nearly three, but some multiple W-C bonding must still be present in order to break the degeneracy of the d_{xz}/d_{yz} set and yield a diamagnetic complex.

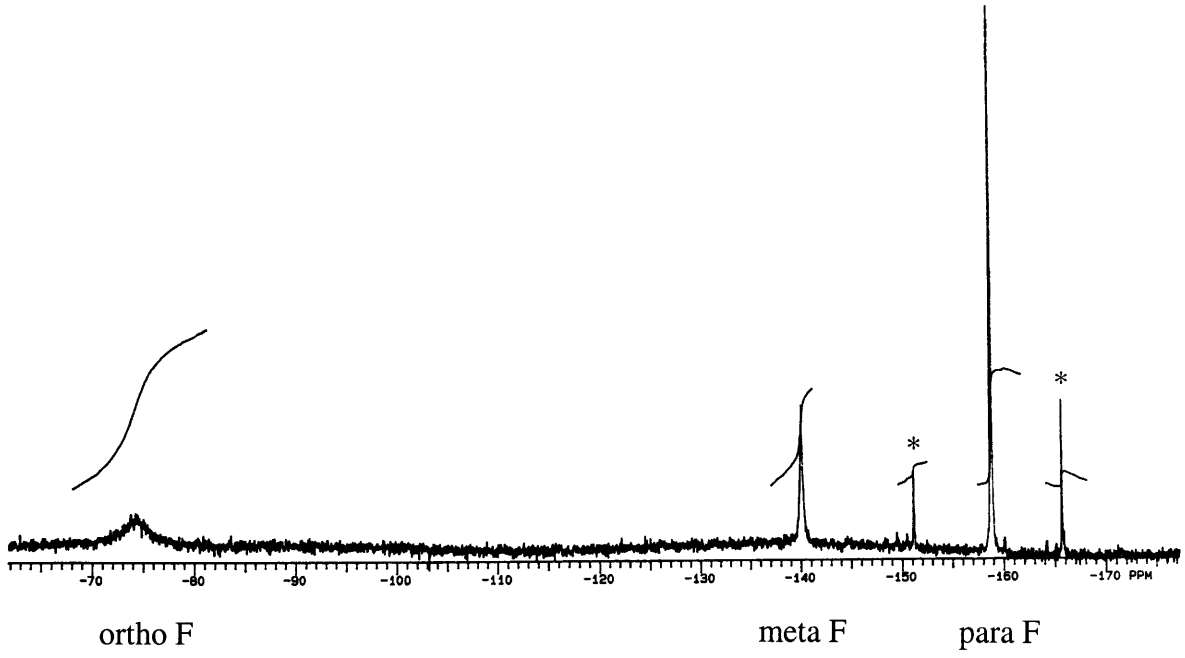

Figure 4.5. The ^{19}F NMR spectrum of [N_3N_F]W(CN-*t*-Bu) (**11**) in CH_2Cl_2 at 22 °C.
* A diamagnetic impurity, see text.

References begin on page 176.

An X-ray study of **11** was carried out, and a view of the structure is shown in Figure 4.6. Table 4.5 contains selected bond lengths and angles, and Table 4.6 contains the crystallographic data. The *t*-butyl isocyanide ligand in **11** is unusually bent, with C(7)-N(5)-C(8) = 132.2(10)°. Additionally, the W-C(7) distance is 1.913(11) Å, in the range normally observed for tungsten-carbon double bonds. The isocyanide C(7)-N(5) distance is 1.249(14) Å, elongated from that in free isocyanides. The metrical data are consistent with strong π-backbonding from tungsten to the isocyanide, in line with the low IR C-N stretching frequency of 1684 cm^{-1}. Based on the data in hand, the complex could be considered a W(V) imidocarbene rather than a W(III) isocyanide adduct. Isocyanide ligands with C_α-N-R angles of less than 170° are rare, with most of the other examples occurring in low-valent complexes of middle transition metals in which the isocyanide ligand is the best π-acceptor ligand present in the coordination sphere.[24] The isocyanide in **11** is canted slightly from the pseudo-C_3 axis; the torsion angle between the N(4)-W and C(7)-N(5) vectors is equal to 11.0°. This is presumably a result of steric pressure between the *t*-Bu group and the C_6F_5 rings attached to N(1) and N(3). N(4)-W-N_{ax}-C_6F_5 dihedral angles range from 169.3 to 179.0°, indicative of no substantial distortions of the "pocket" geometry.

Solid-State Magnetic Susceptibility Measurements

The magnetic susceptibility of **11** in the solid state can be readily modeled using the Curie Law ($\chi_M = (\mu^2/(7.997 \times T)) - C$). μ obtained in this manner is 1.70 ± 0.05 μ_B, close to the spin-only value for one unpaired electron. This data lends credence to the formulation of **11** as a W(V) imidocarbene complex. Figure 4.7 shows a plot of χ_M versus T for **11**. The magnetic susceptibilities of [N_3N_F]WCl and [N_3N_F]MoCl are unexceptional. Behavior very similar to what is seen with silylated analogs [N_3N]WCl and [N_3N]MoCl is observed (see chapters I and II). The magnetic moment of [N_3N_F]WCl falls smoothly as temperature decreases, most likely a result of a combination of spin-orbit coupling and low-symmetry ligand field components which result in zero field splitting of the d^2 ground state triplet.[25] These effects are less pronounced in the molybdenum complex, where Curie-Weiss behavior is observed down to 50 K (μ = 2.76 μ_B; θ = -6.9). Figures 4.8 through 4.10 show the data obtained by SQUID for these complexes.

References begin on page 176.

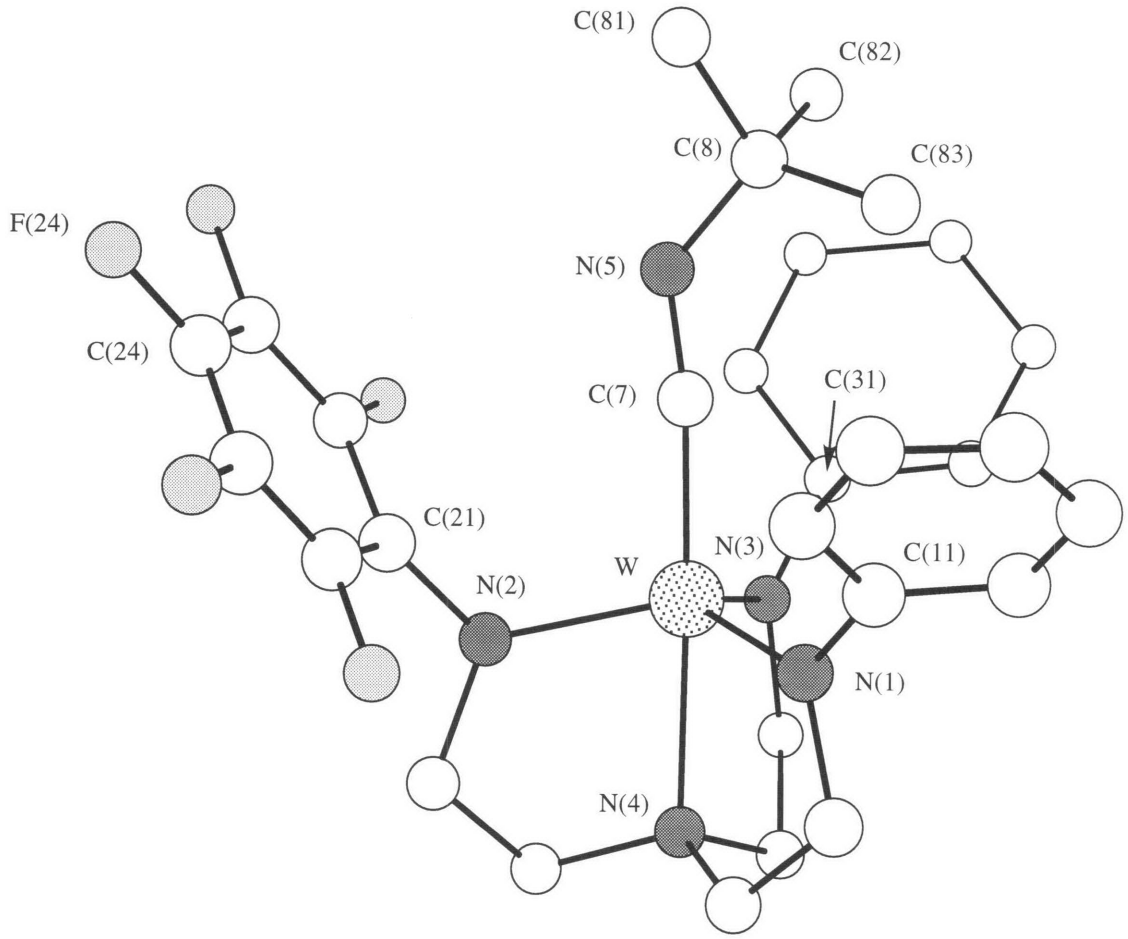

Figure 4.6. A view of the structure of [N_3N_F]W(CN-*t*-Bu) (**11**). The fluorine atoms from the C_6F_5 rings attached to N(1) and N(3) were omitted for clarity.

References begin on page 176.

Table 4.5. Selected bond distances (Å) and angles (deg.) for [N_3N_F]W(CN-*t*-Bu) (**11**).

Distances (Å)

W - C(7)	1.913(11)	C(7) - N(5)	1.249(14)
N(5) - C(8)	1.42(2)	W- N(1)	1.975(8)
W - N(2)	1.967(8)	W- N(3)	1.980(8)
W - N(4)	2.243(8)	C(24) - F(24)	1.349(11)
N(1) - C(11)	1.409(12)	N(3) - C(31)	1.423(13)

Angles (deg.)

C(7) - N(5) - C(8)	132.2(10)	W - C(7) - N(5)	172.1(8)
N(1) - W - N(2)	114.7(3)	N(2) - W - N(3)	117.8(3)
W - N(1) - C(11)	127.9(6)	W - N(3) - C(31)	125.5(6)
W - N(1) - C(1)	118.9(6)	N(4) - W - N(2)	78.7(3)
N(5) - C(8) - C(83)	116.5(11)	N(5) - C(8) - C(81)	111.3(13)

Dihedral Angles (deg.)[a]

N(4) - W - N(2) - C(21)	169.3
N(4) - W - N(1) - C(11)	179.0
N(4) - W - N(3) - C(31)	172.8

Torsion Angle (deg.)[a]

N(4) - W – C(7) - N(5)	169.0

[a] Obtained from a Chem 3D drawing

References begin on page 176.

Table 4.6. Crystallographic data, collection parameters, and refinement parameters for [N_3N_F]W(CN-*t*-Bu) (**11**).

Empirical Formula	$C_{29}H_{21}F_{15}N_5W$
Formula Weight	908.36
Diffractometer	Siemens SMART/CCD
Crystal Dimensions (mm)	0.21 × 0.14 × 0.08
Crystal System	Monoclinic
a (Å)	9.344 (4)
b (Å)	27.09 (2)
c (Å)	12.237 (10)
β (deg)	97.26 (5)
V (Å^3)	3073 (4)
Space Group	$P2_1/c$
Z	4
D_{calc} (Mg/m^3)	1.964
μ (absorption coefficient) (mm^{-1})	3.881
F_{000}	1756
λ (MoK_α)	0.71073 Å
Temperature (K)	153 (2)
θ Range for Data Collection (deg)	1.50 to 23.32
Reflections Collected	9917
Independent Reflections	4215
Absorption Correction	Semi-empirical from ψ-scans
Max. and Min. Transmission	0.3124 and 0.2333
R [I > 2σ(I)]	0.0494
R_W [I > 2σ(I)]	0.1103
GoF	1.216
Extinction Coefficient	0.0012 (2)
Largest Diff. Peak and Hole (eÅ^{-3})	1.633 and -0.997

References begin on page 176.

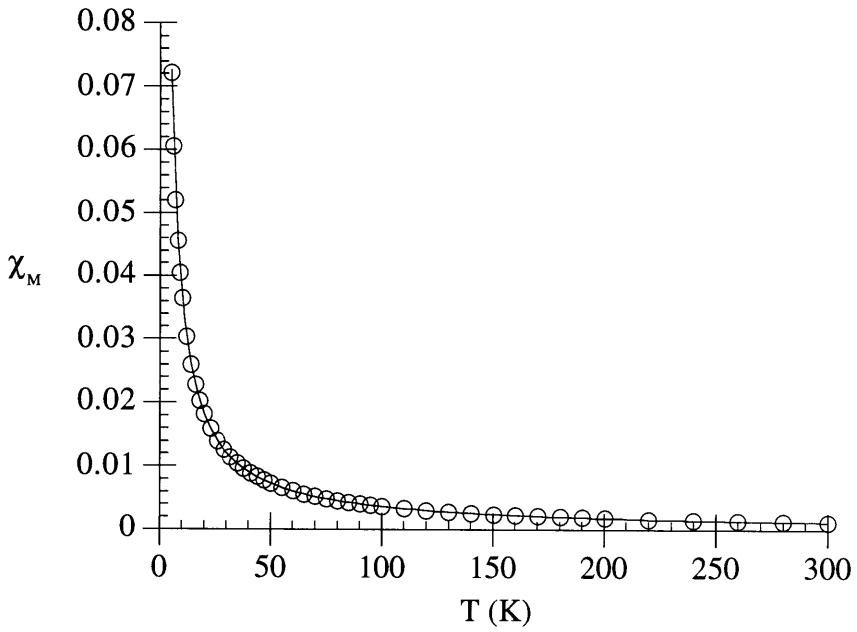

Figure 4.7. A plot of χ_M versus T for [N_3N_F]W(CN-*t*-Bu).

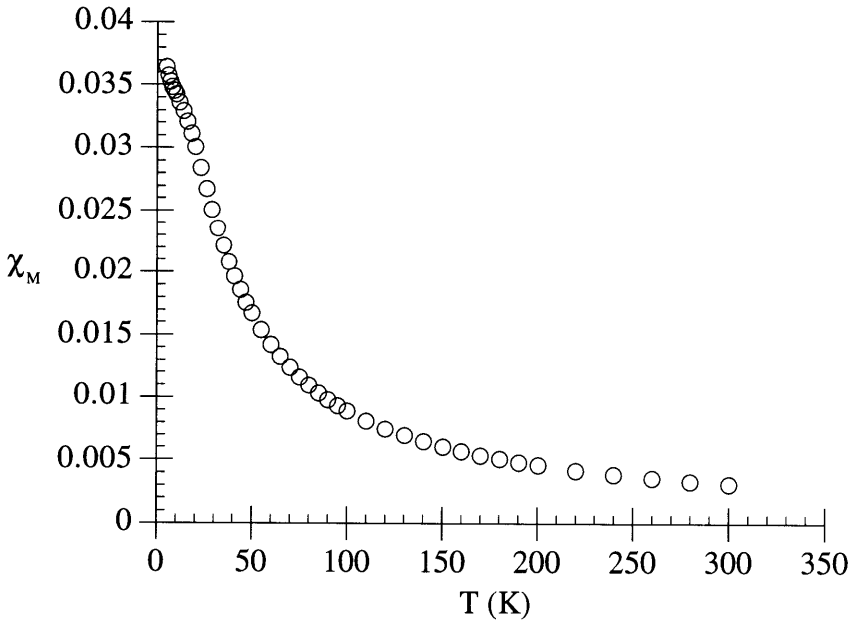

Figure 4.8. A plot of χ_M versus T for [N_3N_F]MoCl.

References begin on page 176.

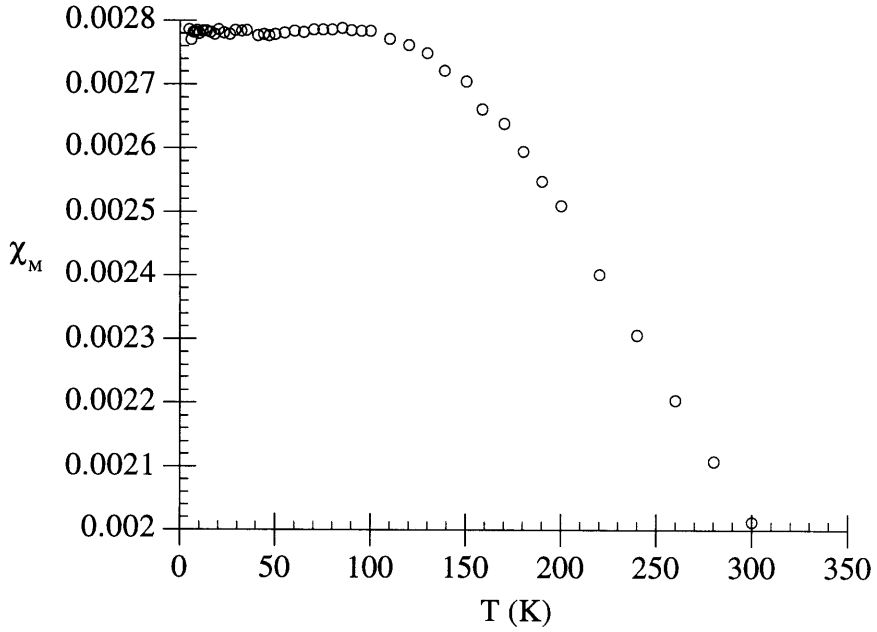

Figure 4.9. A plot of χ_M versus T for [N_3N_F]WCl.

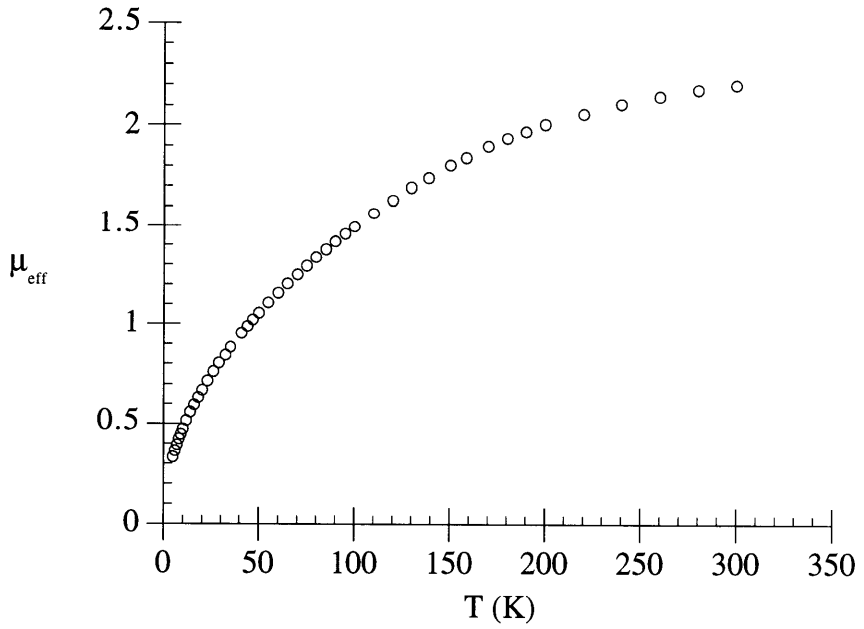

Figure 4.10. A plot of μ_{eff} versus T for [N_3N_F]WCl.

References begin on page 176.

Unstable Isocyanide Complexes and Formation of Other Adducts

When [N_3N_F]WCl is reacted with sodium amalgam in the presence of *n*-butyl isocyanide under conditions identical to those used to synthesize **11**, a paramagnetic species can be observed by ^{19}F NMR after ~1 h. The ^{19}F chemical shifts and peak widths are similar to those observed for **11**, and we propose that [N_3N_F]W(C≡N-*n*-Bu) (**12a**) is present at this point. However, after normal workup and attempting to crystallize from CH_2Cl_2, the solid isolated is contaminated with diamagnetic impurities as evidenced by NMR. Diamagnetic peaks can also be observed by simply allowing the reaction mixture to stir for periods longer than 1 h. If the crude solid is recrystallized from toluene, conversion to the diamagnetic material(s) is nearly complete. The gated-decoupled ^{13}C NMR spectrum of the decomposition product(s) displays two low-field resonances, a singlet at 240 ppm and a doublet at 173 ppm (J_{CH} = 164 Hz). The IR spectrum shows a weak, broad band at 3291 cm^{-1} and an intense stretch at 1647 cm^{-1}. ^1H NMR is consistent with two different types of *n*-butyl groups. Based on these data, we speculate that the decomposition products could arise from hydrogen atom abstraction from toluene. Hydrogen atom transfer from the solvent to **12a** could lead to [N_3N_F]W≡C-NH-*n*-Bu if H· reacts at nitrogen, and the iminoformyl complex, [N_3N_F]W(CH=N-*n*-Bu) if H· reacts at carbon. One problem with this hypothesis is that when **12a** was allowed to stand in toluene-d_8 for 12 h, decomposition to the diamagnetic material was again observed, but ^2H NMR showed that the product(s) did not contain any deuterium. We cannot rule out other decomposition pathways involving intermolecular processes, possibly via hydrogen atom abstraction from the triamidoamine ligand backbone. An equally likely possibility is the some type of dimer forms, an isoelectronic tungsten acetylide complex containing the TMS-substituted triamidoamine ligand, [N_3N]W(C≡CH), has been shown to couple at the β-carbon, leading to a dimeric complex with an olefinic bridging group.[16] It is worth noting that both [N_3N_F]W(CO) and [N_3N_F]W(CN-*t*-Bu) are always contaminated with a *trace* (< 5% by NMR) of a diamagnetic impurity, although this did not prevent the successful C, H, and N analysis of both products. For [N_3N_F]W(^{13}CO), a ^{13}C NMR study revealed a sharp resonance at 205.1 ppm which displayed tungsten satellite

References begin on page 176.

peaks (J_{CW} = 131 Hz), which we attribute to the diamagnetic impurity. Upon proton coupling, this peak splits into a doublet with J_{CH} = 7.5 Hz. Based on these data alone, we cautiously postulate that the diamagnetic impurity present is a carbonyl hydride complex, [N_3N_F]W(CO)(H), analogous to crystallographically characterized [$(TMSNCH_2CH_2)_3N$]-W(CO)(H).[4]

When [N_3N_F]WCl is reduced with sodium amalgam in the presence of MeN≡C, complete decomposition is observed. An interesting progression based on the size of the isocyanide ligand appears to be in effect. The *t*-butyl isocyanide adduct of [N_3N_F]W is stable, a complex proposed to be the *n*-butyl isocyanide adduct can be observed in solution but decomposes upon workup, and the MeN≡C adduct is not even detected before total decomposition occurs. Moving to molybdenum changes the situation somewhat. [N_3N_F]MoCl is cleanly reduced by sodium amalgam in the presence of *n*-butyl isocyanide to yield red, crystalline [N_3N_F]Mo(C≡N-*n*-Bu) (**12b**) in good yield. NMR parameters and the magnetic moment (measured to be 2.3 ± 0.1 μ_B) are similar to those of the paramagnetic [N_3N_F]W(III) π-acid adducts. The C-N stretch in the IR spectrum of **12b** is seen at 1790 cm^{-1}, 106 cm^{-1} higher than that in [N_3N_F]W(CN-*t*-Bu), consistent with a lower degree of backbonding in the molybdenum complex. Again, a trace of diamagnetic material is present in spectra of **12b**, although it again did not prevent successful C, H, and N analysis.

[N_3N_F]WCl is reduced with sodium amalgam in the presence of an excess of nitric oxide to yield [N_3N_F]W(NO) (**13**) in high yield as a diamagnetic tan powder. [N_3N_F]W(OTf) can also be used as a starting material with identical results. A band in the IR spectrum is observed at 1614 cm^{-1}, abnormally low for a terminal nitrosyl. We presume that the metal-based HOMO of the molecule, the d_{xz}/d_{yz} set, is completely filled as a result of the additional electron present in NO compared to isolobal CO or CN-*t*-Bu. This orbital set is of the proper symmetry for donation into the π^* orbitals of the NO ligand, which is evidently a efficacious process considering the low NO stretching frequency. Related chromium[26] and molybdenum[27] nitrosyl complexes of the form (*t*-BuArN)$_3$M(NO) (Ar = 3,5-dimethylphenyl) have recently been

References begin on page 176.

reported, and are also diamagnetic and have a low NO stretching frequency (M = Cr, 1662 cm^{-1}; M = Mo, 1604). The authors found that the NO bond in these complexes was susceptible to cleavage by tris(mesityl)vanadium(THF)[28] to yield (*t*-BuArN)$_3$M≡N species. Treatment of **13** with two equivalents of V(Mes)$_3$(THF) at room temperature led to no reaction, while heating to 70 °C for 14 h gave decomposition. **13** is also not deoxygenated by trimethylphosphine at room temperature.

[N_3N_F]W(CO) (**9**) does react with V(Mes)$_3$(THF) in toluene at room temperature to yield [N_3N_F]W(CO)V(Mes)$_3$ (**14**) in high yield as a black crystalline solid. Broadened and slightly shifted ^{1}H NMR resonances for the mesityl rings are observed at 17.5, 16.2, and 6.6 ppm. The effective magnetic moment at 22 °C is 2.1 ± 0.1 μ_B. Resonances for the [N_3N_F] half of the molecule, however, are located at the normal diamagnetic positions, although the typical H-H and F-F coupling is not observed. No ^{13}C resonance for the CO ligand is observed, even after a long acquisition time using [N_3N_F]W(^{13}CO)V(Mes)$_3$. Apparently the unpaired spin present in the molecule renders this resonance unobservable. No band assignable to the C-O stretch is observed in the IR spectrum, indeed spectra of [N_3N_F]W(CO)V(Mes)$_3$ and [N_3N_F]W(^{13}CO)V(Mes)$_3$ are line-for-line the same.

Crystals suitable for X-ray diffraction were obtained from a toluene solution at -40 °C. The structure was determined and a view of the molecule is given in Figure 4.11. Table 4.7 contains selected interatomic distances and angles. One toluene molecule per **14** is observed in the crystal. Crystallographic data are located in Table 4.8. The proposed connectivity was verified, although the structure is not of high quality (only W, V, O, N, and F atoms were refined anisotropically, see ORTEP diagram, appendix II). The errors in most of the bond lengths are too large to comment extensively on them. The metrical parameters for the triamidoamine side of the molecule are all typical and do not suggest much steric strain in the complex. The N(4)-W-N_{eq}-C_6F_5 dihedral angles are close to 180°, thus the pocket formed by the rings is nearly undistorted. The mesityl rings on vanadium adapt a propeller-like orientation, probably to minimize steric interactions between the ortho methyl groups present on the rings. The V-O

References begin on page 176.

distance of 1.824(14) Å similar to that observed for some vanadium alkoxides,[29] and a nearly tetrahedral geometry at the vanadium center is observed. Although both the W-C(1)-O and V-O-C(1) angles are close to 180°, the torsion angle between the W-C(1) and O-V bond is 167°, a substantial deviation from linearity even considering the error in the structure. Distances between some of the mesityl ring carbons and the C_6F_5 ring carbons range from 3.3 to 3.5 Å, short enough for a van der Waals interaction to be present, although the rings do not lie flat against each other as a result of the twisted mesityl groups.[12-14]

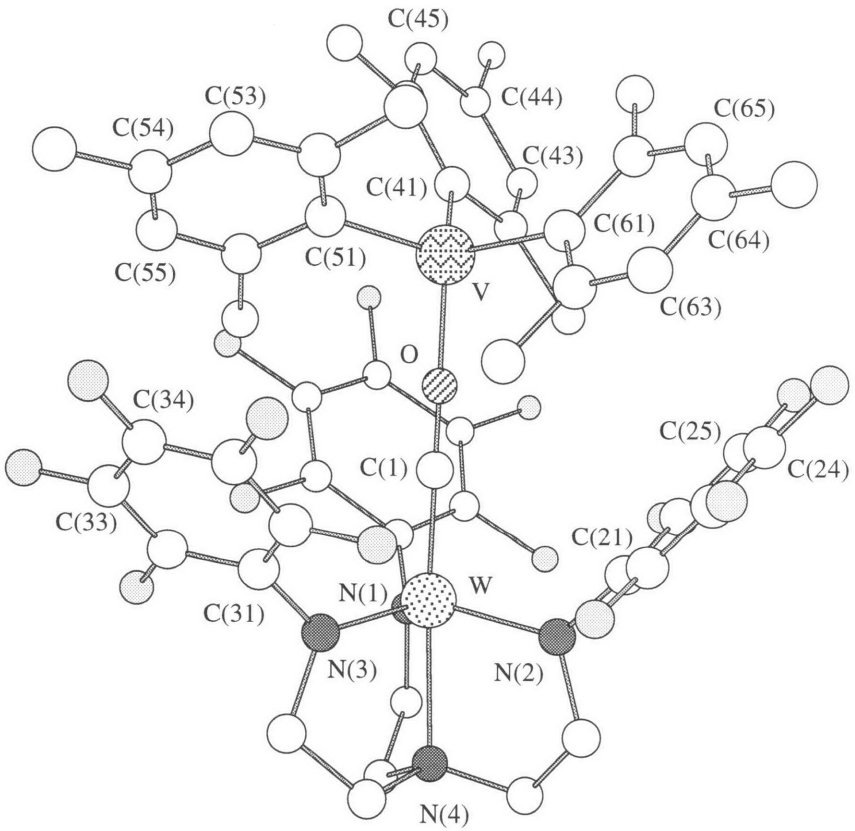

Figure 4.11. A view of the structure of $[N_3N_F]W(CO)V(Mes)_3$ (**14**), with toluene omitted.

References begin on page 176.

Table 4.7. Selected interatomic distances (Å) and angles (deg.) for [N_3N_F]W(CO)V(Mes)$_3$ (**14**).

Distances (Å)

W - C(1)	1.88(2)	O - C(1)	1.19(2)
W - N(1)	1.98(2)	V - O	1.824(14)
W - N(2)	1.98(2)	V - C(41)	2.05(2)
W - N(3)	1.95(2)	V - C(51)	2.03(2)
W - N(4)	2.31(2)	V - C(61)	2.05(2)
C(14) - C(43)	3.55[a]	C(24) - C(63)	3.41[a]
C(34) - C(55)	3.32[a]	C(33) - C(55)	3.64[a]
N(3) - C(31)	1.45(3)	N(2) - C(21)	1.40(2)

Angles (deg.)

W - C(1) - O	178(2)	N(3) - W - N(1)	116.4(7)
C(1) - O - V	176(2)	N(2) - W - N(3)	118.4(7)
O - V - C(41)	112.5(8)	N(2) - W - N(1)	114.9(7)
O - V - C(51)	105.0(8)	N(4) - W - N(3)	80.1(8)
W - N(3) - C(31)	127.4(13)	N(4) - W - N(1)	81.4(7)
W - N(2) - C(21)	124.9(13)	N(3) - W - C(1)	101.0(8)
N(2) - W - C(1)	99.8(8)	N(1) - W - C(1)	101.7(8)

Dihedral Angles (deg.)[a]

N(4) - W - N(2) - C(21)	176
N(4) - W - N(1) - C(11)	179
N(4) - W - N(3) - C(31)	178

Torsion Angle (deg.)

W - C(1) – O - V	166.6

[a] Obtained from a Chem 3D drawing

References begin on page 176.

Table 4.8. Crystallographic data, collection parameters, and refinement parameters for [N_3N_F]W(CO)(3,5-Me_2Ph) · CH_2Cl_2 (**7b**) and [N_3N_F]W(CO)V($Mes)_3$ (**14**)

	[N_3N_F]W(CO)(3,5-Me_2Ph) · CH_2Cl_2	[N_3N_F]W(CO)V($Mes)_3$ · toluene
Empirical Formula	$C_{34}H_{23}Cl_2F_{15}N_4OW$	$C_{59}H_{52}F_{15}N_4OVW$
Formula Weight	1043.31	1352.84
Diffractometer	Siemens SMART/CCD	Siemens SMART/CCD
Crystal Dimensions (mm)	n/a	0.12 × 0.12 × 0.10
Crystal System	Monoclinic	Monoclinic
a (Å)	12.32550 (10)	12.1785 (7)
b (Å)	20.6113 (5)	17.3080 (10)
c (Å)	15.6883 (5)	26.374 (2)
β (deg)	111.4180 (10)	95.6570 (10)
V ($Å^3$)	3710.29 (12)	5532.2 (5)
Space Group	$P2_1/n$	$P2_1/c$
Z	4	4
D_{calc} (Mg/m^3)	1.868	1.624
Absorption Coefficient (mm^{-1})	3.368	2.342
F_{000}	2024	2696
λ (MoK_α)	0.71073 Å	0.71073 Å
Temperature (K)	183 (2)	188 (2)
θ Range for Data Collection (deg)	1.71 to 23.26	1.41 to 20.00
Reflections Collected	14753	15746
Independent Reflections	5314	5147
Absorption Correction	Semi-empirical from ψ-scans	Semi-empirical from ψ-scans
Max. and Min. Transmission	0.4609 and 0.2132	0.2986 and 0.2177
R [$I > 2\sigma(I)$]	0.0399	0.1078
R_W [$I > 2\sigma(I)$]	0.0861	0.1955
R (all data)	0.0496	0.1272
R_W (all data)	0.0943	0.2191
GoF	1.211	1.400
Extinction Coefficient	0.00043 (9)	0.00047 (12)
Largest Diff. Peak and Hole ($eÅ^{-3}$)	0.741 and -0.745	0.732 and -1.501

References begin on page 176.

[N_3N_F]W(OTf) reacts slowly with sodium amalgam in THF under ~3 atmospheres of ethylene to give [N_3N_F]W(C_2H_4) (**15**) in good yield. The molecule is paramagnetic, and is the only compound in this chapter for which no ^{1}H NMR signal is observed. The magnetic moment measured in solution at 22 °C is 1.8 μ_B, the lowest value for any [N_3N_F]W(L) complex in this chapter. Three resonances are observed by ^{19}F NMR (Figure 4.12), although the one which we assign to the ortho fluorines is ~2,500 Hz wide at half-height. Even after precipitation, the brown solid product contains a trace of a paramagnetic impurity, as Figure 4.12 shows. The chemical shifts of this impurity are the same as the species observed when [N_3N_F]W(OTf) is reduced in the absence of any trapping ligand (see above). More bulky olefins such as 2-butene or cyclopentene do not trap "[N_3N_F]W" efficiently enough, only the decomposition product observed without any trap present (see above) is observed. [N_3N_F]W(OTf) reacts with sodium amalgam in the presence of excess bromotrifluoroethylene to yield a paramagnetic complex tentatively formulated as [N_3N_F]WBr (**16**) based on ^{1}H and ^{19}F NMR and C, H, and N analysis. **16** might be more expediently synthesized from [N_3N_F]WCl and TMSBr (cf. the synthesis of [N_3N_F]WI (chapter III)), although we have not attempted that reaction.

A TMS-substituted triamidoamine ethylene complex of tantalum ([N_3N]Ta(C_2H_4)) has been synthesized, and has been shown to react smoothly with various weak acids to yield Ta-ligand multiply-bonded species.[22,30] **15**, however, either did not react or decomposed when treated with acids such as aniline, phenylphosphine, pyridinium triflate, or HCl in ether. The cyclic voltammagram of **15** shows a reversible oxidation wave at 0.40 V. Treatment with [(Cp_2Fe][OTf] in THF led to the formation of [[N_3N_F]W(C_2H_4)][OTf] (**17**) as a red diamagnetic powder in high yield, along with ferrocene. The ^{1}H NMR spectrum displays a peak at 3.10 ppm which we assign to the ethylene ligand. Attempts were made to attack the ethylene ligand in **17** with nucleophiles such as lithium phenylphosphide or Grignard reagents, with no success.

References begin on page 176.

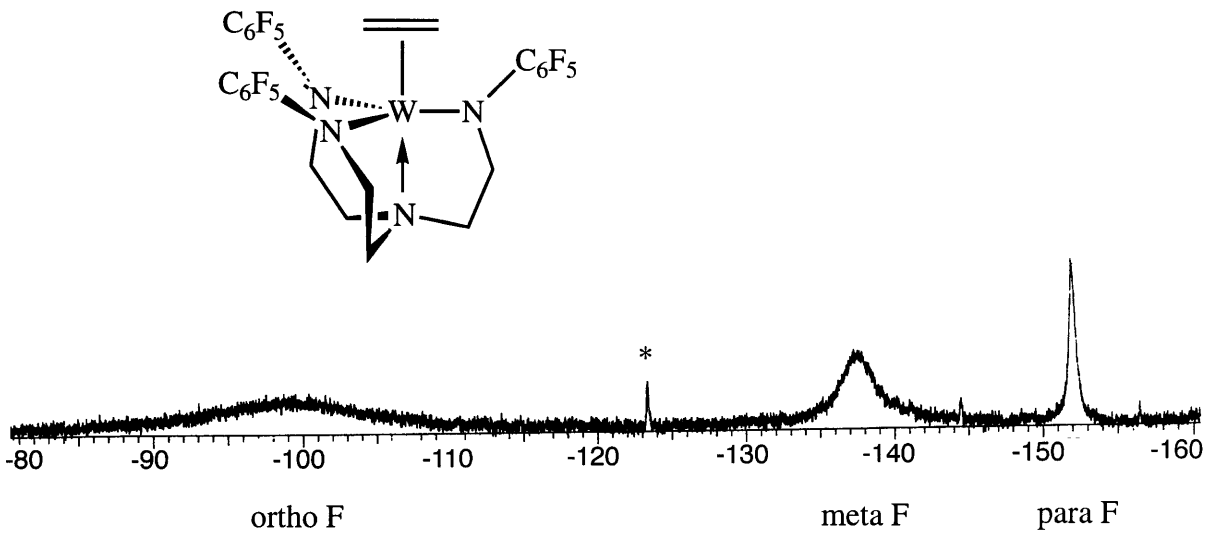

Figure 4.12. The ^{19}F NMR spectrum of [N_3N_F]W(C_2H_4) (**15**) in C_6D_6 at 22 °C.
* An unknown impurity, see text.

Table 4.9. Selected characterization data for [N_3N_F]W(X) and [N_3N_F]W(L) complexes.

[N_3N_F] Complex	% Yield	Morphology	μ_{eff} (μ_B units)	$E_{1/2}$ (V)	IR ν (cm^{-1})
W(CO)	92	red blocks	2.6	0.16 (red.)	1846
W(CN-*t*-Bu)	92	orange plates	1.70[a]	0.33 (ox.)	1684
W(CN-*t*-Bu)$^+$	53	brown powder	diamagnetic	0.33 (red.)	2107
Mo(CN-*n*-Bu)	76	red needles	2.3	0.36 (ox.)	1790
W(NO)	86	tan powder	diamagnetic	—	1614
W(C_2H_4)	79	brown blocks	1.8	0.40 (ox.)	—
W(CO)V($Mes)_3$	88	black blocks	2.1	—	—
W(O-3,5-Me_2Ph)	84	purple needles	3.2	0.33 (ox.)	—
W(3,5-Me_2Ph)	81	burgundy needles	3.0	0.39 (ox.)	—

Satisfactory C, H, and N analyses were obtained for all complexes. μ_{eff} values were obtained by the Evan's method at 22 °C using TMS_2O as an internal standard, the estimated error is ± 0.1 μ_B.

Electrochemical measurements were performed in CH_2Cl_2 under nitrogen, potentials listed are for the lowest energy reversible wave.

[a]Obtained in the solid state using SQUID.

References begin on page 176.

DISCUSSION

The nature of the product of the reaction between [N_3N_F]W(3,5-Me_2Ph) and pyridine *n*-oxide, [N_3N_F]W(O)(3,5-Me_2Ph) (**2b**) was initially somewhat enigmatic since the product appeared to a typical C_{3v}-symmetric triamidoamine complex by NMR. Such a geometry would have limited the tungsten-oxygen bond order at two, since only the d_z^2, d_{xz}, and d_{yz} orbitals would be available for binding both the oxo ligand and the xylyl group. In an undistorted pseudo-C_{3v} triamidoamine complex, the d_{xy} and $d_{x^2-y^2}$ orbitals are of the proper symmetry for π-bonding with the amides, therefore only two amide-to-metal π-bonds are possible. Oxo ligands which are only doubly-bonded to the metal are rare, and high reactivity of the oxo in such complexes is often observed.[31] The oxo ligand in **2b** proved relatively unreactive, suggesting that it was actually pseudo-triply bonded to tungsten. The X-ray structure showed that this is the case, and is rendered possible from a molecular orbital standpoint by an unusually distorted triamidoamine coordination environment (Figures 4.1 and 4.2). Since the molecule is now closer to pseudo-octahedral, the oxo ligand can bond with the d_z^2, d_{xz}, and d_{yz} orbitals (taking the W-dative nitrogen bond as the z axis), resulting in a pseudo-triple bond. Additional π-bonding from oxygen must occur at the expense of π-bonding from the amido ligands, since now only the d_{xy} orbital is of the proper symmetry to π-bond with the amides. Figure 4.13 shows a simplified

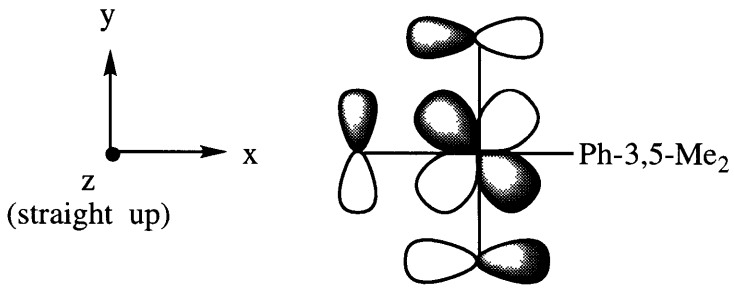

Figure 4.13. Molecular orbital for the interaction between the d_{xy} orbital on tungsten and amido p-orbitals for complex **2b**.

diagram of the approximate molecular orbital for the one amide-tungsten π-bond possible in this situation. The complex is thus an 18 electron species, with the triamidoamine acting as a 10

References begin on page 176.

electron donor. The display of structural flexibility evidenced by this X-ray structure may be an important aspect of triamidoamine chemistry: similar distortions might occur in sterically or electronically unfavorable reaction intermediates, with subsequent reorganization to a stable C_{3v}-symmetric complex.

We became interested in investigating reductions of [N_3N_F]WX complexes from the point of view of dinitrogen fixation. Previous efforts in this area from our laboratories have made use of the Cp^*MMe_3 core,[32,33] with M = Mo and especially W. When the Cp^*MMe_3 fragment assumes a square pyramidal geometry with one empty basal coordination site, two π bonding orbitals (d_z^2 and d_{xy}, taking the z axis as the M-Cp vector) and a σ bonding orbital are available for binding dinitrogen and reduced dinitrogen fragments, an arrangement isolobal with the [N_3N]M fragment. The successful fixation of dinitrogen by [N_3N_F]Mo(OTf)[1] and the fact that previous efforts with the Cp^*MMe_3 system were superior with tungsten instead of molybdenum led us to attempt the synthesis of an [N_3N_F]W dinitrogen complex, and it may seem somewhat surprising that we have been unable to isolate one. However, no [N_3N_F] vanadium dinitrogen complex could be synthesized either,[34] despite the fact that similar vanadium dinitrogen complexes are fairly common.[35,36] In fact, both [N_3N]VCl[37] and [N_3N_F]VCl[38] can be reduced in noncoordinating solvents to give crystallographically-characterized trigonal-monopyramidal vanadium triamidoamine complexes, neither of which has any tendency to bind dinitrogen. Therefore, especially in light of the ready syntheses of the [N_3N_F]W(L) (L = a strong-field π-acid ligand) complexes described in this chapter, it could be that the reason [N_3N_F]W(N_2) proved elusive is that upon reduction of [N_3N_F]W(OTf), the triamidoamine complex decomposes at a rate much faster than it binds dinitrogen.

An interesting observation regarding the chemistry presented here is that no complexes with σ-donor ligands, such as trimethylphosphine, could be prepared. Pyridine also did not react cleanly with [N_3N_F]W(OTf) upon reduction, nor did acetonitrile. It would seem that the *e* set of orbitals in the [N_3N_F]W(L) complexes overlaps well with the π^* orbitals of a suitable acceptor ligand, considering the low IR stretching frequencies for diatomics bound to [N_3N_F]W (Table

References begin on page 176.

4.9). It may be that a relatively low-energy π* orbital on the ligand is needed in order to sequester [N_3N_F]W before decomposition ensues, if in fact hypothetical [N_3N_F]W is a reaction intermediate during the formation of [N_3N_F]W(L) complexes. This proposal could also explain why no dinitrogen complex is formed when the reduction is carried out under N_2 alone; overlap between the high-energy π* orbitals of dinitrogen and the *e* set of orbitals on tungsten may not be great enough for binding to occur.

Several of the X-ray structures present in this chapter show relatively close contacts between C_6F_5 carbons and 3,5-Me_2Ph or 2,4,6-Me_3Ph rings. These could be a result of C_6F_5-$C_6H_3Me_2$ interaction, an arene-arene interaction rendered particularly strong by the fact that in benzene, the polarization of the C-H bonds is such that the hydrogens are rendered partially positive, and the carbons partially negative. The situation is reversed in C_6F_6 as a result of the high electronegativity of fluorine. These perfluorophenyl-phenyl van der Waals interactions thus tend to be stronger than other arene-arene interactions, and are a matter of considerable current interest.[12] In the structure of [N_3N_F]W(O-3,5-Me_2Ph) (**4b**) distances are between 3.15 and 3.92, well within the range normally observed for a perfluoroaryl-aryl interaction.[13,14] Of course, the coordination environment in the apical site of a complex containing the $[N_3N_F]^{3-}$ ligand is fairly crowded, and it may also be that the 3,5-Me_2Ph ring in **4b** simply resides slightly closer to one of the C_6F_5 rings on steric grounds alone. The structure of [N_3N_F]W(CO)(3,5-Me_2Ph) (**7b**) also displays fairly close 3,5-Me_2Ph to C_6F_5 distances, and in this case *two* of the C_6F_5 rings appear to be involved. The geometrical constraints placed by the acyl moiety would seem to guarantee that the 3,5-Me_2Ph ring lies in between two C_6F_5 rings, however, the fact that the angle between the amido ligands to which those two C_6F_5 rings are attached is the smallest of the three N_{eq}-W-N_{eq} angles would indicate an attractive interaction. In the structure of [N_3N_F]W(CO)V($Mes)_3$ (**14**), close contacts between *some* of the perfluorophenyl and mesityl ring carbons are observed, but the twisted, propeller-like orientation of the mesityl rings and the O-V-$C_{mesityl}$ and W-N_{eq}-C_6F_5 angles do not allow them to lie parallel to the C_6F_5 rings, thus any van der Waals interaction between them is likely to be relatively weak.

References begin on page 176.

A noteworthy difference between complexes containing the $[(TMSNCH_2CH_2)_3N]^{3-}$ and $[(C_6F_5NCH_2CH_2)_3N]^{3-}$ ligands is in reactions with lithium phenylphosphide and lithium phenyl arsenide. Although $[N_3N]W{\equiv}P$ is formed readily by reacting $[N_3N]WCl$ with two equivalents of LiPHPh or from $[N_3N]W(PHPh)$,[7] no terminal phosphide has yet been synthesized containing the $[N_3N_F]^{3-}$ ligand. Formation of a terminal phosphide in this manner involved formal oxidation of the metal. These types of reactions have been shown to be slower for complexes containing $[N_3N_F]^{3-}$. For example, $[N_3N_F]W(CH_2SiMe_3)$ loses hydrogen relatively slowly while the reaction between $[N_3N]WCl$ and $LiCH_2SiMe_3$ yields $[N_3N]W{\equiv}CSiMe_3$ rapidly (see chapter III), presumably via intermediate $[N_3N]W(CH_2SiMe_3)$, as has been observed for other $[N_3N]W(CH_2R)$ complexes.[21] Kinetic studies have shown that $[N_3N_F]Mo(CH_2CMe_3)$ loses dihydrogen 12 times more slowly than $[N_3N]Mo(CH_2CMe_3)$ at 121 °C to yield the corresponding alkylidynes (chapter III). The electron withdrawing nature of the C_6F_5 rings renders the metal more electron poor and therefore less susceptible to oxidation to the 6+ oxidation state. Since $[N_3N_F]M$ complexes are also less sterically crowded in the trigonal pocket than are $[N_3N]M$ complexes (see above), there is presumably also less steric pressure on the phenyl group bonded to phosphorus to be lost to give the $[N_3N_F]M{\equiv}P$. During the attempted synthesis of $[N_3N_F]W{\equiv}P$, the C_6F_5 rings of $[N_3N_F]W(PHPh)$ might also be subject to electron transfer from or nucleophilic attack by a lithium reagent.

In general, it seems that chemistry involving nucleophilic attack at the metal center is sometimes complicated by side reactions with $[N_3N_F]$ complexes, whereas these types of reactions with $[N_3N]$ complexes tend to be relatively clean. For example, $[N_3N]M(Me)$,[21] $[N_3N]W(H)$(cyclopentylidene),[39] and $[N_3N]MH^4$ (M = Mo, W) can be prepared in high yield and purity, whereas $[N_3N_F]$-containing analogs of these complexes have yet to be prepared (see chapter III). Conversely, reactions involving reduction of $[N_3N_F]M(X)$ complexes tend to proceed more smoothly than with $[N_3N]M(X)$ complexes (M= Mo, W). Reduction of $[N_3N]Mo(OTf)$ leads to a dimeric decomposition product resulting from formal loss of TMS(OTf),[40] and attempts to synthesize $[N_3N]Mo(CO)$ are limited by formation of

References begin on page 176.

[N_3N]Mo≡C-O-TMS as a by-product, presumably arising from intermolecular migration of a TMS group to oxygen.[41] The electron-withdrawing nature of the $[N_3N_F]^{3-}$ ligand along with the relatively high stability of the N-C_6F_5 linkage are probably what render the formation of the [N_3N_F]W(L) (L = π-acid ligand) complexes so facile. Current interests involve the synthesis of other types of C_6F_5-substited amine ligands, particularly ones containing phosphine donors instead of amine donors (chapter V).

EXPERIMENTAL

General Details. All experiments were conducted under nitrogen in a Vacuum Atmospheres drybox, using standard Schlenk techniques, or on a high vacuum line ($<10^{-4}$ torr). Glassware was dried in a 135 °C oven overnight. Pentane was washed with HNO_3/H_2SO_4 (5/95 v/v), sodium bicarbonate, H_2O, stored over $CaCl_2$ and then distilled from sodium benzophenone with tetraglyme under nitrogen. Ether and THF were purified by sparging with nitrogen and passing through alumina columns.[42] Reagent grade benzene was distilled from sodium benzophenone under nitrogen. Toluene was distilled from molten sodium. Acetonitrile was distilled from P_2O_5. Methylene chloride was distilled from CaH_2. All solvents were stored in the drybox over activated 4 Å molecular sieves. Deuterated solvents were freeze-pump-thaw degassed and vacuum transferred from an appropriate drying agent. ^1H NMR spectra were recorded at either 250 or 300 MHz at 25 °C. ^{13}C, ^{19}F, and ^{31}P NMR spectra were recorded at 75.4, 282, and 121 MHz respectively. ^1H and ^{13}C data are listed in parts per million downfield from tetramethylsilane and were referenced using the solvent peak. ^{19}F NMR are listed in parts per million downfield of $CFCl_3$ as an external standard. ^2H NMR spectra were obtained at 46.0 MHz and referenced to external C_6D_6 (7.15 ppm). ^{31}P NMR spectra are listed in parts per million downfield from H_3PO_4. Coupling constants are given in Hertz, and routine couplings are not listed. Magnetic susceptibility measurements were done by NMR using the Evans method[43] with TMS_2O as an internal standard. Elemental analyses (C, H, N) were performed on a Perkin-

References begin on page 176.

Elmer 2400 CHN analyzer in our own laboratory. Cyclic voltammetry measurements were performed in methylene chloride versus Ag/AgCl using $[Bu_4N][PF_6]$ as the supporting electrolyte and a scan rate of 100 mV/sec. Ferrocene was used as an internal standard (0.47 V).

Starting materials. $[N_3N]WCl$, $[N_3N_F]MoCl$, and $[N_3N_F]W(OTf)$ were synthesized as described in the literature,[1] except $WCl_4(dme)$[44] was used instead of $WCl_4(Et_2S)_2$ for the synthesis of the tungsten chloride. $[N_3N_F]WI$ was prepared as described in chapter III. Phenyllithium and 3,5-xylyllithium were prepared by treatment of the aryl bromide with BuLi in ether/hexane at -35 °C. Pyridine *n*-oxide (Alfa) was sublimed onto a 0 ° probe under dynamic vacuum prior to use. Ferrocenium triflate was prepared by the literature procedure.[45] Sodium amalgam (0.5% by weight) was freshly prepared from sodium spheres and triply-distilled mercury (Aldrich). Methyl isocyanide was prepared by a literature procedure.[23] CO (99.99%) and H_2 were purchased from Matheson and used directly from the cylinder. Electronic grade NO was used directly from the cylinder. *t*-Butyl and *n*-butyl isocyanides were purchased commercially.

$[N_3N_F]WPh$ (1a). $[N_3N_F]WI$ (500 mg, 0.525 mmol) was dissolved in 10 mL of toluene by stirring the solution for 30 minutes. A solution of phenyllithium (59 mg, 0.63 mmol, 1.2 equiv.) was prepared by addition of 3 drops of THF to solid phenyllithium followed by 5 mL of toluene. This solution was added dropwise to the iodide over fifteen minutes. The reaction was stirred for seven hours, at which point 0.3 more equivalents of phenyllithium (15 mg, 0.161 mmol) in 1 mL of toluene were added. The reaction was stirred for another 15 hours. The solvents were removed *in vacuo* and the residue was extracted with dichloromethane. The extract was filtered through Celite and the dichloromethane was removed *in vacuo* to yield the crude product as an orange solid; yield 413 mg (87%). The crude product proved sufficiently pure for subsequent reactions. The product could be purified further by recrystallization from methylene chloride/pentane mixtures; yield 279 mg (59%): ^1H NMR (C_6D_6) δ -16.7 (br s, $\Delta_{1/2}$ = 52), NCH_2), -58.1 (br s, $\Delta_{1/2}$ = 47), NCH_2); ^{19}F NMR (toluene) δ 22.2 (br s, *o*-C_6F_5), -120 (s, *m*-C_6F_5), -139.6 (s, *p*-C_6F_5).

References begin on page 176.

[N_3N_F]W(3,5-$Me_2C_6H_3$) (1b). [N_3N_F]WI (985 mg, 1.03 mmol) was suspended in 20 mL of toluene and a solution of 3,5-xylyllithium (139 mg, 1.24 mmol, 1.2 equiv.), prepared by addition of 5 drops THF to the solid aryllithium followed by 10 mL toluene, was added dropwise to the iodide. The reaction was stirred for 2 hours and then allowed to stand ~ 1 hour and the precipitated LiI filtered off (74 mg). The toluene was removed *in vacuo* and the residue taken up in a minimum amount of dichloromethane. The solution was allowed to stand for ~ 1 hour and filtered through Celite to yield an additional 30 mg of precipitate (78% yield of LiI). The dichloromethane extract was layered with pentane and the mixture was chilled to -40 °C for 15 hours to give 590 mg of burgundy microcrystals. The volume was reduced in vacuo and the process repeated to give a second crop (188 mg); total yield 778 mg (81%): ^{1}H NMR (C_6D_6) δ -16.5 (br s, $\Delta_{1/2}$ = 64), NCH_2), -53.9 (s, 3,5-dimethylphenyl), -59.0 (br s, $\Delta_{1/2}$ = 54), NCH_2); ^{19}F NMR (C_6D_6) δ 12.5 (br s, *o*-C_6F_5), -120.2 (s, *m*-C_6F_5), -136.0 (s, *p*-C_6F_5); $E_{1/2}$(ox) = 0.39 V (reversible); μ_{eff} = 3.0 μ_B (Evan's method). Anal. Calcd. for $C_{32}H_{21}N_4F_{15}W$: C, 41.31; H, 2.28; N, 6.02. Found: C, 40.69; H, 2.55; N, 5.72. The sample may have still been contamined with LiI.

[N_3N_F]WH_3 (1c). A 300 mL glass bomb was charged with [N_3N_F]W(3,5-Me_2-Ph) (400 mg, 0.430 mmol), a teflon coated stir bar, and 25 mL toluene. The bomb was attached to a high vacuum line and degassed by 3 freeze pump thaw cycles. It was then chilled to 77 K and dihydrogen (640 mmHg, 39.9 mmol, 92 equiv.) was introduced by vacuum transfer. The bomb was sealed, warmed to room temperature, and placed in a 40 °C oil bath, and the reaction mixture was stirred for 15 hours. The volatile components were removed under reduced pressure and the crude product recrystallized by layering a concentrated toluene solution with pentane and cooling to -40 °C. The brown product was isolated in two crops; yield 214 mg (60%). The trideuteride was prepared similarly, employing D_2 instead of H_2: ^{1}H NMR (C_6D_6) δ 11.1 (s, $^1J_{HW}$ = 25, 3, hydride, T_1 (22 °C) = 344(5) msec), 3.27 (t, 6, NCH_2), 2.28 (t, 6, NCH_2); ^{19}F NMR (C_6D_6) δ -152.6 (d, 6, *o*-C_6F_5), -163.9 (t, 3, *p*-C_6F_5), -165.7 (t, 6, *m*-C_6F_5). IR (KBr):

References begin on page 176.

2908 m, 2875 m, 1898 ms, hydride, 1508 s, 1314 w, 1261 w cm^{-1}. Anal. Calcd. for $C_{24}H_{15}N_4F_{15}W$: C, 34.80; H, 1.83; N, 6.76. Found: C, 34.48; H, 1.73; N, 6.42.

[N_3N_F]W(O)(Ph) • $(dme)_{1.5}$ (2a). To a THF (5 mL) solution of [N_3N_F]W(Ph) (100 mg, 0.111 mmol) was added pyridine *n*-oxide (11 mg, 0.11 mmol). The reaction was stirred for 8 h and the volatiles removed by rotary evaporation. Recrystallization from DME layered with pentane at -40 °C yielded 69 mg red crystals (68%): ^{1}H NMR (CD_2Cl_2) δ 7.96 (d, 2, *o*-C_6H_5), 7.20 (m, 3, *m*- and *p*-C_6H_5), 4.31 (t, 6, NC*H*$_2$N), 3.63 (s, 6, dme C*H*$_2$), 3.51 (t, 6, NC*H*$_2$N), 3.48 (s, 9, dme C*H*$_3$). ^{19}F NMR (CD_2Cl_2) δ -146.8 (s, 6, *o*-C_6F_5), -163.7 (t, 3, *p*-C_6F_5), -165.3 (t, 6, *m*-C_6F_5).

[N_3N_F]W(O)(3,5-$Me_2C_6H_3$) (2b). [N_3N_F]W[3,5-$Me_2C_6H_3$] (150 mg, 0.161 mmol) was dissolved in 5 mL dimethoxyethane. Pyridine *n*-oxide (15 mg, 0.16 mmol, 1 equiv.) was added as a solid and the reaction was stirred for 15 hours. The solvent was removed *in vacuo* and the red residue recrystallized by layering a concentrated DME solution with pentane and cooling the solution to -40 °C overnight. The red crystalline product was isolated by decantation of the mother liquor and drying *in vacuo* (95 mg, 62%): ^{1}H NMR (C_6D_6) δ 7.70 (s, 2, H_{ortho}), 6.72 (s, 1, H_{para}), 3.69 (t, 6, NC*H*$_2$N), 2.58 (t, 6, NC*H*$_2$N), 2.22 (s, 6, C_6H_3*Me*$_2$). ^{19}F NMR (dme) δ -146.8 (d, 6, *o*-C_6F_5), -164.9 (t, 3, *p*-C_6F_5), -166.7 (t, 6, *m*-C_6F_5). IR (Nujol mull): 1514 s, 1076 w, 988 s, 848 w. Anal. Calcd. for $C_{32}H_{21}N_4F_{15}OW$: C, 40.61; H, 2.24; N, 5.92. Found: C, 40.65; H, 2.09; N, 5.80.

[N_3N_F]W(3,5-Me_2Ph)(=N-TMS) (3). To a stirred solution of [N_3N_F]W(3,5-Me_2Ph) (100 mg, 0.108 mmol) in 5 mL THF was added trimethylsilylazide (14 μL, 0.11 mmol) via syringe. The color changed instantly from red to light orange. Stirring was continued for 4 h and then the THF was removed under reduced pressure. The orange solid was recrystallized from CH_2Cl_2 / pentane at -40 °C. Orange plates formed after 15 h, 75 mg in two crops (69%): ^{1}H NMR (C_6D_6): δ 7.91 (s, 2, H_{ortho}), 6.98 (s, 1, H_{para}), 3.9, 3.6, 3.4, 2.8 (br s, diastereotopic NCH_2N), 2.43 (s, 6, 3,5-(Me)$_2$-Ph), 2.34 (br s, diastereotopic NCH_2N), -0.40 (s, 9, TMS). ^{19}F NMR (C_6D_6): δ -143.8 (s, 4, F_{ortho}), -148.4 (d, 2, F_{ortho}), -164.6 (t, 4, F_{meta}), -165.0 (t, 2, F_{para}),

References begin on page 176.

-165.7 (t, 2, F_{meta}), -166.5 (t, 1, F_{para}). IR (Nujol mull): cm^{-1} 1509, 1119, 1072, 1036, 990, 844. Anal. Calc. for $C_{35}H_{30}N_5F_{15}SiW$. Calc.: C, 41.31; H, 2.97; N, 6.88. Found: C, 41.45; H, 3.18; N, 6.56.

[N_3N_F]W(OC_6F_5) (4a). [N_3N_F]WOTf (250 mg, 0.257 mmol) was covered with 8 mL THF and the mixture cooled to -40 °C. C_6F_5OK (57 mg, 0.26 mmol) was added as a solid and the reaction was warmed to room temperature and stirred for 6 hours. The solvent was then removed under reduced pressure and the red residue extracted with CH_2Cl_2. The extract was reduced in volume, layered with ether, and cooled to -40 °C overnight. The red crystalline product was isolated by decantation of the supernatant and drying *in vacuo*, 129 mg in two crops (50%): $E_{1/2}$(ox) = 0.41 V (reversible), $E_{1/2}$(ox) = 0.49 (quasireversible). ^1H NMR (CD_3CN) δ -18.5 (br s, NCH_2N), -51.5 (s, NCH_2N). ^{19}F NMR (CD_3CN) δ -4.53 (s, 2, phenoxide ortho), -54.1 (s, 6, *o*-C_6F_5), -100.4 (s, 2, phenoxide meta), -125.9 (s, 6, *m*-C_6F_5), -147.3 (s, 3, *p*-C_6F_5), -170.8 (s, 1, phenoxide para). Anal. Calcd. for $C_{30}H_{12}N_4F_{20}OW$: C, 35.74; H, 1.20; N, 5.56. Found: C, 35.92; H, 1.21; N, 5.72.

[N_3N_F]W(O-3,5-$Me_2C_6H_3$) (4b). To a stirred -40 °C solution of [N_3N_F]WCl (200 mg, 0.232 mmol) in 10 mL THF was added solid potassium 3,5-dimethylphenoxide (37 mg, 0.23 mmol). The color of the reaction changed from orange to deep purple within seconds. After 3 hours the solvent was removed *in vacuo* and the residue extracted with CH_2Cl_2. The potassium salts were filtered off and the extract was concentrated, layered with pentane, and cooled to -40 ° for 15 hours. Purple needles formed and were isolated by decantation of the mother liquor and drying *in vacuo*, 184 mg (84%): ^1H NMR (CD_3CN) δ -8.5 (s, 6, 3,5-dimethylphenyl), -15.1 (br s ($\Delta_{1/2}$ = 46 Hz), 6, NCH_2N), -27.8 (s, 1, H_{para}), -42.2 (br s ($\Delta_{1/2}$ = 10 Hz), 2, H_{ortho}), -47.6 (br s ($\Delta_{1/2}$ = 23 Hz), 6, NCH_2N). ^{19}F NMR (CD_3CN) δ -59.8 (br s, *o*-C_6F_5), -123.4 (s, *m*-C_6F_5), -142.6 (s, *p*-C_6F_5). $E_{1/2}$(ox) = 0.33 V (reversible). μ_{obs} = 3.2 μ_B. Anal. Calc. for $C_{32}H_{21}N_4OF_{15}W$. Calc.: C, 40.61; H, 2.24; N, 5.92. Found: C, 40.79; H, 2.30; N, 5.73.

[N_3N_F]W(O-3,5-Me_2Ph)(O) (5). Pyridine *n*-oxide (11 mg, 0.11 mmol) was added as a solid to a solution of [N_3N_F]W(O-3,5-Me_2Ph) (107 mg, 0.113 mmol) in 5 mL dimethoxyethane

References begin on page 176.

with good stirring. The color of the solution changed from purple to light orange. After 20 min., the solvent was removed under reduced pressure and the orange residue recrystallized from dimethoxyethane layered with pentane at -40 °C. The product was obtained as a light orange fluffy solid, 90 mg (83%): ^{1}H NMR ($CDCl_3$) δ 6.60 (s, 2, H_{meta}), 6.50 (s, 1, H_{para}), 4.41, 4.28, 4.18, 3.71, 3.42 (m, diastereotopic NCH_2N), 2.20 (s, 6, 3,5-(Me)$_2$-Ph). ^{19}F NMR ($CDCl_3$) δ -145.9 (d, 4, *o*-C_6F_5), -148.6 (d, 2, *o*-C_6F_5), -162.29 (t, 1, *p*-C_6F_5), -162.32 (t, 2, *p*-C_6F_5), -163.93 (t, 4, *m*-C_6F_5), -164.33 (t, 2, *m*-C_6F_5). Anal. Calc. for $C_{32}H_{21}N_4O_2F_{15}W$. Calc.: C, 39.94; H, 2.20; N, 5.82. Found: C, 39.98; H, 2.36; N, 6.12.

[N_3N_F]Mo(PPhH) (6a). Solid LiPPhH (45 mg, 0.39 mmol) was added to a stirred slurry of [N_3N_F]MoCl (300 mg, 0.388 mmol) in 20 mL toluene. Ten drops THF were then added, which caused the mixture to become homogeneous. After 1 hour, more LiPPhH (14 mg, 0.12 mmol) was added and the mixture stirred for three hours. A ^{19}F NMR spectrum showed the reaction to be complete. The reaction was filtered through Celite and the solvent removed *in vacuo*. The brown residue was recrystallized from CH_2Cl_2 layered with pentane at -40° C. The product was obtained as a brown microcrystalline solid, 263 mg in two crops (80%): ^{1}H NMR δ 11.2 (d, J_{PH} = 281, 1, MoPPh*H*), 6.99 (m, Ph), 6.87 (m, Ph), 3.29 (t, 6, CH_2), 2.44 (t, 6, CH_2); ^{19}F NMR δ -150.1 (d, 6, F_{ortho}), -164.5 (t, 3, F_{para}), -165.3 (t, 6, F_{meta}); ^{31}P NMR δ 189.6 (d). Anal. Calcd for $C_{30}H_{18}N_4F_{15}PMo$: C, 42.57; H, 2.14; N, 6.62. Found: C, 42.57; H, 2.32; N, 6.37.

[N_3N_F]W(PPhH) (6b). To a stirred slurry of [N_3N_F]WCl (500 mg, 0.581 mmol) in 30 mL toluene was added solid LiPPhH (67 mg, 0.58 mmol) followed by 20 drops of THF. Addition of THF caused the reaction to become homogeneous. After 30 minutes, a second portion of LiPPhH (20 mg, 0.17 mmol) was added. The reaction was stirred for another 30 minutes, at which point ^{19}F NMR showed it was complete. The solution was filtered through Celite and the volatiles removed *in vacuo*. The brown solid was recrystallized from CH_2Cl_2 layered with pentane at -40° C, 469 mg (86%) brown crystals isolated in three crops: ^{1}H NMR δ 17.5 (dd, J_{PH}=295 Hz, $^2J_{WH}$ = 22, 1, PPh*H*), 6.97 (t, 4, phenyl), 6.82 (m, 1, phenyl), 3.23 (t, 6,

References begin on page 176.

CH_2), 2.35 (t, 6, CH_2); ^{19}F NMR δ -150.4 (s, 6, F_{ortho}), -164.0 (t, 3, F_{para}), -165.1 (s, 6, F_{meta}); ^{31}P NMR δ 118.1 (2, J_{PW} = 742, *P*HPh). Anal. Calcd for $C_{30}H_{18}N_4F_{15}PW$: C, 38.57; H, 1.94; N, 6.00. Found: C, 38.57; H, 2.11; N, 5.55.

[N_3N_F]W(OC)Ph (7a). A 50 mL round bottomed flask was charged with [N_3N]WPh (200 mg, 0.222 mmol), 10 mL THF, and a stir bar. It was fitted with a vacuum adapter and attached to a high vacuum line. The solution was degassed by 3 freeze pump thaw cycles and CO (67 mmHg, 0.22 mmol, ~1 equiv.) was introduced. The reaction was sealed and warmed to room temperature. Within minutes the color of the reaction has changed to jet black. After 40 minutes the volatiles were removed *in vacuo* and the black residue dissolved in 4 mL CH_2Cl_2, layered with 8 mL pentane and chilled to -40 °C for 15 hours. The black crystalline product was isolated by decanting off the mother liquor and drying *in vacuo*, 166 mg in two crops (81%): ^1H NMR (C_6D_6) δ 6.83 (t, 2, H_{ortho}), 6.62 (d, 2, H_{meta}), 6.20 (t, 1, H_{para}), 3.45 (br s, 6, NCH_2N), 2.37 (br s, 6, NCH_2N). ^{19}F NMR (C_6D_6) δ -150.7 (s, 6, *o*-C_6F_5), -163.6 (t, 3, *p*-C_6F_5), -164.9 (t, 6, *m*-C_6F_5). ^{13}C {^1H} NMR (C_6D_6) δ 256.9, 131.9, 131.6, 125.9, 53.9. IR ($CDCl_3$): 2930 w, 2864 w, 2361 w, 2254 w, 1504 s, 1066 w, 989 s, 912 s. $E_{1/2}$(ox) = 0.35 V (reversible).

[N_3N_F]W(OC)(3,5-$Me_2C_6H_3$) (7b). A 50 mL round-bottomed flask was charged with [N_3N_F]W[3,5-$Me_2C_6H_3$] (200 mg, 0.215 mmol), 10 mL THF, and a stir bar. The flask was fitted with a vacuum adapter and attached to a vacuum manifold. The solution was degassed at -78 °C and carbon monoxide (60 mmHg, ~1 equivalent (headspace volume estimated to be 47 mL)) was introduced and the flask sealed. The reaction was warmed to room temperature with stirring, and after 5 minutes at room temperature the volatiles were removed *in vacuo*. The product was recrystallized by layering a concentrated CH_2Cl_2 solution with pentane, 135 mg in two crops (66%): ^1H NMR (C_6D_6) δ 6.31 (s, 2, H_{ortho}), 6.01 (s, 1, H_{para}), 3.49 (t, 6, NCH_2N), 2.42 (t, 6, NCH_2N), 1.76 (s, 6, 3,5-(C_6H_3*Me*$_2$)). ^{19}F NMR (C_6D_6) δ -150.9 (s, 6, *o*-C_6F_5), -166.4 (t, 3, *p*-C_6F_5), -167.1 (s, 6, *m*-C_6F_5). ^{13}C NMR (C_6D_6) δ 252.3, 145.6, 142.3, 139.2, 135.9, 133.6, 132.6, 130.0, 127.3, 58.2, 54.0, 20.7. IR (KBr): 2921 w, 2872 w, 1506 s, 1356 m,

References begin on page 176.

1310 m, 1244 m, 1131 m, 1067 s, 986 s, 859 s. Anal. Calcd. for $C_{33}H_{21}F_{15}N_4OW$: Calc: C, 41.36; H, 2.21; N, 5.85. Found: C, 41.09; H, 2.10; N, 5.75.

[N_3N_F]W(CO) (9). A 100 mL round bottomed flask was charged with [N_3N_F]WOTf (500 mg, 0.513 mmol), 25 mL THF, 0.5% Na/Hg amalgam (2.36 g, 0.513 mmol, 1 equiv.), and a stir bar. The flask was fitted with a vacuum adapter and attached to a high vacuum line. It was degassed by 3 freeze pump thaw cycles and CO (99 mmHg, 2.05 mmol, 4 equiv.) was introduced by vacuum transfer at 77 K. The reaction was then sealed, warmed to room temperature, and stirred for 2.5 hours. The volatiles were removed *in vacuo* and the red residue extracted with CH_2Cl_2. The solution was filtered through Celite and the volume reduced to ~ 4 mL. 10 mL pentane was layered on and the solution stored at -40 °C for 3 days. 330 mg of red crystalline product (in two crops) were isolated by decantation of the mother liquor and drying *in vacuo*. (76%). The ^{13}C labeled compound was prepared similarly. $E_{1/2}$(ox) = 0.50 V (quasireversible), $E_{1/2}$(red) = 0.16 V (reversible). μ_{eff} = 2.6 μ_B. ^1H NMR (C_6D_6): δ 29.3 (br s, $\Delta_{1/2}$ = 553 Hz, NCH_2N), -19.2 (br s, $\Delta_{1/2}$ = 415 Hz, NCH_2N). ^{19}F NMR (C_6D_6): δ -132.1 (br s, $\Delta_{1/2}$ = 277 Hz), -170.5 (s). IR (Nujol mull): 1846 s, 1510 s, 1006 m, 983 s, 856 w cm^{-1}. Anal. Calcd. for $C_{25}H_{12}N_4F_{15}OW$: C, 35.19; H, 1.42; N, 6.57. Found: C, 35.45; H, 1.45; N, 6.74.

[N_3N_F]W≡C-O-TMS (10). A solution of [N_3N_F]W(CO) (100 mg, 0.117 mmol) in 5 mL THF was added to 0.5 % Na/Hg amalgam (539 mg, 0.117 mmol). The reaction was stirred for 1 hour, at which point ^{19}F NMR indicated clean formation of the anion. The reaction was filtered and trimethylsilyl chloride (18 μL, 0.14 mmol, 1.2 equiv.) was added via syringe. After stirring for 3 hours, the volatiles were removed *in vacuo* and the brown residue extracted with CH_2Cl_2. Reduction in volume of the extract, layering with pentane, and cooling to -40 °C for 15 hours gave the product as brown blocks. It was isolated by decantation of the mother liquor and drying *in vacuo*, 73 mg (67%). The ^{13}C labeled compound was prepared similarly. ^1H NMR (C_6D_6): δ 3.33 (t, 6, NCH_2N), 2.10 (t, 6, NCH_2N), -0.487 (s, 9, TMS). ^{19}F NMR (C_6D_6): δ -151.1 (s, 6, *o*-C_6F_5), -165.7 (s, 9, *m*-C_6F_5 and *p*-C_6F_5). ^{13}C NMR (C_6D_6): δ 216.9 (W≡*C*-O-TMS), 144.8 (C_6F_5), 141.6 (C_6F_5), 139.3 (C_6F_5), 137.2 (C_6F_5), 136.0 (C_6F_5), 56.8 (NCH_2N), 52.1 (NCH_2N),

References begin on page 176.

-1.4 ($(H_3C)_3Si$). Anal. Calc. for $C_{28}H_{21}N_4F_{15}OSiW$. Calc.: C, 36.30; H, 2.28; N, 6.05. Found: C, 35.92; H, 2.18; N, 5.99.

[N_3N_F]W(CN-*t*-Bu) (11). [N_3N_F]WCl (700 mg, 0.813 mmol) and 0.5% Na/Hg amalgam (3.74 g, 0.813 mmol) were added to a 100 mL round bottomed flask. A solution of *t*-butyl isocyanide (92 µl, 0.813 mmol) in 20 mL THF was prepared and subsequently added to the reaction flask. The mixture was stirred for 1.25 hours, at which point ^{19}F NMR showed it to be complete. The solution was decanted from the amalgam and the volatiles removed under reduced pressure. The orange-brown residue was extracted with CH_2Cl_2 and filtered through Celite. The volume was reduced until the solution was saturated with the product at room temperature, ~20 mL solvent. It was then chilled to -40 °C overnight. Orange plates of the product were isolated by decantation of the mother liquor and drying *in vacuo*, 683 mg in two crops (92%): $E_{1/2}(ox)$ = 0.33 V (reversible), $E_{1/2}(red.)$ = -0.020 V. μ_{eff} = 2.2 μ_B. ^1H NMR (C_6D_6): δ 13.6 (br s, $\Delta_{1/2}$ = 67 Hz, *t*-Bu), 8.0 (br s, $\Delta_{1/2}$ = 132 Hz, NCH_2N), -25.8 (br s, $\Delta_{1/2}$ = 99 Hz, NCH_2N). ^{19}F NMR (C_6D_6): δ -77.0 (br s, $\Delta_{1/2}$ = 86 Hz, F_{ortho}), -142.5 (s, F_{meta}), -161.2 (s, F_{para}). IR (Nujol mull): 1684 ms 1509 s, 1061 m, 1009 s, 984 s, 853 m, 644 w cm^{-1}. Anal. Calc. for $C_{29}H_{21}F_{15}N_5W$: Calc.: C, 38.35; H, 2.33; N, 7.71. Found: C, 38.20; H, 2.22; N, 7.75.

[N_3N_F]W(CN-*t*-Bu)][OTf] (11b). A solution of **11** (100 mg, 0.110 mmol) in 5 mL THF was prepared. [Cp_2Fe][OTf] (39 mg, 0.11 mmol) was added as a solid, giving an immediate color change. The reaction was stirred for 20 min, at which point ^{19}F NMR showed it to be complete. It was then filtered and the volume reduced to 2 mL. 12 mL pentane was then added with stirring to precipitate the cation. The brown precipitate was allowed to settle and the supernatant decanted off. Pentane was again added (to wash the product) and then decanted off. Drying *in vacuo* gave 63 mg of a brown powder (54%). ^1H NMR ($CDCl_3$) δ 4.19 (br t, 6, NCH_2N), 3.78 (br t, 6, NCH_2N), 1.09 (s, 9, CMe_3). ^{13}C NMR ($CDCl_3$) δ 157.3 (s, W-$C{\equiv}N$, J_{CW} = 93 Hz), 144, 142, 140, 138, 136, 135 (br s, C_6F_5), 63.7 (s, NCH_2N), 59.9 (s, CMe_3), 53.9 (s, NCH_2N), 30.2 (CMe_3). ^{19}F NMR ($CDCl_3$) δ -78.4 (br s, OTf), -147.6 (d, *o*-C_6F_5), -158.4 (t, *p*-

References begin on page 176.

C_6F_5), -161.8 (s, *m*-C_6F_5). IR (Nujol mull) cm^{-1} (2111, 2104 (C≡N)), 1503 (N-C_6F_5), 1273, 1195, 1155, 1031, 988, 860, 722. 638.

[N_3N_F]Mo(CN-*n*-Bu) (12b). [N_3N_F]MoCl (200 mg, 0.259 mmol) and 0.5% sodium amalgam (1.19 g, 0.259 mmol) were added to a vial. A solution of *n*-butyl isocyanide (27 μL, 0.26 mmol) in 10 mL THF was prepared and added all at once to the molybdenum chloride and amalgam. The reaction was stirred for 3 hr, at which point ^{19}F NMR showed it was complete. It was then filtered and the volatiles were removed under reduced pressure. The product was recrystallized from CH_2Cl_2 layered with excess pentane at -40 °C. After 15 hr large reddish needles formed which were isolated by decanting away the mother liquor and drying *in vacuo*, 162 mg (76%): ^1H NMR (C_6D_6): δ 5.7 (br s ($\Delta_{1/2}$ = 81 Hz), 6, NC*H*$_2$N), 5.2 (br s ($\Delta_{1/2}$ = 25 Hz), *n*-butyl), 4.0 (br s ($\Delta_{1/2}$ = 12 Hz), *n*-butyl), -0.1 (br s ($\Delta_{1/2}$ = 25 Hz), *n*-butyl), -27.6 (br s ($\Delta_{1/2}$ = 94 Hz), 6, NC*H*$_2$N). ^{19}F NMR (C_6D_6): δ -67 (br s ($\Delta_{1/2}$ = 716 Hz), 6, *o*-C_6F_5), -144.0 (s, 3, *p*-C_6F_5), -161.2 (s, 6, *m*-C_6F_5). IR (Nujol mull): cm^{-1} 1790 (RNC). $E_{1/2}$(ox) = 0.36 V. μ_{eff} = 2.3 μ_B. Anal. Calc. for $C_{29}H_{21}N_5F_{15}Mo$. Calc.: C, 42.46; H, 2.58; N, 8.54. Found: C, 42.14; H, 2.55; N, 8.53.

[N_3N_F]W(NO) (13). A 50 mL round bottomed flask was charged with [N_3N_F]WCl (200 mg, 0.232 mmol), sodium amalgam (1.07 g, 0.232 mmol), and THF (10 mL). It was fitted with a vacuum adapter, sealed, and attached to a high vacuum line. After degassing by freeze pump thawing, nitric oxide (0.82 mmol) was introduced by vacuum transfer. The reaction was sealed and warmed to room temperature, during which time the color changed from black-red to light yellow. It was stirred for 1 hour and the solution was decanted off the amalgam, filtered, stripped, and extracted with CH_2Cl_2. The volume of the CH_2Cl_2 was reduced until the solution was saturated with the product at room temperature. The solution was then kept at -40 °C for 15 h, and the light yellow powder isolated by decantation of the supernatant, 171 mg (86%): ^1H NMR (CD_3CN): δ 4.06 (t, 6, NCH_2N), 3.35 (t, 6, NCH_2N). ^{19}F NMR (CD_3CN): δ -151.7 (s, 6, F_{ortho}), -164.1 (t, 3, F_{meta}), -166.0 (s, 6, F_{meta}). IR (Nujol mull): cm^{-1} 1614 (NO). Anal. Calc. for $C_{24}H_{12}N_5F_{15}OW$. Calc.: C, 33.71; H, 1.41; N, 8.19. Found: C, 33.41; H, 1.49; N, 8.59.

References begin on page 176.

[N_3N_F]W-C≡O-V(Mes)$_3$ • toluene (14). A scintillation vial was charged with [N_3N_F]W(CO) (100 mg, 0.117 mmol) and V(mesityl)$_3$·THF (56 mg, 0.12 mmol). 4 mL toluene was added, resulting in a deep black solution. The reaction was stirred for one hour, at which point ^{19}F NMR showed complete conversion to product. The reaction was filtered and the volume of the toluene reduced to ca. 2 mL. Pentane was layered on and the vial cooled to -40 °C. After 15 h, black crystals had formed and were isolated by decanting off the mother liquor and drying *in vacuo*, 130 mg in two crops (88%). The ^{13}C labeled compound was prepared similarly. ^{1}H NMR (C_6D_6): δ 17.5 (br s($\Delta_{1/2}$ = 22 Hz), 9, mesityl Me_{para}), 16.2 (br s($\Delta_{1/2}$ = 300 Hz), 18, mesityl Me_{ortho}), 6.6 (br s($\Delta_{1/2}$ = 45 Hz), 6, mesityl H_{meta}), 3.38 (s, 6, NCH_2N), 2.06 (s, 6, NCH_2N). ^{19}F NMR(C_6D_6): δ -153.2 (s, 6, *o*-C_6F_5), -162.9 (s, 3, *p*-C_6F_5), -164.3 (s, 6, *m*-C_6F_5). IR (KBr press): cm^{-1} 2916, 2867, 1587, 1501, 1278, 985, 851, 756, 729. μ_{eff} = 2.1 μ_B. Anal. Calc. for $C_{59}H_{53}N_4F_{15}OVW$. Calc.: C, 52.34; H, 3.95; N, 4.14. Found: C, 52.28; H, 3.77; N, 3.96.

[N_3N_F]W(C_2H_4) (15). A 300 mL glass bomb was charged with [N_3N_F]W(OTf) (500 mg, 0.513 mmol), 0.5% sodium amalgam (2.60 g, 0.564 mmol Na), 50 mL THF, and a Teflon coated stir bar. It was sealed and attached to a high vacuum line. The solvent was degassed by freeze pump thawing and then ethylene (~40 mmol) was introduced by vacuum transfer. The reaction was allowed to thaw and stirred efficiently at room temperature for 15 h. Efficient stirring is required for the reaction to proceed at a reasonable rate. The brown solution was decanted from the amalgam and the volatiles removed under reduced pressure. The residue was extracted with CH_2Cl_2 and filtered through Celite. The volume of the CH_2Cl_2 was reduced and the solution layered with pentane. Storage at -40 °C for 15 h resulted in precipitation of the product as a brown powder, 346 mg (79%) in two crops: ^{19}F NMR (C_6D_6): δ -100 (v br s ($\Delta_{1/2}$ = 2,500 Hz), 6, F_{ortho}), -137 (br s ($\Delta_{1/2}$ = 650 Hz), 6, H_{meta}), -152.1 (br s ($\Delta_{1/2}$ = 140 Hz), 3, H_{para}). $E_{1/2}$(ox) = 0.40 V. μ_{eff} = 1.8 μ_B. Anal. Calc. for $C_{26}H_{16}N_4F_{15}W$. Calc.: C, 36.60; H, 1.89; N, 6.57. Found: C, 36.54; H, 2.03; N, 6.36.

References begin on page 176.

[N_3N_F]WBr (16). A flask was charged with [N_3N_F]W(OTf) (100 mg, 0.103 mmol), THF, and sodium amalgam (0.5%, 519 mg, 0.113 mol Na). It was attached to a vacuum line and degassed by freeze-pump-thawing. Bromotrifluoroethylene (1.6 mmol) was introduced by vacuum transfer at 77 K and the reaction was sealed and warmed to room temperature. After stirring overnight, the solution was decanted from the amalgam and the volatiles removed *in vacuo*. The solid remaining was extracted with CH_2Cl_2 and filtered. Recrystallization from minimum CH_2Cl_2 layered with pentane at -40 °C gave the product as orange crystals, 40 mg (43%, not optimized). ^{1}H NMR (C_6D_6) δ -25.0 (br s, 6, NCH_2N), -52.2 (br s, 6, NCH_2N). ^{19}F NMR (C_6D_6) δ -76.9 (br s, 6, *o*-C_6F_5), -123.4 (s, 6, *m*-C_6F_5), -144.8 (s, 3, *p*-C_6F_5). Anal. Calcd. for $C_{24}H_{12}F_{15}BrN_4W$: C, 31.85; H, 1.34; N, 6.19. Found: C, 32.23; H, 1.42; N, 6.24.

[N_3N_F]W(C_2H_4) OTf (17). Ferrocenium triflate (83 mg, 0.23 mmol) was added as a solid to a solution of [$(C_6F_5NCH_2CH_2)_3N$]W(C_2H_4) (200 mg, 0.234 mmol) in 8 mL THF. The solution turned deep red instantly. After 15 min., the solution was filtered and the THF removed *in vacuo*. The ferrocene was sublimed away from the product onto a -78 °C probe. The solid which remained was recrystallized from CH_2Cl_2 / pentane to give the product as a red solid, 215 mg (91%): ^{1}H NMR (C_6D_6): δ 4.42 (br s, 6, NCH_2CH_2N), 3.96 (br s, 6, NCH_2CH_2N), 3.10 (s, 4, C_2H_4). ^{19}F NMR ($CDCl_3$): δ -78 (br s, 3, OTf), -143.7 (s, 6, F_{ortho}), -152.7 (s, 3, F_{para}), -159.8 (s, 6, F_{meta}). Anal. Calc. for $C_{27}H_{16}N_4F_{18}O_3SW$. Calc.: C, 32.35; H, 1.61; N, 5.59. Found: C, 32.53; H, 1.63; N, 5.46.

References begin on page 176.

REFERENCES

(1) Kol, M.; Schrock, R. R.; Kempe, R. *J. Am. Chem. Soc.* **1994**, *116*, 4382.

(2) Schrock, R. R.; Seidel, S. W.; Zanetti-Mösch, N. C.; Dobbs, D. A.; Shih, K.-Y.; Davis, W. M. *Organometallics* , in press.

(3) Schrock, R. R.; Seidel, S. W.; Mösch-Zanetti, N. C.; Shih, K.-Y.; O'Donoghue, M. B.; Davis, W. M.; Reiff, W. M. *J. Am. Chem. Soc.* , in press.

(4) Dobbs, D. A.; Schrock, R. R.; Davis, W. M. *Inorg. Chim. Acta.* , in press.

(5) Jessop, P.; Morris, R. *Coord. Chem. Rev.* **1992**, *121*, 155.

(6) Nugent, W. A.; Mayer, J. A. *Metal-Ligand Multiple Bonds*, Wiley: New York, 1988.

(7) Zanetti-Mösch, N. C.; Davis, W. M.; Schrock, R. R.; Wanniger, K.; Seidel, S. W.; O'Donoghue, M. B. , in press.

(8) Duan, Z.; Verkade, J. G. *Inorg. Chem.* **1995**, *34*, 1576.

(9) Steffey, B. D.; Fanwick, P. E.; Rothwell, I. P. *Polyhedron* **1990**, *9*, 963.

(10) Schrock, R. R. *Polyhedron* **1995**, *14*, 3177.

(11) Kerschner, J. L.; Fanwick, P. E.; Rothwell, I. P.; Huffman, J. C. *Inorg. Chem.* **1989**, *28*, 780.

(12) Coates, G. W.; Dunn, A. R.; Henling, L. M.; Dougherty, D. A.; Grubbs, R. H. *Angew. Chem. Int. Ed. Engl.* **1997**, *36*, 248.

(13) Dahl, T. *Acta Chem. Scand.* **1994**, *48*, 95.

(14) Williams, J. H. *Acc. Chem. Res.* **1993**, *26*, 593.

(15) Durfee, L. D.; Rothwell, I. P. *Chem. Rev.* **1988**, *88*, 1059.

(16) Shih, K.-Y.; Schrock, R. R.; Kempe, R. *J. Am. Chem. Soc.* **1994**, *116*, 8804.

(17) Pretsch, E. *Tables of Spectral Data for Structure Determination of Organic Compounds*, Springer-Verlag: New York, 1989.

(18) Schrock, R. R.; Rosenberger, C.; Seidel, S. W.; Shih, K.-Y.; Davis, W. M., in preparation.

(19) Collman, J. P.; Hegedus, L. S.; Norton, J. R.; Finke, R. G. *Principles and Applications of Organotransition Metal Chemistry*, University Science Books: Mill Valley, 1987.

(20) Bronk, B. S.; Protasiewicz, J. D.; Pence, L. E.; Lippard, S. J. *Organometallics* **1995**, *14*, 2177.

(21) Shih, K.-Y.; Totland, K.; Seidel, S. W.; Schrock, R. R. *J. Am. Chem. Soc.* **1994**, *116*, 12103.

(22) Freundlich, J. S.; Schrock, R. R.; Davis, W. M. *J. Am. Chem. Soc.* **1996**, *118*, 3643.

(23) Malatesta, L.; Bonati, F. *Isocyanide Complexes of Metals*, Wiley: New York, 1969; Vol. IV.

(24) Hu, C.; Hodgeman, W. C.; Bennett, D. W. *Inorg. Chem.* **1996**, *35*, 1621.

(25) Figgis, B. N.; Lewis, J. *Prog. Inorg. Chem.* **1964**, *6*, 37.

(26) Odom, A. L.; Cummins, C. C.; Protasiewicz, J. D. *J. Am. Chem. Soc.* **1995**, *117*, 6613.

(27) Laplaza, C. E.; Odom, A. L.; Davis, W. M.; Cummins, C. C.; Protasiewicz, J. D. *J. Am. Chem. Soc.* **1995**, *117*, 4999.

(28) Seidel, W.; Kreisel, G. *Z. Anorg. Allg. Chem.* **1977**, *435*, 146.

(29) Carrano, C. J.; Mohan, M.; Holmes, S. M.; de la Rosa, R.; Butler, A.; Charnock, J. M.; Garner, C. D. *Inorg. Chem.* **1994**, *33*, 646.

(30) Freundlich, J. S.; Schrock, R. R.; Cummins, C. C.; Davis, W. M. *J. Am. Chem. Soc.* **1994**, *116*, 6476.

(31) Parkin, G.; Bercaw, J. E. *J. Am. Chem. Soc.* **1989**, *111*, 391.

(32) O'Regan, M. B.; Liu, A. H.; Finch, W. C.; Schrock, R. R.; Davis, W. M. *J. Am. Chem. Soc.* **1990**, *112*, 4331.

(33) Schrock, R. R.; Glassman, T. E.; Vale, M. G. *J. Am. Chem. Soc.* **1991**, *113*, 725.

(34) Nomura, K.; Schrock, R. R.; Davis, W. M. *Inorg. Chem.* **1996**, *35*, 3695.

(35) Song, J.-I.; Berno, P.; Gambarotta, S. *J. Am. Chem. Soc.* **1994**, *116*, 6927.

(36) Berno, P.; Hao, S.; Minhas, R.; Gambarotta, S. *J. Am. Chem. Soc.* **1994**, *116*, 7417.

(37) Cummins, C. C.; Lee, J.; Schrock, R. R. *Angew. Chem. Int. Ed. Engl.* **1992**, *104*, 1501.

(38) Rosenberger, C.; Schrock, R. R.; Davis, W. M. *Inorg. Chem.* **1997**, *36*, 123.

(39) Schrock, R. R.; Shih, K.-Y.; Dobbs, D.; Davis, W. M. *J. Am. Chem. Soc.* **1995**, *117*, 6609.

(40) Shih, K.-Y., unpublished results.

(41) O'Donoghue, M. B., unpublished results.

(42) Pangborn, A. B.; Giardello, M. A.; Grubbs, R. H.; Rosen, R. K.; Timmers, F. J. *Organometallics* **1996**, *15*, 1518.

(43) Evans, D. F. *J. Chem. Soc.* **1959**, 2003.

(44) Persson, C.; Andersson, C. *Inorg. Chim. Acta* **1993**, *203*, 235.

(45) Schrock, R. R.; Sturgeoff, L. G.; Sharp, P. R. *Inorg. Chem.* **1983**, *22*, 2801.

CHAPTER V

Transition Metal Complexes Containing Multiamidophosphine Ligands,
Including Zirconium Alkyl Complexes as Catalyst Precursors for Olefin Polymerization

INTRODUCTION

Given the success of the triamidoamine ligand in the development of a range of new transition metal chemistry,[1] we became interested in making some extensions of it. In particular, we would like to determine what the ramifications of replacing the dative amine donor by a phosphine donor would be on the observed reactivity of such complexes. We also would like to prepare ligands which are less susceptible towards some documented decomposition reactions of the $[(TMSNCH_2CH_2)_3N]^{3-}$ ligand, such as Si-N bond cleavage[2,3] and abstraction of a hydrogen β to one of the amides.[3] A phosphine ligand would be expected to be a better donor than an amine ligand, at least for later transition metals, which should result changes in the chemistry proceeding in the "steric pocket" of such complexes. Another ongoing project is to develop *di*amido-donor ligands which allow for more flexibility in terms of the types of complexes which can be prepared. Such $[N_2$ donor$]^{2-}$ ligands form complexes with d^0 metals in group IV and d^2 metals in group VI which have two sites where reactivity can take place, as opposed to $[N_3N]^{3-}$ complexes, where reactions can only be carried out at the apical site. $[N_2$ donor$]^{2-}$ complexes containing zirconium are of interest as catalyst precursors for olefin polymerization as the next logical step in the progression from bis(Cp)[4] to "hybrid" Cp-amido[5] to bis(amido) zirconium catalyst precursors.

A resurgence of research by organometallic chemists in the area of Ziegler-Natta catalysis has come with the discovery that bent metallocene complexes activated by methyl aluminoxanes can be used to polymerize α-olefins at high activities.[6] Since this discovery, a large body of research has been carried out in an attempt to understand and make improvements upon the reaction.[4] Complexes containing one amido ligand and one cyclopentadienyl ligand[5] or two amido ligands[7-10] are of current interest as analogs to the bent metallocene catalysts which have a comparatively low formal electron count at the metal. A living system utilizing a zirconium catalyst which contains a chelating diamido ligand with a dative oxygen donor has recently been developed in our laboratories.[11] We became interested in preparing zirconium complexes containing a chelating diamido*phosphine* donor and investigating "activated" forms of them as

References begin on page 221.

olefin polymerization catalysts. We will detail the preparation of such complexes as well as our results regarding their ability to polymerize olefins.

RESULTS

Synthesis of a Hexamethyltriaminophosphine Ligand

Our initial preparations of phosphorus-containing derivatives of triamidoamine ligands utilized ring opening of tosyl aziridines with phosphides. $LiPH_2(dme)$ (see experimental section for notes on handling this material) reacts with *n*-tosyl-2,2-dimethylaziridine (readily prepared in 85 gram quantities) in THF to yield a primary phosphine as evidenced by proton-coupled ^{31}P NMR (δ = -161 ppm, J_{PH} = 192 Hz). (PH_3 itself does not react with three equivalents of *n*-tosyl-2,2-dimethylaziridine in THF or CH_2Cl_2 at room temperature.) Addition of two equivalents of BuLi to the primary phosphine at -40 °C followed by two additional equivalents of the tosyl aziridine and subsequent quenching with water yields $P(CH_2CMe_2NHTs)_3$ (**1**). The reaction can also be performed stepwise (forming the secondary phosphine first and then the tertiary phosphine) but the streamlined procedure described is preferred. Treatment of **1** with an excess of sodium naphthalide in DME yields $P(CH_2CMe_2NH_2)_3$ (**2**) in low isolated yield (27-37%). Scheme 5.1 details the one-pot synthesis of **2** from *n*-tosyl-2,2-dimethylaziridine and $LiPH_2(dme)$ (Scheme 5.1). The tosyl amide cleavage reaction was problematic for the several reasons. A large quantity of insoluble side-products are produced which are difficult to separate from the product. Also, after extraction of the product from this mixture, it remains contaminated with substantial quantities of naphthalene. Pure **2** was finally obtained as a white crystalline solid by fractional distillation followed by recrystallization.

Attempts to convert **2** to a tris(perfluorophenyl) derivative by reaction with C_6F_6 in DMSO in the presence of K_2CO_3, analogous to the preparation of $[(C_6F_5NCH_2CH_2)_3N]H_3$,[12] were unsuccessful. ^{19}F NMR showed no reaction after 24 h at 70 °C, and higher temperatures and longer reaction times led to decomposition. We were able to convert **2** to $^*[N_3P_F]H_3$ (**3**)

References begin on page 221.

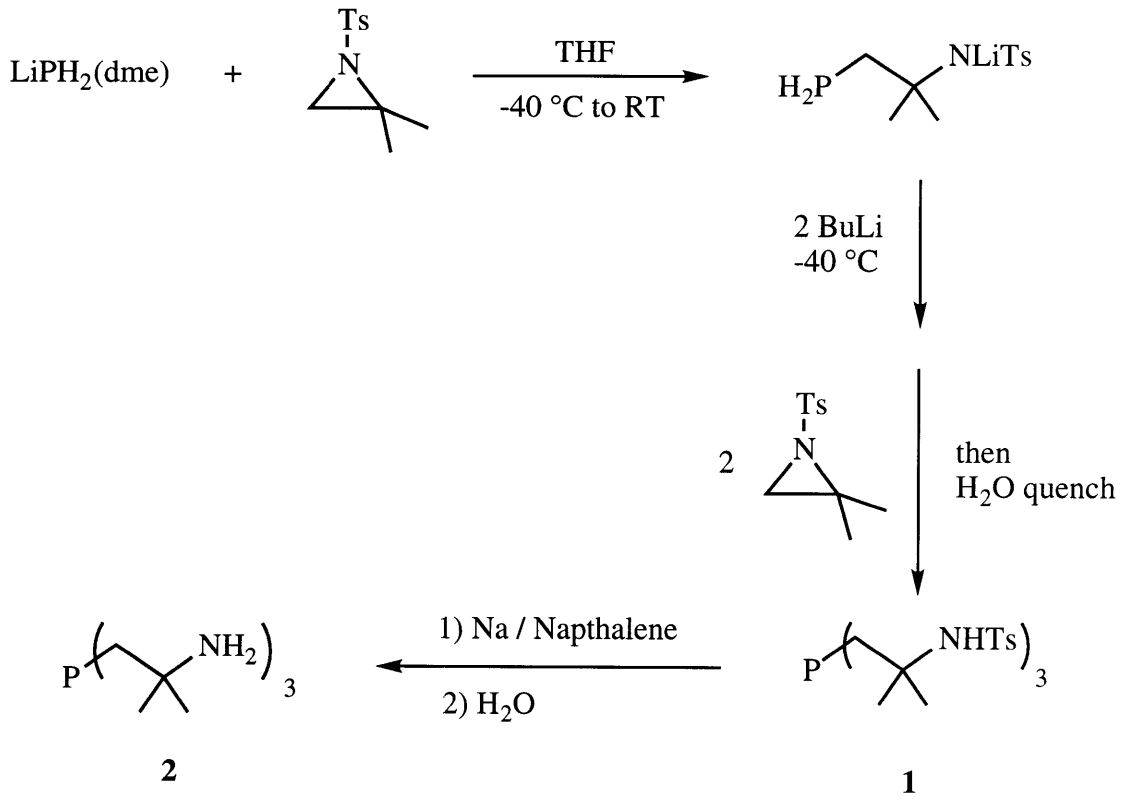

Scheme 5.1. The one-pot synthesis of $P(CH_2CMe_2NH_2)_3$ (**2**) from $LiPH_2(dme)$.

($^*[N_3P_F]H_3$ = $(P(CH_2CMe_2NHC_6F_5)_3)$) by a different method. Deprotonation of **2** with two equivalents of BuLi followed by treatment with one equivalent of C_6F_6 at -40 °C leads to mono C_6F_5-substituted, monolithiated **2** by ^{19}F NMR. Two equivalents of BuLi are required because the amine proton of $RNHC_6F_5$ formed during the reaction is more acidic than those of $P(CH_2CMe_2NH_2)_3$, therefore, as lithiated **2** begins to react with C_6F_6 the $RN\underline{H}C_6F_5$ proton is removed by another lithiated **2**, giving $RNLiC_6F_5$. The second equivalent of BuLi serves to keep a CH_2CMe_2NHLi fragment present so that the arylation reaction goes to completion. ^{19}F NMR shows upfield-shifted resonances for "$P(CH_2CMe_2NLiC_6F_5)(CH_2CMe_2NHC_6F_5)_2$" at -167.2,

References begin on page 221.

-171.2, and -199.2 ppm. Repeating the process twice and quenching with water leads to **3** in moderate yield (30-40%) on small scales (~500 mg product obtained, equation 1). When the reaction was run on a larger scale (10.6 mmol of **2**) the yield dropped to below 15%. This

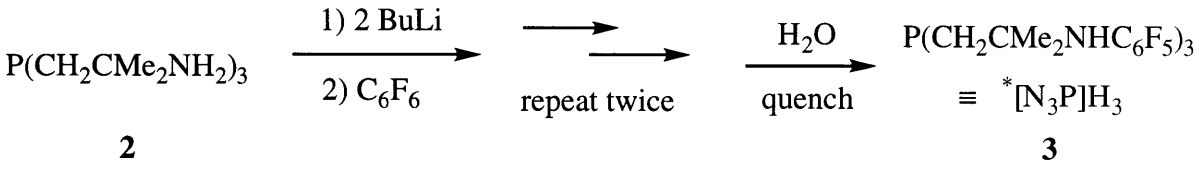

2 **3** (1)

method for obtaining **3** is thus quite limited. The reaction does not proceed cleanly by ^{19}F NMR, decomposition peaks are evident at all stages of the sequence. It seems likely that some of the difficulties involve instability of the presumed trilithiated intermediate, $^{*}[N_3P_F]Li_3$ (**4**). Although high-field peaks ascribable to this trilithium salt are observed in the ^{19}F NMR at the end of the reaction, **4** may be inherently unstable with respect to loss of LiF or other decomposition routes (no trilithium salts of a series of fluorinated aryl-substituted triamidoamine ligands, including $[(C_6F_5NLiCH_2CH_2)_3N]$ have been isolated either).[12] A species proposed to be $[N_3N_F]K_3$ ($[N_3N_F]^{3-} = [(C_6F_5NCH_2CH_2)_3N]^{3-}$) has been prepared in situ, but was shown to be unstable in solution.[13]

The problems with the preparation of **3** led us to seek a more direct route for its preparation. 2,2-dimethylaziridine reacts with C_6F_6 in DMSO in the presence of K_2CO_3 to give *n*-C_6F_5-2,2-dimethylazidine (**5**) in low yield. Presumably, the reaction is sluggish because of the relatively low nucleophilicity of the aziridine nitrogen. It was hoped that **5** would react with lithium phosphides to yield **3** directly. Unfortunately, addition of **5** to LiPPhH in THF leads only to decomposition according to ^{19}F NMR (equation 2). The C_6F_5 ring in **5** is probably too susceptible to electron transfer or nucleophilic attack by LiPHPh.

References begin on page 221.

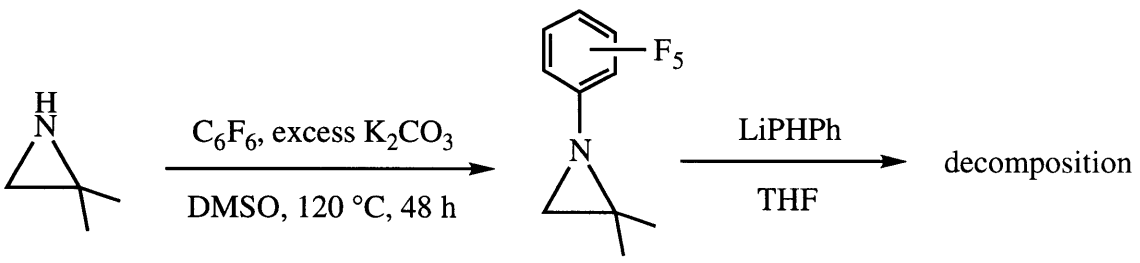

(2)

5

Despite the laborious and low-yield preparation of $^{*}[N_3P_F]H_3$ (**3**), we were able to investigate the possibility of forming transition metal complexes containing it. **3** does not react with $Ti(NMe_2)_4$ or $Mo(NMe_2)_4$ in refluxing toluene after 15 h. Treatment of **3** with $TiCl_4(THF)_2$ in THF in the presence of triethylamine resulted in no reaction. When **3** is treated with three equivalents of BuLi in THF at -40 °C, ^{19}F NMR shows clean conversion to the species proposed to be $^{*}[N_3P_F]Li_3$ (**4**) within 20 min. **4** is not formed as cleanly in diethyl ether. The proposed trilithium salt did not prove to be useful synthetically. Addition of $TiCl_4(THF)_2$ or $WCl_4(DME)$ to THF solutions of **4** led to either decomposition or regeneration of **3**. $^{*}[N_3P_F]H_3$ does react with $Zr(NMe_2)_4$, giving a species which we propose is the corresponding zirconium dimethylamide complex, $^{*}[N_3P_F]Zr(NMe_2)$ (**6**) as a pentane-soluble colorless solid. **6** remains incompletely characterized due to the difficulties associated with obtaining substantial quantities of the $^{*}[N_3P_F]H_3$ ligand. A single resonance in the ^{31}P NMR spectrum of $^{*}[N_3N_F]Zr(NMe_2)$ is observed at -23.7 ppm, 32 ppm downfield from the ^{31}P resonance in $^{*}[N_3P_F]H_3$. The ^{1}H NMR spectrum shows that the methyl groups on the apical amido ligand are inequivalent, suggesting that rotation about the Me_2N-Zr bond is slow on the NMR time scale. Although the ^{1}H resonances for the ligand backbone $C\underline{H}_2$ and $C\underline{Me}_2$ groups are observed as singlets at 1.06 and 0.115 ppm respectively, the ^{19}F NMR spectrum displays three resonances of equal intensity for the ortho fluorines, possibly resulting from hindered rotation of the apical dimethylamido ligand (leading to a C_s-symmetric complex) *as well as* hindered rotation about the N-C_6F_5 bonds. In this situation, the C_6F_5 ring attached to the amide which lies in the mirror plane would give rise to one ortho fluorine resonance, and the other two C_6F_5 rings would have "inside" and "outside"

References begin on page 221.

fluorines, giving rise to three fluorine resonances. A more complicated pattern is observed for the meta and para resonances because these are less well-separated. The situation is much the same as what is seen in $[(C_6F_5NCH_2CH_2)NH]W{\equiv}CCMe_3(Cl)$ (chapter III), hindered rotation of the C_6F_5 rings was also used to explain the ^{19}F spectrum, although only two C_6F_5 rings are present in that molecule. For $^*[N_3P_F]Zr(NMe_2)$, another possibility is that the complex is not C_{3v}-symmetric, although integration of the ^1H NMR spectrum does imply only one NMe_2 ligand is present on zirconium. These NMR data should be compared to those observed with $[(C_6F_5NCH_2CH_2)_3N]Mo(NMe_2)$.[12] In this molybdenum complex, a single resonance for the dimethylamido ligand is observed by ^1H NMR at room temperature, and the ^{19}F NMR spectrum shows the typical three-peak pattern seen for diamagnetic $[N_3N_F]^{3-}$ complexes; thus, the NMe_2 ligand rotates freely. The difficulties associated with the synthesis of gram quantities of $^*[N_3P_F]H_3$ led us to switch directions towards more easily synthesized ligands before **6** could be more fully characterized. Considering the unusual NMR data associated with **6**, we cannot be completely certain that our formulation of it as $^*[N_3P_F]Zr(NMe_2)$ is correct without satisfactory analytical data.

Synthetic Attempts Towards α-Methylated Triamidoamine Ligands

n-Tosyl-2,2-dimethylaziridine reacts with NH_3 (~22 psi) in ethanol to give the ring-opened diamine product, $H_2NCH_2CMe_2NHTs$ (**7**) in good yield (Scheme 5.2). This product reacts with two equivalents of *n*-tosyl-2,2-dimethylaziridine in DMSO at room temperature to give the dialkylated product, $HN(CH_2CMe_2NHTs)_2$ (**8**) in moderate yield. The reaction does not proceed 100% regioselectively; some of what is proposed to be $HN(CH_2CMe_2NHTs)$-(CMe_2CH_2NHTs) is detected by ^1H NMR in the crude product mixture. The regiochemistry of the product is easily determined by ^1H NMR by comparison with literature compounds.[14] **8** does not react further with aziridine to give trialkylated product, even upon increasing the reaction temperature. Forcing conditions tend to lead to elimination and other decomposition reactions. For example, refluxing a mixture of **7** and *n*-Ts-2,2-dimethylaziridine in the presence of ytterbium(III) triflate (known to assist aziridine ring opening reactions[15]) leads to ring-opening

References begin on page 221.

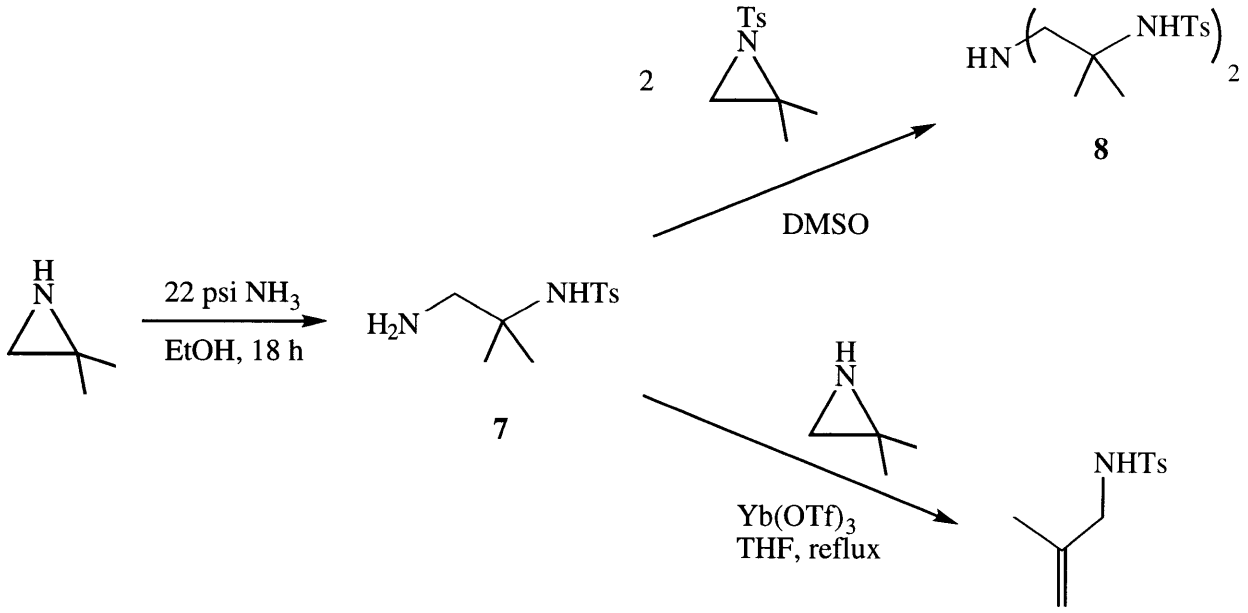

Scheme 5.2. Ring-opening reactions with amine nucleophiles.

via elimination, yielding $H_2C{=}C(Me)(CH_2NHTs)$, a literature compound.[16] We found that lithium amides do not react cleanly with *n*-Ts-2,2-dimethylaziridine, ruling out the possibility of using these more potent nucleophiles to effect ring opening. Even if the reactions discussed here had been more successful, the fact that the products are tosyl amides would probably seriously limit the syntheses because of the difficulty of cleaving this functionality.

Preparation of TMS-Substituted Diamidophosphine Ligands

$ClCH_2CH_2NH_2 \cdot HCl$ reacts with $Me_2ClSiCH_2CH_2SiMe_2Cl$ in the presence of triethylamine to give the protected β-chloroethylamine, $ClCH_2CH_2$(cyclo-$NSiMe_2CH_2CH_2$-$SiMe_2$) (**9**). Addition of butyllithium at -10 °C to a THF solution of two equivalents of **9** and phenylphosphine results in the formation of $PhP(CH_2CH_2$(cyclo-$NSiMe_2CH_2CH_2SiMe_2))$ (**10**) in quantitative yield as an air-stable oil. Removal of the silyl protecting group is effected by treatment with aqueous HCl in ether. $PhP(CH_2CH_2NH_2) \cdot 2\ HCl$ (**11**) is isolated by recrystallization in 65% overall yield from phenylphosphine. This dihydrochloride salt has been

References begin on page 221.

prepared previously from $ClCH_2CH_2NH_2$ and phenylphosphine in NH_3 (l),[17] but we find the preparation in THF from **9** more convenient. **11** reacts with four equivalents of BuLi followed

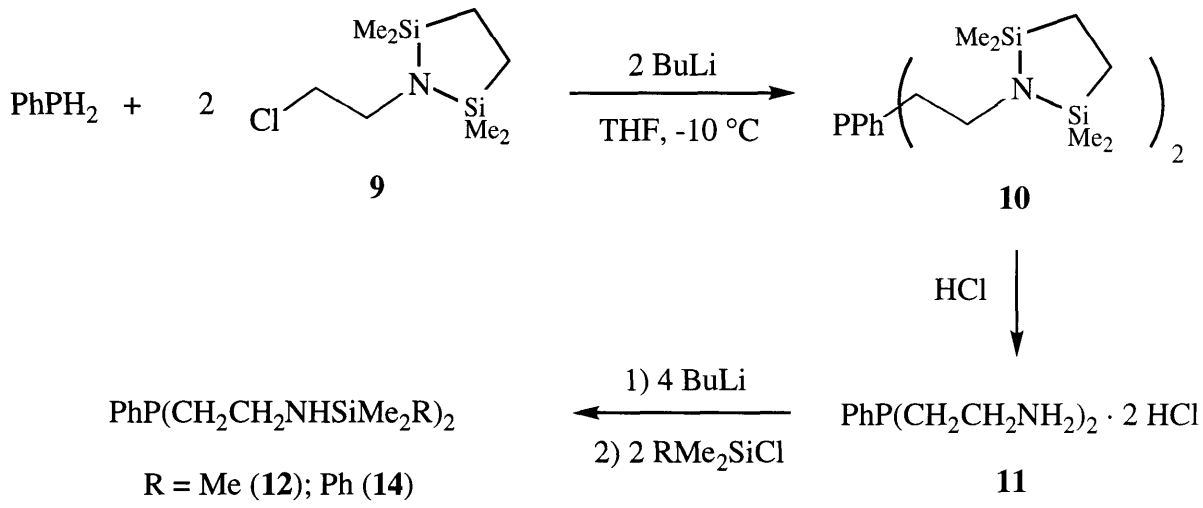

Scheme 5.3. Synthesis of silylated diaminophosphine ligands.

by two equivalents of TMSCl to yield $[N_2P]H_2$ (**12**) ($[N_2P]^{2-}$ = $[(TMSNCH_2CH_2)_2PPh]^{2-}$) quantitatively. A dilithium salt, $[N_2P]Li_2$ (**13**), can be prepared from **12** and two equivalents of BuLi as a white, pentane-soluble crystalline solid in moderate to good yield. A phenyldimethylsilyl-substituted ligand $[PhN_2P]H_2$ (**14**) ($[PhN_2P]^{2-}$ = $[(PhMe_2SiNCH_2CH_2)_2PPh]^{2-}$) can be prepared quantitatively simply by replacing $PhMe_2SiCl$ with TMSCl in the synthesis.

$[N_2P]H_2$ reacts with $Zr(NMe_2)_4$ in pentane to yield $[N_2P]Zr(NMe_2)_2$ (**15**) as an oil. ^1H NMR spectra of **15** display inequivalent dimethylamido ligands as well as diastereotopic ligand backbone methylene protons, consistent with the C_s-symmetric structure shown in equation 2. A single resonance is observed in the ^{31}P NMR spectrum at -10.5 ppm. **15** is converted to white, crystalline $[N_2P]ZrCl_2$ (**16**) by treatment with two equivalents of TMSCl in pentane. Within minutes, analytically pure **16** begins to crystallize directly from the reaction mixture. Workup is effected by simply filtering the product off and drying it *in vacuo*. The backbone methylene protons of $[N_2P]ZrCl_2$ are diastereotopic, again suggesting a C_s-symmetric structure, and δ (^{31}P)

References begin on page 221.

for the complex is 1.94 ppm. Phenyldimethylsilyl-substituted analogs, $[PhN_2P]Zr(NMe_2)_2$ (**17**) and $[PhN_2P]ZrCl_2$ (**18**) are readily prepared by analogous methods.

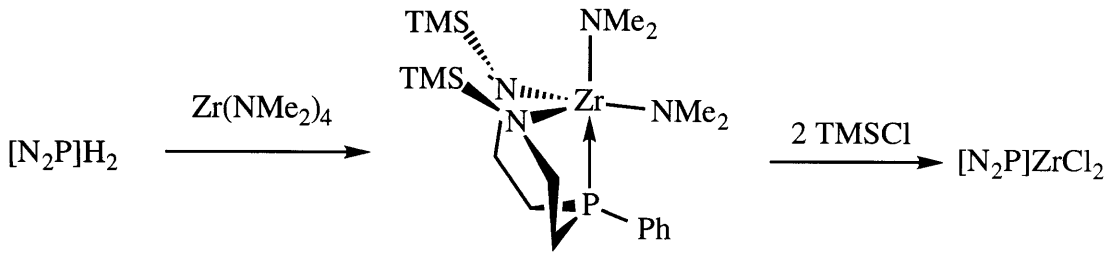

(2)

15 **16**

$[N_2P]ZrCl_2$ reacts with 2 equivalents of CH_3MgCl to yield $[N_2P]Zr(CH_3)_2$ (**19**) as an oil. Attempts to crystallize this highly soluble complex were unsuccessful, and we were therefore unable to obtain analytical data. ^1H NMR spectra of the product isolated after extraction with pentane show no impurities. ^1H NMR parameters for the $[N_2P]$ ligand backbone in **19** are similar to those observed for **17** and **18**. The methyl groups are observed at 0.80 ($^3J_{HP}$ = 6 Hz) and 0.60 ($^3J_{PH}$ < 1 Hz). By extension from some similar complexes which will be described below, we propose that the methyl group with the larger $^3J_{PH}$ value is cis to phosphorus and one with the smaller $^3J_{PH}$ value is trans to phosphorus. The ^{13}C-labeled complex ($[N_2P]Zr(^{13}CH_3)_2$) displays two resonances in the ^{13}C NMR spectrum in ether (unlocked) at 35.9 ppm with $^2J_{PC}$ = 29 Hz and at 40.9 ppm with $^2J_{PC} \approx 2$ Hz. The higher $^2J_{PC}$ value is indicative of a methyl trans to phosphorus. $[PhN_2P]ZrCl_2$ also reacts with two equivalents of MeMgCl to yield $[PhN_2P]Zr(Me)_2$ (**20**), but the complex is also an oil which could not be crystallized.

Alkyl-chloride and mixed alkyl species can also be prepared. Treatment of an ethereal solution of $[N_2P]ZrCl_2$ with one equivalent of MeMgCl (3.0 M in THF) leads to the formation of $[N_2P]Zr(Me)(THF)Cl$ (**21**) as a white crystalline solid (equation 3) in moderate yield. Analytical data and ^1H NMR are consistent with the formulation as a six-coordinate mono THF adduct, as one equivalent of THF per zirconium remains after extraction with pentane, removal of the volatiles *in vacuo*, and recrystallization from pentane. The ^{31}P resonance is observed at -0.49

References begin on page 221.

ppm. Again by extension from a similar complex (see below), we propose that the THF is bound in the equatorial plane which contains the two amides and the methyl ligand, since $^3J_{PH}$ = 7 Hz. Such a six-coordinate structure has also been proposed for a tungsten diamidoamine complex (see chapter III). $[N_2P]ZrCl_2$ is methylated in the absence of THF with Me_2Mg to give base-free $[N_2P]Zr(Me)Cl$ (**22**), δ (^{31}P) = -1.6. The CH_3 ligand is observed at 0.9 ppm with no proton-phosphorus coupling, therefore, we propose that the structure is a base analog of that of **21** with a cis CH_3 ligand.

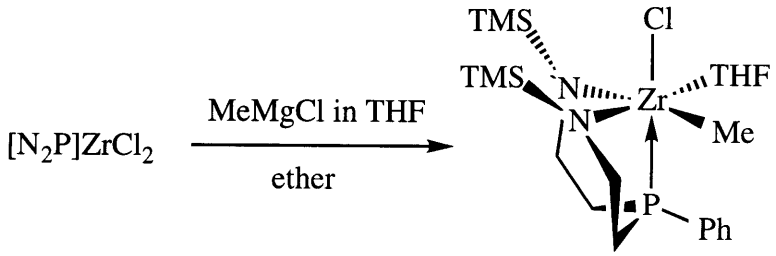

(3)

21

$[N_2P]ZrCl_2$ reacts with one equivalent of Me_2CHCH_2MgCl to form $[N_2P]Zr(Cl)(CH_2\text{-}CHMe_2)$ (**23**). C_α from the *i*-Bu ligand is observed in the ^{13}C NMR spectrum at 70.9 ppm with no coupling to phosphorus, indicative of a cis(*i*-Bu), trans(Cl) arrangement. C_β is observed at 29.9 ppm, and here phosphorus coupling *is* observed (J_{CP} = 5 Hz). Whether or not a β-agostic interaction is present has not been probed by VT NMR. The ^1H NMR of **23** shows a virtual triplet at 1.5 ppm for $C\underline{H}_2CHMe_2$, with $^3J_{PH}$ = 7.7 Hz and $^3J_{HH}$ = 6.8 Hz, as determined by a phosphorus-decoupled ^1H spectrum. **23** is not very stable thermally, decomposing over days in solution. Treatment of $[N_2P]ZrCl_2$ with two equivalents of *i*-BuMgCl yields only **23**; no evidence for the dialkyl is observed, possibility because such a species is too crowded. **23** also decomposes when treated with MeMgCl. $[N_2P]ZrCl_2$ reacts with one equivalent of EtMgCl to give a mixture of products, none of which were identified.

Treatment of $[N_2P]ZrCl_2$ with one equivalent of MeMgCl followed by one equivalent of BnMgCl (Bn = $C_6H_5CH_2$) leads to the formation of white, crystalline $[N_2P]Zr(CH_3)(Bn)$ (**24**) in

References begin on page 221.

good yield. The ^1H NMR spectrum displays a resonance for the benzylic protons at 2.83 ppm ($^3J_{PH}$ = 9 Hz) and a resonance at 0.588 ppm for the CH_3 ligand ($^3J_{PH}$ not observed). The ^{13}C NMR spectrum shows a resonance at 62.4 ppm ($^2J_{CP}$ = 4.6 Hz, $^1J_{CH}$ = 130 Hz) for the benzylic carbon, and a resonance at 38.2 ppm ($^2J_{CP}$ = 27.9 Hz, $^1J_{CH}$ = 112 Hz) for the $^{13}CH_3$ group. As we have done for all $[N_2P]Zr$ alkyls thus far, we propose that the ligand with the large value of $^2J_{CP}$ (in this case CH_3) is trans to the phosphine, and the ligand with the small value of $^2J_{CP}$ is cis. For **24**, crystals suitable for X-ray diffraction were obtained from pentane at -40 °C, allowing us to test this proposal.

A view of the structure of $[N_2P]Zr(CH_3)(Bn)$ is shown in Figure 5.1, and Table 5.1 contains selected bond lengths and angles. Crystallographic data are located in Table 5.3. The structure verified that the methyl group is trans to phosphorus, and showed that the ipso carbon of the benzyl ligand is within bonding distance of zirconium (Zr-C(41) = 2.835(4) Å). The Zr - C(47) - C(41) angle is 95.4°. These metrical data are consistent with a weak zirconium-C_{ipso} interaction, more typical values for η^2 benzyl M-C_{ipso} distances and M-C_α-C_{ipso} angles are 2.50-2.65 Å and 87-88°.[18,19] The $^1J_{CH}$ value observed (130 Hz) by NMR in C_6D_6 is consistent with the weak η^2 interaction observed in the solid state.[18] The Zr-P distance is 2.9343(11) Å, relatively long in comparison to related complexes[20-22] (the structures in the cited works have Zr-P distances from 2.75-2.85 Å, but they do not have methyl ligands trans to phosphorus). A diamidophosphine $ZrMe_2$ complex similar to **24** with silicon present in the ligand backbone, $[(2,6\text{-}Me_2PhNSiMe_2CH_2)_2PPh]Zr(Me)_2$ (**25**), has been prepared and crystallographically characterized in our laboratories, and the Zr-P bond length is 2.916(2) Å.[23] It may be that a trans effect from the strongly σ-donating methyl ligand in **24** and **25** results in a weaker Zr-P interaction than what has been observed previously. The TMS groups in **24** are fairly twisted, with P-Zr-N-Si dihedral angles of 139.6 and 144.7°, and N(1)-Zr-N(2) is 102.35(13)°. These data indicate substantial distortion from a trigonal-bipyramidal geometry.

References begin on page 221.

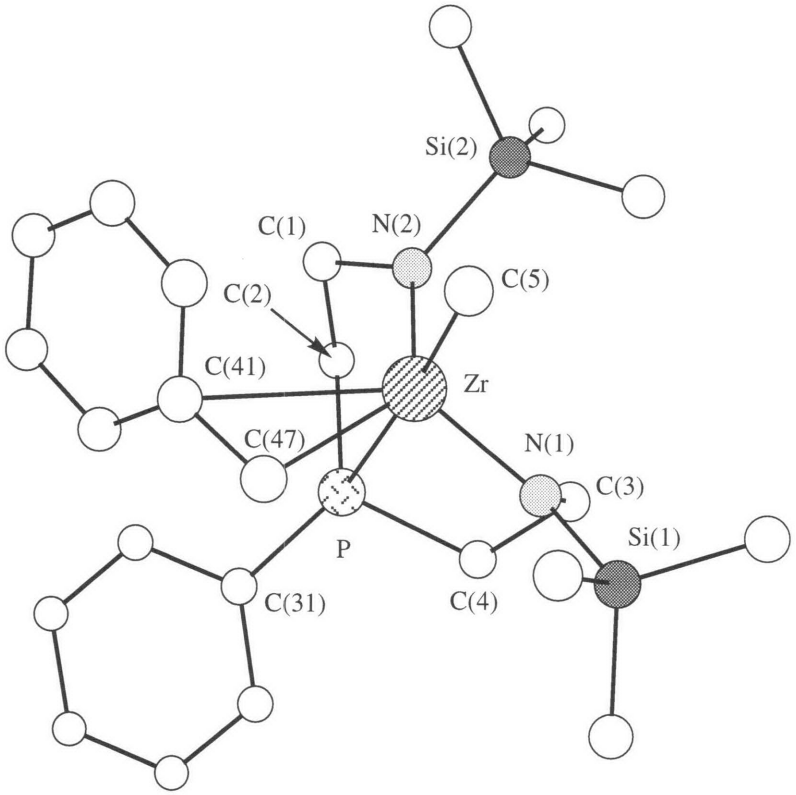

Figure 5.1. A view of the structure of $[N_2P]Zr(CH_3)(Bn)$ (**24**).

References begin on page 221.

Table 5.1. Selected bond distances (Å) and angles (deg.) for $[N_2P]Zr(CH_3)(Bn)$ (**24**).

Distances (Å)

Zr - P	2.9343(11)	Zr - C(5)	2.294(4)
Zr - N(1)	2.054(3)	Zr - C(47)	2.295(4)
Zr - N(2)	2.062(3)	Zr - C(41)	2.835(4)
C(41) - C(47)	1.464(5)	P - C(31)	1.822(4)
C(2) - P	1.843(4)	C(4) - P	1.836(4)
N(1) - Si(1)	1.733(3)	N(2) - Si(2)	1.746(3)

Angles (deg.)

N(1) - Zr - N(2)	102.35(13)	Zr - C(47) - C(41)	95.4(2)
Zr - P - C(31)	144.66(13)	C(5) - Zr - P	174.65(12)
C(31) - P - C(4)	104.6(2)	C(31) - P - C(2)	105.0(2)
C(2) - P - C(4)	106.7(2)	C(3) - N(1) - Si(1)	115.6(3)
C(47) - Zr - N(2)	127.56(13)	Zr - N(1) - Si(1)	125.0(2)
C(5) - Zr - N(1)	109.96(14)	C(47) - Zr - N(1)	114.25(14)

Dihedral Angles (deg.)[a]

P - Zr - N(1) - Si(1)	139.6	P - Zr - N(2) - Si(2)	144.7

[a] Obtained from a Chem 3D drawing

References begin on page 221.

A bis(benzyl) complex can be prepared from $[N_2P]ZrCl_2$ and two equivalents of BnMgCl (equation 4). Light yellow, crystalline $[N_2P]Zr(Bn)_2$ (**26**) is obtained in good yield after recrystallization from ether/pentane mixtures. ^1H NMR shows inequivalent benzyl groups, at 2.75 (d, $^3J_{PH}$ = 6.6 Hz) and 2.69 (d, $^3J_{PH}$ = 2.4 Hz) ppm. ^{13}C NMR shows two resonances that we assign as the C_α cis to the phosphine (at 69.3 ppm, $^1J_{CH}$ = 126 Hz (c.f. 130 Hz for **24**), $^2J_{CP}$ = 3.2 Hz) and the C_α trans to the phosphine (at 65.9 ppm, $^1J_{CH}$ = 118 Hz, $^2J_{CP}$ = 22 Hz).

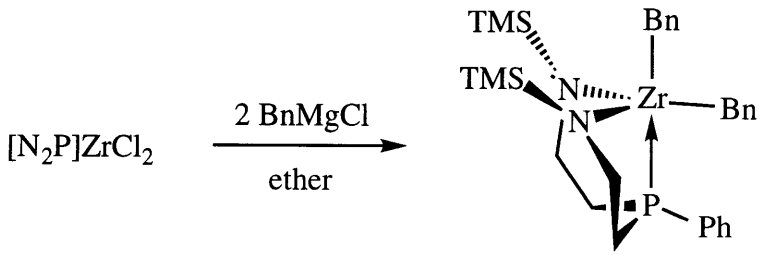

(4)

25

Activation of $[N_2P]Zr$ Dialkyl Complexes and Polymerization Studies

$[N_2P]Zr(^{13}CH_3)_2$ (**19**) reacts with $[Ph_3C][B(C_6F_5)_4]$ in bromobenzene-d_5 at -30 °C to yield $[[N_2P]Zr(^{13}CH_3)][B(C_6F_5)_4]$ (**27**) along with $Ph_3C^{13}CH_3$. The ^{13}C NMR spectrum at -30 °C (Figure 5.2) shows a peak at 55.1 ppm (14 ppm downfield from the lower field $\underline{C}H_3$ resonance in **19**) which we assign to $[[N_2P]Zr(^{13}CH_3)]^+$, as well as a resonance for $Ph_3C^{13}CH_3$ at 30.5 ppm. The peak for the organic product is much more intense that for **27**, presumably a result of a large difference in relaxation times between the $Ph_3C^{13}\underline{C}H_3$ and $[[N_2P]Zr(^{13}\underline{C}H_3)]^+$. A similar variation in peak heights is observed during the preparation of $[[t\text{-Bu-}o\text{-}C_6H_4)_2O]Zr(^{13}CH_3)]^+$,[24] a living catalyst for 1-hexene polymerization.[11] Thus, we are reasonably confident that variable relaxation times, rather than significant decomposition of **27**, are the origin of the disparity in peak heights. The ^{31}P NMR spectrum shows a relatively broad

References begin on page 221.

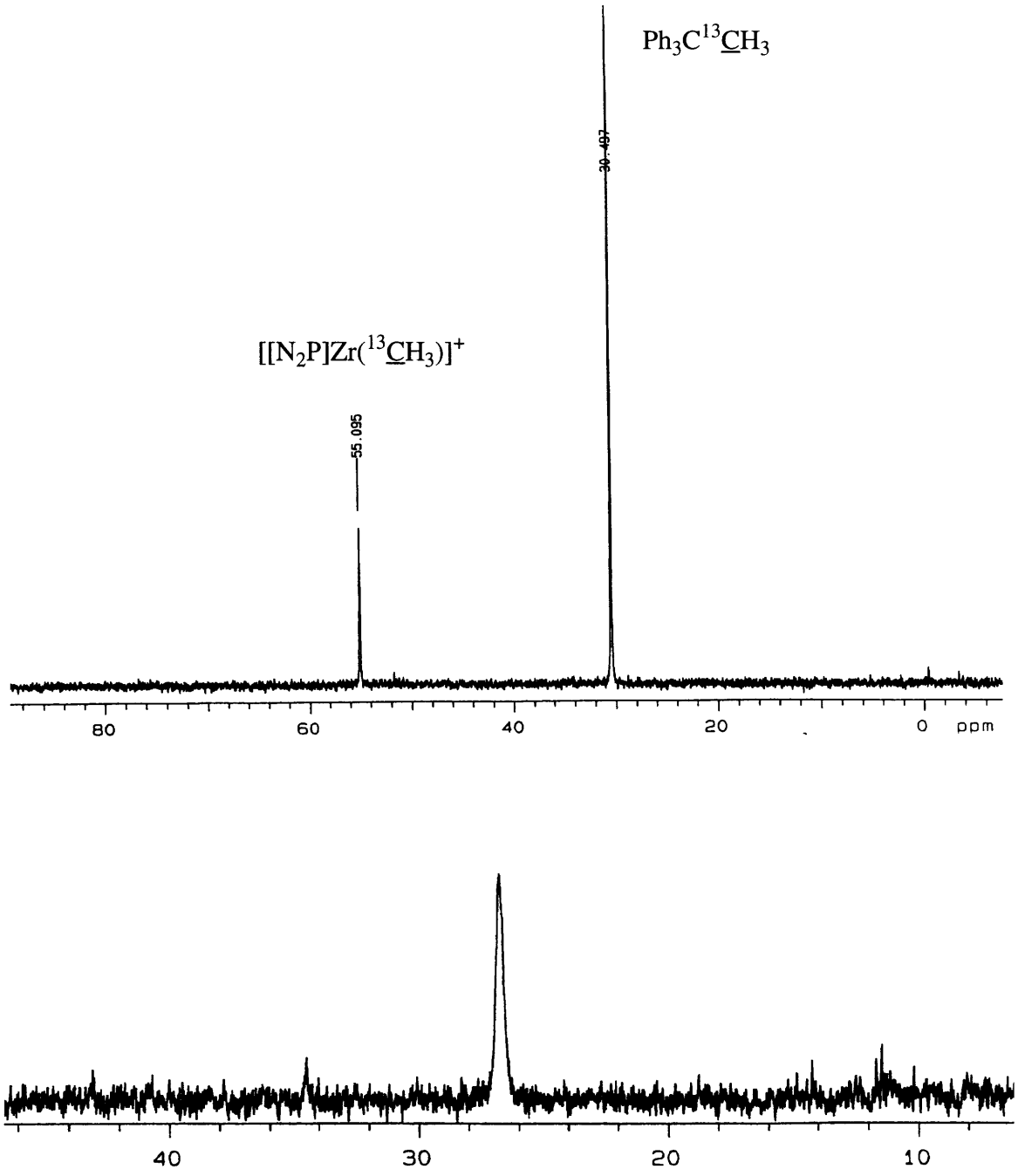

Figure 5.2. The ^{13}C (top) and ^{31}P (bottom) NMR spectra of $[[N_2P]Zr(^{13}CH_3)]^+$ $[B(C_6F_5)_4]^-$ (**27**) in bromobenzene-d_5 recorded at -30 °C.

resonance at 26.8 ppm, 42.5 ppm downfield of that in **19**. The proton NMR spectrum at -30 °C shows a fairly broad TMS signal. No resonance for $[[N_2P]Zr(^{13}C\underline{H}_3)]^+$ could be resolved, possibly because what would be expected to be a relatively weak doublet near 0 ppm is obscured by the broad TMS resonance. Since no C-P coupling is seen in either the ^{31}P or ^{13}C spectrum, we propose that the methyl group is cis to phosphorous and the apical site is vacant or contains loosely coordinated solvent (equation 5). **27** is not very thermally stable. Evidence of decomposition is observed by ^{13}C and ^{31}P NMR within minutes of warming to room temperature.

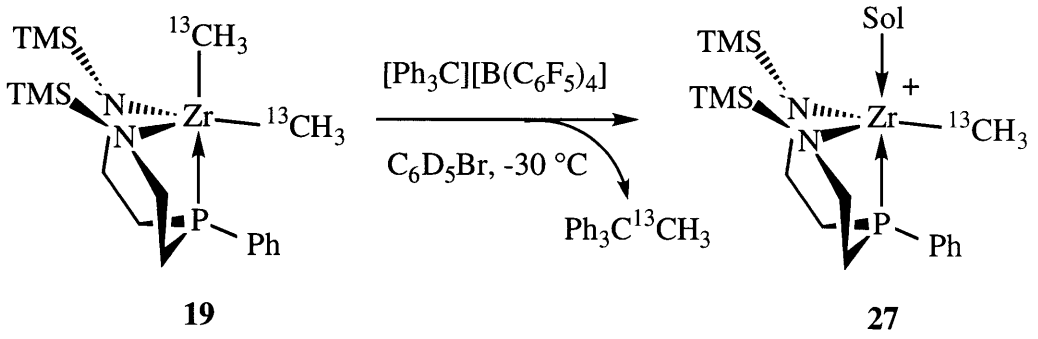

19 **27** (5)

The thermal instability of **27** led us to search for more robust cations. It was hoped that the ability of benzyl ligand to act as more than a two electron donor would stabilize a cationic species. $[N_2P]Zr(Bn)_2$ (**26**) reacts with $[Ph_3C][B(C_6F_5)_4]$ in bromobenzene-d_5 at -30 °C to yield a species proposed to be $[[N_2P]Zr(Bn)][B(C_6F_5)_4]$ (**28**). The ^1H NMR spectrum at -30 °C shows a peak at 3.88 ppm (c.f. 2.75 and 2.69 ppm for the $C\underline{H}_2Ph$ ligands in **26**) which we assign as $[[N_2P]Zr(C\underline{H}_2Ph)]^+$. No proton-phosphorous coupling is observed, leading us to again assign the stereochemistry of this benzyl ligand as cis to phosphorus. A single TMS resonance is observed at 0.096 ppm. The ^{31}P NMR spectrum displays a broad peak at 22 ppm, close to that observed for **27**. Warming the sample to room temperature results in decomposition in a matter of minutes as evidenced by ^1H and ^{31}P NMR. Apparently, no additional stability is imparted to the cation by the benzyl ligand. $[[N_2P]Zr(Me)(Bn)]$ also reacts with $[Ph_3C][B(C_6F_5)_4]$ in bromobenzene-d_5 at -30 °C, although a mixture of products is formed as determined by NMR at -30 °C,

References begin on page 221.

presumably a result of a lack of selectivity towards removal of the benzyl ligand over the methyl, or vice versa. No increase in cation stability was observed by ^{31}P NMR upon attempted generation of [[N_2P]Zr(Me)][$B(C_6F_5)$] in C_6H_5Cl instead of bromobenzene-d_5, unlike the behavior observed with the species proposed to be [[(2,6-$Me_2PhNCH_2CH_2)_2S$]-Zr(Me)][$B(C_6F_5)$].[25]

Cation formation with phenyldimethyl-substituted complexes was also investigated in the hope that the phenyl group might stabilize the cation by some π-interaction. [PhN_2P]Zr($^{13}CH_3)_2$ (**20**) reacts with [Ph_3C][$B(C_6F_5)_4$] in bromobenzene-d_5 at -30 °C to give a mixture of several species, as evidenced by ^1H, ^{31}P, and ^{13}C NMR at this temperature. It appears that the phenyldimethylsilyl substituents allow for other decomposition pathways to occur rather than garner additional stability.

Addition of *n,n*-dimethylaniline to [[N_2P]Zr($^{13}CH_3$)][$B(C_6F_5)_4$] (**27**) immediately after it is generated leads to a new species which can be observed spectroscopically at -30 °C. We cautiously propose that a base adduct, [[N_2P]Zr($^{13}CH_3$)(NMe_2Ph][$B(C_6F_5)_4$] (**29**) is formed, although other species are present by ^{31}P and ^{13}C NMR. Interestingly, the $^{13}CH_3$ group in **29** appears as a doublet at 44.7 ppm, $^2J_{CP}$ = 25 Hz. A doublet is also observed in the ^{31}P spectrum, again with a 25 Hz coupling constant. We interpret these data by proposing that the methyl group in **29** is trans to the phosphine, and the dimethylaniline base is bound in the equatorial site. Resonances for both free (2.64 ppm) and bound (2.77 ppm) NMe_2Ph are observed in the ^1H NMR spectrum. Although **29** is not formed cleanly, warming to room temperature for 30 min and re-cooling results in no change in the spectra, thus whatever species are present are much more thermally stable than "cations" generated in the absence of NMe_2Ph. Attempts to generate cationic base adducts from [($PhNMe_2H$][$B(C_6F_5)_4$] and [N_2P]ZrR_2 complexes directly at room temperature in C_6D_5Br were unsuccessful, only decomposition was observed.

Addition of 20 equivalents of 1-hexene to [[$N_2PZr(CH_3)$][$B(C_6F_5)_4$] (**27**) in bromobenzene-d_5 and allowing the reaction to stand at 0 °C for 1 h results in the formation of some polymer as evidenced by ^1H NMR, although >50% monomer is still present. Longer

References begin on page 221.

reaction times result in almost no additional polymer. Despite the increased thermal stability of **29**, a similarly sluggish reaction with 1-hexene was observed. Both **27** and [[N_2P]Zr(Bn)][B(C_6F_5)] (**28**) appear to be effective catalysts for the polymerization of ethylene in chlorobenzene at 0 °C. A white solid was obtained from the reactions which has not been characterized, "activities" at ~1 atm ethylene are 2.3 x 10^5 and 5.4 x 10^4 g/mol-h-atm for **27** and **28**, respectively.

P-C Bond Cleavage During the Attempted Synthesis of a [N_2P]$^{2-}$ Molybdenum Complex

[N_2P]Li_2 reacts with $MoCl_4(THF)_2$ in THF to yield [N_2P][NP]Mo(IV) (**30**) ([NP]$^{2-}$ = [$TMSNCH_2CH_2PPh]^{2-}$) in 5% yield as a diamagnetic, dark orange crystalline solid. Presumably, the reaction is plagued by the same problems which occur during the synthesis of [$(TMSNCH_2CH_2)_3$N]MoCl, rupture of the TMS-N linkage and formation of TMSCl. Here, an additional problem is observed, namely cleavage of one of the P-(CH_2CH_2NTMS) linkages to yield the [NP]$^{2-}$ ligand. Two resonances are observed in the ^{31}P NMR spectrum, one at 210 ppm for the phosphide and one at 62 ppm for the phosphine. Both are doublets with $^2J_{PP} \approx 10$ Hz, consistent with a cis arrangement. Two TMS groups are observed in the ^{1}H NMR at 2.21 and 0.452 ppm in a 2:1 ratio.

An X-ray structural determination of **30** was carried out, and a view of the structure is shown in Figure 5.3. Table 5.2 contains selected bond lengths and angles, and Table 5.3 contains the crystallographic data. The molybdenum-phosphine distance (Mo-P(1)) is 2.525(3) Å, in the range normally observed for molybdenum phosphines.[26] The Mo-phosphide distance is ~0.2 Å shorter, at 2.223(4) Å. Several of the metrical parameters indicate a high degree of steric strain in the complex. Most notable are the P(1)-Mo-N_{eq}-Si dihedral angles, 131.8 and 118.3°. The TMS groups are thus substantially twisted towards Mo, whereas in **24** they are twisted away from Zr. **30** is presumably diamagnetic for the same reason as [N_3N_F]Mo(NMe_2) is,[12] π-bonding from the apical amido ligand results in energetically inequivalent d_{xz} and d_{yz} orbitals, leading to a singlet ground state.

References begin on page 221.

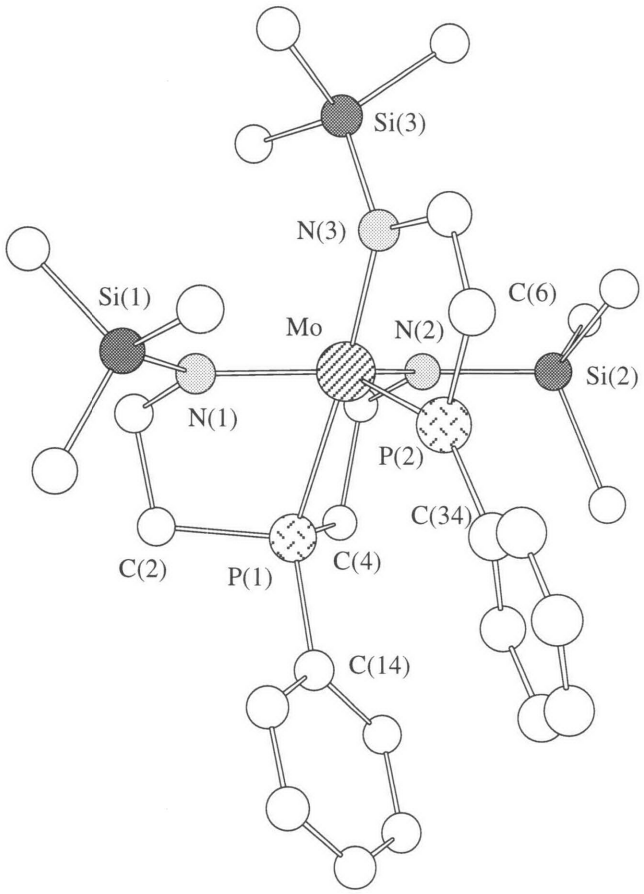

Figure 5.3. A view of the structure of $[N_2P][NP]Mo$ (**30**).

Table 5.2. Selected bond distances (Å) and angles (deg.) for $[N_2P][NP]Mo$ (**30**).

Distances (Å)

Mo - P(1)	2.525(3)	Mo - P(2)	2.223(4)
Mo - N(1)	2.001(9)	Mo - N(3)	2.063(10)
Mo - N(2)	2.004(9)	C(6) - P(2)	1.855(12)
P(1) - C(4)	1.837(12)	P(2) - C(34)	1.796(12)
C(2) - P(1)	1.805(13)	P(1) - C(14)	1.821(13)
N(1) - Si(1)	1.762(10)	N(2) - Si(2)	1.739(10)
N(3) - Si(3)	1.781(10)		

Angles (deg.)

N(1) - Mo - N(2)	126.6(4)	P(1) - Mo - P(2)	102.74(12)
N(3) - Mo - P(2)	82.4(2)	N(1) - Mo - P(2)	119.3(3)
Mo - N(3) - Si(3)	122.8(5)	N(2) - Mo - P(2)	111.0(3)
C(2) - P(1) - C(4)	107.2(6)	C(2) - P(1) - C(14)	103.7(6)
P(1) - Mo - N(3)	174.7(2)	C(6) - P(2) - C(34)	106.9(6)
Mo - N(2) - Si(2)	126.8(5)	Mo - N(1) - Si(1)	129.4(5)

Dihedral Angles (deg.)[a]

P(1) - Mo - N(1) - Si(1)	131.8
P(1) - Mo - N(2) - Si(2)	118.3

[a] Obtained from a Chem 3D drawing

Table 5.3. Crystallographic data, collection parameters, and refinement parameters for $[N_2P]Zr(CH_3)(Bn)$ (**24**) and $[N_2P][NP]Mo$ (**30**).

	$[N_2P]Zr(CH_3)(Bn)$	$[N_2P][NP]Mo$
Empirical Formula	$C_{24}H_{41}N_2PSi_2Zr$	$C_{27}H_{49}MoN_3P_2Si_3$
Formula Weight	535.96	657.84
Diffractometer	Siemens SMART/CCD	Siemens SMART/CCD
Crystal Dimensions (mm)	$0.26 \times 0.12 \times 0.08$	$0.38 \times 0.12 \times 0.12$
Crystal Color	Colorless	Orange
Crystal System	Monoclinic	Monoclinic
a (Å)	13.677 (3)	11.2882 (8)
b (Å)	11.936 (3)	16.6242 (11)
c (Å)	17.646 (3)	17.8030 (12)
β (deg)	96.182 (14)	93.5440 (10)
V (Å^3)	2863.9 (11)	3334.5 (4)
Space Group	$P2_1/c$	$P2_1/c$
Z	4	4
ρ_{calc} (Mg/m^3)	1.243	1.310
Absorption Coefficient (mm^{-1})	0.536	0.618
F_{000}	1128	1384
λ (MoK_α)	0.71073 Å	0.71073 Å
Temperature (K)	183 (2)	183 (2)
Scan Type	ω	ω
θ Range for Data Collection (deg)	1.50 to 23.26	1.68 to 20.00
Reflections Collected	8939	9797
Independent Reflections	3928	3112
Absorption Correction	None	None
R [I > 2σ(I)]	0.0450	0.0999
R_W [I > 2σ(I)]	0.0912	0.2507
GoF	1.164	1.030
Extinction Coefficient	0.0016 (3)	n/a
Largest Diff. Peak and Hole (eÅ^{-3})	0.373 and -0.332	1.753 and -1.028

References begin on page 221.

Preparation of Complexes Containing the $[(C_6F_5NCH_2CH_2)_2PPh]^{2-}$ Ligand

The low yields observed for the preparations of $[N_2P][NP]Mo$ and $[N_3N]MoCl$ stand in stark contrast to the high yields obtained for the preparation of $[N_3N_F]MCl$ (M = Mo, W) complexes.[12] We thus became interested in preparing a C_6F_5-substituted diamidophosphine ligand in the hope of extending such chemistry towards complexes containing middle transition metals. $PhP(CH_2CH_2NH_2)_2 \cdot 2HCl$ reacts with an excess of C_6F_6 in DMSO in the presence of K_2CO_3 under nitrogen to give $PhP(CH_2CH_2NHC_6F_5)_2$, $[N_2P_F]H_2$, (**31**) as a white crystalline solid which is air-stable enough to be chromatographed on alumina under air. **31** reacts with $Mo(NMe_2)_4$ in pentane to give $[N_2P_F]Mo(NMe_2)_2$ (**32**). The ^{31}P NMR spectrum of **32** shows a single resonance at 61.6 ppm, ~90 ppm downfield from that of **31**, and very similar to the chemical shift for the phosphine ligand in $[N_2P][NP]Mo$. A diastereotopic ligand backbone is observed by ^1H NMR, as well as two dimethylamido resonances. **32** is probably diamagnetic because π-bonding from the apical NMe_2 ligand renders the d_{xz} and d_{yz} orbitals acutely inequivalent. We propose that the structure of **32** is similar to analogous $[N_2P]Zr(NMe_2)_2$ (**15**), as shown in equation 6. ^{19}F NMR spectra show a pattern typical of diamagnetic C_6F_5-substitued complexes in which the rings rotate readily on the NMR time scale, a doublet at -150.9 ppm for the ortho fluorines and a multiplet at -165.5 ppm for the meta and para fluorines.

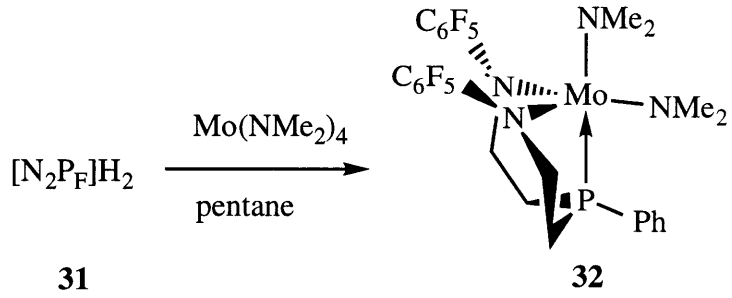

31 **32** (6)

$[N_2P_F]H_2$ reacts with $MoCl_4(THF)_2$ in the presence of triethylamine in THF to give an orange, paramagnetic species which we formulate as an anionic amido-amine-phosphine complex, $[[PhP(CH_2CH_2NHC_6F_5)(CH_2CH_2NC_6F_5)]MoCl_4][HNEt_3]$. (**33**) C, H, and N analyses

References begin on page 221.

are consistent with this formulation. The ^{19}F NMR spectrum displays five paramagnetic signals which we assign to the amido C_6F_5 ring (presumably not rotating on the NMR time scale) and 3 diamagnetic signals (chemical shifts of these fluorines are very similar to those of $[N_2P_F]H_2$) which we assign to the amino C_6F_5 ring. No ^{31}P resonance is observed, as would be expected if the phosphine is bound directly to the paramagnetic center. A band at 3346 cm^{-1} is observed in the IR spectrum, assigned as an N-H stretch. The ^1H NMR spectrum shows two large, broad peaks at 1.63 and 1.38 ppm for the $HNEt_3^+$ cation, and eight resonances for the ligand backbone protons, in two groups of four (presumably each group comes from one ethylene backbone unit). The chemical shifts of the first group are 15.7, 13.2, 10.7, and 8.8 ppm, and those for the second are -7.05, -20.68, -23.8, and -38.35 ppm. These high-field peaks are in the range normally observed for $[N_3N]$ and $[N_3N_F]MoX$ complexes;[12,27] therefore, we cautiously assign them to the ethylene unit bonded to the amide, and the other, less-shifted set to the amino ethylene unit. Based on the fact that the ^1H and ^{19}F resonances assigned to the amino ethylene unit are not significantly shifted, we feel that the most likely structure is that shown in equation 7, with an

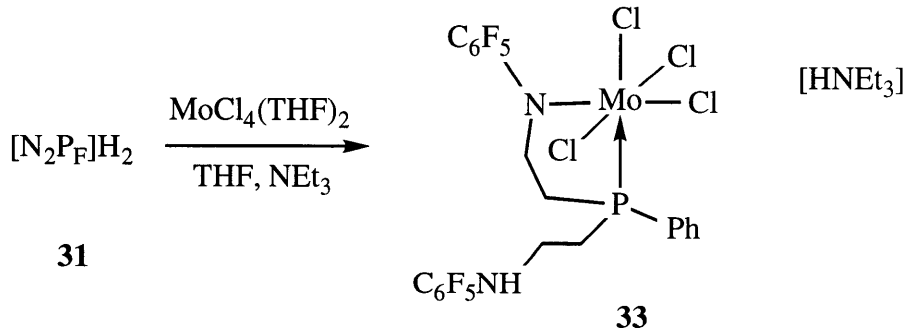

(7)

octahedral geometry and the amine ligand dissociated. In C_s symmetry, the z-axis is conventionally perpendicular to the mirror plane. Thus, the two d electrons in **33** reside in the d_{xy} and d_{yz} orbitals, which are *not* rigorously degenerate (cf. d_{xz}/d_{yz} in C_{3v} symmetry, which are). However, the energy difference between them in this case is evidently so small that the complex remains paramagnetic. $RuCl_2(PPh_3)_3$ reacts with $[N_2P_F]H_2$ in the presence of triethylamine to give a diamagnetic complex. NMR data are consistent with a structure similar to

References begin on page 221.

that proposed for **33**, but we have not yet obtained the ruthenium complex in pure enough form to verify its composition by elemental analysis.

DISCUSSION

We became interested in preparing a chelating triamido ligand without any protons β to the amides after the observation that a 16 electron tantalum ethylene complex containing the $[N_3N]^{3-}$ ligand rearranges via what is formally an abstraction of one of the triamidoamine ligand β-protons to give a triamido-monoamido product.[3,28] Presumably, replacement of all six β-protons in a triamidoamine complex by methyl groups would result in a ligand framework less susceptible to such decomposition reactions. However, we found that hexamethyltriamido ligands were difficult to prepare, the only success being the low-yield synthesis of $[(C_6F_5NCMe_2CH_2)_3P]H_3$ (abbreviated as $^*[N_3P_F]H_3$ (**3**)) from $LiPH_2(DME)$ and *n*-Ts-2,2-dimethylaziridine. Attempts to prepare transition metal complexes containing **3** were seriously limited by the fact that the ligand is to date only available in milligram quantities.

Another continual goal in our laboratories has been the preparation of a chelating, triamido *phosphine* ligand in order to investigate the effect of changing the dative donor from nitrogen to phosphorus. The successful preparation of $[(TMSNCH_2CH_2)_2PPh]^{2-}$ ($[N_2P]^{2-}$) has allowed us to initiate studies with some phosphine-containing diamido ligands. 10-12 gram quantities of $[N_2P]H_2$ are available in three steps from phenylphosphine (~60% overall yield). This has allowed for the synthesis of a class of zirconium(IV) complexes containing the $[N_2P]^{2-}$ ligand. The coordination environment in $[N_2P]ZrX_2$ complexes is unique in several ways. The phosphine ligand's high barrier to inversion (relative to nitrogen or oxygen) through a planar phosphorus intermediate imparts stereochemical rigidity to the complexes, thus complexes such as $[N_2P]Zr(NMe_2)_2$ and $[N_2P]Zr(Me)_2$ have inequivalent axial and equatorial X ligands on the NMR time scale at room temperature (c.f. $[(t\text{-Bu-}o\text{-}C_6H_4)_2O]ZrX_2$,[11] where such inversion is fast on the NMR time scale). We note that even if the phosphine ligand in an $[N_2P]$ complex dissociates from the metal, interconversion of axial and equatorial X ligands would still be slow

References begin on page 221.

due to the fact that a planar phosphine is a high-energy species. This chemical inequivalence of axial and equatorial ligands stands in contrast to ubiquitous Cp_2ZrX_2 species, where the X ligands are related by a mirror plane.

The presence of the phosphine donor in $[N_2P]^{2-}$ complexes provides a valuable NMR handle, both for monitoring reactions by ^{31}P NMR, and in making stereochemical assignments of axial and equatorial ligands based on $^2J_{CP}$ and $^3J_{HP}$ values. For $[N_2P]Zr$ dialkyls, one of the alkyls usually has a $^2J_{CP}$ value of ~25 Hz, and the other is much lower, ≤ 5 Hz. Trans couplings through a transition metal center are generally observed to be greater than the corresponding cis couplings,[29] and we propose that the complexes in this chapter are no exception. For one complex, $[N_2P]Zr$(*trans*-Me)(*cis*-Bn), we were able to verify the stereochemistry predicted by $^2J_{CP}$ coupling constants by X-ray crystallography. Interestingly, $^3J_{PH}$ values for cis alkyls are observed to be ~6 Hz, and those for trans are ≤ 2 Hz (for mixed alkyl and alkyl-chloride complexes where such a distinction can be made).

The X-ray structure of **24** displays a long Zr-P distance (2.9343(11) Å). At least for the zirconium complex studied, it appears that changing the dative donor from N to P results in a relatively weak interaction, possibly because Zr prefers harder donors such as N or O. The structure of $[N_2P][NP]Mo$, however, shows a molybdenum-phosphine distance of 2.525(3) Å, indicative of a more tightly-bound phosphine ligand. It appears that $[N_2P]$ ligands may be more appropriate for the synthesis of complexes of later transition metals. However, it has generally been found that TMS-substituted multiamidoamine complexes of metals such as Mo and W have been difficult to prepare, presumably because of the propensity for Si-N bond cleavage during the reactions. This problem has been resolved for molybdenum and tungsten complexes by replacing the TMS amide substituents with C_6F_5 rings.[12] $[N_2P_F]H_2$ would thus seem to be a good choice for the synthesis of complexes of later transition metals, and the preliminary experiments carried out indicate that this is the case for metals such as molybdenum and ruthenium.

References begin on page 221.

Considering the recent interest in using diamido ligands as Ziegler-Natta catalysts (both with a dative amine donor[8] and with no dative donor[9,30]) and the development of a living system for the polymerization of 1-hexene with a catalyst containing a dative oxygen,[11] we attempted to generate several cationic zirconium alkyl complexes. Species proposed to be [[N_2P]ZrMe][$B(C_6F_5)_4$] (**27**) and [[N_2P]ZrBn][$B(C_6F_5)_4$] (**28**) were observed spectroscopically at -30 °C, but decomposed upon warming to room temperature. Given the observed thermal instability, it is perhaps not surprising that both species are poor 1-hexene polymerization catalysts at 0 °C. However, both do generate a white insoluble solid, presumably polyethylene, at activities one or two orders of magnitude lower than those observed in typical zirconocene/MAO or zirconocene/$MeB(C_6F_5)_3$ systems.[31] The thermal instability of **27** and **28** might stem from the relatively labile Si-N linkage, decomposition via cleavage of this functionality is now a well-documented transformation in complexes containing the $[(TMSNCH_2CH_2)_3N]^{3-}$ ligand.[2,3,32] Another possible decomposition pathway is via rupture of the P-(CH_2CH_2NTMS) linkage, as observed during the synthesis of [N_2P][NP]Mo (**30**). Coordination of the phosphine to a cationic zirconium center would be expected to activate the P-C bond towards this type of reaction. Based on the data obtained so far, it seems that diamidophosphine ligands are inferior to diamido-ether ligands in terms of stabilizing a zirconium cation. The phosphine may also provide too much electron density to the metal, resulting in a poor catalyst. We feel that the results with the $[N_2P_F]H_2$ ligand are more promising in terms of creating a new framework upon which to build middle transition metal complexes.

EXPERIMENTAL

General Details. All experiments were conducted under nitrogen in a Vacuum Atmospheres drybox, using standard Schlenk techniques, or on a high vacuum line ($< 10^{-4}$ torr). Pentane was washed with HNO_3/H_2SO_4 (5/95 v/v), sodium bicarbonate, H_2O, stored over $CaCl_2$ and then distilled from sodium benzophenone under nitrogen. Regent grade benzene was

References begin on page 221.

distilled from sodium benzophenone under nitrogen. Toluene was distilled from molten sodium. Methylene chloride was distilled from CaH_2. Reagent grade ether and THF were sparged with nitrogen and passed through alumina columns.[33] Aldrich anhydrous grade DME was sparged with argon and brought in the drybox. All solvents were stored in the drybox over activated 4 Å molecular sieves. Deuterated solvents were freeze-pump-thaw degassed and vacuum transferred from an appropriate drying agent, or sparged with argon and stored over 4 Å sieves. NMR spectra are recorded in C_6D_6 unless noted otherwise. ^1H and ^{13}C data are listed in parts per million downfield from tetramethylsilane and were referenced using the residual protonated solvent peak. ^2H NMR spectra usually were obtained at 46.0 MHz and are referenced externally to C_6D_6 (7.15 ppm) in C_6H_6. Unless otherwise noted, NMR experiments were run in C_6D_6 solution and ^{13}C and ^{31}P spectra were proton-decoupled. Probe temperatures during variable temperature studies were calibrated with methanol (low T) or ethylene glycol (high T). Coupling constants are given in hertz, and routine couplings are not listed. Elemental analyses (C, H, N) were performed on a Perkin-Elmer 2400 CHN analyzer in our own laboratory. Column chromatography was performed by the method of Still.[34]

$LiPH_2$(dme) was prepared as described in the literature.[35] All precautions detailed in the procedure regarding handing PH_3 (*g*) should be followed and the experimental carried out exactly as stated, including the use of a mercury safety valve and a special gas inlet. We found it more convenient to destroy excess PH_3 by entraining it in a stream of argon and bubbling through aqueous $CuSO_4$ rather than by burning. PH_3 (*g*) is a toxic and pyrophoric species, thus all operations should be carried out in an efficient fume hood under rigorously anaerobic conditions. 2,2-Dimethylaziridine was prepared by a modification (given below) of the literature procedure.[36] It was converted to the *n*-tosyl derivative as previously described.[37] $Zr(NMe_2)_4$ was prepared by a literature procedure.[38] DMSO was stored over activated molecular sieves before use. $^{13}CH_3MgI$ was prepared from $^{13}CH_3I$ (Cambridge Isotopes) and magnesium in ether. Grignard reagents were titrated with *n*-propanol using 1,10-phenathroline as an indicator

References begin on page 221.

before use. Me_2Mg was a gift from Dr. Timothy Warren. $MoCl_4(THF)_2$[37] and $Mo(NMe_2)_4$[39] were prepared by literature procedures.

Modified preparation of 2,2-dimethylaziridine. A solution of 2-amino-2-methyl-propanol (100 g, 1.12 mol) in 200 mL water had a solution of 60 mL conc. H_2SO_4 in 200 mL water added. The reaction was heated under argon and the water distilled away until the reaction temperature reached 115 °C. The distillation was then continued, now under aspirator pressure, and the reaction temperature slowly increased to 210 °C, at which point the material thickened and began to darken. It was then cooled to room temperature and the reaction flask broken with a hammer to remove the solid mass of product. This was broken up with a screwdriver and ground to a coarse powder in a mortar and pestle. 200 mL of 40% aqueous NaOH was added to the powder and the dark slurry which formed was distilled. The first 125 mL of aziridine/water azeotrope was collected, bp 78-100 °C. KOH was added to this distillate to remove the water and the aziridine was then dried over KOH followed by sodium. The dry aziridine was now distilled from sodium, bp 72-73 °C, 48.6 g obtained (61%): ^{1}H NMR ($CDCl_3$) δ 1.53 (s, 2, CH_2), 1.21 (s, 6, Me_2), 0.50 (s, 1, N*H*).

$P(CH_2CMe_2NH_2)_3$ (2). To a stirred solution of $LiPH_2$(dme) (7.50 g, 40.3 mmol) in 125 mL THF was added a solution of *n*-tosyl-2,2-dimethylaziridine (9.08 g, 40.3 mmol) in 125 mL THF dropwise. After the addition was complete, the reaction was stirred at room temperature for 2 h, at which point ^{31}P NMR showed that the primary phosphine was present. The reaction was cooled to -40 °C and BuLi (2.5 M, 32.2 mL, 80.5 mmol) was added via syringe. After warming and stirring at room temperature for 10 min, it was recooled to -40 °C and *n*-tosyl-2,2-dimethylaziridine (18.2 g, 80.6 mmol) was added as a solid in portions. The reaction mixture was allowed to stand overnight, the volume reduced to ~125 mL, and the reaction was quenched with water (2.2 mL, 3.1 equiv.). The rest of the THF was removed by rotary evaporation to yield proposed tosylamide **1** as a light yellow solid.

References begin on page 221.

A 500 mL round bottomed flask was charged with naphthalene (20.7 g, 161 mmol), sodium spheres (12.0 g, 524 mmol), and 250 mL DME. The tosylamide was slowly added in 70 mL DME and the reaction stirred overnight. Water (10 mL, 352 mmol) was added slowly via syringe and the solvents were removed under reduced pressure. The residue was extracted with ~300 mL pentane/toluene (50/50 v/v) and filtered. The insolubles were rinsed carefully with pentane. The filtrate was stripped on the rotary evaporator and the yellow oil left behind was distilled using a flame heat source. Naphthalene was removed as the first fraction. A 15 cm vigereux column was introduced to the distillation apparatus and the product distilled over, bp 105-140 °C (0.065 torr). It was obtained as an air-stable colorless oil. The oil was dissolved in 20 mL pentane and cooled to -40 °C overnight to give the product as white crystals which melt around room temperature, 3.7 g (37%): ^{1}H NMR (C_6D_6): δ 1.52 (d, $^2J_{PH}$ = 4.0 Hz, 6, CH_2), 1.13 (s, 18, $C(CH_3)_2$), 0.99 (br s, 6, NH_2). ^{31}P NMR (C_6D_6): δ -58.0. ^{13}C NMR (C_6D_6): δ 50.3 (d, $^1J_{PC}$ = 13.8 Hz), 48.3 (d, $^2J_{PC}$ = 13.2 Hz), 32.4 (d, $^3J_{PC}$ = 7.8 Hz). IR (neat, salt plates): cm^{-1} 3336, 3264 (NH_2 stretch), 1596 (NH_2 bend), 884 (br s, NH wag).

$P(CH_2CMe_2NHC_6F_5)_3$ (3). A solution of **2** (648 mg, 2.62 mmol) was prepared in 20 mL THF. It was cooled to -40 °C and BuLi (2.5 M, 2.10 mL, 2 equiv.) was added via syringe. The reaction was stirred for 2 h, cooled to -40° C, and C_6F_6 (302 μL, 2.62 mmol, 1 equiv.) was added via syringe. ^{19}F NMR at this point showed no C_6F_6. The reaction was re-cooled, two more equivalents BuLi added, and stirred 45 minutes. It was then cooled again and one equivalent C_6F_6 added. After stirring 1.5 hr, it was re-cooled and 2 equivalents BuLi added. After stirring for 45 minutes, one final equivalent C_6F_6 was added slowly at room temperature. The reaction was then stirred overnight and then quenched at 0 °C with water (189 μL, 4 equiv.). After stirring 15 minutes, the solvents were removed *in vacuo*. The residue was partitioned between 50 mL CH_2Cl_2/H_2O, washed with brine, and dried over Na_2SO_4. The methylene chloride was removed on the rotovap and the residue subjected to flash chromatography on Al_2O_3 using 40% CH_2Cl_2/hexane as the eluant. The product came off with the solvent front in the first few fractions along with a brown impurity. It was then recrystallized from minimum

References begin on page 221.

pentane and isolated as off-white crystals, yield 416 mg (21%). ^{1}H NMR (C_6D_6): δ 3.12 (br s, 3, NH), 1.70 (d, $^2J_{PH}$ = 3 Hz, 6), 1.08 (s, 18, C(CH_3)$_2$). ^{31}P NMR (C_6D_6): δ -54.6. ^{13}C NMR (C_6D_6): δ 144.4, 141.2, 139.9, 138.2, 136.6, 135.4, 121.0 (C_6F_5), 57.6 (d, $^1J_{PC}$ = 14 Hz), 45.6 (d, $^2J_{PC}$ = 13 Hz), 28.7 (d, $^3J_{PC}$ = 9 Hz). ^{19}F NMR (C_6D_6): -149.7 (d, F_{ortho}, 6), -163.5 (t, F_{para}, 3), -164.0 (t, F_{meta}, 6). IR (Nujol mull): 3343, 3309, 1514, 1002, 972. FABMS (m/e) = 746 (M + 1).

***n*-C_6F_5-2,2-dimethylaziridine (5).** 2,2-Dimethylaziridine (1.00 g, 14.1 mmol), hexafluorobenzene (3.40 g, 18.3 mmol), potassium carbonate (2.33 g, 16.9 mmol), and 16 mL DMSO were added to a round bottomed flask. The reaction was heated for 2 days at 120 °C, at which point ^{19}F NMR showed the C_6F_6 had been consumed. It was cooled to room temperature, poured onto 100 mL water and extracted with 30 mL $CHCl_3$. The chloroform was then washed twice with water and once with brine to remove all the DMSO. It was dried over Na_2SO_4 and the chloroform removed *in vacuo* to yield a brown liquid. This was distilled under aspirator pressure to give a clear, colorless liquid, bp 80 °C, 400 mg (12%, not optimized): ^{1}H NMR ($CDCl_3$) δ 2.32 (s, 2, CH_2), 1.30 (s, 6, Me_2). ^{19}F NMR ($CDCl_3$) δ -155 (br s, 2, F_{ortho}), -164.2 (br s, 2, F_{meta}), -166.6 (t, 3, F_{para}). ^{13}C NMR ($CDCl_3$) δ 143.2, 139.9, 137.5, 136.6, 134.2, 126.2 (m, C_6F_5), 42.2 (CH_2), 41.4 (CMe_2), 22.3 (CMe_2).

$H_2NCH_2CMe_2NHTs$ (7). A 200 mL Fisher porter bottle was charged with *n*-tosyl-2,2-dimethylaziridine (3.45 g, 15.3 mmol) dissolved in 15 mL THF. 65 mL ethanol were then added and the bottle sealed and pressurized with ammonia (22 psi). The volume of the solution increased to 100 mL over the course of an hour due to absorbed NH_3 and the mixture was stirred under NH_3 pressure for 17 more hours behind a blast shield. The pressure was then released, the ammonia sparged out, and the ethanol removed *in vacuo*. The oil which resulted crystallized after being under vacuum for ~1 hr. This solid was recrystallized by dissolving in minimum hot toluene, hot filtering off insoluble impurities, and adding hexane to the point of precipitation while hot. Upon slow cooling to room temperature, 2.86 g of white crystalline product was obtained (77%): ^{1}H NMR ($CDCl_3$) δ 7.77 (d, 2, TsH_{ortho}), 7.26 (d, 2, TsH_{meta}), 2.56 (s, 2,

References begin on page 221.

CH_2), 2.40 (s, 3, Ts-CH_3), 1.11 (s, 6, CMe_2), 1.08 (s, 1, N*H*-Ts). ^{13}C NMR ($CDCl_3$) δ 142.9 (Ts-C_{ipso}), 140.8 (Ts-C_{para}), 129.6 (Ts-C_{ortho}), 127.1 (Ts-C_{meta}), 57.0 (CMe_2), 52.6 (CH_2), 25.3 (CMe_2), 21.6 (Ts-CH_3). IR ($CDCl_3$) cm^{-1} 3288 (br w), 3155 w, 2254, 1470, 1385, 1320. Anal Calc. for $C_{11}H_{18}N_2O_2S$. Calc.: C, 54.52; H, 7.49; N, 11.56. Found: C, 54.81; H, 7.45; N, 11.37.

$HN(CH_2CMe_2NHTs)_2$ (8). A vial was charged with $H_2NCH_2CMe_2NHTs$ (0.75 g, 3.1 mmol) and *n*-Ts-2,2-dimethylaziridine (1.39 g, 6.19 mmol). DMSO (1.5 mL) was added and the reaction stirred at room temperature for 2 days. TLC (35% EtOAc/hexanes) showed no $H_2NCH_2CMe_2NHTs$ was remaining. The reaction was worked up by pouring onto 100 mL water and extracting with 60 mL ether. The extract was washed twice with water, once with brine, and dried over sodium sulfate. The volatiles were removed *in vacuo* and the residue purified by flash chromatography on silica (35% EtOAc/hexanes eluant). 0.63 g (44%) of the desired product was obtained. The less mobile $HN(CH_2CMe_2NHTs)(CMe_2CH_2NHTs)$ regioisomer could be obtained by continued elution (0.18 g). Characterization data for $HN(CH_2CMe_2NHTs)_2$: ^1H NMR ($CDCl_3$) δ 7.78 (d, 4, Ts), 7.28 (d, 4, Ts), 5.75 (br s, NH), 2.67 (s, 2, CH_2), 2.40 (s, 6, TsCH_3), 1.17 (s, 12, CMe_2). FABMS (m/e) = 468 (M + 1).

$ClCH_2CH_2$(cyclo-$NSiMe_2CH_2CH_2SiMe_2$) (9). A 1 L flask was charged with $ClCH_2CH_2NH_2 \cdot HCl$ (32.3 g, 0.278 mol), triethylamine (128 mL, 0.835 mol, 3.3 equiv.), and 600 mL CH_2Cl_2 (dry solvent is unnecessary). A solution of $ClMe_2SiCH_2CH_2SiMe_2Cl$ in 200 mL CH_2Cl_2 was prepared in the drybox. It was added slowly via dropping funnel to the well-stirred $ClCH_2CH_2NH_2 \cdot HCl$ slurry over one hour, giving a mild exotherm. The reaction was stirred overnight and the voluminous $NEt_3 \cdot HCl$ precipitate was filtered off. The CH_2Cl_2 solution was evaporated and the residue extracted with hexanes. The $NEt_3 \cdot HCl$ was also thoroughly extracted with hexanes and the combined extracts evaporated. Vacuum distillation of the liquid remaining gave the product as a colorless liquid which clouded slightly upon standing, bp. 45 °C (100 mtorr), 45.3 g (73%). ^1H NMR δ 3.18 (m, 2, CH_2), 3.00 (m, 2, CH_2), 0.665 (s, 4,

References begin on page 221.

$SiCH_2CH_2Si$), 0.040 (s, 12, Me_2Si). ^{13}C NMR δ 45.6 (CH_2), 45.1 (CH_2), 8.12 ($SiCH_2CH_2Si$), -0.158 (Me_2Si).

$PhP(CH_2CH_2(cyclo\text{-}NSiMe_2CH_2CH_2SiMe_2))_2$ (10). In the drybox, a 500 mL Schlenk flask was charged with 300 mL THF, $ClCH_2CH_2(cyclo\text{-}NSiMe_2CH_2CH_2SiMe_2)$ (50.0 g, 0.225 mol), and a stir bar. It was fitted with a septum and brought out to the Schlenk line. Phenylphosphine (12.4 mL, 0.113 mol) was introduced via syringe. The flask was cooled to -10 °C (ice/acetone bath) and fitted with an addition funnel containing 2.5 M BuLi in hexanes (90.1 mL, 0.225 mol). The butyllithium solution was added dropwise in over 1.5 h. After the addition was complete, the reaction was warmed to room temperature and stirred overnight. ^{31}P NMR clean conversion to product, which is air-stable enough to allow for workup under air. The volatiles were removed by rotary evaporation and the heterogeneous residue extracted with hexanes (200 mL). This solution was filtered through a bed of Celite and the volatiles removed under reduced pressure, leaving the product as a light yellow oil, 54.3 g, 100%. ^1H NMR δ 7.50 (t, 2, Ph), 7.36 (d, 3, Ph), 2.81 (m, 4, CH_2), 1.80 (m, 4, CH_2), 0.655 (s, 8, $SiCH_2CH_2Si$), -0.0153 (s, 24, $SiMe_2$). ^{13}C NMR δ 139.1 (d, Ph_{ipso}), 132.7 (d, Ph_{meta}), 129.1 (Ph_{para}), 128.7 (d, Ph_{ortho}), 39.8 (d, $^1J_{CP}$ = 24 Hz, NCH_2CH_2P), 34.6 (d, $^2J_{CP}$ = 15 Hz, NCH_2CH_2P), 8.37 ($SiCH_2CH_2Si$), 0.19 ($Si(CH_3)_2$). ^{31}P NMR (THF) -33.2 (s).

$PhP(CH_2CH_2NH_2)_2 \cdot 2HCl$ (11). Under air, a 500 mL round-bottomed flask was charged with $PhP(CH_2CH_2(cyclo\text{-}NSiMe_2CH_2CH_2SiMe_2))_2$ (54.3 g, 0.113 mol) and 350 mL ether. It was cooled on an ice bath. A dilute solution of HCl was prepared by adding 12 M HCl (24 mL, 0.29 mol, 2.5 equiv.) to 75 mL water. This was added to the ethereal solution over 5 min and the reaction was stirred overnight. The layers were separated and the aqueous extract washed with ether (2 x 100 mL). The water was removed by rotary evaporation with a bath temperature of 60 °C to leave the crude product as an off-white oily mass. Ethanol (800 mL, sparged with argon) was added and the mixture heated under argon in an 80 °C oil bath for 20 min with good stirring. White microcrystals formed which were isolated on a Büchner funnel. A second crop was obtained by reducing the volume of the mother liquor to ~250 mL, resulting

References begin on page 221.

in oiling out of more product. Heating this mixture as before led to formation of a second crop of microcrystals which were filtered off. The product was dried at 50 °C *in vacuo* to remove the last traces of EtOH, 19.9 g (65%). ^{1}H NMR (DMSO-d_6) δ 8.22 (6, NH_3^+), 7.55 (2, Ph), 7.41 (3, Ph), 2.78 (br m, 4, NCH_2P), 2.10 (t, 4, NCH_2P). ^{31}P NMR (DMSO-d_6) δ -29.6.

$PhP(CH_2CH_2NHTMS)_2$ (12). In the drybox, a 500 mL round-bottomed flask was charged with $PhP(CH_2CH_2NH_2)_2 \cdot 2HCl$ (10.0 g, 37.2 mmol) and 300 mL THF. The slurry was cooled to -40 °C and BuLi (2.5 M in hexanes, 59.4 mL, 149 mmol) was slowly added via syringe. The reaction was re-cooled several times during the addition. Once all the BuLi was added the mixture was stirred at room temperature for 2.5 h. It was again cooled to -40 °C and TMSCl (9.9 mL, 78.0 mmol) was added via syringe. After stirring at 22 °C for 3 h, the volatiles were removed *in vacuo* and the oily residue extracted with 180 mL pentane. Filtration through a bed of Celite and removal of the pentane under reduced pressure left the product as a brown oil in quantitative yield, 12.6 g. ^{1}H NMR δ 7.58 (t, 2, Ph), 7.12 (m, 3, Ph), 2.82 (m, 4, NCH_2P), 1.79 (m, 4, NCH_2P), 0.3 (br s, 2, NH), 0.01 (s, 18, $Si(CH_3)_3$). ^{31}P NMR δ -35.7 (s). ^{13}C NMR δ 139.0 (d, Ph_{ipso}), 132.7 (d, Ph_{meta}), 129.0 (d, Ph_{para}), 128.8 (d, Ph_{ortho}), 39.7 (d, $^1J_{CP}$ = 24 Hz, NCH_2CH_2P), 34.6 (d, $^2J_{CP}$ = 15 Hz), 8.37 ($SiCH_2CH_2Si$), 0.191 ($Si(CH_3)_2$).

$PhP(CH_2CH_2NLiTMS)_2$ (13). A 100 mL round-bottom was charged with $PhP(CH_2CH_2NHTMS)_2$ (4.00 g, 11.7 mmol) and 70 mL pentane. It was cooled to -40 °C and BuLi (2.5 M in hexanes, 9.4 mL, 24 mmol) was added. The reaction was stirred at 22 °C for 50 min and the volume reduced to ~30 mL. Cooling to -40 °C with seeding led to crystallization of the product. It was filtered off and rinsed quickly with cold pentane. A second crop was obtained similarly for a combined yield of 2.54 g (62%). ^{1}H NMR (THF-d_8) δ 7.45 (t, 2, Ph), 7.24 (m, 3, Ph), 3.23 (m, 4, NCH_2P), 1.91 (m, 4, NCH_2P), -0.068 (s, 18, $Si(CH_3)_3$). ^{31}P NMR (THF-d_8) δ -29.2. ^{13}C NMR δ 143.6, 132.1, 128.8, 128.1 (Ph), 46.2 (d, $^1J_{CP}$ = 16 Hz, NCH_2CH_2P), 36.4 (NCH_2CH_2P), 2.11 ($Si(CH_3)_3$). Several attempts to obtain satisfactory analytical data for this dilithium salt have failed.

References begin on page 221.

$PhP(CH_2CH_2NH(SiPhMe_2)_2$ (14). This ligand was prepared by the same procedure used for $PhP(CH_2CH_2NHTMS)_2$; using $PhP(CH_2CH_2NH_2)_2 \cdot 2HCl$ (1.50 g, 5.57 mmol), 70 mL THF, 2.5 M BuLi in hexanes (8.92 mL, 22.3 mmol), and $PhMe_2SiCl$ (1.87 mL, 11.2 mmol). The product was obtained as an oil, 2.51 g (97%). ^1H NMR δ 7.56, 7.44, 7.24, 7.11 (m, Ph), 2.82 (m, 4, NCH_2P), 1.66 (m, 4, NCH_2P), 0.585 (br t, 2, NH), 0.225 (s, 12, $Si(CH_3)_2$).

$[N_2P]ZrCl_2$ (16). $[N_2P]H_2$ (2.00 g, 5.87 mmol) was dissolved in 60 mL pentane. The solution was cooled to -40 °C and $Zr(NMe_2)_4$ (1.57 g, 5.87 mmol) was added as a solid. The reaction was stirred overnight, filtered to remove a small amount of precipitate, and the volatiles then removed under reduced pressure. $[N_2P]Zr(NMe_2)_2$ was left as an oil. ^1H NMR δ 7.35 (tt, 2, Ph), 7.02 (d, 3, Ph), 3.5 (m, 2, NCH_2P), 3.2 (m, 2, NCH_2P), 3.13 (s, 6, NMe_2), 3.05 (s, 6, NMe_2), 1.99 (m, 2, NCH_2P), 1.68 (m, 2, NCH_2P), 0.30 (s, 18, $SiMe_3$). ^{31}P NMR δ -10.5 (s). The bis(dimethylamido) compound was dissolved in 40 mL pentane and TMSCl (1.49 mL, 11.7 mmol) was added by syringe. The reaction was stirred vigorously for 10 min and then allowed to stand for two hours. The off-white crystalline solid which formed was isolated on a frit and dried *in vacuo*, 2.36 g (80%). No further purification was necessary, although the complex may be recrystallized from toluene/pentane mixtures. ^1H NMR δ 7.63 (t, 2, Ph), 7.13 (m, 3, Ph), 2.94 (br m, 2, NCH_2P), 2.73 (m, 2, NCH_2P), 1.91 (m, 4, NCH_2P), 0.37 (s, 18, $SiMe_3$). ^{31}P NMR δ 1.94 (s). ^{13}C NMR δ 133.0, 130.1, 129.0, 125.6 (Ph), 50.0 (d, J_{PC} = 15 Hz, NCH_2P), 38.3 (d, J_{CP} = 20 Hz, NCH_2P), 1.30 ($Si(CH_3)_3$). Anal. Calc. for $C_{16}H_{31}N_2PSi_2ZrCl_2$: C, 38.38; H, 6.24; N, 5.59. Found: C, 38.53; H, 6.20; N, 5.52.

$[PhN_2P]ZrCl_2$ (18). The complex was prepared by the same method used for $[PhN_2P]ZrCl_2$; starting from $[PhN_2P]H_2$ (1.00 g, 2.15 mmol), $Zr(NMe_2)_4$ (576 mg, 2.15 mmol), and 40 mL pentane. $[PhN_2P]Zr(NMe_2)_2$ was obtained as an oil. ^1H NMR δ 7.74 (d, Ph), 7.23 (m, Ph), 7.03 (m, Ph), 3.5 (m, 2, NCH_2P), 3.19 (s, 6, NMe_2), 3.06 (s, 6, NMe_2), 1.78 (br t, 2, NCH_2P), 1.60 (m, 2, NCH_2P), 0.57 (s, 6, $SiMe_2$), 0.54 (s, 6, $SiMe_2$). ^{31}P NMR δ -10.2 (s). The bis(dimethylamido) compound was dissolved in 20 mL pentane and TMSCl (546 μL, 4.30 mmol) added by syringe. After 15 min of stirring, the reaction was allowed to stand overnight.

References begin on page 221.

The off-white microcrystalline product was isolated on a frit, washed with cold pentane, and dried *in vacuo*, 1.08 g (80%). No further purification was necessary. ^{1}H NMR δ 7.7 (d, Ph), 7.3 (t, Ph), 7.15 (m, Ph), 7.0 (m, Ph), 3.5 (br m, 4, NCH_2P), 1.6 (br m, 4, NCH_2P), 0.87 (s, 6, $SiMe_2$), 0.74 (s, 6, $SiMe_2$). Anal. Calc. for $C_{26}H_{35}N_2PSi_2ZrCl_2$: C, 49.98; H, 5.65; N, 4.48. Found: C, 50.11; H, 5.31; N, 4.49.

$[N_2P]Zr(CH_3)_2$ (19). $[N_2P]ZrCl_2$ (260 mg, 0.519 mmol) was dissolved in 15 mL ether. The solution was cooled to -40 °C and MeMgCl (3.0 M in THF, 346 μL, 1.04 mmol) was added by syringe. The reaction was stirred for 45 min at room temperature and then the volatiles were removed under reduced pressure. The residue was extracted with 12 mL pentane for 1 h, filtered, and the volatiles removed. The product was left as an oil, 220 mg (92%). The complex could not be crystallized and therefore was not purified further. ^{1}H NMR δ 7.3 (m, 2, Ph), 7.0 (m, 3, Ph), 3.4 (m, 2, NCH_2P), 3.1 (m, 2, NCH_2P), 1.8 (m, 2, NCH_2P), 1.62 (m, 2, NCH_2P), 0.80 (d, $^2J_{HP}$ = 6 Hz, 3, *cis*-Me), 0.60 (s, 3, *trans*-Me). ^{13}C NMR of $[N_2P]Zr(^{13}CH_3)_2$ (ether) δ 35.9 ($^2J_{CP}$ = 29 Hz, $^1J_{CH}$ = 113 Hz), 40.9 ($^2J_{CP}$ = 2 Hz, $^1J_{CH}$ = 114 Hz). ^{31}P NMR δ -15.7 (s). The $[N_2P]Zr(^{13}CH_3)_2$ complex was prepared similarly.

$[PhP(CH_2CH_2N(SiPhMe_2)_2]Zr(CH_3)_2$ (20). $[PhP(CH_2CH_2N(SiPhMe_2)_2]ZrCl_2$ (150 mg, 0.240 mmol) was dissolved in 10 mL ether and the solution cooled to -40 °C. MeMgCl (3.0 M in THF, 160 μL, 0.480 mmol) was added by syringe. A white precipitate formed and after 2 h, ^{31}P NMR showed the alkylation was complete. Dioxane (45 μL, 0.53 mmol, 2.2 equiv.) was added and the resultant precipitate allowed to settle for ~15 min. The reaction was filtered through a short plug of Celite and the ether removed *in vacuo*. The product was left as a thick oil, 138 mg (99%). The $^{13}CH_3$ complex was prepared similarly from $^{13}CH_3MgI$. ^{1}H NMR δ 7.73 (m, Ph), 7.18 (m, Ph), 7.0 (m, Ph), 3.41 (m, 2, NCH_2P), 3.04 (m, 2, NCH_2P), 1.52 (m, 4, NCH_2P), 0.86 (d, $^2J_{PH}$ = 4.5 Hz, 3, *cis*-Me), 0.75 (s, 12, $SiMe_2$), 0.67 (s, 3, *trans*-Me). ^{31}P NMR δ -15.9 (s).

$[N_2P]Zr(CH_3)(THF)Cl$ (21). $[N_2P]ZrCl_2$ (300 mg, 0.599 mmol) was dissolved in 20 mL ether and the solution cooled to -40 °C in the drybox freezer. MeMgCl (3.0 M in THF, 100

References begin on page 221.

μL, 0.300 mmol) was added via syringe over 4 min. The solution was placed back in the freezer for 15 min and then another portion of MeMgCl (100 μL, 0.300 mmol) was added. After stirring at room temperature for 30 min, the volatiles were removed under reduced pressure. The reside was extracted with 40 mL pentane for 2 h. The extract was filtered through Celite and the volatiles removed. Recrystallization from pentane at -40 °C gave the product as white crystals, 140 mg (42%). ^{1}H NMR δ 7.32 (m, 2, Ph), 7.02 (m, 3, Ph), 3.64 (m, 4, THF), 3.2 (m, 4, NCH_2P), 1.8 (m, 4, NCH_2P), 1.33 (m, 4, THF), 0.84 (d, $^2J_{PH}$ = 7 Hz, 3, Me), 0.42 (s, 18, $SiMe_3$). ^{31}P NMR δ -0.49 (s). Anal. Calc. for $C_{21}H_{42}N_2PSi_2ClOZr$: C, 45.66; H, 7.66; N, 5.07. Found: C, 45.54; H, 7.85; N, 5.02.

[N_2P]Zr(CH_3)Cl (22). [N_2P]$ZrCl_2$ (350 mg, 0.699 mmol) was dissolved in 20 mL ether and the solution cooled to -40 °C. Me_2Mg (0.82 M in ether, 426 μL, 0.350 mmol) was added by syringe and the reaction stirred for 1 h at room temperature. The ether was removed *in vacuo* and the residue extracted with 40 mL pentane. The extract was filtered through Celite and the volume reduced to ~20 mL. Storage at -40 °C for 15 h resulted in precipitation of the product, 223 mg in two crops (66%). ^{1}H NMR δ 7.3 (m, 2, Ph), 6.95 (m, 3, Ph), 3.25 (m, 4, NCH_2P), 1.8 (m, 4, NCH_2P), 0.9 (s, 3, CH_3), 0.40 (s, 18, $SiMe_3$). ^{31}P NMR δ -1.6 (s). Several attempts to obtain analytical data for the complex have failed.

[$PhP(CH_2CH_2NTMS)_2$]Zr(*i*-Bu)Cl (23). [N_2P]$ZrCl_2$ (200 mg, 0.399 mmol) was dissolved in 15 mL ether and the solution cooled to -40 °C. *i*-BuMgCl (2.16 M in ether, 185 μL, 0.399 mmol) was added by syringe and the reaction was stirred at room temperature for 2 h. Dioxane (41 μL, 0.479 mmol) was added and the precipitate allowed to settle for 30 min. The mixture was filtered through a short plug of Celite and the volatiles removed *in vacuo*. Recrystallization from ~1 mL ether layered with pentane yielded the product as a light yellow powder, 137 mg (66%). ^{1}H NMR δ 7.34 (m, 2, Ph), 7.03 (m, 3, Ph), 3.3 (dt, 4, NCH_2P), 2.1 (sept., 1, $CH_2CH(CH_3)_2$), 1.88 (m, 4, NCH_2P), 1.5 (virtual triplet, $^3J_{PH}$ = 7.7 Hz, $^3J_{HH}$ = 6.8 Hz, 2, $CH_2CH(CH_3)_2$), 1.07 (d, 6, $CH_2CH(CH_3)_2$), 0.37 (s, 18, $SiMe_3$). ^{31}P NMR δ 1.19 (s). ^{13}C NMR δ 134, 132, 130, 129 (Ph), 70.9 ($CH_2CH(CH_3)_2$), 48 (d, NCH_2P), 37.8 (d, NCH_2P),

References begin on page 221.

29.9 (d, $^3J_{CP}$ = 5 Hz, $CH_2CH(CH_3)_2$), 28.2 (s, $CH_2CH(CH_3)_2$), 1.1 (s, $Si(CH_3)_3$). Anal. Calcd. for $C_{20}H_{40}N_2Si_2PClZr$: C, 45.99; H, 7.72; N, 5.36. Found: C, 45.52; H, 7.53; N, 5.37.

[PhP(CH$_2$CH$_2$NTMS)$_2$]Zr(Bn)(^{13}CH$_3$) (24). $[N_2P]ZrCl_2$ (250 mg, 0.499 mmol) was dissolved in 20 mL ether and the solution cooled to -40 °C. $^{13}CH_3MgI$ (1.4 M in ether, 423 µL, 0.50 mmol) was added by syringe and the reaction was stirred for 40 min. It was again cooled to -40 °C and BnMgCl (1.0 M in ether, 500 µL, 0.499 mmol) was added. After stirring for 1.3 h, dioxane (98 µL) was added. The precipitate was allowed to settle for 45 min and the solution filtered through a plug of Celite. The ether was removed *in vacuo* and the crude product recrystallized from ether, 169 mg (63%). ^{1}H NMR δ 7.4 (t, Ph), 7.1 (m, Ph), 6.8 (t, Ph), 3.25 (m, 2, NCH_2P), 2.82 (d, $^3J_{HP}$ = 9 Hz, *cis*-$CH_2C_6H_5$), 2.61 (m, 2, NCH_2P), 1.8 (m, 2, NCH_2P), 1.62 (m, NCH_2P), 0.588 (d, 3, *trans*-^{13}Me), 0.304 (s, 18, $SiMe_3$). ^{31}P NMR δ -6.56 (d), ^{13}C NMR δ 131.9 , 129,7 128.9, 127.4, 122.3, 62.4 (*cis*-$CH_2C_6H_5$, $^2J_{CP}$ = 4.6 Hz, $^1J_{CH}$ =130 Hz), 48.7 (NCH_2P), 38.2 (d, *trans*-$^{13}CH_3$, $^2J_{CP}$ = 27.9 Hz), 37.7 (NCH_2P), 0.927 ($SiMe_3$). Anal. Calc. for $C_{24}H_{41}N_2PSi_2Zr$: C, 53.69; H, 7.70; N, 5.22. Found: C, 54.08; H, 7.32; N, 5.17.

[PhP(CH$_2$CH$_2$NTMS)$_2$]Zr(Bn)$_2$ (26). $[N_2P]ZrCl_2$ (150 mg, 0.300 mmol) was dissolved in 10 mL ether. The solution was cooled to -40 °C and $C_6H_5CH_2MgCl$ (1.0 M in ether, 599 µL, 0.599 mmol) was added by syringe. After 3 h, ^{31}P NMR showed that the reaction was complete. Dioxane (56 µL, 0.66 mmol) was added and the precipitate allowed to settle. The reaction was filtered through Celite and the volatiles removed under reduced pressure. Recrystallization from ether/pentane at -40 °C left the product as yellow crystals, 120 mg in two crops (65%). ^{1}H NMR δ 7.28 (d, 4, Bn), 7.05 (m, 2, Ph), 6.95 (m, 2, Ph), 6.7 (m, 2, Ph), 3.15 (m, 2, NCH_2P), 2.8 (m, 2, NCH_2P), 2.75 (d, $^3J_{PH}$ = 6.6 Hz, 2, *cis*-$CH_2C_6H_5$), 2.69 (d, $^3J_{HP}$ = 2.4 Hz, 2, *trans*-$CH_2C_6H_5$), 1.65 (m, 4, NCH_2P), 0.294 (s, 18, $SiMe_3$). ^{31}P NMR δ -7.08 (s). ^{13}C NMR δ 149.6 (Bn-ipso), 143.5 (Bn-ipso), 135.9 (Ph-ipso), 131.7 (Ph-ortho), 129.3, 128.9, 128.8, 128.7, 127.3, 126.8, 122.3, 120.8, 69.3 ($^2J_{CP}$ = 3.2 Hz, $^1J_{CH}$ = 126 Hz, *cis*-$CH_2C_6H_5$), 65.9 ($^2J_{CP}$ = 22 Hz, $^1J_{CH}$ = 118 Hz, *trans*-$CH_2C_6H_5$), 47.7 (d, NCH_2P), 37.1 (d, NCH_2P), 1.40 ($SiMe_3$).

References begin on page 221.

Anal. Calc. for $C_{30}H_{45}N_2PSi_2Zr$: C, 58.87; H, 7.41; N, 4.58. Found: C, 58.71; H, 7.55; N, 4.47.

[[N_2P]Zr(Bn)][B(C_6F_5)$_4$] (28). A solution of [N_2P]Zr(Bn)$_2$ (16 mg, 26 μmol) in ~0.3 mL C_6D_5Br was prepared and cooled to -40 °C. A solution of [Ph_3C][B(C_6F_5)$_4$] (24 mg, 26 μmol) in ~0.3 mL C_6D_5Br was prepared and cooled similarly. The cold solutions were quickly mixed and added to an NMR tube with a 14/20 joint attached. A needle valve was placed on and the tube was removed from the drybox and immediately frozen. It was evacuated, flame-sealed, and transported to the NMR instrument. It was then thawed at ~ -30 °C and placed in a -30 °C NMR probe for spectroscopic analysis. ^{1}H NMR (C_6D_5Br, -30 °C) δ 7.2 (m, Ph), 6.72 (d, 2, ortho-Ph), 6.39 (d, 2, ortho-Ph), 3.88 (s, 2, PhC*H*$_2$Ph), 3.6 (m, 2, NCH_2P), 3.25 (m, 2, NCH_2P), 2.3 (m, 2, NCH_2P), 1.95 (m, 2, NCH_2P), 0.096 (s, 18, $SiMe_3$). ^{31}P NMR (C_6D_5Br, -30 °C) δ 22 (br s). Within minutes of warming the sample to room temperature, decomposition became evident in both the ^{1}H and ^{31}P spectra.

[[N_2P]Zr($^{13}CH_3$)][B(C_6F_5)$_4$] (27). This cation was observed as described above using [N_2P]Zr($^{13}CH_3$)$_2$ (10 mg, 22 μmol) and [Ph_3C][B(C_6F_5)] (20 mg, 22 μmol). ^{1}H NMR (C_6D_5Br, -30 °C) δ 7.0 (m, Ph), 3.3 (br m, NCH_2P), 2.1 (br m, NCH_2P), 1.8 (d, $^{13}CH_3CPh_3$), 0.08 (s, $SiMe_3$). ^{31}P NMR (C_6D_5Br, -30 °C) δ 26.8 (s). ^{13}C NMR (C_6D_5Br, -30 °C) δ 55.1 (s, Zr($^{13}CH_3$)$^+$), 30.5 (s, $^{13}CH_3CPh_3$). Decomposition was evident within minutes of warming to room temperature, $\tau_{1/2}$ at 20 °C ≈ 15 min.

[[N_2P]Zr($^{13}CH_3$)(NMe_2Ph)][B(C_6F_5)$_4$] (29). This species was prepared as described above using [N_2P]Zr($^{13}CH_3$)$_2$ (10 mg, 22 μmol) and [Ph_3C][B(C_6F_5)] (20 mg, 22 μmol). After mixing, NMe_2Ph (2.8 μL, 22 μmol) was added by syringe. The sample was then prepared as before. NMR spectra indicate more than one species is present at -30 °C, the major species appears to be the Zr(*trans*-Me)(NMe_2Ph)$^+$ complex. ^{13}C NMR (C_6D_5Br, -30 °C) δ 44.7 (d, $^2J_{CP}$ = 25 Hz, *trans*-$^{13}CH_3$). ^{31}P NMR (C_6D_5Br, -30 °C) δ -1.1 (d, $^2J_{CP}$ = 25 Hz).

Polyethylene. (a) From [[N_2P]Zr(Bn)][B(C_6F_5)$_4$]. A 100 mL schlenk was charged with [N_2P]Zr(Bn)$_2$ (20 mg, 33 μmol) and 50 mL chlorobenzene. The reaction was cooled to -40 °C

References begin on page 221.

and a -40 °C solution of $[Ph_3C][B(C_6F_5)_4]$ (30 mg, 33 μmol) in 4 mL chlorobenzene was added. The flask was fitted with a septum, removed from the drybox, and attached to the schlenk line. It was placed in an ice bath and ethylene was introduced with a needle through the septum. The gas flow was directed just over the surface of the solution and allowed to escape through the argon manifold. The reaction was stirred vigorously during gas addition. After 4.00 min, the polymerization was quenched with methanol (1.25 mL). The chlorobenzene was removed by rotary evaporation and the white solid remaining titruated with methanol. The residual volatiles were removed by heating at ~50 °C under high vacuum overnight. The polymer was obtained as a white solid, 117 mg (5.4×10^4 g / mol · h).

(b) From $[[N_2P]Zr(Me)][B(C_6F_5)_4]$. The procedure is identical to that described above except that $[N_2P]Zr(Me)_2$ (18 mg, 39 μmol) and $[Ph_3C][B(C_6F_5)_4]$ (36 mg, 39 μmol) were employed. Ethylene was introduced for 2.00 min and the reaction quenched as before. 295 mg of a white flaky solid was obtained (2.3×10^5 g / mol · h).

$[PhP(CH_2CH_2NTMS)_2][PhPCH_2CH_2NTMS]Mo$ (30). A solution of $[N_2P]Li_2$ (849 mg, 2.41 mmol, 1.7 equiv.) in 20 mL THF was cooled to -40 °C. Solid $MoCl_4(THF)_2$ (541 mg, 1.42 mmol) was added and the mixture stirred at room temperature overnight. The volatiles were removed under reduced pressure and the dark brown solid left was washed with pentane (2 x 5 mL). The insolubles were extracted with 2 : 1 ether : pentane (30 mL). The extract was filtered through Celite and the volatiles removed. Recrystallization from ether gave the product as dark orange blocks, 50 mg (6%). ^1H NMR δ 7.53 (t, 2, Ph), 7.21 (t, 3, Ph), 7.03 (br m, 2, Ph), 6.82 (br m, 3, Ph), 4.38 (m, 2, NCH_2P), 3.9 (m, 2, NCH_2P), 3.0 (m, 4, NCH_2P), 2.0 (m, 4, NCH_2P), 0.40 (s, 9, $SiMe_3$), 0.07 (s, 18, $SiMe_3$). ^{31}P NMR δ 209.7 (d, $^2J_{PP}$ = 9 Hz, phosphide), 62.5 (d, $^2J_{PP}$ = 11 Hz, phosphine). ^{13}C NMR δ 131.5, 131.4, 129.8, 129.0, 128.8, 126.2 (Ph), 54.4 (br s, NCH_2P), 52.6 (d, NCH_2P), 37.2 (br s, NCH_2P), 34.7 (d, NCH_2P), 2.21 (s, TMS), 0.452 (s, TMS). Anal. Calcd. for $C_{27}H_{49}MoN_3P_2Si_3$: Calcd.: C, 49.30; H, 7.51; N, 6.39. Found: C, 49.41; H, 7.28; N, 6.35.

References begin on page 221.

$[N_2P_F]H_2$ (31). A 100 mL schlenk flask was charged with $PhP(CH_2CH_2NH_2)_2 \cdot 2HCl$ (5.00 g, 18.6 mmol), K_2CO_3 (11.6 g, 83.6 mmol, 4.5 equiv.), and 50 mL DMSO. It was then sparged with argon for 20 min. C_6F_6 (degassed and dried over 4 Å sieves) was then added via syringe. The reaction was heated at 60 °C for 24 h. As this preparation has not been optimized, a slightly higher temperature or longer reaction time may increase the yield. The reaction is conveniently monitored by ^{19}F NMR. The reaction was worked up under anaerobic conditions since the product decomposed upon exposure to oxygen-containing H_2O. The DMSO solution was partitioned between 50 mL CH_2Cl_2 and 100 mL H_2O (both degassed) and washed with 100 mL H_2O followed by 100 mL brine. The relatively dry CH_2Cl_2 solution is now air-stable enough to be further dried with $MgSO_4$ under air and evaporated. Flash chromatography (under air) on a 10 × 5 cm Al_2O_3 (neutral, not activated) column with CH_2Cl_2/hexane mixtures as the eluant gave the product as a white crystalline solid, 2.13 g (22%, not optimized). ^1H NMR ($CDCl_3$) δ 7.53 (m, 2, C_6H_5), 7.39 (m, 3, C_6H_5), 3.65 (br s, 2, N*H*), 3.40 (q, 4, NCH_2CH_2P), 2.13 (m, 4, NCH_2CH_2P). ^{19}F NMR ($CDCl_3$) δ -160.7 (d, 4, *o*-C_6F_5), -165.6 (t, 4, *m*-C_6F_5), -172.7 (*p*-C_6F_5). ^{31}P NMR ($CDCl_3$) δ -36.4. ^{13}C NMR ($CDCl_3$) δ 139, 137, 134, 124 (m, C_6F_5), 132.6 (d, J_{CP} = 21 Hz, *p*-C_6H_5), 130.2 (s, *p*-C_6H_5), 128.9 (d, J_{CP} = 8 Hz, *m*-C_6H_5), 43.2 (d, NCH_2P), 29.5 (d, NCH_2P). Anal. Calcd. for $C_{22}H_{15}N_2PF_{10}$: Calcd.: C, 50.02; H, 2.86; N, 5.30. Found: C, 49.86; H, 2.97; N, 5.25.

$[N_2P_F]Mo(NMe_2)_2$ (32). A solution of $[N_2P_F]H_2$ (150 mg, 0.284 mmol) in 5 mL pentane was prepared and cooled to -40 °C. A solution of $Mo(NMe_2)_4$ (77 mg, 0.284 mmol) in 5 mL pentane was prepared and cooled similarly. The ligand solution was added to that containing $Mo(NMe_2)_4$ via pipette over 2 min and the reaction stirred for 2 h. ^{31}P NMR indicated conversion to a new material. Crystallization from ~20 : 1 pentane : toluene yielded 75 mg of the product as a dark solid, (37%, not optimized). ^1H NMR δ 7.57 (br t, P*Ph*), 7.17 (m, P*Ph*), 3.5, 3.25, 2.07, 1.55 (2, m, NC*H*HP resonances), 3.06 (6, s, NMe_2), 2.91 (6, s, NMe_2). ^{19}F NMR δ -150.9 (d, *o*-C_6F_5), -165.5 (m, *m*- and *p*-C_6F_5). ^{31}P NMR δ 61.6 (s).

References begin on page 221.

[[PhP($CH_2CH_2NHC_6F_5$)($CH_2CH_2NC_6F_5$)]$MoCl_4$][$HNEt_3$] (33). Solid $MoCl_4(THF)_2$ (108 mg, 0.284 mmol) was added to a stirred solution of $[N_2P_F]H_2$ (150 mg, 0.284 mmol) in 10 mL THF. Triethylamine (83 μL, 0.625 mmol, 2.2 equiv.) was added via syringe. The reaction was stirred overnight at which point ^{19}F NMR indicated clean formation of the product. Removal of the volatiles *in vacuo* left an orange residue which was recrystallized from ~2 mL DME layered with ~3 mL pentane, 223 mg orange microcrystalline product obtained (92%). ^1H NMR δ 15.7, 13.2, 10.7, 8.8 (br singlets, $PCH_2CH_2N_{amine}$), 1.63, 1.38 (br singlets, $HNEt_3$), -7.05, -20.68, -23.8, -38.35 (br singlets, $PCH_2CH_2N_{amide}$). ^{19}F NMR δ -46.5 (br s, C_6F_5-N_{amide}), -54.1 (br s, C_6F_5-N_{amide}), -130.4 (s, C_6F_5-N_{amide}), -131.9 (s, C_6F_5-N_{amide}), -148.4 (s, C_6F_5-N_{amide}), -158.0 (s, C_6F_5-N_{amine}), -164.4 (s, C_6F_5-N_{amine}), -173.6 (s, C_6F_5-N_{amine}). IR (Nujol) cm^{-1} 3346 (NH), 1525, 1503, 1025, 987, 801, 743. Anal. Calcd. for $C_{28}H_{30}Cl_4F_{10}MoN_3P$: Calcd.: C, 38.78; H, 3.49; N, 4.85. Found: C, 38.48; H, 3.74; N, 4.77.

References begin on page 221.

REFERENCES

(1) Schrock, R. R. *Acc. Chem. Res.* **1997**, *30*, 9.

(2) Schrock, R. R.; Rosenberger, C.; Seidel, S. W.; Shih, K.-Y.; Davis, W. M., in preparation.

(3) Freundlich, J. S.; Schrock, R. R.; Davis, W. M. *J. Am. Chem. Soc.* **1996**, *118*, 3643.

(4) Brintzinger, H. H.; Fischer, D.; Mülhaupt, R.; Rieger, B.; Waymouth, R. M. *Angew. Chem. Int. Ed. Engl.* **1995**, *34*, 1143.

(5) Shapiro, P. J.; Bunel, E.; Schaefer, W. P.; Bercaw, J. E. *Organometallics* **1990**, *9*, 867.

(6) Sinn, H.; Kaminsky, W. *Adv. Organomet. Chem.* **1980**, *18*, 99.

(7) Guérin, F.; McConville, D. H.; Vittal, J. J. *Organometallics* **1996**, *15*, 5586.

(8) Cloke, F. G. N.; Geldbach, T. J.; Hitchcock, P. B.; Love, J. B. *J. Organomet. Chem.* **1996**, *506*, 343.

(9) Scollard, J. D.; McConville, D. H. *J. Am. Chem. Soc.* **1996**, *118*, 10008.

(10) Scollard, J. D.; McConville, D. H.; Payne, N. C.; Vittal, J. J. *Macromolecules* **1996**, *29*, 5241.

(11) Baumann, R.; Schrock, R. R.; Davis, W. M. *J. Am. Chem. Soc.* **1997**, *119*, 3830.

(12) Kol, M.; Schrock, R. R.; Kempe, R. *J. Am. Chem. Soc.* **1994**, *116*, 4382.

(13) Freundlich, J. S., unpublished observations.

(14) Stamm, H.; Assithianakis, P.; Buchholz, B.; Weiß, R. *Tetrahedron Lett.* **1982**, *23*, 5021.

(15) Merguro, M.; Asao, N.; Yamamoto, Y. *Tetrahedron Lett.* **1994**, *35*, 7395.

(16) Onistschenko, A.; Buchholz, B.; Stamm, H. *Tetrahedron Lett.* **1987**, *43*, 565.

(17) Issleib, K.; Oehme, H. *Chem. Ber.* **1967**, *100*, 2685.

(18) Latesky, S. L.; McMullen, A. K.; Niccolai, G. P.; Rothwell, I. P. *Organometallics* **1985**, *4*, 902.

(19) Warren, T. H.; Schrock, R. R.; Davis, W. M. *Organometallics* **1996**, *15*, 562.

(20) Fryzuk, M. D.; Mao, S. S. H.; Zaworotko, M. J.; MacGillivray, L. R. *J. Am. Chem. Soc.* **1993**, *115*, 5336.

(21) Fryzuk, M. D.; Haddad, T. S.; Mylvaganam, M.; McConville, D. H.; Rettig, S. J. *J. Am. Chem. Soc.* **1993**, *115*, 2782.

(22) Fryzuk, M. D.; Love, J. B.; Rettig, S. J.; Young, V. G. *Science* **1997**, *275*, 1445.

(23) Schrodi, Y.; Davis, W. M., unpublished results.

(24) Baumann, R., unpublished results.

(25) Turculet, L., unpublished results.

(26) Parkin, G. *Chem. Rev.* **1993**, *93*, 887.

(27) Schrock, R. R.; Seidel, S. W.; Mösch-Zanetti, N. C.; Shih, K.-Y.; O'Donoghue, M. B.; Davis, W. M.; Reiff, W. M. *J. Am. Chem. Soc.* , in press.

(28) Freundlich, J. S.; Schrock, R. R.; Davis, W. M. *Organometallics* **1996**, *15*, 2777.

(29) Mann, B. E.; Taylor, B. F. *^{13}C NMR Data for Organometallic Compounds*, Academic Press: New York, 1981.

(30) Scollard, J. D.; McConville, D. H.; Vittal, J. J. *Organometallics* **1995**, *14*, 5478.

(31) Yang, X.; Stern, C. L.; Marks, T. J. *J. Am. Chem. Soc.* **1994**, *116*, 10015.

(32) Schrock, R. R.; Seidel, S. W.; Zanetti-Mösch, N. C.; Dobbs, D. A.; Shih, K.-Y.; Davis, W. M. *Organometallics* , in press.

(33) Pangborn, A. B.; Giardello, M. A.; Grubbs, R. H.; Rosen, R. K.; Timmers, F. J. *Organometallics* **1996**, *15*, 1518.

(34) Still, W. C.; Kahn, M.; Mitra, A. *J. Org. Chem.* **1978**, *43*, 2923.

(35) Baudler, M.; Glinka, K. *Inorg. Synth.* **1990**, *27*, 227.

(36) Cairns, T. L. *J. Am. Chem. Soc.* **1941**, *63*, 871.

(37) Woods, C. W.; Borkovec, A. B.; Hart, F. M. *J. Med. Chem.* **1964**, *7*, 371.

(38) Diamond, G. M.; Rodewald, S.; Jordan, R. F. *Organometallics* **1995**, *14*, 5.

(39) Bradley, D. C.; Chisholm, M. H. *J. Chem. Soc. (A)* **1971**, 2741.

APPENDIX I

Attempts to Gain Evidence for α-Agostic Interactions in

$[WCp^*(Me)_4][PF_6]$ and $[Cp_2Ta(Me)_2][BF_4]$

A portion of the material covered has appeared in print:

Maus, D. C.; Copié, V.; Sun, B.; Griffiths, J. M.; Griffin, R. G.; Luo, S.; Schrock, R. R.; Liu, A. L.; Seidel, S. W.; Davis, W. M.; Grohmann, A. *J. Am. Chem. Soc.* **1996**, *118*, 5665.

Studies of $[Cp^*WMe_4][PF_6]$

NMR has been used extensively to investigate dynamic processes in liquids and solids because of the wide range of kinetic time scales that are accessible. Usually these studies involve analysis of line shapes or relaxation times, which directly yield information concerning the rates and mechanism of motion. We have been interested in obtaining evidence for an α-agostic interaction in $[Cp^*WMe_4][PF_6]$ (**1**) for some time. The methyl groups in trigonal-bipyramidal **1** are highly acidic. **1** reacts with triethylamine to give unstable $Cp^*W(Me)_3(CH_2)$,[1] in which the methylene protons are grossly inequivalent, presumably as a consequence of an α-agostic interaction[2] with one of the methylene C-H bonds with the metal, a characteristic of some alkylidene complexes of early transition metals.[3] "Activation" of an α-hydrogen through an α-agostic interaction could conceivable be the source of the high acidity of $[WCp^*Me_4]^+$. Solution NMR studies of **1** indicated that the molecule is fluxional, the equatorial and axial methyl groups exchange readily on the NMR time scale (k ~50 sec^{-1} at 25 °C), presumably via a square-pyramidal intermediate. An X-ray study of **1** verified the trigonal-pyramidal geometry, although disorder prevented accurate determination of bond lengths.[1]

A solid-state ^{13}C NMR study of $[WCp^*(^{13}CH_3)_4][PF_6]$ showed an unusually slow rate of hopping for the three protons attached to the axial methyl group (E_a = 26.8 ± 1.7 kJ/mol or 6.4 ± 0.4 kcal/mol).[4] The rate of hopping for protons bound to equatorial methyl groups was determined by solid-state ^2H NMR with $[WCp^*(CD_3)_4][PF_6]$ to be 10.9 ± 0.4 kJ/mol (2.6 ± 0.1 kcal/mol).[4] In order to determine if the origin of slowed "hopping" (rotation) of the axial methyl group compared to the equatorial methyl groups was a result of an α-agostic interaction, a high-quality crystal structure of **1** was required. In an attempt to circumvent the problems with disorder seen in structural determinations of **1**, crystals of $[(\eta^5\text{-}C_5Me_4EtW(Me)_4]\ [PF_6]$ (**2**) were grown and the X-ray structure solved. The structure of **2** is ordered and of high quality. Two independent molecules per one molecule of CH_2Cl_2 are found in the unit cell. Two views of the structure are given in Figure 1. Selected bond distances and angles are located in Table 1, and crystallographic data are located in Table 2.

References are located on page 229.

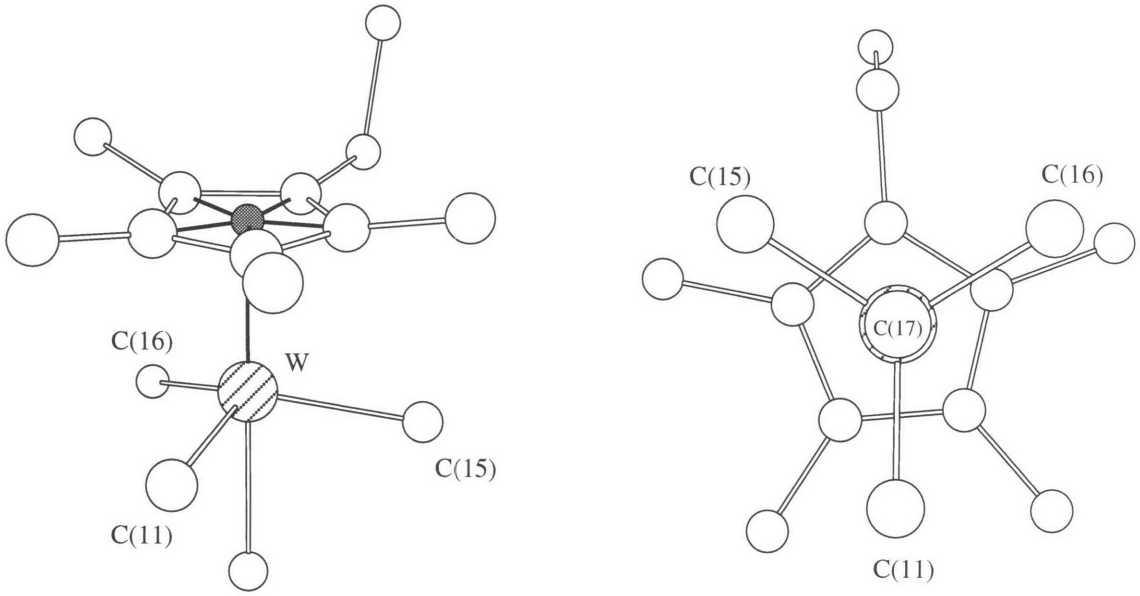

Figure 1. Two views of the structure of one of the independent molecules of $[W(\eta^5\text{-}C_5Me_4Et)(Me)_4]^+$ (**2**), CH_2Cl_2 and $[PF_6]^-$ removed. The shaded atom in the structure on the left is the ring centroid, the view on the right is down the C(17)-W bond.

Table 1. Selected bond lengths (Å) and angles (deg.) for (**2**).

	Molecule 1	**Molecule 2**
	Distances (Å)	
W-C(11)	2.132(11)	2.143(11)
W-C(15)	2.114(11)	2.114(11)
W-C(16)	2.122(11)	2.122(10)
W-C(17)	2.182(11)	2.182(10)
	Angles (deg.)	
C(15)-W-C(11)	117.0(5)	115.5(5)
C(15)-W-C(16)	111.4(5)	112.9(5)
C(16)-W-C(11)	116.9(5)	116.5(5)
C(17)-W-C(16)	77.7(5)	77.0(4)
C(17)-W-C(11)	75.8(5)	76.4(5)
C(17)-W-C(15)	77.6(5)	77.1(4)

References are located on page 229.

Table 2. Crystallographic data, collection parameters, and refinement parameters for $[W(\eta^5\text{-}C_5Me_4Et)(Me)_4][PF_6] \cdot 0.5\ CH_2Cl_2$ (**2**).

Empirical Formula	$C_{15.50}H_{30}ClF_6PW$
Formula Weight	580.67
Diffractometer	Siemens SMART/CCD
Crystal Dimensions (mm)	0.32 × 0.32 × 0.18
Crystal System	Orthorhombic
a (Å)	25.462 (2)
b (Å)	25.295 (2)
c (Å)	12.6030 (7)
V (Å^3)	8117.0 (8)
Space Group	Pbca
Z	16
ρ_{calc} (Mg/m^3)	1.901
Absorption Coefficient (mm^{-1})	5.952
F_{000}	4528
λ (MoK_α)	0.71073 Å
Temperature (K)	188 (2)
Scan Type	ω
θ Range for Data Collection (deg)	1.60 to 23.28
Reflections Collected	30453
Independent Reflections	5835
Absorption Correction	None
R [I > 2σ(I)]	0.0542
R_W [I > 2σ(I)]	0.1172
GoF	1.221
Extinction Coefficient	0.000059 (11)
Largest Diff. Peak and Hole (eÅ^{-3})	1.209 and -1.359

References are located on page 229.

The three W-Me_{eq} bond distances in **2** are statistically the same, averaging 2.12 Å. The W-Me_{ax} bond length is slightly longer, at 2.18 Å. This bond could be longer as a result of steric repulsion from the equatorial methyls, which are pushed towards Me_{ax} by the C_5Me_4Et ring (Me_{eq}-W-Me_{ax} angles deviate little from 77°). The only deviation from local 3-fold symmetry of the WMe_4 core is a marginally smaller value for one of the Me_{eq}-W-Me_{eq} angles (~112.2° average for the two molecules) versus the other two such angles (~116.5° average). However, as the view down the C(17)-W bond in Figure 1 shows, the slightly smaller C(16)-W-C(15) angle is the one with only one of the cyclopentyl carbon atoms (and its ethyl substituent) projected between the two methyl groups. Therefore, steric effects alone are sufficient to explain the slight distortions from local three-fold symmetry observed and the very slightly longer W-Me_{ax} bond. The structural study allows us to conclude that there is no evidence for any interaction between W and a CH bond in either an equatorial or an axial methyl group in $[W(\eta^5\text{-}C_5Me_4Et)(Me)_4][PF_6]$. If we assume that the structure of a $\eta^5\text{-}C_5Me_5$ complex is virtually identical to the structure of a $\eta^5\text{-}C_5Me_4Et$ complex, then we can say that an α-agostic interaction in **1** in the solid state is unlikely. The slowed rotation of the axial methyl group which was observed by solid-state NMR studies could be a result of a more crowded steric environment for Me_{ax} as compared to the Me_{eq} ligands.

Studies of $[Cp_2Ta(Me)_2][BF_4]$

The studies discussed above on $[WCp^*Me_4][PF_6]$ raised a question: would the methyl group "hopping" rates vary in a similar cationic species, $[Cp_2Ta(CH_3)_2][BF_4]$ (**3**)? This complex is also acidic and is deprotonated by $Me_3P{=}CH_2$ to give structurally characterized $Cp_2Ta(CH_2)(CH_3)$.[5] $[Cp_2Ta(CD_3)_2][BF_4]$ (**4**) and $[Cp_2Ta(^{13}CH_3)_2][BF_4]$ were synthesized and a solid-state NMR study carried out in order to determine the rates of methyl group rotation. Both methyl groups were found to hop within the same fast limit, k ~10^{10} sec^{-1},[6] thus no NMR evidence for an α-agostic interaction was found. A anomaly was found, however, in the solution NMR data of **3** and **4**. The CH_3 groups in **3** are observed by ^1H NMR at 0.55 ppm in CD_3CN solution, and the CD_3 groups in **4** are observed by ^2H NMR at 1.3 ppm in CH_3CN. Generally,

References are located on page 229.

the ^2H NMR chemical shift of a deuterated compound is close to the ^1H NMR chemical shift of the protio analog, leading us to wonder if the observed inconsistency in shifts is the result of an α-agostic interaction. A stronger α-agostic interaction would be expected in $Cp_2Ta(CH_3)_2^+$ compared to $Cp_2Ta(CD_3)_2^+$. The sign of the chemical shift perturbation which might be expected is a complicated issue, since an agostic interaction generally results in an upfield shift of the proton which interacts with the metal center and a downfield shift of the other two protons attached to the particular methyl group. If an α-agostic interaction is occurring in these complexes, it is apparently averaged over all six protons (or deuterons) by a fluxional process, since only a single resonance is observed. A VT NMR study of $[Cp_2Ta(CH_3)][BF_4]$ showed that the chemical shift of the CH_3 ligands is virtually temperature-independent from 20 to -80 °C. Thus, we feel that the chemical shift difference between the ^2H NMR resonance of the CD_3 ligands in $[Cp_2Ta(CD_3)][BF_4]$ and the ^1H NMR resonance of the CH_3 ligands in $[Cp_2Ta(CH_3)][BF_4]$ is not a result of an α-agostic interaction, since a strong chemical shift dependence on temperature would be expected for an α-agostic proton. It is worth noting that the chemical shifts of the methyl ligands in $[Cp^*W(CH_3)_4][PF_6]$ and $[Cp^*W(CD_3)_4][PF_6]$ are identical at -30 °C (a temperature at which the spectrum is not complicated by the fluxional process described above).

EXPERIMENTAL

General methods can be found in the main text of the thesis. $[W(\eta^5\text{-}C_5Me_4Et)(Me)_4][PF_6]$ (**2**) was prepared by a literature procedure.[7] Isotopically-enriched $[Cp_2Ta(Me)_2][BF_4]$ complexes (CD_3 and $^{13}CH_3$) were prepared by a method analogous to the literature procedure for $[Cp_2Ta(CH_3)_2][BF_4]$[5] using $Zn(CD_3)_2$ or $Zn(^{13}CH_3)$. These dimethylzinc reagents were prepared from the corresponding isotopically-enriched methyl iodide and Zn/Cu by the sealed tube method.[8] We note several requirements which we found for the sealed tube reaction to proceed satisfactorily. Copper powder must be activated with HCl before use. Also, the reactions should not be stirred while heating, stirring was found to result in low yields of the product.

References are located on page 229.

REFERENCES

(1) Liu, A. H.; Murray, R. C.; Dewan, J. C.; Santarsiero, B. D.; Schrock, R. R. *J. Am. Chem. Soc.* **1987**, *109*, 4282.

(2) Brookhart, M.; Green, M. L. H. *Prog. Inorg. Chem.* **1988**, *36*, 1.

(3) Schrock, R. R. In *Reactions of Coordinated Ligands*; Braterman, P. R., Ed.; Plenum: New York, 1986.

(4) Maus, D. C.; Copié, V.; Sun, B.; Griffiths, J. M.; Griffin, R. G.; Luo, S.; Schrock, R. R.; Liu, A. H.; Seidel, S. W.; Davis, W. M.; Grohmann, A. *J. Am. Chem. Soc.* **1996**, *118*, 5665.

(5) Schrock, R. R.; Sharp, P. R. *J. Am. Chem. Soc.* **1978**, *100*, 2389.

(6) Maus, D. C., unpublished results.

(7) Green, M. L. H.; Hughes, A. K.; Popham, N. A.; Stephens, A. H. H.; Wong, L.-L. *J. Chem. Soc. Dalton Trans.* **1992**, 3077.

(8) Hota, N. K.; Willis, C. J. *J. Organometal. Chem.* **1967**, *9*, 169.

APPENDIX II

ORTEP Drawings at the 35% Probability Level for X-ray Structures,

Tabulated by Identification Number (see Table of Contents)

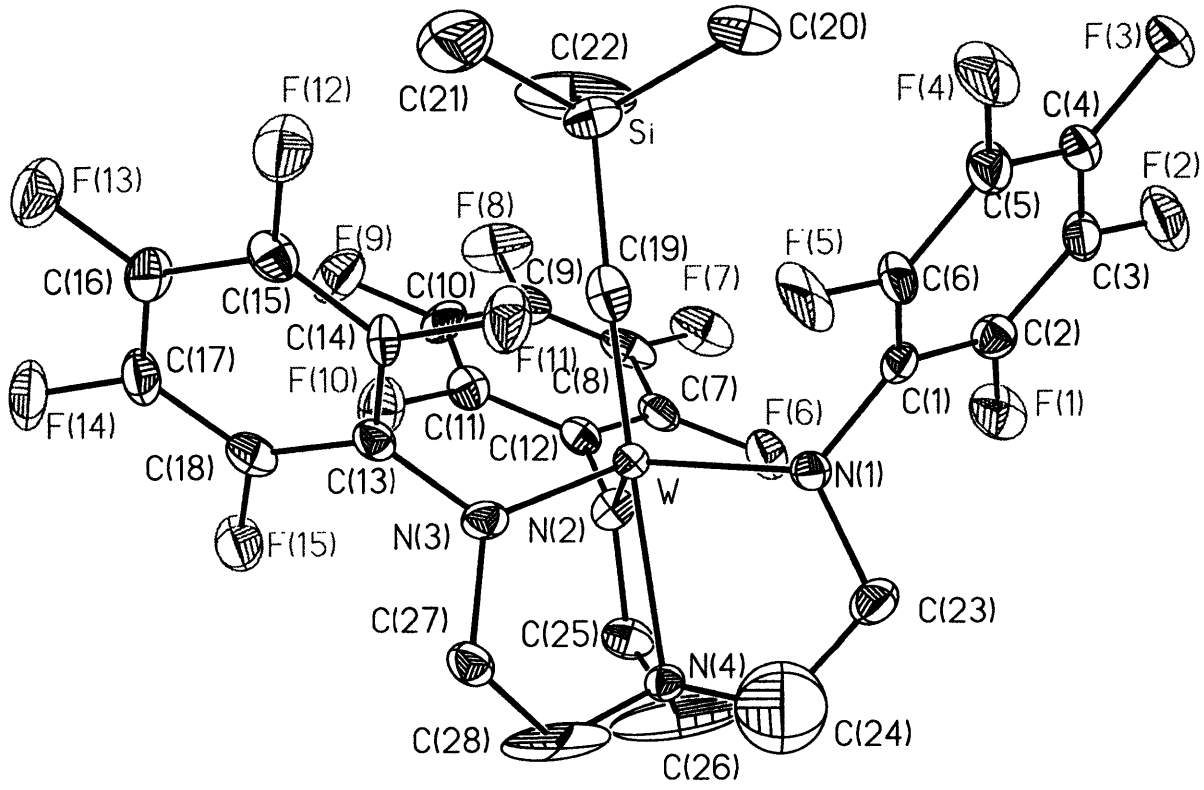
C(22)
C(20)
C(21)
Si
F(12)
F(13)
F(8)
F(9)
C(19)
C(16)
C(15)
C(10)
C(9)
F(7)
C(14)
C(17)
F(10)
F(11)
C(8)
C(7)
F(14)
C(11)
C(12)
F(6)
C(18)
C(13)
W
N(1)
F(15)
N(3)
N(2)
C(27)
C(25)
C(23)
N(4)
C(28)
C(24)
C(26)
F(3)
F(4)
C(4)
F(2)
C(5)
F(5)
C(6)
C(3)
C(2)
C(1)
F(1)

94047

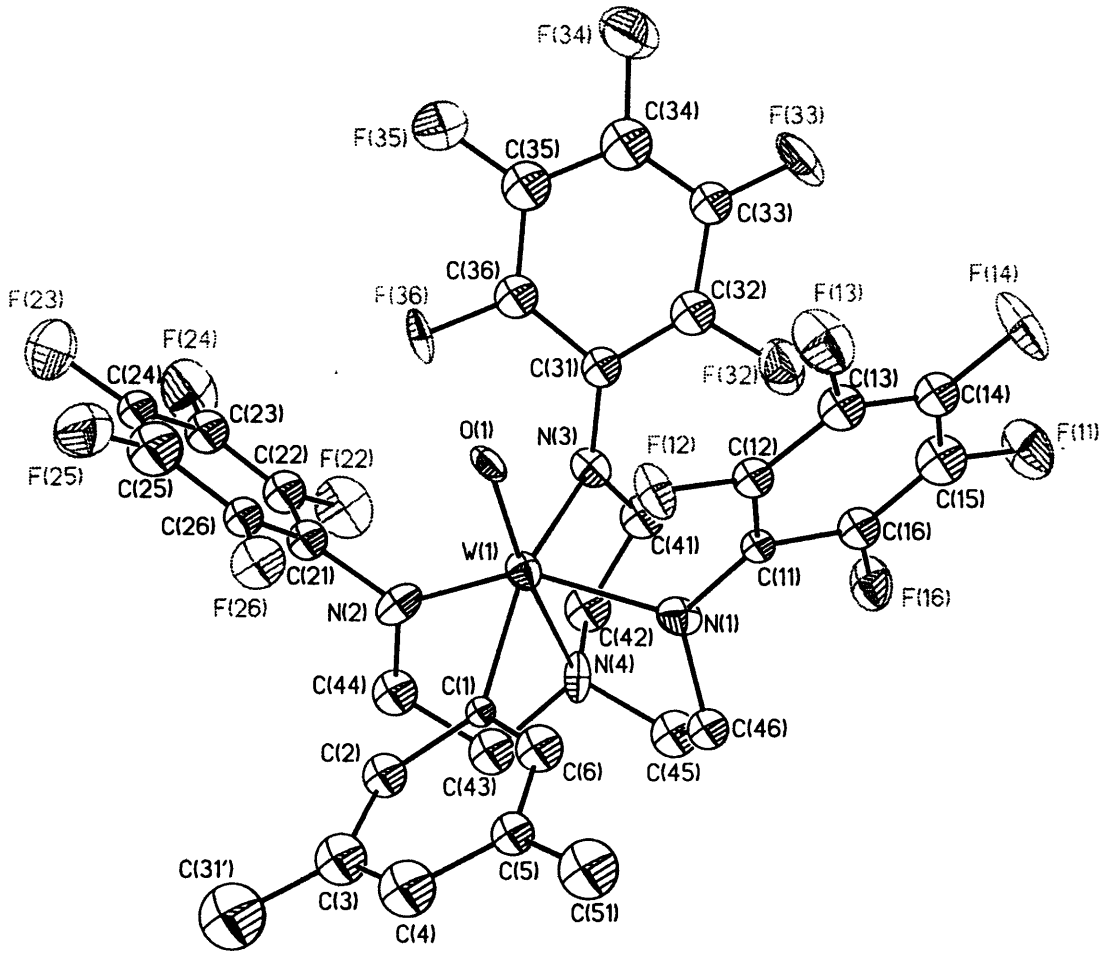
F(34)
C(34)
F(33)
F(35)
C(35)
C(33)
C(36)
C(32)
F(14)
F(23)
F(36)
F(13)
F(24)
C(31)
F(32)
C(13)
C(14)
C(24)
C(23)
O(1)
N(3)
F(12)
C(12)
F(11)
F(25)
C(25)
C(22)
F(22)
C(15)
C(26)
C(41)
C(16)
W(1)
C(21)
C(11)
F(26)
N(2)
F(16)
C(42)
N(1)
N(4)
C(44)
C(1)
C(46)
C(2)
C(43)
C(6)
C(45)
C(31')
C(3)
C(5)
C(51)
C(4)

95095b

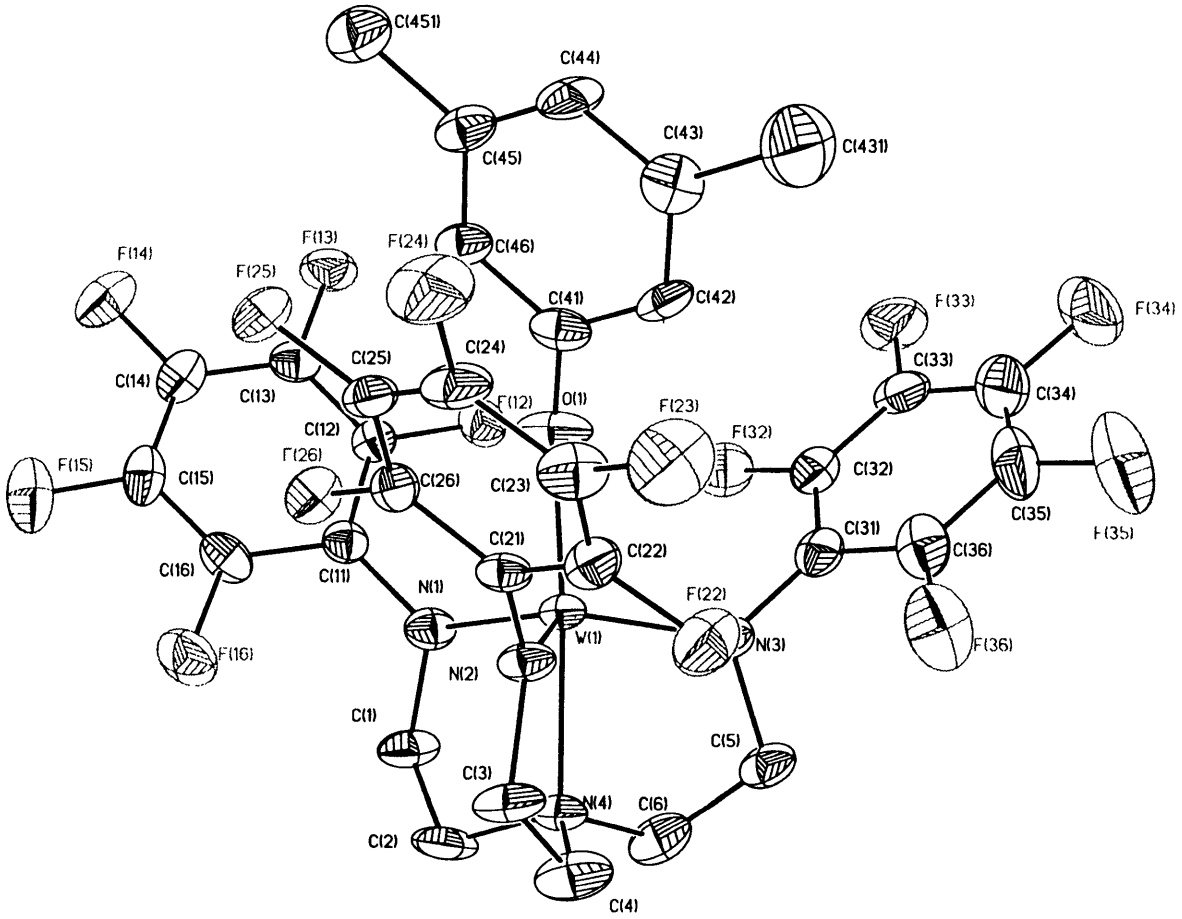
C(451)
C(44)
C(45)
C(43)
C(431)
F(14)
F(25)
F(13)
F(24)
C(46)
C(41)
C(42)
F(33)
F(34)
C(14)
C(13)
C(25)
C(24)
C(33)
C(34)
F(12)
O(1)
F(23)
C(12)
F(32)
F(15)
F(26)
C(15)
C(26)
C(23)
C(32)
C(35)
F(35)
C(21)
C(22)
C(31)
C(16)
C(11)
C(36)
N(1)
F(22)
W(1)
N(3)
F(16)
N(2)
F(36)
C(1)
C(5)
C(3)
N(4)
C(6)
C(2)
C(4)

95091

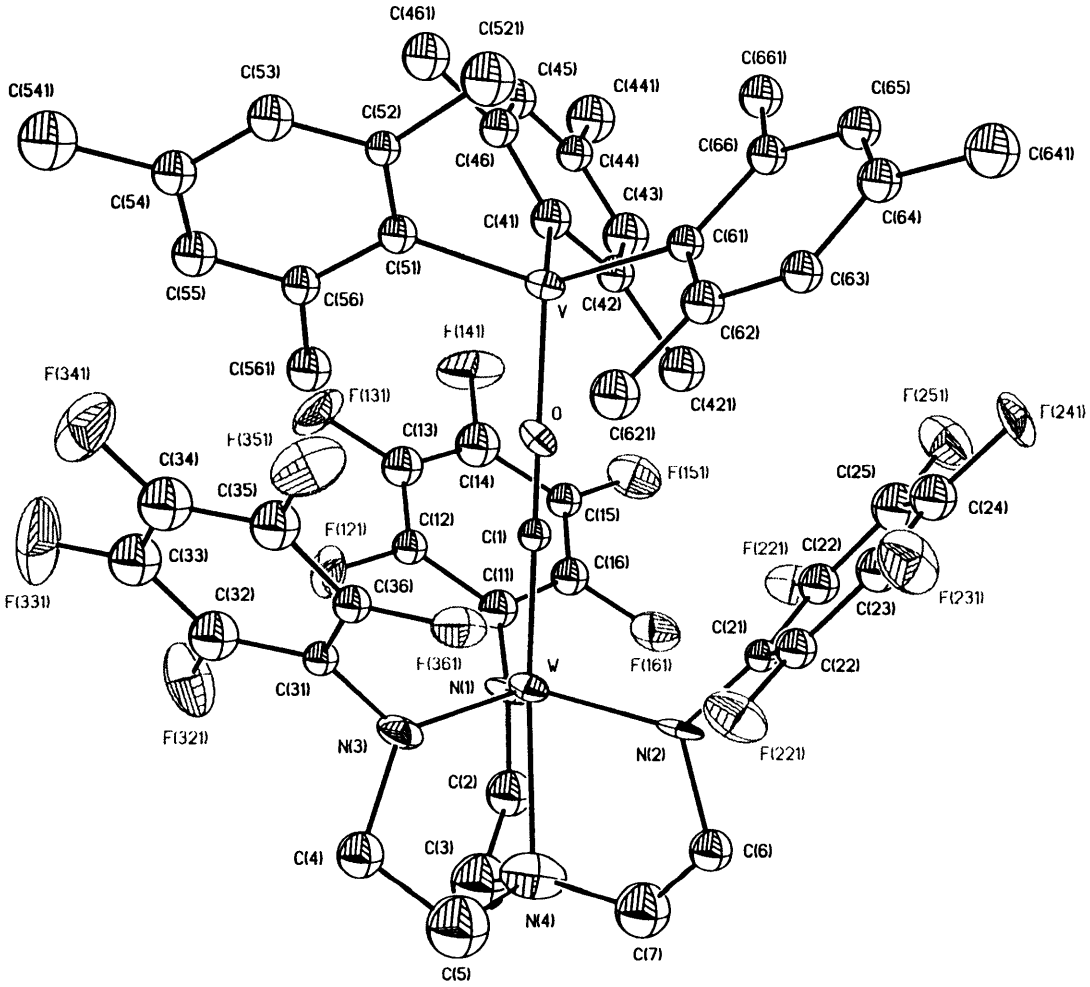
C(461)
C(521)
C(53)
C(45)
C(661)
C(541)
C(441)
C(65)
C(52)
C(46)
C(66)
C(641)
C(54)
C(44)
C(64)
C(43)
C(41)
C(61)
C(51)
C(63)
C(55)
C(56)
V
C(42)
C(62)
F(141)
C(561)
F(341)
F(131)
O
C(421)
F(351)
C(13)
C(621)
F(251)
F(241)
C(34)
C(14)
F(151)
C(25)
C(35)
C(15)
C(24)
C(12)
C(1)
F(121)
C(33)
C(16)
F(221)
C(22)
F(331)
C(36)
C(11)
C(23)
F(231)
C(32)
C(21)
F(361)
F(161)
W
C(31)
N(1)
C(22)
F(321)
N(3)
N(2)
F(221)
C(2)
C(4)
C(3)
C(6)
N(4)
C(7)
C(5)

95155

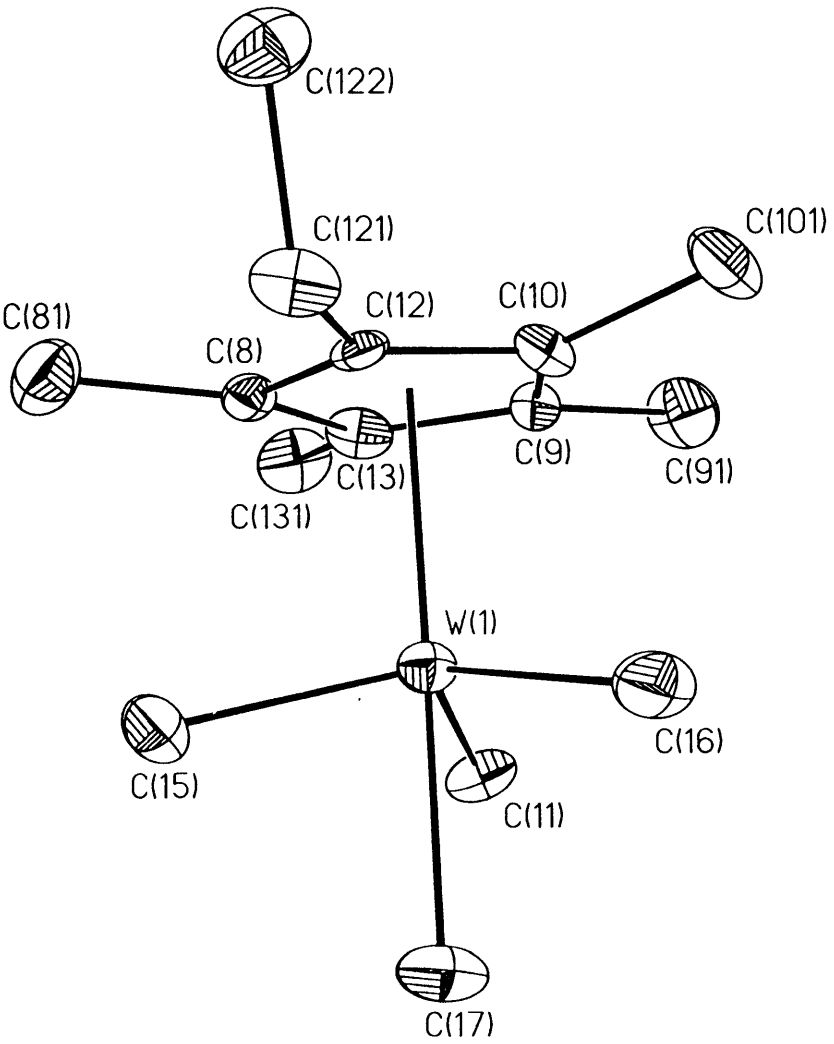

95162

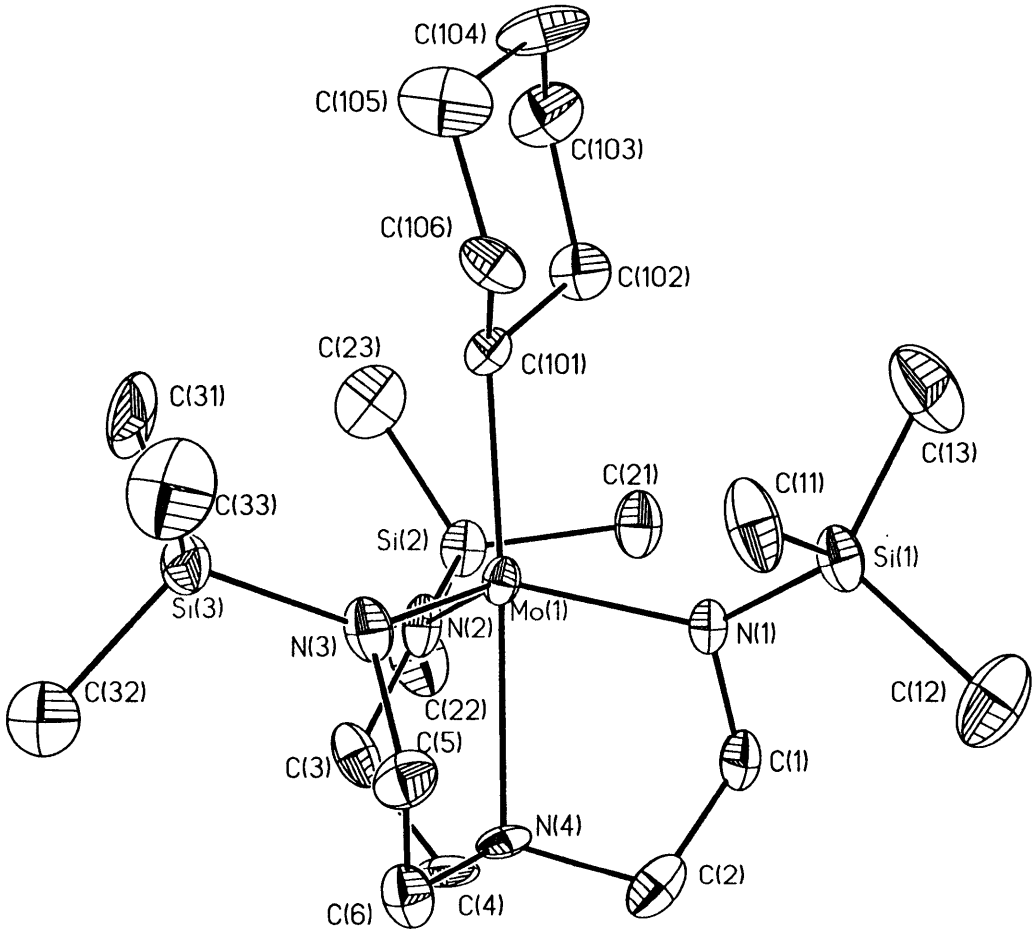
C(104)
C(105)
C(103)
C(106)
C(102)
C(23)
C(101)
C(31)
C(13)
C(21)
C(11)
C(33)
Si(2)
Si(1)
Si(3)
Mo(1)
N(2)
N(3)
N(1)
C(32)
C(12)
C(22)
C(5)
C(3)
C(1)
N(4)
C(2)
C(6)
C(4)

96208

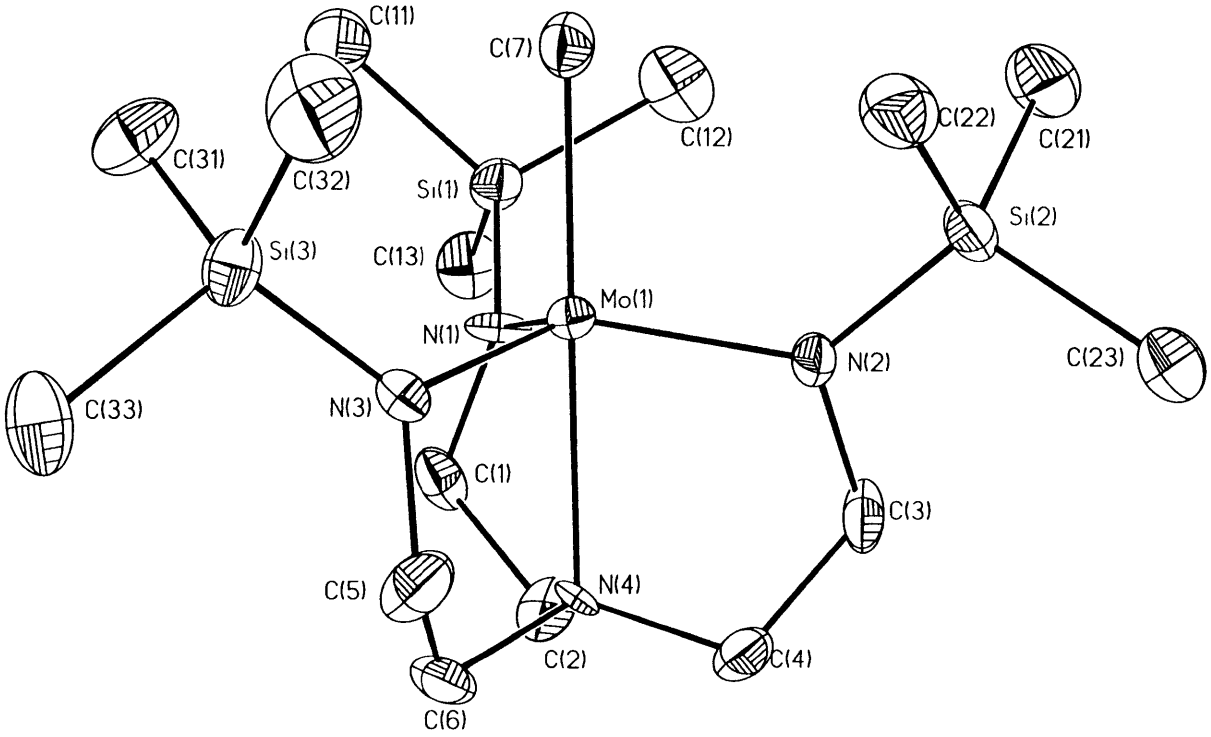
C(11)
C(7)
C(12)
C(22)
C(21)
C(31)
C(32)
Si(1)
Si(2)
Si(3)
C(13)
Mo(1)
N(1)
N(2)
C(23)
C(33)
N(3)
C(1)
C(3)
C(5)
N(4)
C(2)
C(4)
C(6)

97001

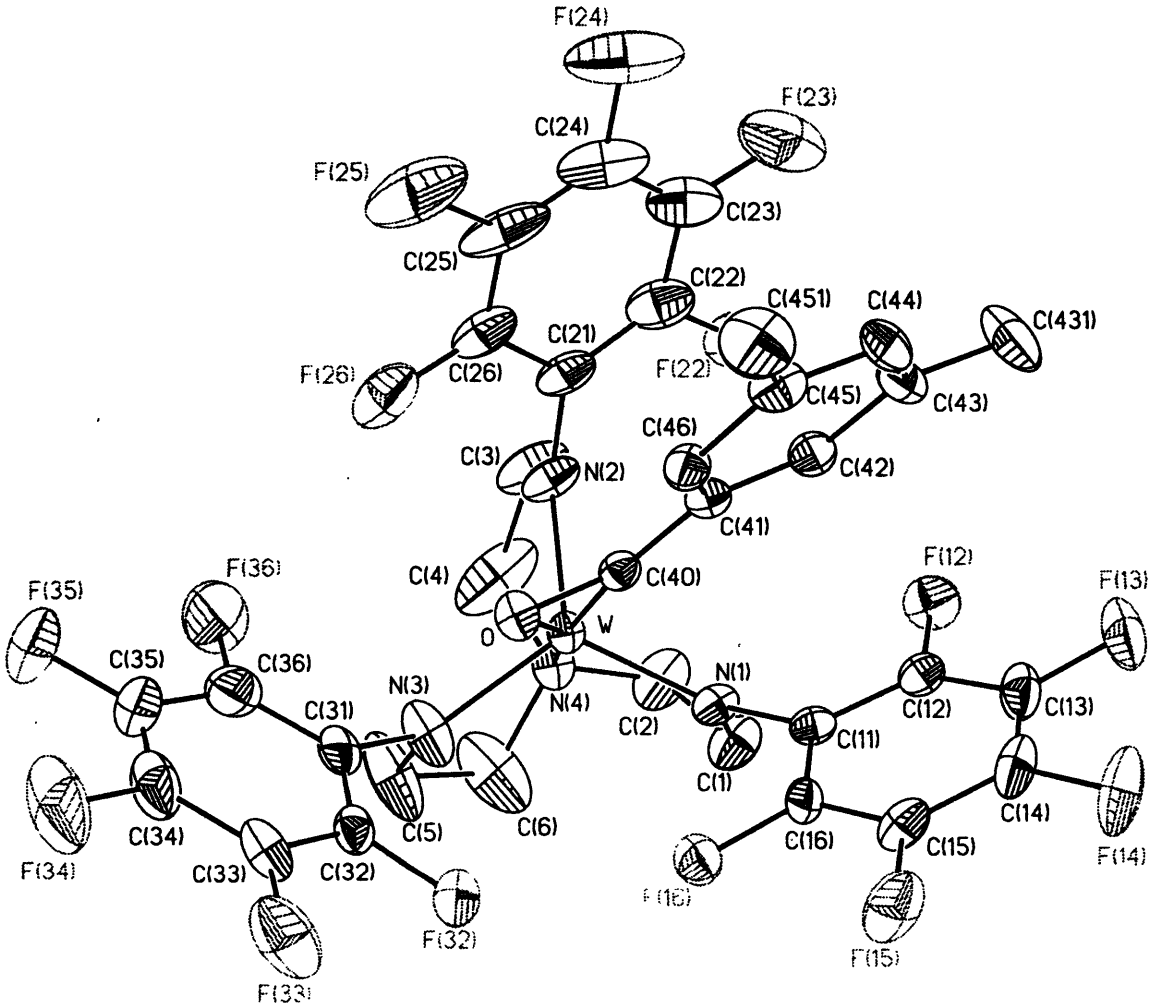
F(24)
F(23)
C(24)
F(25)
C(23)
C(25)
C(22)
C(451)
C(44)
C(431)
C(21)
F(26)
C(26)
F(22)
C(45)
C(43)
C(46)
C(3)
N(2)
C(42)
C(41)
F(36)
F(12)
F(13)
F(35)
C(4)
C(40)
O
W
C(35)
C(36)
N(3)
N(4)
C(2)
N(1)
C(12)
C(13)
C(31)
C(11)
C(1)
C(34)
C(5)
C(6)
C(16)
C(15)
C(14)
F(34)
C(33)
C(32)
F(16)
F(14)
F(32)
F(15)
F(33)

97010

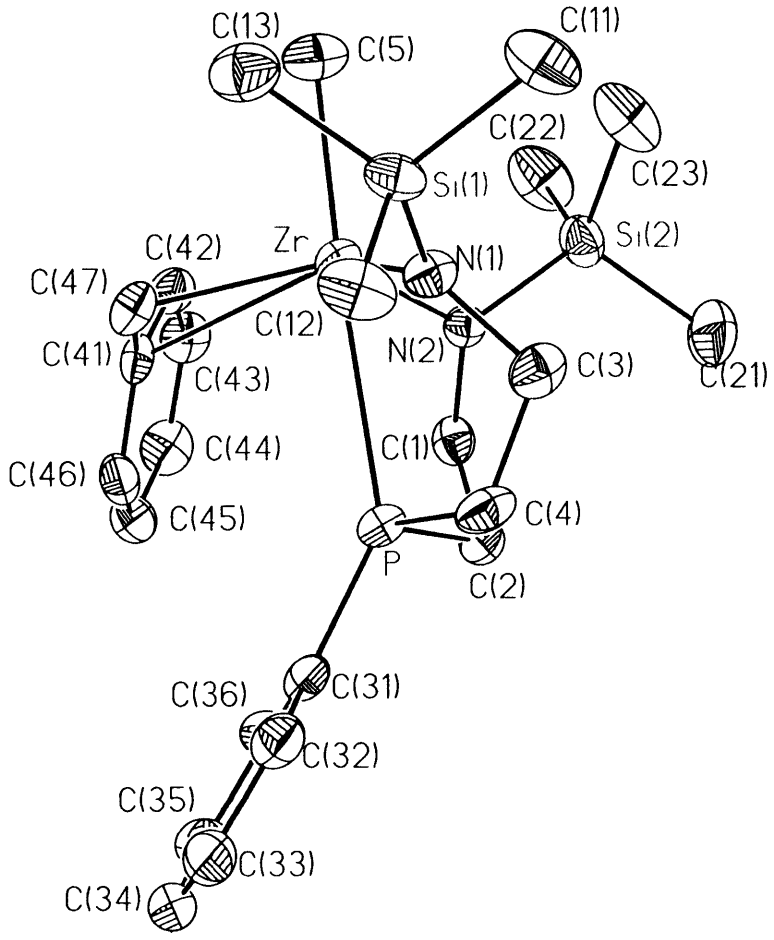
C(13)
C(5)
C(11)
C(22)
C(23)
Si(1)
Si(2)
Zr
C(42)
N(1)
C(47)
C(12)
C(41)
N(2)
C(3)
C(21)
C(43)
C(44)
C(1)
C(46)
C(4)
C(45)
P
C(2)
C(36)
C(31)
C(32)
C(35)
C(33)
C(34)

97048

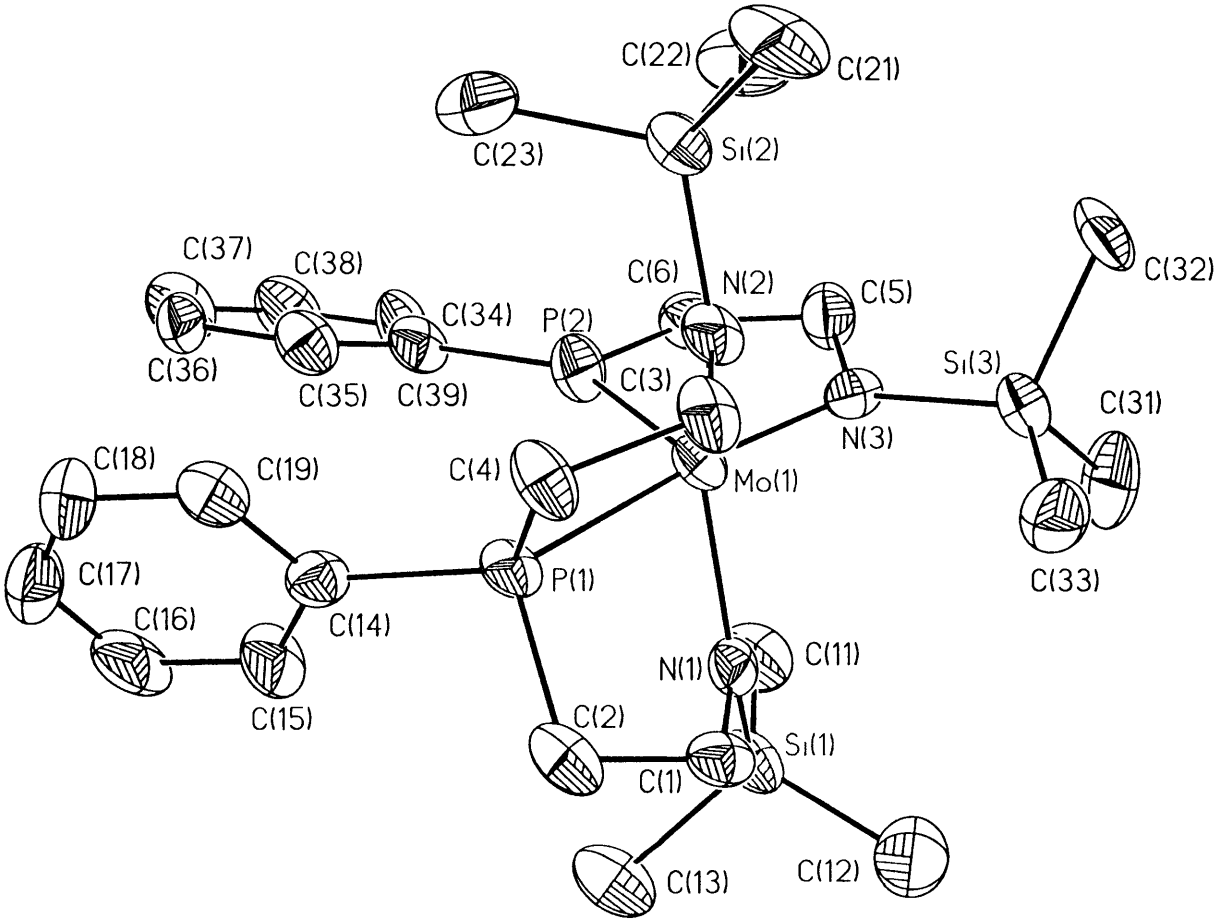
C(22)
C(21)
C(23)
Si(2)
C(37)
C(38)
C(6)
N(2)
C(5)
C(32)
C(34)
P(2)
C(36)
C(35)
C(39)
C(3)
Si(3)
C(31)
N(3)
C(18)
C(19)
C(4)
Mo(1)
C(17)
P(1)
C(33)
C(16)
C(14)
N(1)
C(11)
C(15)
C(2)
Si(1)
C(1)
C(13)
C(12)

97063

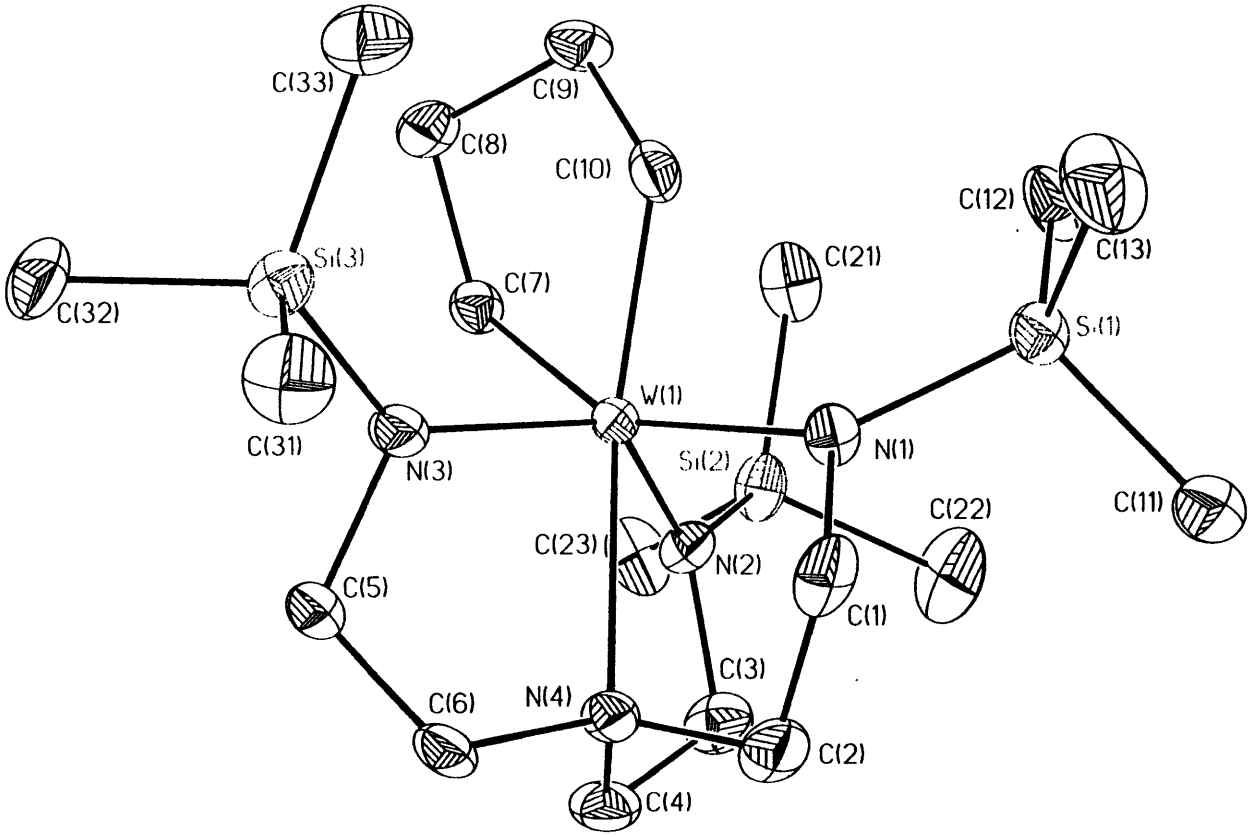
C(33)
C(9)
C(8)
C(10)
C(12)
C(13)
C(32)
Si(3)
C(7)
C(21)
Si(1)
W(1)
C(31)
N(3)
N(1)
Si(2)
C(22)
C(11)
C(23)
N(2)
C(5)
C(1)
C(3)
C(6)
N(4)
C(2)
C(4)

97072

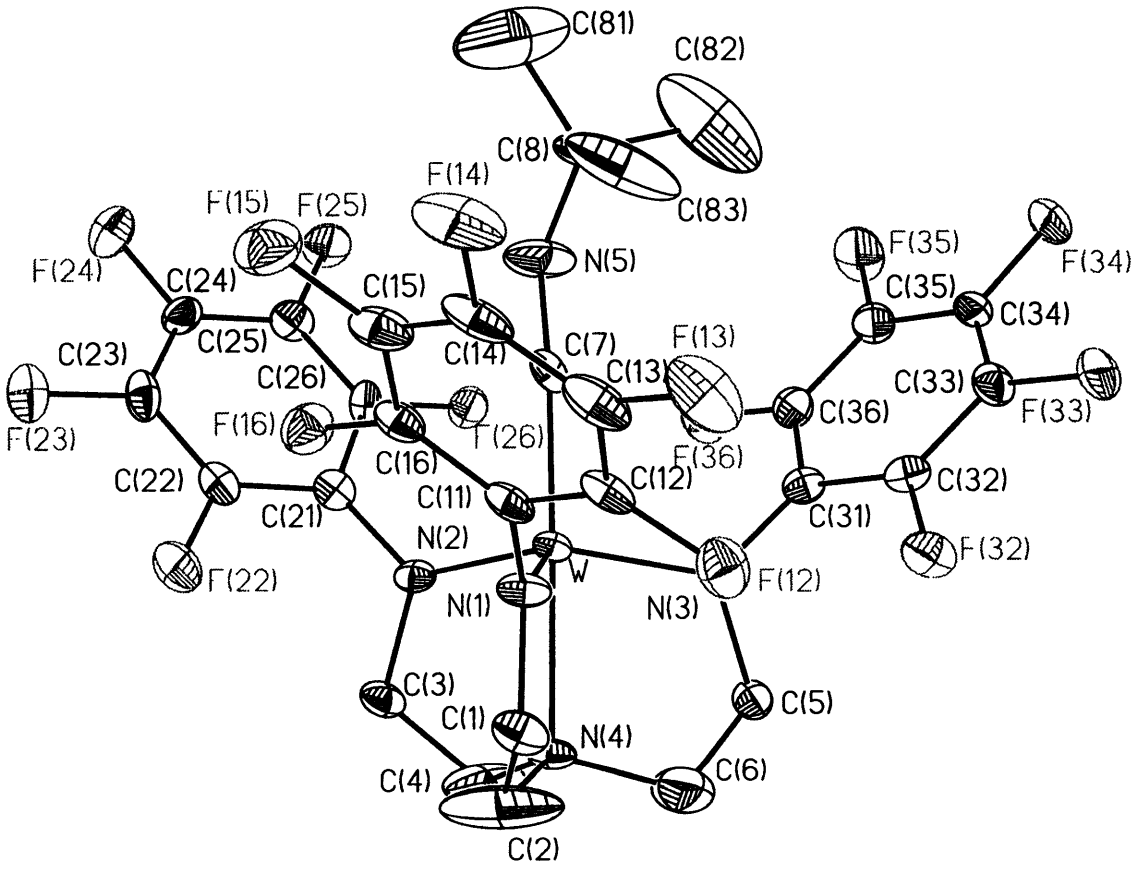
C(81)
C(82)
C(8)
C(83)
F(14)
F(15)
F(25)
N(5)
F(35)
F(34)
F(24)
C(24)
C(15)
C(35)
C(34)
C(25)
C(14)
C(7)
F(13)
C(23)
C(26)
C(13)
C(33)
C(36)
F(33)
F(16)
F(26)
F(23)
C(16)
F(36)
C(22)
C(11)
C(12)
C(32)
C(21)
C(31)
N(2)
F(32)
F(22)
W
F(12)
N(1)
N(3)
C(3)
C(5)
C(1)
N(4)
C(4)
C(6)
C(2)

97129

ACKNOWLEDGMENTS

It's almost a cliché to begin one's acknowledgment section by saying how this is the hardest part to write, since the vast majority of people who open this thesis are going to: (1) find out how many pages I wrote; (2) *maybe* glance at the preface (I've got some quotes up there, have a look!); and (3) read the acknowledgments. Since everybody is, first and foremost, curious as to how many pages this is, (incidentally, I think the number of pages a thesis contains is a poor measure of how much work the person actually got done) maybe you're also curious, as I was, about some other facts concerning this thesis. It's 64,169 words long. It contains 353,336 characters, for an average word length of 5.5063 letters.

I must begin by thanking Dick Schrock for all the guidance over the past four years. I feel that we in the Schrock group are extremely fortunate to have an advisor who is really a part of our chemistry, and who makes research a high priority. I also thank Dick for treating me as an adult, which has made my life here enjoyable. Dick is a true advisor, and most of the work which led to chapters in this thesis was spawned from our discussions. But he also provided me with the freedom to run with things, which is probably where I learned the most.

The Schrock group has been an amazing place to work. The enthusiasm is high and I have had the chance to learn from some great chemists. I thank everyone I worked with, past and present. Ivan Shih was one of the first that I would consider an influence. His flying-by-the-seat-of-the-pants style of churning out results impressed me. That style led him to open the door on triamidoamine chemistry with Mo and W, and it was gratifying that I was also able to reap some of the reward of what Ivan began with those silylated complexes. He also taught me to mitigate my enthusiasm slightly until I knew what the product was, and to think critically about my own research results. Nadia Zanetti is another one who knows how to make compounds, and with a style similar to Ivan's made her own extensions into Mo and W chemistry. Between those two 6-430 was always a good place to stop by. Flo Schattenmann and Tim Warren made a great team. The 6-427 lab was really something! Two great chemists, athletes, and partiers came together, and whenever I was in their lab I was guaranteed to have some fun and learn something. I've also enjoyed spending time with Flo's fiancee Sheree Stokes, and I hope I continue to see much of the two of them.

I've been fortunate to have some great labmates. Shifang Luo got stuck with me as a first-year and we ended up having some great times together. My first I.A.P. in the lab with Shifang really stands out in my mind as a transition period during which I became a graduate student, with his help. He got me on track and was always willing to spend his time showing me the ropes. Deryn Fogg and I also had some great times, and I thank her for teaching me much about late metals and physical chemistry. Equally importantly, she knows how to have a good time (a "party girl" [sic]) and I think some of that rubbed off as well. My newer labmates, Laura Turculet, Sherry Zsu, and Dave Graf (I drove Dave out before long) kept me company and dealt well with my erratic lab schedule while writing up. Thanks go to Gretchen for staying on top of things.

I thank Prof. Scott Virgil for being approachable and taking some time to teach me some organic chemistry when I seriously needed it. Profs. Dan Nocera and Bill Reiff provided us with some valuable insights on magnetochemistry. Bill Davis got us some pretty neat structures. Bill and I had an 86% att/comp record. If we were in the NFL we'd be millionaires! I also gratefully acknowledge Aaron Odom, without whom I never would have gotten the structure of $[N_3N_F]W(CO)(3,5\text{-}Me_2Ph)$ (one of the best crystals (jet-black) I ever grew). Steve ("the Bone") Reid and Melissa Hirsch also helped me with some structures. Anybody who ever analyzed one of my compounds for me, thanks for helping me get those important data.

Joel Freundlich provided me with a number a good chemical leads to pursue over the time we worked together. Myra O'Donoghue has always made coming to work fun, and has been great to talk and collaborate with on the group VI projects. I also truly appreciate Joel and Myra's suggestions and comments during the preparation of this thesis. Tom Boyd and I had some good laughs over the years about the MIT-Delaware connection. Robert Baumann and I both appreciate a good pint in a Cambridge bar on a weeknight! I also thank him and Tim Warren for helpful discussions on Zr chemistry and an endless supply of Grignard reagents. John the-Dartmouth-

hacker Alexander has been a good guy to work with and also got me on-line at home which provided me with a connection to the outside world while I was living like a monk writing up this thesis. George Greco taught me a little bit about Brooklyn and the history of the DuPhos ligand. Eric Liang and Jesse Lee really got me started with thinking about the diamido ligands and were good guys to talk with. Mike Aizenberg taught me much about coordination chemistry and X-ray crystallography. He's another one with whom a chat almost invariably leads to (1) learning something or (2) a good joke (or both!).

Doug Maus and I had a nice collaboration on some solid-state NMR work. I did what I like to do (make compounds, especially isotopically enriched) and he did what he liked to do (put them in sapphire rotors, spin at ~1700 Hz, and record the solid-state NMR spectrum). It was fun to see the Griffin group's setup. Back at the ranch, I thank Jeanne Owens and Jeff Simpson for teaching me some neat tricks at the NMR lab.

I thank the entire Cummins group for helping out from time to time in terms of trading reagents and ideas. I think the fact that Kit stayed here provided us with a uniquely synergistic environment in which to do chemistry. Mike Fickes has been a great friend literally from day one here at MIT, when we both realized that we were actually peers, and had unknowingly been so for 2 years a Berkeley. All the great bike rides we took were great inspirations for me. We did some great trips, and we also had some great beers together over the years. My only solace in the fact that we have to split up now comes from knowing that we will meet (and ride!) again, hopefully sooner rather than later. Seble Wagaw and Dan Lecloux have also been cool to spend time with. Tom Reisz helped get us out on some great rides this summer, very important during thesis writing! It was also a pleasure to drink a few good beers with Tomás G. while writing up.

Yann Schrodi and I have had some great times since he joined the group. I predict he will take the projects we've worked on to new heights. The group received three talented and hard-working UROPs this summer, Maria, Laura, and John; who have really come in and gotten some good projects going. I've enjoyed what little interaction I've had with them.

I also need to thank my undergraduate advisor, Bruce Novak, for giving me my first research position, despite the fact that he swore to his graduate students that he wouldn't take any more undergrads! My friends Tim Deming and Andy Goodwin from the Novak group were very influential in terms of getting me starting in research.

This brings me to the person that I owe the most to, and unfortunately someone who is no longer on the planet, my father, a chemist with duPont for 20 years. All arguments about whether chemistry is "nature or nurture" aside, it is plain to me that he influenced me greatly in my choice of a career. I think he was brilliant in that he saw an interest in science in me and gently encouraged me in that direction, but never pushed too hard. I can't explain the anger and grief that I feel as a result of the fact that fact that he's not here to see me get this degree. It's a horrible injustice. Equally unjust is the fact that my grandfather, also a chemist, died several months before I finished this. So my two great chemical fathers never lived to see me finish the thing that they started, my chemical education. I am somewhat consoled by that fact that my mom and both of my grandmothers are still here to witness this. They gave, and continue to give, me lots of love and support over the years both before and after my dad died. I still feel the influence of the first Dr. Seidel strongly, and it is because he can't be here to enjoy this with me that I have dedicated this thesis to his memory.